Julius-Maximilians-
UNIVERSITÄT
WÜRZBURG

OTH
OSTBAYERISCHE
TECHNISCHE
HOCHSCHULE
REGENSBURG

Conformal Mappings onto Simply and Multiply Connected Circular Arc Polygon Domains

Dissertationsschrift zur Erlangung des naturwissenschaftlichen
Doktorgrades der Julius-Maximilians-Universität Würzburg

vorgelegt von

Ulrich Josef Bauer

aus

Dietfurt/Töging, Deutschland

Würzburg 2015

Eingereicht am 23.04.2015
bei der Fakultät Mathematik und Informatik
der Julius-Maximilians-Universität Würzburg

1. Gutachter: Prof. Dr. Stephan Ruscheweyh
2. Gutachter: Prof. Dr. Wolfgang Lauf

Tag der Disputation: 20.11.2015

Contents

Acknowledgments

I would like to express my deepest gratitude to all those who supported me on my way to finish this thesis.

I wish to especially thank my supervisors Professor Dr. Stephan Ruscheweyh and Professor Dr. Wolfgang Lauf for providing me this great opportunity and for all their support.

I want to thank all current and former members of chair IV of the Department of Mathematics in Würzburg for their backing. I also owe thanks to those of the OTH Regensburg who supported me in any way.

Last but not least, I am grateful to my parents, my sisters and my girlfriend for their patience and support.

1 Introduction

1.1 The Mapping Problem

Since the publication of the famous Riemann mapping theorem, it is known that every simply connected domain can be conformally mapped onto the unit disk. It was extended later to also ensure the conformal mapping of any multiply connected domain onto a conformally equivalent canonical region like a circular domain (Definition 4.1).[1] While the existence of such mappings for all finitely connected domains is guaranteed, the search for the mapping formulas has since remained an open topic.

The Schwarz-Christoffel transformation and its variations represent a class of mappings onto polygonal domains and other similar domains. A historical summary of the evolution of the Schwarz-Christoffel mapping can be found in Section 1.2.
The two common features of these mappings are that each of them conformally maps a canonical domain onto a domain whose boundary contains several vertices and that the mapping formulas contain at least two kinds of parameters. The issue with these parameters is that they define the shape of the image domain, but the actual shape can only be seen by evaluating the mapping. The search for the correct parameters for a given image domain is known as the "parameter problem".

The goal of this thesis is to investigate conformal mappings onto circular arc polygon domains, i.e. domains that are bounded by polygons consisting of circular arcs instead of line segments. This includes the investigation of the third kind of parameters of these mappings in the case of simply connected image domains. A new version for conformal mappings onto multiply connected domains will also be constructed. We will moreover discuss the necessary concepts of the numerics to give an approach to the parameter problem. A summary of the results of our thesis can be found in Section 1.3 and an outline of the different chapters can be found in Section 1.4.

1.2 Historical Overview

The first known reference to conformal mappings from the upper half plane onto polygonal domains (Figure 1) can be found in an article by Elwin Bruno Christoffel published in the year 1867. Some years later Hermann Amandus Schwarz discovered the same mappings independently of Christoffel. Referring to both mathematicians, the mapping onto a polygonal domain is known as the "Schwarz-Christoffel transformation".
While all domains can be approximated by polygonal domains, the common mapping formula (Lemma 3.5) has two major drawbacks. First, the mappings are from standard domains like the upper half plane onto polygonal domains. However, in most scenarios, the mappings are needed the other way around, i.e. from a polygonal domain onto a

[1] The corresponding theorems and more canonical regions can, for example, be found in the book of Conway [Con95, Chapter 15].

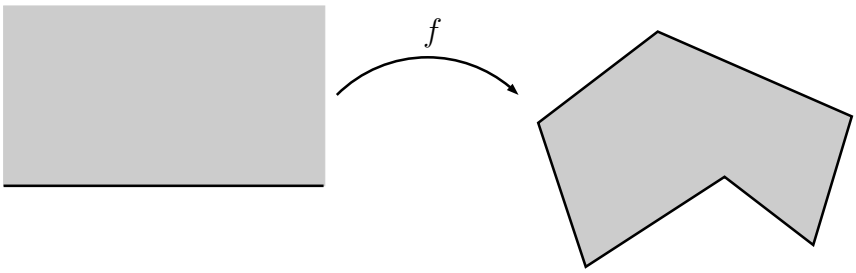

Figure 1: Schwarz-Christoffel transformation: The upper half plane is mapped onto a domain bounded by a polygon.

standard domain.
The second problem is in choosing the correct parameters. The mapping formula contains two kinds of parameters (the preimages of the corners of the polygon and the interior angle at these corners) and the shape of the image domain depends on these choices, but the result of an actual mapping can only be attained by evaluating the mapping. This problem is normally simply referred to as the "parameter problem" in the context of the Schwarz-Christoffel transformation.
Christoffel and Schwarz also expanded this topic to different forms of the mapping formula by changing some of the properties of the image domains. This includes mappings onto the exterior of a polygon, domains with curved boundary parts and domains bounded by circular arc polygons (Figure 2). The circular arc polygon domains, e.g.

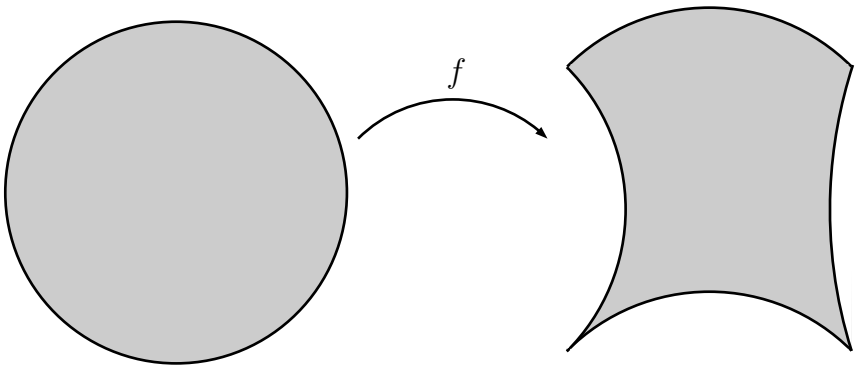

Figure 2: Circular arc polygon domain mapping: The unit disk is mapped onto a domain bounded by a polygon, where the sides are circular arcs.

domains, where the boundary is a polygon while the straight sides are replaced by circular arcs, will be the main topic of this thesis.
While they have discovered many mapping formulas, the parameter problem restricted them to simple examples.

This topic became of interest again in the second half of the twentieth century. With

the invention of the computer and its improvements, there was a way to handle the parameter problem. By the start of the next century a lot of articles were published about the different aspects of the numerics of the Schwarz-Christoffel transformation. In the late nineties, software packages for most topics regarding the Schwarz-Christoffel transformation were available.
The numerics of conformal mappings onto circular arc polygon domains was especially investigated by Bjørstad and Grosse [BG87] and Howell [How90],[How93].
A more detailed view on the history until this point, with many references and an in-depth discussion of the numerics, can be found in the book [DT02] of Trefethen and Driscoll.

The major improvement in the 21th century was the discovery of the mapping formula for mappings onto multiply connected polygonal domains. Conformal mappings onto doubly connected polygonal domains were already known for quite some time. Komatu stated a formula in 1945 [Kom45] and Hu later on wrote a software package (DSC-PACK) to handle it [Hu98]. An alternative approach to the mappings onto doubly connected domains [DEP01] from DeLillo, Elcrat and Pfaltzgraff led to the mappings for a connectivity greater than two (Figure 3) [DEP04]. Some years later, Crowdy used

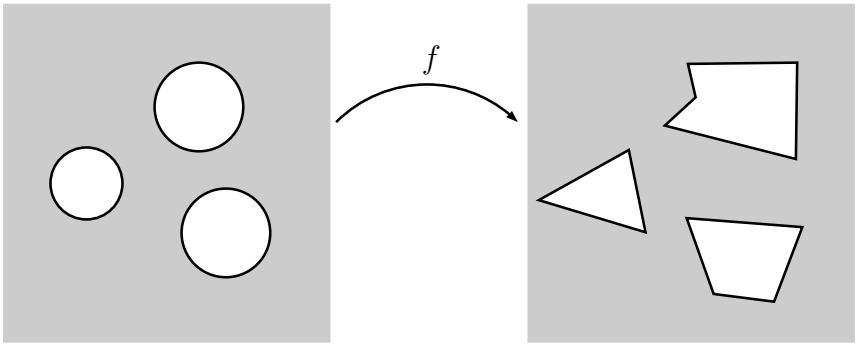

Figure 3: Multiply connected Schwarz-Christoffel transformation: The plane minus some disks is mapped onto an unbounded multiply connected polygonal domain.

a tool from the area of Kleinian groups, the Schottky-Klein prime function, to state another version of the mapping formula for multiply connected domains [Cro05]. These newer activities are also described in [Cas08].

From this point on, the topic evolved similarly to the simply connected case. There were efforts to construct further mappings with the tools gathered so far (e.g. [CM06]). On the other hand, the numerics used for the mappings was improved and algorithms were created to cope with the parameter problem (e.g. [DK11]).
Some formulas for conformal mappings onto multiply connected circular arc polygon domains (Figure 4) were already published by Crowdy [CF07], [CFG11], but an approach using methods similar to the ones of DeLillo, Elcrat and Pfaltzgraff is still missing.

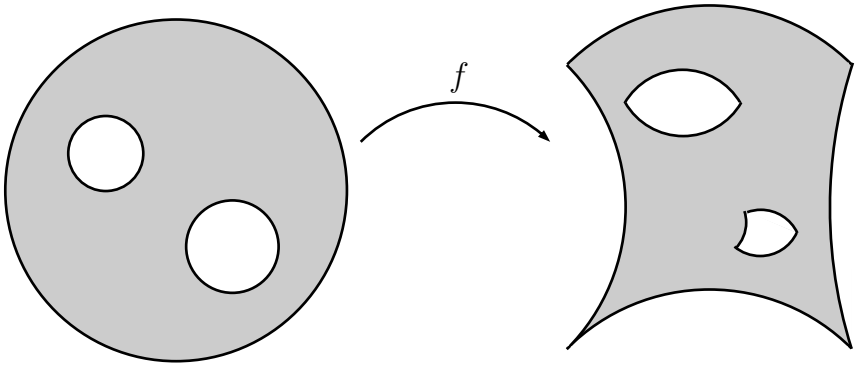

Figure 4: Multiply connected circular arc polygon domain mapping: A circular domain is mapped onto a bounded multiply connected circular arc polygon domain.

1.3 Main Results of this Thesis

Our thesis makes some essential contributions to handling the open topics in the context of the conformal mappings onto circular arc polygon domains.

Conformal mappings onto circular arc polygon domains contain parameters in addition to the classical parameters of the Schwarz-Christoffel transformation. To contribute to the parameter problem of conformal mappings from the unit disk onto circular arc polygon domains, we investigate two special cases of these mappings. In the first case we can describe the additional parameters if the bounding circular arc polygon is a polygon with straight sides (Lemma 3.6). In the second case we provide an approximation for the additional parameters if the circular arc polygon domain satisfies some symmetry conditions (equation (3.9)). These results allow us to draw conclusions on the connection between these additional parameters and the classical parameters of the mapping.
We are also able to prove a formula for the change of the additional parameters if an automorphism of the unit disk is applied before a fixed conformal mapping onto a circular arc polygon domain is used (equation (3.6)).

For conformal mappings onto multiply connected circular arc polygon domains, we provide an alternative construction of the mapping formula without using the Schottky-Klein prime function. In the process of constructing our main result, mappings for domains of connectivity three or greater (Theorem 4.43), we also provide a formula for conformal mappings onto doubly connected circular arc polygon domains (Theorem 4.22). The comparison of these mapping formulas with already known mappings (Sections 4.3 and 4.5) allows us to provide values for some of the parameters of the mappings onto doubly connected circular arc polygon domains if the image domain is a polygonal domain (Lemmas 4.27 and 4.28).
The different components of the mapping formula are constructed by using a slightly modified variant of the Poincaré theta series. This construction includes the design of a

function to remove unwanted poles (Section 4.4.2) and of different versions of functions that are analytic on the domain of definition of the mapping functions and satisfy some special functional equations (Sections 4.4.4 to 4.4.6).
As a result of our investigations, we have found conformal mappings from circular domains onto conformally equivalent circular arc polygon domains of arbitrary finite connectivity.

We also provide the necessary concepts to numerically evaluate the conformal mappings onto multiply connected circular arc polygon domains. As the evaluation of such a map requires the solution of a differential equation, we provide a possible configuration of curves inside the preimage domain to solve the equation along them (Algorithm 2) in addition to a description of the procedure for computing either the formula for the doubly connected case (Section 5.3) or the case of connectivity three or greater (Section 5.4). We also describe the procedures for solving the parameter problem for multiply connected circular arc polygon domains (Section 5.5).

1.4 Structure of this Thesis

Our thesis can be split up in four main chapters not including the introduction (Chapter 1) and the conclusion (Chapter 6).

Basic Information

The second chapter is mainly a collection of different information scattered among different books and articles. The intention is to have all the tools needed for the later discussion in one common place. Only the quintessences of the different results are stated. Any further or in depth discussion can therefore be found in the original sources. We will also present some minor conclusions in this chapter. They are not directly mentioned in the literature as they are of no common interest, but will simplify the reasoning in the following chapters of the thesis.
This section consists of the topics

- **Möbius Transformations**: The Möbius transformations and their main properties and classification are stated.
- **Schwarzian Derivative**: Here the main features and some further properties of the differential operator “Schwarzian derivative” are listed.
- **Kleinian Groups**: Results regarding groups of Möbius transformations are presented.
- **Schottky Groups**: The behavior of Schottky groups, a subtype of the Kleinian groups, is described. We provide some additional results regarding the behavior of such groups.
- **Poincaré Theta Series**: A series covering all transformations of a Kleinian group is introduced and investigated. We further introduce a generalization of the series.

Simply Connected Circular Arc Polygon Domains

The third chapter covers conformal mappings onto simply connected circular arc polygon domains. First the mapping formula itself is introduced in different versions. Thereafter, one kind of parameters contained in the formula receives some in-depth discussion. This includes the investigation by us for the case where the parameters change by the application of an automorphisms to the preimage domain.
We further investigate the behavior of these parameters for two classes of image domains. Each of these classes is identified by special geometric properties. First the mapping formula is compared with the classical Schwarz-Christoffel transformation, i.e. the image domains are bounded by polygons. The second domain type is characterized by a symmetry against rotation around the origin.

Multiply Connected Circular Arc Polygon Domains

In the fourth chapter, we construct the Schwarzian derivative of conformal mappings onto multiply connected circular arc polygon domains. The construction of the Schwarzian derivative is done in three steps:

1. We collect the basic properties of the Schwarzian derivative.
2. We construct the Schwarzian derivative of the conformal mappings onto doubly connected circular arc polygon domains.
3. The obtained results are extended to a Schwarzian derivative of conformal mappings onto circular arc polygon domains with connectivity three or greater.

The section for the mappings onto doubly connected domains and the section for the mappings onto multiply connected domains are followed by comparisons with already known Schwarzian derivatives of functions, which can also be seen as mappings onto circular arc polygon domains.
Each construction step consists of several smaller steps as we have to verify the properties we found like functional equations, correct principal parts and convergence.

Numerical Approaches to the CAPD Mapping

Different aspects regarding the numerical conformal mappings onto circular arc polygon domains (CAPDs) are discussed in the fifth chapter. The focus will be on mappings onto multiply connected domains, since the results can also be used for simply connected domains. However, the multiply connected scenario also includes several additional problems.
We establish curves in order to evaluate the Schwarzian derivative in a multiply connected domain, discuss possible implementations of the Schwarzian derivative and present some generated images. We also give a basic approach to the parameter problem for mappings onto multiply connected circular arc polygon domains.

2 Basic Information

Since Möbius transformations will play an important role in the following sections, we will introduce in advance several terms and facts regarding these mappings.
Many details are taken from the monograph of Ford [For51], as this text is a key reference regarding Möbius transformations and especially groups of them. An alternative reference would be the book of Maskit [Mas88].
We will also add some own statements to better illustrate the behavior of the different entities. We will especially provide some information about the behavior of Schottky groups (items 2.32 to 2.37) and expand the concept of the Poincaré theta series (Lemmas 2.42 and 2.43).
If a lemma is taken from a specific article or book, it is marked accordingly.

For economy in notation, we will from now on call a conformal mapping simply connected if it maps a simply connected domain onto another simply connected domain. Hence, we will call a conformal mapping multiply connected if it maps a multiply connected domain onto another domain of the same connectivity.

2.1 Möbius Transformations

Definition 2.1
The transformation

$$T(z) = \frac{az+b}{cz+d}$$

where $a, b, c, d \in \mathbb{C}$ are constants and $ad - bc \neq 0$, is called a Möbius transformation. If not stated otherwise, the transformation is normalized by $ad - bc = 1$. The set of all Möbius transformations is denoted by $\mathbb{M}$.

Some basic properties of Möbius transformations are:

Lemma 2.2 ([For51, pp. 2, 4, 9, 12])
The following statements are true for Möbius transformations:

- *The inverse of a Möbius transformation is a Möbius transformation.*
- *Any composition of a finite number of Möbius transformations is equivalent to a single Möbius transformation.*
- *Each Möbius transformation carries a circle or straight line into a circle or straight line.*
- *Any composition of an even number of reflections (against a circle or line) is equivalent to a Möbius transformation.*

The next definition will clarify the term “reflection” used in the lemma above.

Definition 2.3
A reflection s against a circle with center c and radius r is defined by

$$s(z) := \frac{r^2}{\bar{z} - \bar{c}} + c.$$

Möbius transformations have either one or two fixed points. They are divided into four different classes according to their fixed points.
If a transformation has only one fixed point, it is called a *parabolic* transformation. Transformations with two fixed points are called one of *elliptic*, *hyperbolic* or *loxodromic*. We differentiate between these three cases by the fact whether the fixed points are attractive, repelling or indifferent. The hyperbolic and the loxodromic transformations have one attractive and one repelling fixed point, while the elliptic transformations have two indifferent fixed points.
The class of a transformation can easily be found by the following lemma:

Lemma 2.4 ([For51, p. 23])
The transformation $T(z) = \frac{az+b}{cz+d}$, where $ad - bc = 1$, is of the type stated if, and only if, the following conditions on $a + d$ hold:

Hyperbolic *if $a + d$ is real and $|a + d| > 2$*

Elliptic *if $a + d$ is real and $|a + d| < 2$*

Parabolic *if $a + d = \pm 2$*

Loxodromic *if $a + d$ is complex.*

Since hyperbolic and loxodromic transformations have a similar behavior regarding their fixed points, some books like [Mas88] define the hyperbolic transformations as a subtype of the loxodromic transformations. Hence, they refer to both kinds of transformations by the term loxodromic.

The mapping behavior of a Möbius transformation can partially be described by the so called isometric circle.

Definition 2.5
The circle

$$|cz + d| = 1, \qquad c \neq 0,$$

which is the complete locus of points in the neighborhood of which lengths and areas are unaltered in magnitude by the transformation $T(z) = \frac{az+b}{cz+d}$ normalized by $ad-bc = 1$, is called the isometric circle of the transformation. The circle has the center $u := -\frac{d}{c}$ and radius $|c|^{-1}$.

Lemma 2.6 ([For51, p. 25])
For the isometric circle of a transformation T the following is true:

- *Lengths and areas inside the isometric circle are increased in magnitude, and lengths and areas outside the isometric circle are decreased in magnitude, by the transformation.*
- *A transformation carries its isometric circle into the isometric circle of the inverse transformation.*

2.2 The Schwarzian Derivative

The Schwarzian derivative is a differential operator, which is invariant against Möbius transformations. It is used in many parts of complex analysis. A good overview of its many applications can be found in [Osg98].
We will list in this section the properties of the Schwarzian derivative necessary for our discussion. For the following lemmas, we suppose all functions to be sufficiently often differentiable.

Definition 2.7
The Schwarzian derivative $\{f, z\}$ of a function f of one complex variable is defined by

$$\{f, z\} := \left(\frac{f''(z)}{f'(z)}\right)' - \frac{1}{2}\left(\frac{f''(z)}{f'(z)}\right)^2.$$

The Schwarzian derivative is often simply called the Schwarzian.

For a composition of functions, the Schwarzian has the property:

Lemma 2.8
The Schwarzian derivative of a composition of two functions can be written as

$$\{f \circ g, z\} = \{f, g(z)\}\, g'(z)^2 + \{g, z\}.$$

The main property of the Schwarzian derivative is its invariance against Möbius transformations.

Lemma 2.9
The Schwarzian derivative $\{T, z\}$ is identically zero if and only if T is a Möbius transformation $T \in \mathbb{M}$.

This allows us to state:

Lemma 2.10
The Schwarzian derivative of a composition of a holomorphic function f and a Möbius transformation T, is either of the form

$$\{T \circ f, z\} = \{f, z\} \quad \text{or} \quad \{f \circ T, z\} = T'(z)^2\{f, T(z)\}.$$

Pre-Schwarzian

In the context of the classical Schwarz-Christoffel mapping, the pre-Schwarzian is used. It is a pre-stage of the Schwarzian derivative with the property of being invariant against translation, rotation and scaling.

Definition 2.11
The pre-Schwarzian of a function f is defined by the quotient $\frac{f''}{f'}$.

The pre-Schwarzian has no special notation in the common literature.

The main property of the pre-Schwarzian can easily be derived by calculation:

Lemma 2.12
The pre-Schwarzian is invariant under translation, rotation and scaling.
For two functions f and $g = af + b$, where $a \in \mathbb{C} \setminus \{0\}$ and $b \in \mathbb{C}$, it is true

$$\frac{f''}{f'} = \frac{g''}{g'}.$$

2.2.1 Solving the Schwarzian Derivative

The Schwarzian derivative is in most cases not solved in the form of a differential equation of the third order, but as a system of second order differential equations according to the following lemma.

Lemma 2.13 ([Hil76, Chapter 10])
Let y_1 and y_2 be two linearly independent solutions of the equation

$$y'' + Q(z)y = 0, \tag{2.1}$$

which are defined and holomorphic in some simply connected domain D in the complex plane. Then

$$f(z) = \frac{y_1(z)}{y_2(z)}$$

satisfies the equation

$$\{f, z\} = 2Q(z) \tag{2.2}$$

at all points of D where $y_2(z) \neq 0$. Conversely, if $w(z)$ is a solution of (2.2), holomorphic in some neighborhood of a point $z_0 \in D$, then one can find two linearly independent solutions, $u(z)$ and $v(z)$, of (2.1) defined in D so that

$$f(z) = \frac{u(z)}{v(z)},$$

and if $v(z_0) = 1$ the solutions u and v are uniquely defined.

It is important to note that this version of solving the Schwarzian demands a simply connected domain. This is less a necessity of the Schwarzian, but of differential equations in the complex domain.
The common way of solving differential equations is to start at some point z_0 with some initial values and then solve along different curves. Each curve allows us to extend the domain by usage of the monodromy theorem [Hen74, Theorem 3.5c]. Hence, we get a solution for the whole domain by using enough curves and merging the results.
However, this method demands that the results of the different curves match, i.e. every solution from z_0 to z_1 should yield the same value for z_1. While this property is guaranteed for simply connected domains, it is not ensured for domains of greater connectivity. As the curves surround the boundary components in different ways, they can lead to different solutions at the same end point (Figure 5). For example, if one curve

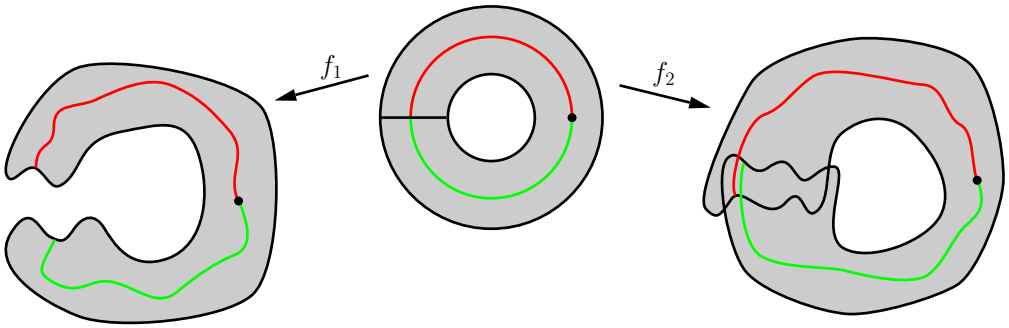

Figure 5: The image of a cut up domain can contain a gap or overlap. Hence, two different curves starting in the same point can yield different values for points on the cut.

surrounds one of the holes of the domain clockwise, it could lead to another branch, as the curve surrounding the hole counterclockwise.
Hence, it is possible to solve the Schwarzian by the method given above on multiply connected domains, but it may lead to multivalued results. These multivalued results indicate that the mapping is not a valid, i.e. well-defined, multiply connected mapping.

A simple example would be the function $f(z) = \sqrt{z+a}$. The result of the mapping of the annulus $r < |z| < 1$ depends on the choice of the shifting parameter a. If a is in the interior of the smaller bounding circle of the annulus $|a| < r$, we need to insert a suitable slit into the domain for a well defined mapping. In this case, we then only have a simply connected mapping (Figure 6(a)).
If the parameter lies outside of the annulus $|a| > 1$, the function is a well defined doubly connected mapping (Figure 6(b)).[2] In the case where the parameter is inside

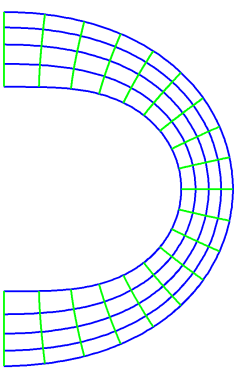

(a) The simply connected image of the slitted annulus for a=$\frac{1}{4}$.

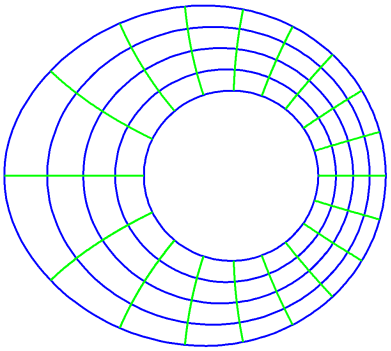

(b) The doubly connected image of the annulus for a=$\frac{5}{4}$.

Figure 6: The image of the annulus $\frac{1}{2} < |z| < 1$ for the mapping $\sqrt{z+a}$ is either a simply connected domain for $|a| < \frac{1}{2}$ (left image) or a doubly connected domain (right image), depending on the fact, if it is necessary to cut up the annulus.

the annulus $r < |a| < 1$, we have to combine the two versions and insert a suitable slit from a to the outer boundary of the annulus. The result is a mapping of the slitted annulus onto a doubly connected domain.
Therefore, the validity of a given Schwarzian in a multiply connected context may not be clear in advance.

A possible approach to handle this problem would be to cut the domain down to simple connectivity (Figure 7). The differential equation can then be solved on the now simply connected domain. To reassemble the domain afterwards, one needs to ensure that the solutions of both sides of each cut match.[3]
Let D be a doubly connected domain and D_S a simply connected version of D produced by connecting the boundary components by a slit. If we denote the cut by γ with the two sides γ^+ and γ^-, we need to assure for a solution f that $f^{(n)}(\gamma^+) = f^{(n)}(\gamma^-)$, $n = 0, \ldots, \infty$. However, instead of validating the whole cut, one may only examine one point and its derivatives.

[2] The logarithmic slit has to be chosen accordingly.
[3] The reassembling itself can be justified by e.g. [Hen74, Theorem 5.11a].

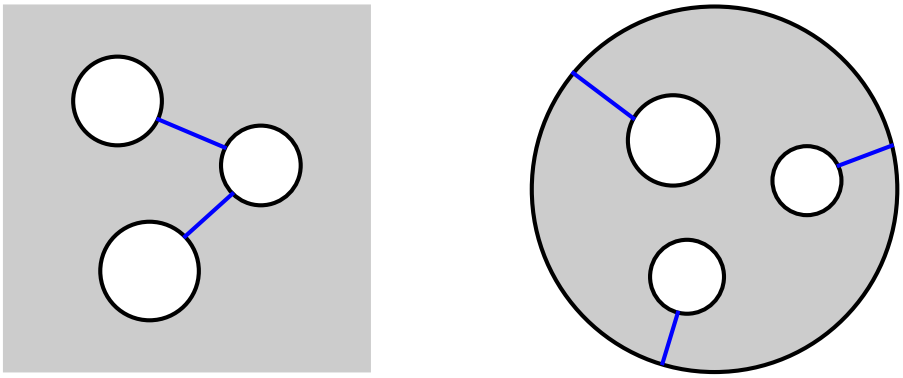

Figure 7: Any $(m+1)$-connected domain can be reduced to simple connectivity by inserting m non-intersecting slits (blue lines) connecting the boundary components. The resulting domain is not unique.

If we use the Schwarzian derivative as an example, the initial values consist of $f(z_0)$, $f'(z_0)$ and $f''(z_0)$ at some point $z_0 \in D$. We can solve twice from z_0 to some point $z_1 \in \gamma$ to get values for $z_1^+ \in \gamma^+$ and $z_1^- \in \gamma^-$ (Figure 8). If we continue the solution process from both points along γ, we get values for γ^+ and γ^- respectively. Hence, if we have for z_1

$$f(z_1^+) = f(z_1^-), \quad f'(z_1^+) = f'(z_1^-), \quad f''(z_1^+) = f''(z_1^-),$$

the solutions starting in z_1 either along γ^+ or γ^- coincide, as they have the same initial values. This means that with equal initial values at one point on γ, we have $f^{(n)}(\gamma^+) = f^{(n)}(\gamma^-)$ for all $n \in \mathbb{N} \cup \{0\}$. Note that the property $f^{(n)}(z_1^+) = f^{(n)}(z_1^-)$ can be verified for a fixed n by

$$\int_\delta f^{(n+1)}(z)dz = 0$$

for a curve $\delta \in D_S$ from z_1^+ to z_1^- enclosing one of the boundary components of D.
If we want to solve the Schwarzian derivative on a $(m+1)$-connected domain bounded by the curves C_j, where $j = 0, \ldots, m$, we can apply the same procedure but with m cuts[4]. Hence, we have to check the $3m$ complex integrals

$$\int_{\delta_j} f^{(k)}(z)dz = 0, \qquad j = 1, \ldots, m, \ k = 1, 2, 3, \tag{2.3}$$

where each δ_j encloses only the boundary component C_j.

2.2.2 Further Properties

We state some further properties of the Schwarzian derivative, which will be of great use in the following chapters.

[4]The layout of the actual cuts is not important as long as it leads to a valid simply connected domain.

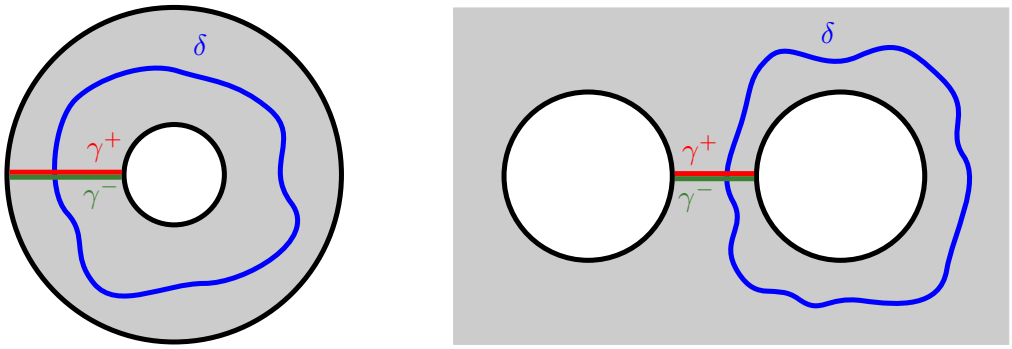

(a) An annulus

(b) An unbounded doubly connected domain

Figure 8: Two examples for a cut γ, with its sides γ^+ and γ^-, connecting the boundary components, and an enclosing curve δ for one of the boundary components.

Lemma 2.14
Simple poles of a meromorphic function f do not appear in its Schwarzian derivative.

Proof. Since the function f is meromorphic, it can be written in the form

$$f(z) = \frac{a_{-1}}{(z-s)} + a_0 + a_1(z-s) + O((z-s)^2)$$

for each of its simple poles s. Therefore, the quotient in the Schwarzian is of the form

$$\frac{f''(z)}{f'(z)} = \frac{-2}{(z-s)} + \left(\frac{-2a_1}{a_{-1}}\right)(z-s) + O((z-s)^2).$$

This leads to

$$\left(\frac{f''(z)}{f'(z)}\right)' = \frac{2}{(z-s)^2} + \left(\frac{-2a_1}{a_{-1}}\right) + O((z-s)^1),$$
$$\left(\frac{f''(z)}{f'(z)}\right)^2 = \frac{4}{(z-s)^2} + \left(\frac{8a_1}{a_{-1}}\right) + O((z-s)^1),$$

and concludes in

$$\{f,z\} = \left(\frac{-2a_1}{a_{-1}}\right) - \frac{1}{2}\left(\frac{8a_1}{a_{-1}}\right) + O((z-s)^1).$$

Therefore, $\{f,z\}$ is holomorphic at s, what proves the lemma. □

The statement above is quite intuitive, as the location of a simple pole can easily be altered by Möbius transformations. A simple pole s of f can be mapped onto a finite point w by a suitable transformation $T \in \mathbb{M}$, where $w = T(\infty)$, and so the function $T \circ f$ is finite at s. However, the Schwarzian must be equal for both functions $\{T \circ f, z\} = \{f, z\}$ as it is invariant against such transformations. This means that this pole can not appear in the Schwarzian derivative.

We also want to state the connection of the Schwarzian derivative of a function with its mapping behavior, a fact that in most textbooks only occurs as an exercise (e.g. [Ahl73, p. 21]). A more explicit form can be found in the article [CP01].

Lemma 2.15 ([CP01])
Let $z = z(t)$ be an arclength parametrized curve contained in the domain of the holomorphic mapping f and let $w(t) = f(z(t))$ be the image curve. The curvature of w is given by

$$\kappa(s) = |f'(z)|^{-1} \left(\operatorname{Im} \left(z' \frac{f''(z)}{f'(z)} \right) + k(t) \right),$$

with s denoting the arclength parameter of the image curve.
The change of the image curvature is further given by

$$\frac{d\kappa}{ds} = \frac{1}{|f'(z)|^2} \left(\operatorname{Im} \left((z')^2 \{f, z\} \right) + \frac{dk}{dt} \right).$$

If z is a circular arc $z(t) = re^{\frac{it}{r}} + c$, this simplifies to

$$\frac{d\kappa}{ds} = \frac{1}{|f'(z)|^2} \left(\operatorname{Im} \left((z')^2 \{f, z\} \right) \right). \tag{2.4}$$

Proof. As implied by the fact that the proof is often an exercise, the lemma can be shown by a straight forward calculation.
Let $z = z(t)$ be an arclength parametrized curve, so the curvature is given by $k(t) = \frac{d}{dt} \arg(z'(t))$. The curvature of the image curve $w(t) = f(z(t))$ is given by

$$\kappa(s) = \frac{d}{ds} \arg(w'(t)) = \frac{1}{|f'(z)|} \left(\operatorname{Im} \left(\left(\frac{f''}{f'}(z) \right) z' \right) + k(t) \right)$$

where s denotes the arclength parameter of the image curve and z should be read as $z(t)$. Further differentiation yields the relation

$$\frac{d\kappa}{ds} = \frac{1}{|f'(z)|^2} \left(\operatorname{Im} \left((z')^2 \{f, z\} \right) + \frac{dk}{dt} \right).$$

If the curve is a circle $z(t) = re^{\frac{it}{r}} + c$, we get $z'(t) = ie^{\frac{it}{r}}$, $k(t) = \frac{1}{r}$ and $k'(t) = 0$. This leads to

$$\frac{d\kappa}{ds} = \frac{1}{|f'|^2} \operatorname{Im}\left((z')^2\{f, z\}\right).$$

□

The lemma above can be simplified to:

Lemma 2.16
For a conformal mapping of a circular arc Γ in the form $z(t) = re^{\frac{it}{r}} + c$ onto a circular arc $f(\Gamma)$, the condition

$$(z - c)^2\{f, z\} \in \mathbb{R}$$

holds for all $z \in \Gamma$.

Proof. If the image curve is a circular arc, its curvature must be constant and therefore the rate of change of the curvature must be identically zero. As a result, equation (2.4) from the preceding lemma simplifies to

$$\frac{d\kappa}{ds} = \frac{1}{|f'(z)|^2}\left(\operatorname{Im}\left((z')^2\{f, z\}\right)\right) = 0 \quad \Rightarrow \quad \operatorname{Im}\left((z')^2\{f, z\}\right) = 0.$$

Replacing $z'(t) = ie^{\frac{it}{r}}$ with $\frac{i}{r}(z - c)$ gives

$$\operatorname{Im}\left((z - c)^2\{f, z\}\right) = 0 \;\Leftrightarrow\; (z - c)^2\{f, z\} \in \mathbb{R}$$

□

There is also a connection between the Schwarzian and the univalence of a function. The first work on this connection was by Nehari, while it was later on extended in several directions.

Lemma 2.17 ([Neh48])
In order that the analytic function f is univalent in $|z| < 1$, it is necessary that

$$|\{f, z\}| \leq \frac{6}{(1 - |z|^2)^2}$$

Many generalized versions are now available. An overview can be found in [Osg98].

2.3 Kleinian Groups

This section will present basic results regarding groups of Möbius transformations.

Definition 2.18
A finite or infinite set of transformations $G \subset \mathbb{M}$ is said to form a group if,

- *the inverse of each transformation of the set is a transformation of the set, i.e. $T \in G \Rightarrow T^{-1} \in G$*
- *the succession of any two transformations of the set is a transformation of the set, i.e. $T, U \in G \Rightarrow T \circ U \in G$.*

We want the groups to satisfy the following property:

Definition 2.19
A group $G \subset \mathbb{M}$ is properly discontinuous at a point $z_0 \in \mathbb{C}_\infty$ if there exits a region S enclosing z_0 such that all transformations of the group, other than the identical transformation, carry z_0 outside of S.
A group $G \subset \mathbb{M}$ who is properly discontinuous at some point $z_0 \in \mathbb{C}_\infty$ is called properly discontinuous.
The set of all points at which $G \subset \mathbb{M}$ is properly discontinuous is denoted by Ω.

We will suppose from now on that every group is properly discontinuous, as it is a requirement for most statements regarding such groups.

A characteristic feature of each group of Möbius transformations is the fundamental region.

Definition 2.20
Two configurations (points, curves, etc.) are said to be congruent with respect to a group if there is a transformation of the group other than the identical transformation, which carries one configuration into the other.

Definition 2.21
A region, connected or not, no two of whose points are congruent with respect to a given group, and such that the neighborhood of any point on the boundary contains points congruent to points in the given region, is called a fundamental region R for the group.

There are some interesting facts about the isometric circles (Definition 2.5) of all the transformations of a group.

Lemma 2.22 ([For51, p. 41])
Let G be a properly discontinuous group of Möbius transformations.
The radii of the isometric circles are bounded and the number of isometric circles with radii exceeding a given positive quantity is finite.
Let $\{I_n\}$ be an infinite sequence of distinct isometric circles $I_1, I_2, \ldots$ of transformations of the group, with the radii being $r_1, r_2, \ldots$, then $\lim_{n\to\infty} r_n = 0$.

The properties of the isometric circles lead to the idea of the limit set.

Definition 2.23
A cluster point of the centers of the isometric circles of the transformations of a group is called a limit point of the group. A point which is not a limit point is called an ordinary point. The set of limit points of a group is denoted by Λ.

The set of all limit points of a group is often called the *limit set* of the group.

With the concept of the limit points, we can distinguish the groups of Möbius transformations.

Definition 2.24 ([For51, p. 66])
A properly discontinuous group is called

Elementary *if the group is finite or has only one or two limit points*

Fuchsian *if all the transformations have a common fixed circle and each transformation carries the interior of the fixed circle into itself*

Kleinian *if none of the above matches*

The term *Kleinian group* is often also used for all types of properly discontinuous groups of Möbius transformations (e.g. in [Mas88, p. 16]). We will also assume the elementary and Fuchsian groups to be special cases of the Kleinian groups for a easier notation.

The set of all limit points of a group has the following interesting properties:

Lemma 2.25 ([For51, p. 43],[Mas88, p. 96])
For the limit set the following is true:

- *The limit set is transformed into itself by any transformation of the group.*
- *If the limit set contains more than two points, it is a perfect set.*
- *The limit set of a non-elementary Kleinian group is the closure of the set of loxodromic and hyperbolic fixed points.*

The introduction of the limit set allows us to partition the Riemann sphere:

Lemma 2.26 ([Mas88, p. 24])
For any group G of Möbius transformations with fundamental region R, $\mathbb{C}_\infty$ is the disjoint union of Λ and $\Omega^* \supset \bigcup_{T\in G} T(R)$.

The set $\Omega^* \supset \Omega$ is the regular set of G and the difference $\Omega^* \setminus \Omega$ are fixed points of elliptic elements of G ([Mas88, p. 23, 25]). Hence, $\Omega^* = \Omega$, if G does not contain elliptic transformations. The difference $\Omega^* \setminus \bigcup_{T\in G} T(R)$ is the union of the transformations of $\partial R \setminus \Lambda$. If the boundary of R does not contain any limit points, we can write Ω^* as the union of the transformations of the closure of R

$$\Omega^* = \bigcup_{T\in G} T(\mathrm{cl}(R)).$$

Hence, every point on the Riemann sphere is in this case either congruent to a point in the closure of the fundamental region or a point in the limit set.

2.4 Schottky Groups

The following chapters will often refer to a subtype of the Kleinian groups known as Schottky groups. Hence, we will present further results regarding these Schottky groups. We will also give some facts, which are not stated explicitly in the standard books about Kleinian groups, but will simplify the later discussion. This particularly covers the topic of the mapping dynamics of the Schottky groups.

Definition 2.27
A Schottky group is defined by $2n$ disjoint circles, $C_1, C_1', \ldots, C_n, C_n'$, which are external to one another and bound a domain $D \subset \mathbb{C}_\infty$, and by n elements $T_1, \ldots, T_n \in \mathbb{M}$. Each T_j carries C_j into C_j' in such a way that the exterior of C_j is carried into the interior of C_j'.
The Schottky group G is generated by $T_1, \ldots, T_n$ and has D as a fundamental region.

We can even further restrict the group by:

Definition 2.28
Suppose the n pairs of circles C_1 and C_1', C_2 and C_2', etc., bounding the fundamental region of a Schottky group are symmetric with respect to a common circle C_0 and let s_j, $j = 0, \ldots, n$, denote the reflection against the circle C_j. If each of the transformations T_j carrying C_j into C_j' (and the exterior of C_j into the interior of C_j') is given by $T_j = s_0 \circ s_j$, we call the Schottky group symmetric.

The name for this specific type of Schottky group is taken from [Bur91].[5]

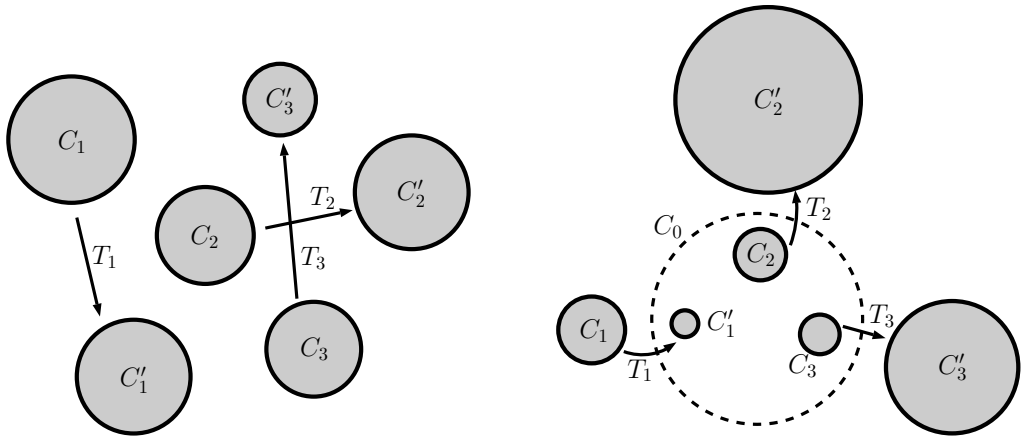

(a) A Schottky group: The group is generated by the transformations T_j, which map the circles C_j onto the circles C'_j.

(b) A symmetric Schottky group: The circles C_j and C'_j are symmetric with respect to the circle C_0.

Figure 9: The images show the circles C_j and C'_j of a general and a symmetric Schottky group. The white area outside of the gray-filled circles is the fundamental region for each of the groups.

The Möbius transformations produced by two consecutive reflections as in the definition above can be written as:

Lemma 2.29
Two consecutive circle reflections

$$s_1(z) = \frac{r_1^2}{\bar{z} - \bar{c_1}} + c_1, \qquad s_2(z) = \frac{r_2^2}{\bar{z} - \bar{c_2}} + c_2,$$

form the Möbius transformation

$$(s_2 \circ s_1)(z) = \frac{(|c_2|^2 - r_2^2 - \bar{c}_1 c_2)z + (|c_1|^2 c_2 - c_1|c_2|^2 + r_2^2 c_1 - r_1^2 c_2)}{(\bar{c_2} - \bar{c_1})z + (|c_1|^2 - r_1^2 - c_1\bar{c_2})}.$$

This allows us to state:

Lemma 2.30
The generators of a symmetric Schottky group are hyperbolic.

[5]Burnside himself refers to Poincaré, but without any exact reference.

Proof. A Möbius transformation is hyperbolic if the "trace" is real and greater than 2 according to Lemma 2.4. Each of the generators can be written as two successive reflections. Without loss of generality, we denote them by s_1 and s_2. The trace of $s_2 \circ s_1$ is (according to the previous lemma) of the form

$$a + d = \frac{(|c_2|^2 - r_2^2 - \bar{c}_1 c_2) + (|c_1|^2 - r_1^2 - c_1\bar{c}_2)}{r_1 r_2} = \frac{|c_1 - c_2|^2 - r_1^2 - r_2^2}{r_1 r_2} \in \mathbb{R}.$$

The denominator $r_1 r_2$ is necessary, as we need to ensure $ad - bc = 1$.
As the circles bounding the fundamental region of the Schottky group are not allowed to touch, we have

$$|c_1 - c_2| > r_1 + r_2$$

what leads to

$$a + d = \frac{|c_1 - c_2|^2 - r_1^2 - r_2^2}{r_1 r_2} > \frac{(r_1 + r_2)^2 - r_1^2 - r_2^2}{r_1 r_2} = 2.$$

□

While the statement above can easily be seen, there is a more general result.

Lemma 2.31 ([Mas88, p. 312])
Let G be a Schottky group, then G consists only of loxodromic and hyperbolic transformations.

As we will use the behavior of Schottky groups in the following chapters, we want to extend the common results by additional information. We will therefore introduce and justify some new notations.

Definition 2.32
For a Schottky group G, the extended generating set $\mathrm{gen}(G)$ *refers to the generating transformations of G and their inverses, i.e. the transformations $T_j^{\pm 1}$, where each $T_j^{\pm 1}$ maps one of the n circles pairs C_1, C_1', …, C_n, C_n' into each other:*

$$\mathrm{gen}(G) := \{T_1, \ldots, T_n, T_1^{-1}, \ldots, T_n^{-1}\}$$

To simplify the notation of the following lemmas and proofs, we will use

$$C_j^{+1} := C_j', \qquad C_j^{-1} := C_j, \qquad T_j^{+1} := T_j.$$

In this way, we are able to state that each

$$T_j^\alpha \in \mathrm{gen}(G) = \{T_j^\alpha \,|\, T_j^\alpha(C_j^{-\alpha}) = C_j^\alpha;\ j = 1, \ldots, n;\ \alpha \in \{-1, +1\}\}$$

maps the fundamental region into the circle C_j^α.
We will also shorten the notation of compositions by $TU = T \circ U$, since we want to write

the transformations of a Schottky group as a sequence of its (extended) generators. If in the following a transformation is split up by

$$U = U_1 \dots U_m,$$

it has to be read as

$$U = U_1 \dots U_m, \quad \text{where } U_j \in \text{gen}(G), U_{j+1} \neq U_j^{-1}, j = 1, \dots, m-1$$

if not stated otherwise. This will allow us to restrict our investigations of the mapping behavior of the group to the mapping behavior of the generating transformations.
One result regarding the position of a point $U(z)$ is:

Lemma 2.33
Let G be a Schottky group and the mapping $U = U_1 \dots U_m$ be an element of G, where $U_j \in \text{gen}(G) = \{T_1, \dots, T_n, T_1^{-1}, \dots, T_n^{-1}\}$ and $U_{j+1} \neq U_j^{-1}$.
Let further z be a point outside of $C_i^{-\eta}$ if $U_m = T_i^{\eta}$, $\eta \in \{-1, 1\}$.
Then the point $U(z)$ is inside the circle C_k^{ν} if and only if $U_1 = T_k^{\nu}$, $\nu \in \{-1, 1\}$.

Proof. By the definition of the Schottky group, T_i^{η} maps the exterior of $C_i^{-\eta}$ onto the interior of C_i^{η}. As a consequence, $U_m(z) = T_i^{\eta}(z)$ is in the interior of C_i^{η} if z is outside of $C_i^{-\eta}$.
Since no consecutive transformations are allowed to be inverse to each other, the "outside of" condition is automatically satisfied for the next transformation U_{m-1}. Therefore $U_{m-1}U_m(z)$ lies in C_l^{μ} for $U_{m-1} = T_l^{\mu}$.
Actually, T_l^{μ} is the only transformation which can move $U_m(z)$ into C_l^{μ}, as any other transformation would map $U_m(z)$ into its corresponding circle. The only exception would be $T_i^{-\eta}$, since it maps the interior of C_i^{η} onto the exterior of $C_i^{-\eta}$ and the interior of C_l^{μ} lies in the exterior of $C_i^{-\eta}$. However, $U_{m-1} = T_i^{-\eta}$ is prohibited by $U_{j+1} \neq U_j^{-1}$.
Successive applications of the remaining transformations yields the result. □

Note that the "outside of" condition in the lemma is satisfied if z lies in the fundamental region. Hence, we can expand the lemma above to the following one.

Lemma 2.34
Let G be a Schottky group and the mapping U be an element of G.
The factorization

$$U = U_1 \dots U_m,$$

where $U_j \in \text{gen}(G)$ and $U_{j+1} \neq U_j^{-1}$, is unique.

Proof. Let z_0 be a point of the fundamental region of G.
Suppose there are two different factorizations $U = U_1 \dots U_m = V_1 \dots V_\mu$. Hence, $W = U_m^{-1} \dots U_1^{-1} V_1 \dots V_\mu$ must be the identity. We rename the transformations of W to $W = W_1 \dots W_\nu$ after removing inverse pairs of transformations to ensure $W_j \neq W_{j+1}^{-1}$ for $j = 1, \dots, \nu - 1$. W does not vanish completely in this process, as the factorizations are different.
The transformation $W_2 \dots W_\nu$ has to map z_0 inside a circle C_k^α, i.e. outside of the fundamental region, or it is itself the identity. If $W_2 \dots W_\nu$ is the identity, so must W_1 also be the identity id $\notin \text{gen}(G)$, violating the condition $W_j \in \text{gen}(G)$.
Therefore $W_2 \dots W_\nu$ maps z_0 inside C_k^α, which means that according to Lemma 2.33 $W_2 = T_k^\alpha \in \text{gen}(G)$. Hence, W_1 has to map $(W_2 \dots W_\nu)(z_0)$ into the fundamental region. However, the only transformation with this property would be $T_k^{-\alpha}$, which is not allowed by the condition $W_j \neq W_{j+1}^{-1}$. This leaves us with no possible choice for W_1.

As either way leads to a contradiction, the assumption must be false, which proofs the lemma. □

While we do not want to introduce too many terms of group theory, there is a fact worth noticing: The uniqueness of the factorization is equivalent to the property that the Schottky group is free. Because this property is true for all Schottky groups [Mas88, p. 312], the proof above is actually redundant.
Nonetheless, uniqueness allows us to define a useful size for the transformations of a Schottky group.

Definition 2.35
Let G be a Schottky group and the mapping U be an element of G.
The length of a transformation U is defined by the number of generating transformations necessary to compose it

$$|U| = |U_1 \dots U_m| = m,$$

where $U_j \in \text{gen}(G)$ and $U_{j+1} \neq U_j^{-1}$ for $j = 1, \dots, m-1$. The length of the identity is zero, i.e. $|id| := 0$.

The set $\text{gen}(G)$ can be seen as the transformations with length one

$$\text{gen}(G) = \{\, T \mid T \in G;\ |T| = 1\}.$$

The same property, but with an alternative definition, is called the grade of a transformation in [Aka64].

We want to continue our investigations by shifting our focus to the limit points of the group. It is known that the images of the fundamental region cluster around the limit points, but we are able to better specify this behavior in the context of Schottky groups.

Lemma 2.36
Let G be a Schottky group and D its fundamental region. Let further l be a fixed point of $T \in G$, where $|T^2| = 2|T|$, and $G_T \subset G$ a set containing transformations $U \in G$, where $|T| < |U|$, that does not begin with neither T nor T^{-1}, i.e. $|T^{-1}U| > |U| - |T|$ and $|TU| > |U| - |T|$.
The distance $|U(z) - l|$, where $z \in D$ and $U(z) \neq \infty$, has a common lower boundary for all $U \in G_T$.

Proof. The domain $T(D)$ is bounded by the circles $T(C_j^\alpha)$, as they are the mappings of the boundary of D. The mappings of D, which lie near to $T(D)$ are $T(W(D))$, where $W \in \text{gen}(G)$, as they have one boundary component in common because of $W_j^\alpha(C_j^{-\alpha}) = C_j^\alpha$. The domain enclosing $T(D)$ is the one with the shortest transformation, i.e. $|TW| < |T|$, what implies for $T = T_1 \dots T_m$ that $W = T_m^{-1}$.
Therefore, each of the holes of $T(D)$ contains one of the domains $T(W(D))$ with the exception of $W = T_m^{-1}$. In this manner, we can reach the domains inside the holes of each $T(W(D))$, by applying further transformations, and so the convex hull $\text{ch}(T(D))$ of $T(D)$ contains all the domains $T(V(D))$, where $V \in G$ and $V_1 \neq T_m^{-1}$, while all other mappings of D must be outside. Additionally, the condition $|T^2| = 2|T|$ implies that $T_1 \neq T_m^{-1}$, and so $T^{n+1}(D) \subset \text{ch}(T^n(D))$.
If l is the attractive fixed point of T, we have

$$\lim_{n\to\infty} T^n(z) = l, \qquad z \in D. \tag{2.5}$$

This means that every neighborhood of l contains points that lie in the interior complement $ch(T(T_1(D)))$ of $T(D)$, and so l has also to be in this complement.
If U does not begin with T, $U(z)$ $(z \in D)$ lies in a domain outside of the convex hull of $T(D)$, while l lies inside of it. Therefore, $|U(z) - l| > \varepsilon$ has a positive lower boundary. Repeating the steps above for T^{-1} and its attractive fixed point (the repelling fixed point of T) yields the result. □

If we investigate the movement of a limit point l under transformations of the group, we get:

Lemma 2.37
The points congruent to a fixed point l of a transformation $T \in G$ of a non-elementary Schottky group G with respect to the group G form a proper subset of the limit set. This subset is given by the fixed points of the transformations UTU^{-1}, where $U \in G$.

Proof. According to Lemma 2.25, $l = T(l)$ is an element of Λ. Hence, each point congruent to l is also an element of Λ. If l is mapped by $V \in G$, we have

$$(VTV^{-1})(V(l)) = (VT)(l) = V(l).$$

This means $V(l)$ is a fixed point of $VTV^{-1} \in G$ and $\{V(l) \,|\, T(l) = l,\, V \in G\} \subset \Lambda$.

If we want to show that $\{V(l) \,|\, T(l) = l,\, V \in G\}$ is a proper subset of Λ, it is enough to prove that the only transformations in G with coinciding fixed points are the powers T^n, $n \in \mathbb{Z} \setminus \{0\}$, of the same transformation T. Hence, there are transformations whose fixed points we can not reach. Note that two transformations of the group can not have only one fixed point in common. Maskit [Mas88, I.D.4] stated that if T has exactly two fixed points and T and U share exactly one fixed point, then $TUT^{-1}U^{-1}$ is parabolic. However, as $TUT^{-1}U^{-1} \in G$ this would contradict Lemma 2.31.
Suppose $T, U \in G$ have the same fixed points, where $T^\alpha \neq X^\beta \neq U^\gamma$ for any combination $\alpha, \beta, \gamma \in \mathbb{N}$ and any $X \in G$, and $|T| = n$, $|U| = m$. Further suppose that they are normalized so that $U_1 \neq U_m^{-1}$, as this allows to conclude that $|U^\gamma| = \gamma|U|$. Otherwise replace $U = \hat{V}\hat{U}\hat{V}^{-1}$ by $\hat{U}$ and T by $\hat{V}^{-1}T\hat{V}$. Let l be the common attractive fixed point and $\hat{l}$ the common repelling fixed point, or else we have to interchange T and/or U with their inverses.
Following the proof of Lemma 2.36, l lies in $\mathrm{ch}(T_1(D))$ as every neighborhood of l contains infinitely many domains $T^j(D)$ that are subsets of $\mathrm{ch}(T_1(D))$. However, l is also in $\mathrm{ch}(U_1(D))$ and we can conclude that $U_1 = T_1$ as $U_1, T_1 \in \mathrm{gen}(G)$. By investigating the location of $\hat{l}$, we obtain $U_m^{-1} = T_n^{-1}$. We can conclude from $U_1 \neq U_m^{-1}$ that also $T_1 \neq T_n^{-1}$. Hence, we have $l \in \mathrm{ch}(T^\alpha(D))$ and $l \in \mathrm{ch}(U^\beta(D))$ for all $\alpha, \beta \in \mathbb{N}$.
The domains $T^{m+2}(D)$ and $U^{n+2}(D)$ are inside $\mathrm{ch}(T^{m+1}(D))$ as they lie in a neighborhood of l and the transformations T^{m+2} and U^{n+2} are of greater length than T^{m+1}. Hence, they have the same starting sequence of transformations of $\mathrm{gen}(G)$, and so $T^m = U^n$, where $|T^m| = |U^n| = nm$. The comparison of both forms yields $T^m = (X^{\frac{n}{k}})^m = (X^{\frac{m}{k}})^n = U^n$ for $|X| = k = \gcd(n, m)$ and $X \in G$. However, this leads to a contradiction. □

2.5 Poincaré Theta Series

In the context of Kleinian groups, there is a special type of functions called the Poincaré theta series. A Poincaré theta series is defined by a sum over all transformations of the group.

Definition 2.38
Let G be a properly discontinuous group of Möbius transformations and $R(z)$ a rational function, none of whose poles is at a limit point of the group. The series

$$\theta(z) := \sum_{T \in G} T'(z)^\nu R(T(z)), \qquad \nu \in \mathbb{N}, \tag{2.6}$$

over all transformations of the group is called the theta series of Poincaré.

The series is also often referred to as the "Poincaré series" to avoid confusion with other theta series.

The most interesting feature of the theta series is its functional equation:

Lemma 2.39 ([For51, p. 103])
Every Poincaré theta series θ for the group G has the property

$$\theta(T(z)) = T'(z)^{-\nu}\theta(z)$$

for every transformation $T \in G$ of the group.

Proof. Calculation yields

$$\begin{aligned}\theta(T(z)) &= \sum_{U\in G} U'(T(z))^{\nu}\, R(U(T(z))) \\ &= T'(z)^{-\nu} \sum_{V\in G} V(z)^{\nu}\, R(V(z)) = T'(z)^{-\nu}\theta(z).\end{aligned}$$

The operations above are allowed as $V = U \circ T$ is also a transformation of the group and the order of summation can be changed since we have absolute convergence, as it can be seen below. □

As with most series, convergence is a great issue. The convergence of the theta series is ensured by the following lemma:

Lemma 2.40 ([For51, p. 105])
If $\nu \geq 2$ and if the point at infinity is an ordinary point of the group, then the theta series (2.6) defines a function which is analytic except possibly for poles in any connected region not containing limit points of the group in its interior.

Proof. While a full proof can be found in [For51], we only want to state the basic idea. If we stay away from the poles of R, their congruent points and the centers of the isometric circles, the function $R(T(z))$ is bounded by

$$|R(T(z))| < m_1.$$

The derivatives of the transformations on the other hand are decreasing with $|c|^{-2}$ as we have

$$|T'(z)| = \left|\frac{1}{(cz+d)^2}\right| = \left|c^{-2}\right| \left|\left(z + \frac{d}{c}\right)^{-2}\right| < |c|^{-2} m_2.$$

Note that $-\frac{d}{c}$ tends to one of the limit points, while $|c|$ goes to infinity. Combining

these information gives

$$\left|\sum_{T\in G} T'(z)^\nu R(T(z))\right| < \sum_{T\in G} |c|^{-2\nu} m_2^\nu m_1.$$

Hence, the theta series converges as stated in the lemma for $\nu \geq 2$ if

$$\sum_{T\in G} |c|^{-4} < \infty.$$

□

The proof above requires the convergence of the sum $\sum |c|^{-4}$. Therefore we also need the following lemma to ensure the convergence of the Poincaré series.

Lemma 2.41 ([For51, p. 104])
If the point at infinity is an ordinary point of the group G, then the series $\sum_{T\in G} |c|^{-2n}$ converges for $n \geq 2$, while in the summation the finite number of terms for which $c = 0$ are omitted.

Note that the values $|c|^{-1}$ represent the radii of the isometric circles (Definition 2.5), which are shrinking by Lemma 2.22. Also we expect the finite subset of transformations with $c = 0$ to be omitted for every sum $\sum_{T\in G} |c|^{-k}$, even if it is not stated explicitly.[6]

One may wonder, why the limit points of the group are prohibited as possible poles of R. This is because otherwise $R(T(z))$ can be unbounded for transformations T with a great length, i.e. $|T| \to \infty$. We want to specify this behavior by the following lemma found by us.

Lemma 2.42
Let G be a Kleinian group, $\infty \notin \Lambda$, $l \in \Lambda$, and M a closed subset of $\mathbb{C}_\infty \setminus \Lambda$.
There is a common constant $m > 0$ for all $T \in G$ with a coefficient $c \neq 0$, where $T(z) = (az + b)/(cz + d)$, so that

$$|c|^{-2} m < |T(z) - l|, \qquad z \in M.$$

If l is an attractive fixed point of $T \in G$, let $G_T = \{\, T^n \,|\, n \in \mathbb{N}, c_n \neq 0 \,\} \subset G$ denote the subset containing the powers $T^n(z) = (a_n z + b_n)/(c_n z + d_n)$ of T and let $\tilde{M}$ be a closed subset of $\mathbb{C}_\infty \setminus (\Lambda \cup \{\, U^{-1}(\infty) \,|\, U \in G_T \,\})$. There are two constants $m_u > m_l > 0$, so that

$$|c_n|^{-2} m_l < |T^n(z) - l| < |c_n|^{-2} m_u, \qquad z \in \tilde{M}. \tag{2.7}$$

[6] If there are infinitely many transformations with $c = 0$, then infinity is a limit point of the group. If G is a Schottky group and infinity an ordinary point, the only transformation with $c = 0$ is the identity.

Proof. Calculation yields

$$T(z) - l = T(z) - T(l') = \frac{z - l'}{c^2(z + \frac{d}{c})(l' + \frac{d}{c})} = \frac{z - l'}{c^2(z - u)(l' - u)},$$

where $u = -\frac{d}{c}$ is the center of the isometric circle of T. Since $\infty \notin \Lambda$, there is a circle around infinity containing neither limit points nor centers of isometric circles. Hence, we have $|l' - u| < \varepsilon_1$ and $0 < \varepsilon_2 < |z - l'|/|z - u|$ for all $z \in M$, $l' \in \Lambda$ and $T \in G$. We therefore find

$$|T(z) - l| = |c|^{-2} \left| \frac{z - l}{(z - u)(l - u)} \right| > |c|^{-2} m.$$

If l is an attractive fixed point of T, $l' = l$. As $u_n = -\frac{d_n}{c_n}$ approaches the repelling fixed point of T we find $|l - u_n| > \varepsilon_3 > 0$ and since $|T^n(z)| < \infty$, we also have $|z - u_n| > \varepsilon_4 > 0$. Hence, we have

$$m_l < \left| \frac{z - l}{(z - u_n)(l - u_n)} \right| < m_u.$$

□

The summands $R(T(z))$ of a Poincaré series can be unbounded for $|T| \to \infty$ according to equation (2.7) if R contains a pole at a limit point. However, the convergence of the Poincaré series depends on the fact that $R(T(z))$ is bounded, and therefore poles at limit points are excluded in the definition of the Poincaré theta series.
To investigate the case where the rational function R has a pole at a limit point, we introduce a *modified Poincaré theta series* by dropping the restriction of Definition 2.38 prohibiting these poles. To show the convergence of this modified series, we found an adapted version of the convergence Lemma 2.40:

Lemma 2.43
Suppose exactly one of the poles of the rational function R of the (modified) Poincaré theta series is at a limit point of the group and of order $k \in \mathbb{N}$.
If $\nu - k \geq 2$ and if the point at infinity is an ordinary point of the group, then the theta series defines a function which is analytic except possibly for poles in any connected region not containing limit points of the group in its interior.

Proof. The concept of the proof is similar to the preceding version for the classical Poincaré series [For51, p. 105]. However, this time we need Lemma 2.42 to find an upper bound for $R(T(z))$

$$|R(T(z))| < |T(z) - l|^{-k} m_1 < |c|^{2k} m_2.$$

The new bound leads to

$$\left|\sum_{T\in G} T'(z)^\nu R(T(z))\right| < \sum_{T\in G} |c|^{-2\nu}|c|^{2k} m_3 = m_3 \sum_{T\in G} |c|^{-2(\nu-k)}.$$

The sum $\sum_{T\in G} |c|^{-2(\nu-k)}$ converges if $\nu - k \geq 2$ according to Lemma 2.41. □

For Poincaré series with a rational function R containing several poles at limit points, we have to split up R by partial fraction expansion to generate several Poincaré series. Then we can apply the lemma to each of them.
In the following, we will not distinguish between the Poincaré theta series and its modified version. A given series can be classified by investigating the poles of the rational function R.

In some special cases, a Kleinian group permits the stronger convergence property $\sum |c|^{-2} < \infty$.[7] In the following, we list some scenarios regarding the convergence of $\sum |c|^{-2}$.

Lemma 2.44 ([For51, p. 106])
For a Fuchsian group G of the second kind[8]*, for which the point at infinity is an ordinary point, the sum $\sum_{T\in G} |c|^{-2}$ converges.*

The lemma above is stated in [For51], where [Bur91] is referred.

Lemma 2.45 ([Sch87])
Let G be a Schottky group, whose fundamental domain is bounded by the $2n$ circles C_1, C_1',...,C_n, C_n'.
The sum $\sum_{T\in G} |c|^{-2}$ converges if it is possible to separate D into a sequence of triply connected domains by adding circles C_j'' that are disjoint with each other and the circles C_k and C_l'.

The original lemma by Schottky stated the convergence of the radii of the circles $T(C_j)$ and $T(C_j')$ instead of the convergence of the sum $\sum |c|^{-2}$. However, the convergences of the sum of the radii and of $\sum |c|^{-2}$ are equivalent. If we denote with $r_{j,T}$ the radius of $T(C_j)$, there is the following lemma. (Note that C_j' can be written as $T(C_j)$ for a suitable T.)

[7] Burnside stated the conjecture that this is always possible for Schottky groups, but it was later disproved by Myrberg. See [Aka64] for references.

[8] A Fuchsian group of the second kind has the property that the limit set is nowhere dense on the common fixed circle of the transformations.

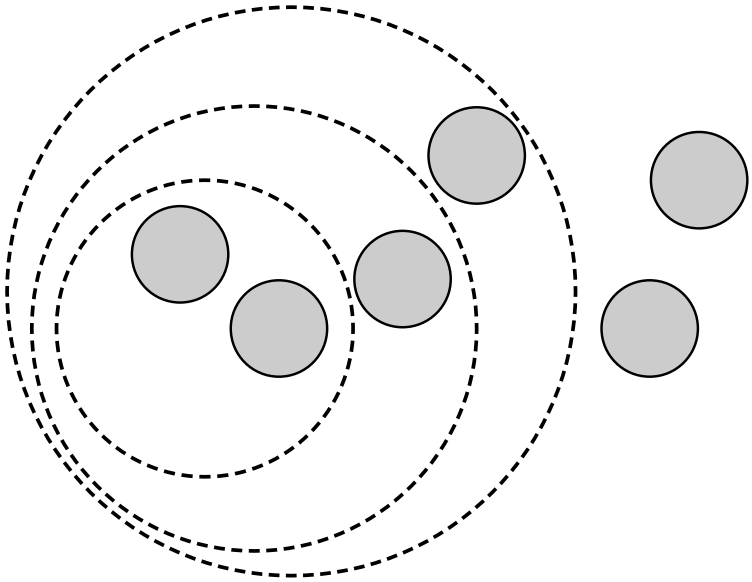

Figure 10: The fundamental domain of the Schottky group bounded by the 6 gray-filled circles can be separated into a sequence of triply connected domains by the dashed circles.

Lemma 2.46 ([Aka64])
Let G be a Schottky group, whose fundamental domain is bounded by the $2n$ circles C_1, C_1',...,C_n, C_n'. Let further $r_{j,T}$ be the radius of $T(C_j)$, where $T \in G$, and $\nu \in \mathbb{N}$.
The series $\sum_{T \in G} |c|^{-\nu}$ converges if and only if $\sum_{T \in G} \sum_{j=1}^{n} (r_{j,T})^{\nu/2}$ converges.

Hence, the convergence of the sum over the radii is equivalent to the convergence of the sum $\sum |c|^{-2}$.

There is also a connection between the convergence of $\sum |c|^{-2\nu}$ and the Hausdorff dimension of the limit set of the group. This topic and some additional conditions for the convergence of $\sum |c|^{-2}$ can be found in the works of Akaza e.g. [Aka64].

3 Simply Connected Circular Arc Polygon Domains

We wish to investigate conformal mappings from the unit disk onto simply connected circular arc polygon domains (Figure 11). This conformal mappings were first investigated by Schwarz in 1869 [Sch69], but still contain some open questions.

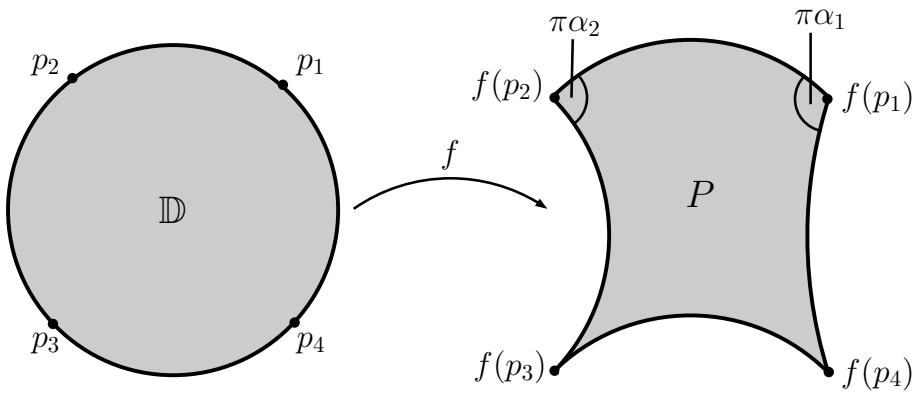

Figure 11: The unit disk is conformally mapped onto a simply connected circular arc polygon domain. The points p_j on the boundary of the unit disk represent the preimages of the vertices of the CAP.

Before we investigate the mappings itself, we define the term "circular arc polygon domain".

Definition 3.1
A circular arc polygon (CAP) is a closed curve $\delta : [0,1] \to \mathbb{C}$ that is a continuous union of finitely many circular arcs and line segments. Hence, there is a finite partition $0 = t_1 < t_2 < \ldots < t_{n+1} = 1$, where $n \geq 2$ and $n \in \mathbb{N}$, of the interval $[0,1]$ such that each interval $[t_k, t_{k+1}]$ for $k = 1, \ldots, n$ is mapped onto a circular arc or line segment. A circular arc polygon domain (CAPD) is a finitely connected domain whose boundary components are circular arc polygons.

Not every circular arc polygon is suitable to be a boundary component of a circular arc polygon domain. Some of them are only able to be a boundary component of a domain if the domain is a subset of a specific component of their complement (Figure 12). For example, a self-intersecting curve can not be the outer boundary of a connected domain. The circular arc polygons that can bound a domain are either simple closed curves, simple arcs[9] or a finite union of these types like a simple curve with an attached arc.
Since we will use the circular arc polygons as boundary components, we suppose for

[9]The term "arc" refers here to a simple not-closed curve. The curve is no longer simple if it is reparametrized to be closed.

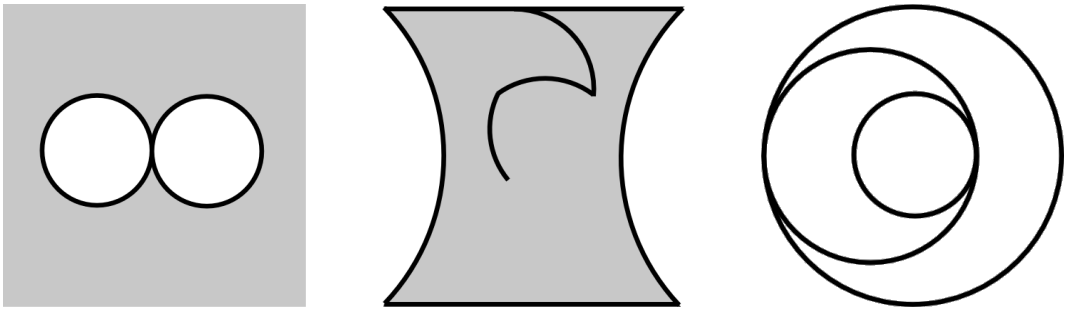

(a) An unbounded CAPD, which is bounded by a self-intersecting CAP.

(b) A CAP containing an arc bounds a bounded CAPD.

(c) A CAP that self-intersects twice can not be a boundary component of a CAPD.

Figure 12: Some CAPs can only be an outer boundary component (figure part (a)) or an inner boundary component (figure part (b)) of a CAPD. Some CAPs can not be a boundary component of a CAPD at all (figure part (c)).

the following investigations that all circular arc polygons are able to bound a domain at least in the required component of their complement. Therefore, it depends on the

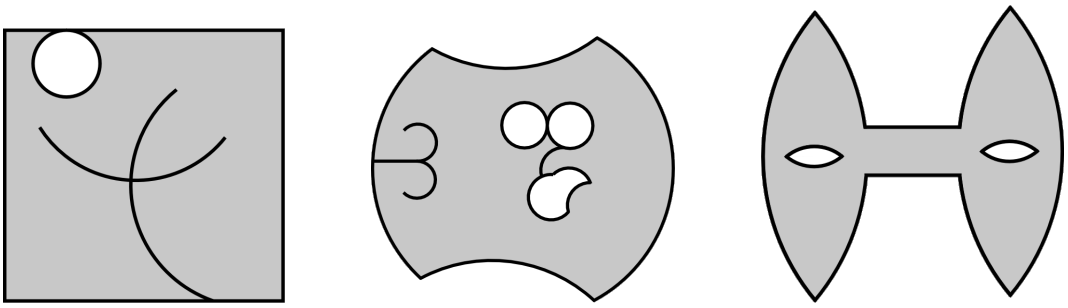

(a) connectivity one

(b) connectivity two

(c) connectivity three

Figure 13: CAPDs can have various shapes and different connectivity.

currently examined domain if a CAP is suitable for our discussion.
Hence, an alternative approach for the definition is to define a circular arc polygon domain as a finitely connected domain bounded by finite unions of circular arcs and to define the set of all circular arc polygons as the set of the boundary components of all circular arc polygon domains.

We also suppose the circular arc polygons to be parametrized in a way that the domain is to the left. Hence, we will interpret a slit to have two sides, as it is (part of) a closed curve. This allows us to define the *vertices* of the boundary as the points $v_k = \delta(t_k)$, $k = 1, \ldots, n$, with the values t_k of the partition $0 = t_1 < t_2 < \ldots < t_{n+1} = 1$, as defined

in Definition 3.1.[10] The interior angle $\pi\alpha$ at such a vertex is the angle between the two consecutive circular arcs measured inside the domain.
From this point on, we will no longer explicitly refer to line segments, as they can be seen as parts of circles that run through infinity.

Note that each conformal mapping onto a circular arc polygon domain can be continuously extended to the boundary, as each boundary component, i.e. circular arc polygon, is locally connected. [Con95, Theorem 15.3.5]

For now, we will focus on the conformal mappings of the unit disk onto simply connected circular arc polygon domains. Conformal mappings onto multiply connected circular arc polygon domains are handled in Chapter 4. Hence, the boundary of a CAPD is at the moment defined by one CAP, which is the union of n circular arcs. This CAP has n vertices v_k and n interior angles $\pi\alpha_k$.

3.1 The Schwarzian Derivative of the Mappings

We wish to investigate conformal mappings of the unit disk onto simply connected circular arc polygon domains. The common[11] mapping formula for these mappings is always given in the form of their Schwarzian derivative. We want to justify this fact, before we continue by actually stating the formula.

A circular arc polygon consists by definition only of circular arcs, and so any conformal transformation, which maps circles onto circles will map a CAPD onto a CAPD with the same interior angles at each vertex. The most general transformation doing this is a Möbius transformation. Hence, for a function f, which conformally maps the unit disk onto a CAPD, we can get new mappings $T \circ f$ onto CAPDs by applying a Möbius transformation $T \in \mathbb{M}$. All the images of these functions $T \circ f$ can be conformally mapped onto each other by Möbius transformations.
To get a unique form for all these mappings, we need to remove the Möbius transformations. This can be done by the application of the Schwarzian derivative, since we have

$$\{T \circ f, z\} = \{f, z\}.$$

Therefore only the Schwarzian is given for these mappings, while the actual mappings $T \circ f$ can be gathered by solving the Schwarzian. The three complex initial values of the Schwarzian correspond to the three complex degrees of freedom of the Möbius transformations.

An alternative approach is to extend such a mapping over a bounding circular arc by the Schwarz reflection principle. The extension itself is a mapping from the plane minus the closed unit disk onto a reflected version of the CAPD. If the Schwarz reflection principle

[10] As we do not demand consecutive circular arcs to be from different circles, one may add "artificial" vertices by splitting an arc.

[11] The Schwarzian derivatives of these mappings are equal, except for the values of the parameters.

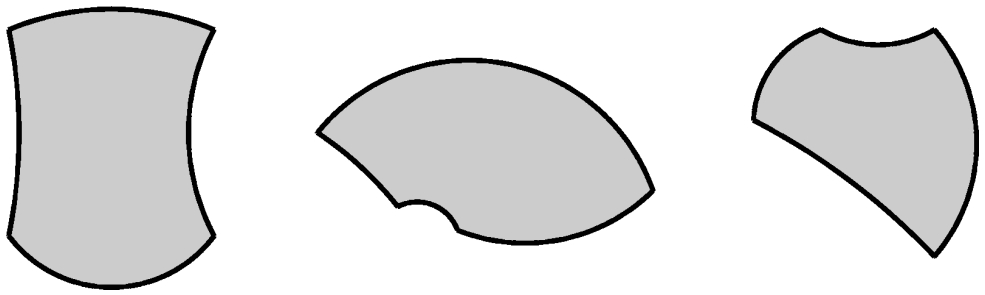

Figure 14: The three circular arc polygon domains shown above can be mapped onto each other by Möbius transformations.

is applied again but on the extension and for a different arc, we get a mapping of the unit disk onto a twice reflected version of the CAPD. However, two successive reflections are equal to a Möbius transformation, and so two extensions lead to a mapping from the unit disk onto a Möbius transformed version of the CAPD (Figure 15). A common mapping formula for both image domains can be gathered by applying the Schwarzian derivative.

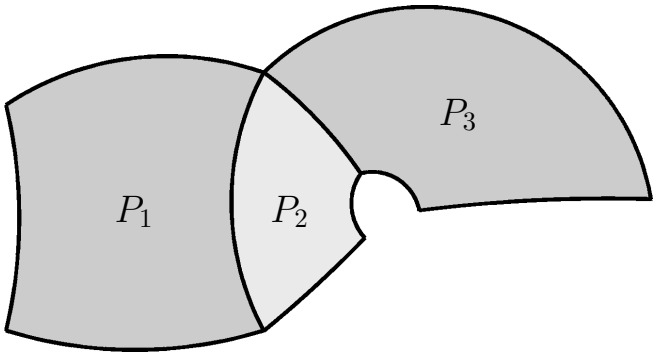

Figure 15: The circular arc polygon domain P_1 (left dark region) is reflected against one of its bounding circular arcs onto P_2 (middle pale region). The reflected domain P_2 is then also reflected against its boundary onto P_3 (right dark region). The two dark regions P_1 and P_3 differ only by a Möbius transformation.

The common form of conformal mappings from the upper half plane onto circular arc polygon domains can be found in most of the standard literature covering the topics of conformal mappings such as [Neh52, Chapter 5][12] or [Hil62]. We will refer here to the core literature regarding all information related to (simply connected) Schwarz-Christoffel-mappings:

[12]Nehari refers to circular arc polygons as curvilinear polygons.

Lemma 3.2 ([DT02, Chapter 4.10])
Let P be a simply connected circular arc polygon domain bounded by a circular arc polygon with vertices $v_1,\dots,v_n$ and interior angles $\alpha_1\pi,\dots,\alpha_n\pi$.
The Schwarzian derivative $\{f,z\}$ of any conformal mapping f of the upper half plane onto P has the form

$$\{f,z\} = \frac{1}{2}\sum_{k=1}^{n}\frac{1-\alpha_k^2}{(z-p_k)^2} + \sum_{k=1}^{n}\frac{\gamma_k}{(z-p_k)},$$

where $f(p_k) = v_k$ for $k = 1,\dots,n$. The parameters have to satisfy the constraints:

$$\sum_{k=1}^{n}\gamma_k = \sum_{k=1}^{n}(2\gamma_k p_k + (1-\alpha_k^2)) = \sum_{k=1}^{n}(\gamma_k p_k^2 + (1-\alpha_k^2)p_k) = 0.$$

Often it is just indicated that the mappings from the unit disk can be acquired by using $\{f\circ T, z\} = T'(z)^2\{f, T(z)\}$. In this case, T is the Möbius transformation, which maps the unit disk onto the upper half plane. A version for mappings from the unit disk onto CAPDs without use of the upper half plane can be found in an article of Porter:

Lemma 3.3 ([Por05])
Let P be a simply connected circular arc polygon domain bounded by a circular arc polygon with vertices $v_1,\dots,v_n$ and interior angles $\alpha_1\pi,\dots,\alpha_n\pi$.
The Schwarzian derivative $\{f,z\}$ of any conformal mapping f of the unit disk onto P has the form

$$\{f,z\} = \sum_{k=1}^{n}\frac{1}{p_k}\left(\frac{2p_k - z}{(z-p_k)^2}a_k + \frac{2ir_k}{(z-p_k)}\right),$$

where $f(p_k) = v_k$, $a_k = \frac{1}{2}(1-\alpha_k)^2$ and $r_k \in \mathbb{R}$ for $k = 1,\dots,n$. The parameters have to satisfy the constraints:

$$\sum_{k=1}^{n} r_k = \sum_{k=1}^{n} p_k(a_k + 2ir_k) = 0.$$

We will present our own version of the conformal mappings from the unit disk onto CAPDs. The result is equal to the one of Porter, but the proof uses a different method. The concept of the following proof is similar to the one we will use in the later sections for multiply connected mappings.
As we will refer very often to the Schwarzian derivative of conformal mappings onto CAPDs, we introduce a new symbol $\mathcal{S}(z) := \{f,z\}$ for it.

Theorem 3.4
Let P be a simply connected circular arc polygon domain bounded by a circular arc polygon with vertices $v_1,\ldots,v_n$ and interior angles $\alpha_1\pi,\ldots,\alpha_n\pi$.
The Schwarzian derivative $\mathcal{S}$ of any conformal mapping f of the unit disk onto P has the form

$$\mathcal{S}(z) = \{f, z\} = \sum_{k=1}^{n} \frac{1}{p_k} \left(\frac{2p_k - z}{(z-p_k)^2} a_k + \frac{i\mu_k}{(z-p_k)} \right),$$

where $f(p_k) = v_k$, $a_k = \frac{1}{2}(1-\alpha_k)^2$ and $\mu_k \in \mathbb{R}$ for $k = 1,\ldots,n$. The parameters have to satisfy the constraints:

$$\sum_{k=1}^{n} \mu_k = \sum_{k=1}^{n} p_k(a_k + i\mu_k) = 0. \tag{3.1}$$

Proof. The mapping function f has to behave at each vertex $v = f(p)$ like

$$f(z) = (z-p)^{\alpha}\psi(z),$$

where $\alpha\pi$ is the interior angle of the bounding CAP at v. In this equation ψ is an analytic function different from zero at p and represents the remaining part of f. As we apply the Schwarzian derivative to this, we obtain

$$\{f, z\} = \frac{a}{(z-p)^2} + \frac{\gamma}{(z-p)} + O((z-p)^0),$$

with the abbreviations

$$a := \frac{1}{2}(1-\alpha^2) \quad \text{and} \quad \gamma := \frac{\psi'(p)}{\psi(p)} \frac{(1-\alpha^2)}{\alpha}.$$

The preimage domain is bounded by $\partial\mathbb{D}$, while the image domain is bounded by arcs from the circles C_k. According to the Schwarz reflection principle, we can extend the mapping beyond its boundary by

$$f(s(z)) = s_k(f(z)),$$

with $s(z) = \frac{1}{\bar{z}}$ being the reflection against the unit circle and $s_k(z) = \frac{r_k^2}{\bar{z}-\bar{c_k}} + c_k$ being a reflection against one of the circles C_k in the image domain. Applying the Schwarzian to this equation yields

$$\{f, z\} = \frac{1}{z^4}\overline{\{f, \frac{1}{\bar{z}}\}}. \tag{3.2}$$

The application of the Schwarzian also combines the different extensions to one form as they only differ by Möbius transformations.

The Schwarzian does not contain any poles in $\mathbb{D}$ as the initial function f is conformal. Neither does its extension $\mathbb{C}_\infty \setminus \overline{\mathbb{D}}$ contain any poles. Hence, the only poles in $\mathbb{C}_\infty$ can be at the prevertices $p_k \in \partial\mathbb{D}$. This allows us to write:

$$\mathcal{S}(z) = \sum_{k=1}^{n} \left(\frac{a_k}{(z-p_k)^2} + \frac{\gamma_k}{(z-p_k)} \right) + \kappa, \qquad \kappa \in \mathbb{C}.$$

Putting this result in (3.2) yields with $\overline{p_k} = p_k^{-1}$

$$\begin{aligned} 0 &= \frac{1}{z^4}\overline{\mathcal{S}\left(\frac{1}{\bar{z}}\right)} - \mathcal{S}(z) \\ &= \sum_{k=1}^{n} \left(\frac{-\overline{p_k(\gamma_k p_k + 2a_k)} - \gamma_k}{(z-p_k)} + \frac{\overline{p_k(\gamma_k p_k + 2a_k)}}{z} + \frac{\overline{\gamma_k p_k + a_k}}{z^2} + \frac{\overline{\gamma_k}}{z^3} \right) - \kappa + \frac{\bar{\kappa}}{z^4}. \end{aligned}$$

This gives immediately the conditions

$$\sum_{k=1}^{n} \gamma_k = \sum_{k=1}^{n} (\gamma_k p_k + a_k) = \sum_{k=1}^{n} p_k(\gamma_k p_k + 2a_k) = \kappa = 0, \tag{3.3}$$

$$-\overline{p_k(\gamma_k p_k + 2a_k)} - \gamma_k = 0. \tag{3.4}$$

The second line can be altered to

$$-\overline{\gamma_k p_k + a_k} = \gamma_k p_k + a_k \iff \operatorname{Re}(\gamma_k p_k + a_k) = 0.$$

Substituting for

$$i\mu_k := \gamma_k p_k + a_k, \qquad \mu_k \in \mathbb{R},$$

ensures equation (3.4) and allows the Schwarzian in the form

$$\mathcal{S}(z) = \sum_{k=1}^{n} \frac{1}{p_k} \left(\frac{2p_k - z}{(z-p_k)^2} a_k + \frac{i\mu_k}{(z-p_k)} \right)$$

while equation (3.3) changes to

$$\sum_{k=1}^{n} \mu_k = \sum_{k=1}^{n} p_k(a_k + i\mu_k) = 0.$$

□

3.1.1 The Parameter Problem

All kinds of mappings similar to the Schwarz-Christoffel (SC) mapping are connected to some kind of parameter problem, i.e. the search for the correct values of the parameters of the mapping formula, if a specific image domain is given.

In the CAPD case, each vertex of the image domain generates one interior angle, one prevertex and one parameter γ or μ (depending on the form) in the Schwarzian. While the significance of the prevertices as preimages of the vertices and the interior angles is clear, the additional parameters γ/μ do not yet have any geometric interpretation. It might be reasonable to assume a connection to the curvature of the boundary arcs, as this is the main difference in comparison to the classical SC mapping. This connection could for example be something like the change of curvature at the corresponding vertices. The position of the prevertices and the interior angles may also influence these values.
Research regarding these parameters was done especially by Porter, e.g. in [Por05] and [PK09]. Both articles cover CAPDs with special geometric properties.
An interesting information about the behavior of γ can be drawn from the work of Porter. The parameters γ of two prevertices tend to infinity in their absolute values as the prevertices become closer.
The following work tries to cover some further special cases of CAPDs and to draw conclusions regarding γ. We will see that the property of a growing γ will also appear several times.

3.2 Moving the Conformal Center

One possible way to investigate the behavior of the parameters μ of the Schwarzian is to apply an automorphism of the unit disk and observe how the μ change.
If we apply the automorphism A, before we map $\mathbb{D}$ by f onto a CAPD, the composition $f \circ A$, must also have a Schwarzian matching the formula stated in Theorem 3.4.
The automorphisms of the unit disk are of the form

$$A(z) = e^{i\varphi}\frac{z-v}{1-\bar{v}z}, \qquad \varphi \in [0, 2\pi[\,,\ v \in \mathbb{D}.$$

First, we only apply a rotation of $\mathbb{D}$ in the form $R(z) = e^{i\varphi}z = \lambda z$. By the properties of the Schwarzian derivative (Lemma 2.10), we have for any Möbius transformation T

$$\{f \circ T, z\} = T'(z)^2\{f, T(z)\}.$$

For a rotation, where $p_k = R(q_k) = \lambda q_k$, we therefore have

$$\begin{aligned}\{f \circ R, z\} = R'(z)^2\{f, R(z)\} &= \lambda^2 \sum_{k=1}^{n} \frac{1}{p_k}\left(\frac{2p_k - \lambda z}{(\lambda z - p_k)^2}a_k + \frac{i\mu_k}{(\lambda z - p_k)}\right) \\ &= \sum_{k=1}^{n} \frac{1}{q_k}\left(\frac{2q_k - z}{(z - q_k)^2}a_k + \frac{i\mu_k}{(z - q_k)}\right).\end{aligned} \tag{3.5}$$

This shows that μ is invariant against rotations of $\mathbb{D}$.[13] Therefore it is enough to investigate automorphisms of the form

$$A(z) = \frac{z-v}{1-\bar{v}z}, \qquad v \in]0, 1[$$

[13] Note that γ is not invariant against such rotations.

(Figure 16). Any other automorphism can be generated by applying a rotation R in the form

$$R^{-1} \circ A \circ R.$$

Retaining the new prevertices $q_k = A^{-1}(p_k)$ and the new parameters η_k, calculation yields a formula for the alternation of the parameters. Hence, we have found the connection

$$\begin{aligned} \eta_k &= \frac{|v + p_k|^2 \mu_k + 2v \operatorname{Im}(p_k) a}{1 - v^2} \\ &= \frac{(1 - v^2)\mu_k + 2v \operatorname{Im}(q_k) a}{|q_k - v|^2}. \end{aligned} \tag{3.6}$$

It is important to notice that since we apply A before f, we have $A(q_k) = p_k$ and

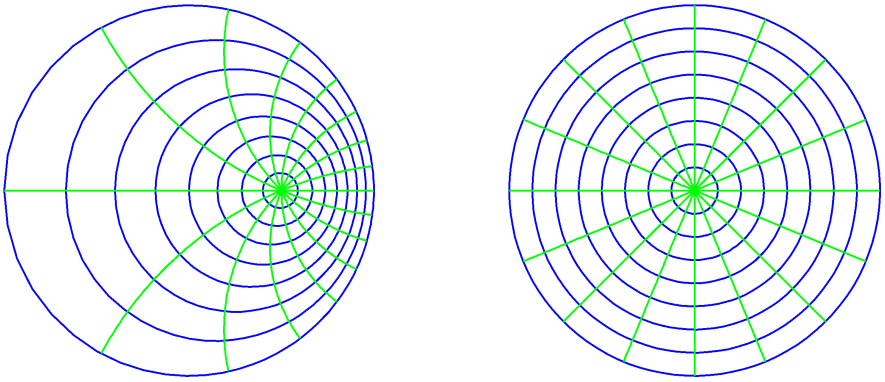

Figure 16: The mapping of the unit disk for an automorphism A, where $A(z) = (z - v)/(1 - \bar{v}z)$ and $v = \frac{1}{2}$. The left image contains the prevertices q, while the right contains the p. Hence, the mapping A^{-1} is from the right to the left domain.

therefore actually mapping p_k by

$$A^{-1}(z) = \frac{z + v}{1 + \bar{v}z}.$$

It can be verified by calculation that 1 is the attractive fixed point of A^{-1}, while -1 is the repelling fixed point for $v \in]0, 1[$.[14] If we therefore place a prevertex p_1 in 1 and another in $-1 = p_2$, we have

$$\begin{aligned} |\eta_1| &= \left| \frac{(v + 1)^2}{1 - v^2} \mu_1 \right| = \left| \frac{1 + v}{1 - v} \right| |\mu_1| > |\mu_1|, \\ |\eta_2| &= \left| \frac{(v - 1)^2}{1 - v^2} \mu_2 \right| = \left| \frac{1 - v}{1 + v} \right| |\mu_2| < |\mu_2| \end{aligned} \tag{3.7}$$

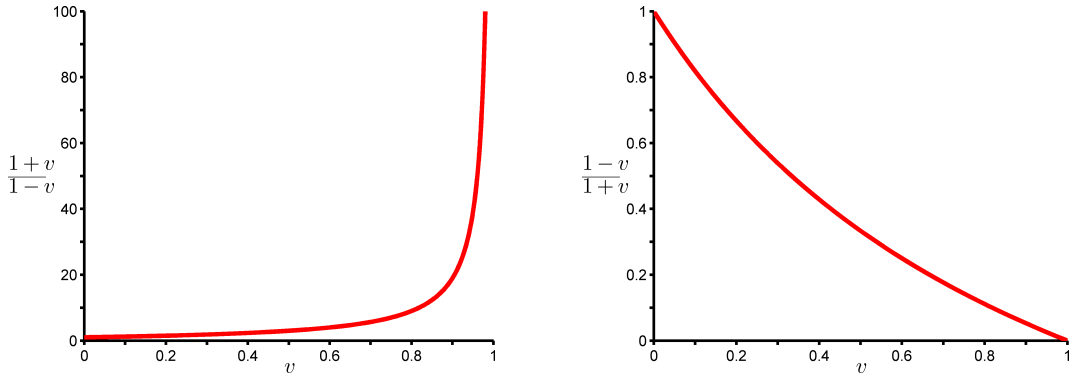

(a) The factor $\frac{1+v}{1-v}$ for $v \in (0,1)$.

(b) The factor $\frac{1-v}{1+v}$ for $v \in (0,1)$.

Figure 17: The behavior of the factors of equation (3.7) is shown above. The first factor (left image) rises to infinity while the second one (right image) tends to zero while v approaches 1.

for $\mu_1 \neq 0$ and $\mu_2 \neq 0$. The parameter is rising in absolute value for the attractive fixed point and shrinking for the repelling one. This effect increases if v gets closer to 1, i.e. the derivative at the attractive fixed point gets closer to zero.
In the case of only two prevertices, the parameters must both be zero to satisfy the restricting equations. For a greater number of prevertices, we can at least notice that the absolute values of the parameters are rising, if they are clustered together by an automorphism. The more they are clustered, the greater the growth of the parameters.

3.3 Comparison to the Schwarz-Christoffel Transformation

The classical Schwarz-Christoffel transformation is a special case of the conformal mappings onto CAPDs. The Schwarz-Christoffel transformation is, in comparison to the CAPD mapping, easier to handle, as a boundary consisting only of line segments permits less geometric variety. This is shown, for example, in the fact that in this context it is not necessary to use the Schwarzian derivative. Instead the simpler pre-Schwarzian $\frac{f''}{f'}$ is used. For the SC mapping, the pre-Schwarzian is of the form

$$S(z) = \frac{f''(z)}{f'(z)} = \sum_{k=1}^{n} \frac{\alpha_k - 1}{z - p_k}.$$

The p_k denote again the prevertices, while the α_k refer to the interior angles $\alpha_k \pi$. Usually the mapping is stated in the form:

[14] The transformation A^{-1} is hyperbolic and has therefore one attractive and one repelling fixed point.

Lemma 3.5 ([DT02])
Let P be the interior of a polygon having vertices $v_1, \ldots, v_n$ and interior angles $\alpha_1\pi, \ldots, \alpha_n\pi$ in counterclockwise order. Let f be any conformal map from the upper half-plane onto P. Then

$$f(z) = A + C \int^z \prod_{k=1}^{n} (\zeta - p_k)^{\alpha_k - 1} d\zeta$$

for some complex constants A and C, where $v_k = f(p_k)$ for $k = 1, \ldots, n$.

Here the classical form for the upper half plane is cited, but the version for the unit disk is equal[15] to the stated form and can for example also be found in [DT02].

To compare the SC mapping with the CAPD mapping, we have to calculate the Schwarzian from the pre-Schwarzian:

$$\begin{aligned}\mathcal{S}(z) &= \left(\frac{f''(z)}{f'(z)}\right)' - \frac{1}{2}\left(\frac{f''(z)}{f'(z)}\right)^2 = \left(\sum_{k=1}^{n} \frac{\alpha_k - 1}{z - p_k}\right)' - \frac{1}{2}\left(\sum_{k=1}^{n} \frac{\alpha_k - 1}{z - p_k}\right)^2 \\ &= \sum_{k=1}^{n} \frac{a_k}{(z - p_k)^2} - \sum_{k=1}^{n} \left(\sum_{j=1, j\neq k}^{n} \frac{(\alpha_j - 1)}{(p_k - p_j)}\right) \frac{(\alpha_k - 1)}{(z - p_k)}.\end{aligned}$$

Here a_k is again defined as

$$a_k := \frac{1}{2}(1 - \alpha_k^2).$$

It is interesting to note that the sum attached to the first order poles is nearly the pre-Schwarzian evaluated at p_k, except for the missing term for p_k. Hence, we define

$$S(z, p_k) := S(z) - \frac{\alpha_k - 1}{z - p_k} = \sum_{\substack{j=1 \\ j\neq k}}^{n} \frac{(\alpha_j - 1)}{(z - p_j)}$$

and rewrite the above to

$$\mathcal{S}(z) = \sum_{k=1}^{n} \left(\frac{a_k}{(z - p_k)^2} + \frac{-(\alpha_k - 1)S(p_k, p_k)}{(z - p_k)}\right).$$

By comparing this with the CAPD formula, we obtain

$$\gamma_k = -(\alpha_k - 1)S(p_k, p_k),$$

and with $i\mu_k = p_k\gamma_k + a_k$ we further have

$$\mu_k = i\left((\alpha_k - 1)p_k S(p_k, p_k) - \frac{1}{2}(1 - \alpha_k^2)\right).$$

[15] Normally the version for the unit disk is reshaped to avoid numerical issues regarding the logarithm.

By multiplying p_k into $S(p_k, p_k)$, terms in the form $\frac{p_k}{p_k - p_j}$ arise, which can be transformed with $p_k = e^{i\varphi_k}$ (since the prevertices are on $\partial\mathbb{D}$) to

$$\frac{p_k}{p_k - p_j} = \frac{1}{1 - \exp\left(i(\varphi_j - \varphi_k)\right)} = \frac{i}{2}\cot\frac{\varphi_j - \varphi_k}{2} + \frac{1}{2}.$$

This allows us to write μ in the form

$$\begin{aligned}\mu_k &= i\left((\alpha_k - 1)\sum_{j\neq k}(\alpha_j - 1)\left(\frac{i}{2}\cot\frac{\varphi_j - \varphi_k}{2} + \frac{1}{2}\right) - \frac{1}{2}(1 - \alpha_k^2)\right) \\ &= -\frac{(\alpha_k - 1)}{2}\sum_{j\neq k}(\alpha_j - 1)\cot\frac{\varphi_j - \varphi_k}{2} + \frac{i}{2}\left((\alpha_k - 1)\sum_{j\neq k}(\alpha_j - 1) - (1 - \alpha_k^2)\right).\end{aligned}$$

The imaginary part in the formula above must be zero, since we know that μ_k must be real. This can easily be verified by using the fact that for a polygon, we have $\sum_{k=1}^{n}(\alpha_k - 1) = -2$. Replacing $\sum_{j\neq k}(\alpha_j - 1)$ with $-2 - (\alpha_k - 1)$ and a straight calculation yield the result.
Hence, we have found an explicit formula for μ_k:

Lemma 3.6
Let P be a CAPD that can be mapped onto a polygonal domain by a Möbius transformation.
The parameters of the Schwarzian derivative of a conformal mapping from the unit disk onto P are given by

$$\mu_k = -\frac{(\alpha_k - 1)}{2}\sum_{j\neq k}(\alpha_j - 1)\cot\frac{\varphi_j - \varphi_k}{2}, \qquad k = 1, \ldots, n.$$

The φ_k refer to the arguments of the prevertices p_k.

The phrasing "can be mapped onto a polygonal domain" is chosen, because the image domain is only a polygonal domain if it is normalized accordingly. Otherwise it looks like an ordinary CAPD.[16]
The restricting equations (3.1) of the CAPD mapping can be verified for the values given in the lemma above. This is done in the appendix at A.1.

There is one more fact of note: Since the cotangents have a pole at zero, we must assume an increase in the absolute value of μ_k, if its neighboring prevertices get close. This matches the result from the preceding section.

[16]The CAPD still has the feature that all circles providing arcs of the boundary have one common intersection point. This point has to be mapped to infinity to get a polygonal domain.

3.4 Domains Symmetric with Respect to Rotations

We wish to investigate the conformal mappings from the unit disk onto CAPDs that are symmetric with respect to rotations. The special structure of the image domains may allow conclusions on the behavior of the parameters. We suppose that each image domain is symmetric with respect to a rotation around zero. Therefore we normalize each mapping f by demanding $f(0) = 0$.
The symmetry of such a mapping can be expressed in the form

$$f(\omega z) = \omega f(z), \qquad \omega = \exp \frac{2i\pi}{m},\ m \in \mathbb{N} \setminus \{1\}.$$

This property of f leads to the property

$$\omega^2 \mathcal{S}(\omega z) = \mathcal{S}(z),$$

of the Schwarzian derivative. The equation above shows that for every prevertex p there are also prevertices $\omega^j p$, where $j = 1, \ldots, m-1$. Each of these sets of prevertices has the same a and μ, as it can be verified by calculation.[17]
Hence all prevertices are given, if we know the prevertices with their arguments in the interval $[0, \frac{2\pi}{m}[$. The remaining ones can be gathered by rotating this initial set by ω^j. To keep the problem as simple as possible, we will use only a small number of prevertices in the initial set.

3.4.1 One Prevertex

If there is only one prevertex independent regarding rotation, then there is only one possible choice for μ. Since all μ have to be equal, they all must be zero by the restricting equations (3.1). Therefore all the parameters depend on the choice of the first prevertex p and the corresponding interior angle. They are given by

$$p_k = \omega^{k-1} p, \quad a_k = a, \quad \mu_k = 0, \qquad k = 1, \ldots, m.$$

We will normalize the preimage domains by a rotation and set p to 1. This means that all prevertices of such a mapping are given by $p_k = \omega^{k-1}$.
With the prevertices set and no choice regarding μ, the curvature of the boundary arcs, which have by the symmetry all the same curvature, depends only on the common interior angle $\pi\alpha$ in the form $a = \frac{1}{2}(1 - \alpha^2)$.
Since the geometry of the image domains is very simple, we can state a formula for the curvature κ of the boundary arcs. If we normalize each image domain by the property that the first prevertex $p = 1$ is mapped onto 1, i.e. $f(1) = 1$, we have

$$\kappa_m(\alpha) = \frac{\sin\left((\alpha/2 + 1/m - 1/2)\pi\right)}{\sin\left(\pi/m\right)}. \tag{3.8}$$

This normalization is necessary, as the curvature depends on the scaling of the image domain. The curvature also has a sign in this case: A negative curvature means that the

[17] This can also be seen in equation (3.5).

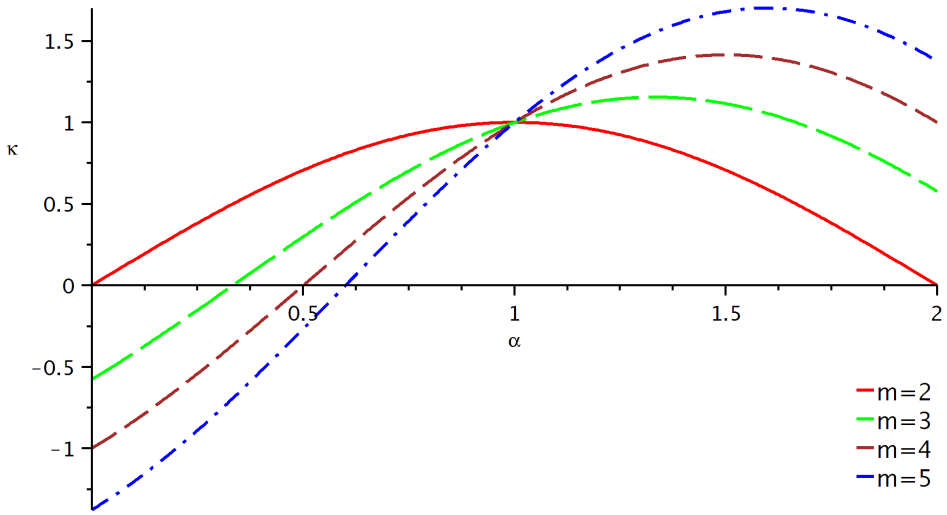

Figure 18: Curvature vs interior angle: The greatest possible curvature rises with the number of vertices. The common intersection point at $\alpha = 1$ is the mapping onto the unit disk.

boundary arc is bent inwards, while a positive curvature indicates a bulging outwards. Therefore the unit circle has a curvature of 1.
The only conclusion we can draw so far is that the curvature of the boundary arcs not only depends on μ, but also on a and the number of prevertices.

3.4.2 Two Prevertices

We again normalize the preimage domains by a rotation. In this case of two prevertices, we use the rotation to place the initial prevertices symmetric to the real axis at p and $\overline{p}$. The normalization is changed compared to the "one prevertex" case, as it will be beneficial later in the work.
With this normalization, we have

$$p = \exp(i\varphi),$$
$$\overline{p} = \exp(-i\varphi),$$

so that the prevertices depend only on one real parameter φ. To keep the preimage domains unique, we allow φ only in the interval $[0, \frac{\pi}{2m}]$. In this way, the arc between $\overline{p}$ and p is shorter than the one between p and $\omega\overline{p}$. Any other scenario can be reached by rotating the preimage domain. For reference, we have a short ($\overline{p}$ to p) and a long (p to $\omega\overline{p}$) edge, and the image domain contains each of these edges m times.
The two different values for the μ must be zero in summation, as demanded by the restricting equations, so they can only differ in their signs. For simplicity, we further

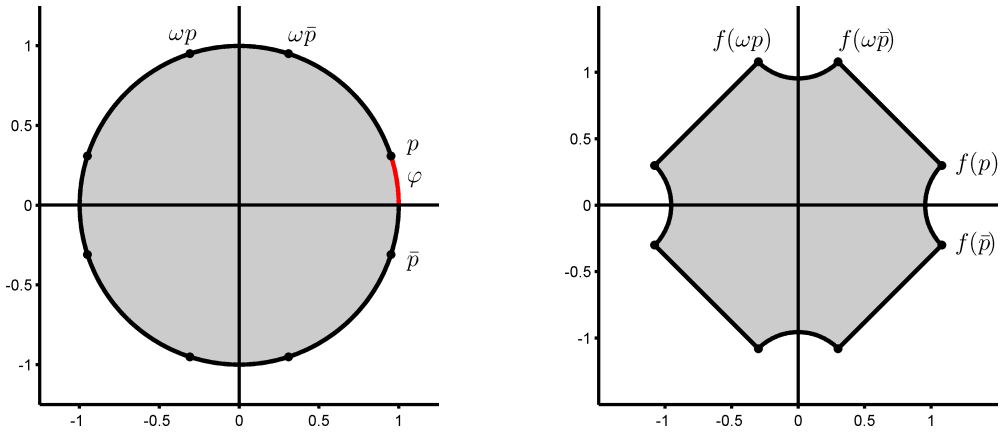

Figure 19: The unit disk is mapped onto a symmetric CAPD with two kinds of edges. $(m = 4)$

set a for all vertices to the same value, and so have

$$
\begin{aligned}
&p_k \in \{p,\, \omega\overline{p},\, \omega p,\, \omega^2\overline{p}, \omega^2 p,\, \ldots\, ,\, \omega^{m-1}\overline{p},\, \omega^{m-1}p,\, \overline{p}\},\\
&\mu_k = \begin{cases} \mu & \text{if } k \text{ is odd} \\ -\mu & \text{if } k \text{ is even} \end{cases},\\
&a_k = a,\\
&k = 1, \ldots, 2m.
\end{aligned}
$$

Note that for $\mu = 0$ and $\varphi = \frac{\pi}{2m}$, we return to the "one prevertex" case, as the prevertices are equally spaced and have the same parameter μ.

Limit Behavior

There is a connection to the "one prevertex" case: If we let φ of any mapping go to zero, the two prevertices $\overline{p}$ and p will merge in the limit, as do all their rotations $\omega\overline{p}$ and ωp. The limit domain then has only one prevertex not generated by a rotation with a power of ω. Since $\overline{p}$ and p collapse at 1, the image domain in the limit is normalized according to the preceding section.
We may also demand from the limit process that the curvature of the long image edge κ is kept constant. This means that the parameters μ have to change, but the convergence process satisfies the conditions of the Carathéodory convergence theorem regarding the image domains. Additionally, this means that the edges of the limit domain all have the same curvature κ of the long edge, as the small edge and its rotations vanish.
The named Carathéodory convergence theorem [Con95, Corollary 4.11] allows us to conclude that the mapping functions, and therefore their Schwarzian derivatives, also

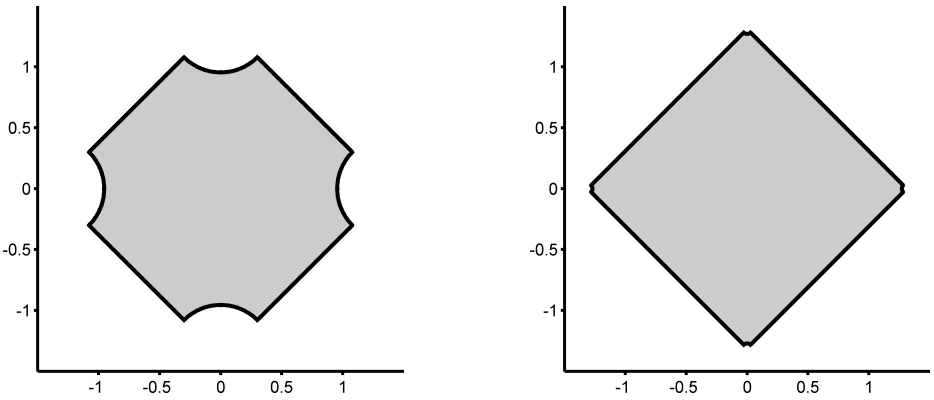

Figure 20: The small arcs of the domain shrink in the limit process, while the curvature of the long edges is kept constant. The small edges vanish in the limit case and only vertices remain. (left image $\varphi = 0.1\pi$, right image $\varphi = 0.001\pi$)

converge. Hence, regarding the residues at p and $\overline{p}$, we have[18]

$$p(a + i\mu) + \overline{p}(a - i\mu) \to \tilde{p}(\tilde{a} + i\tilde{\mu}),$$

where the tilde denotes the new values in the limit case. We know that the new prevertex is 1 and $\tilde{\mu}$ must be zero as this was discussed earlier, so we find

$$\begin{aligned} a(p + \overline{p}) + i\mu(p - \overline{p}) &\to \tilde{a} \\ \Rightarrow 2a\cos\varphi - 2\mu\sin\varphi &\to \tilde{a}. \end{aligned}$$

Hence, if we are getting close to the limit, i.e. when φ is very small, we can approximate μ by

$$\mu \approx \frac{2a\cos\varphi - \tilde{a}}{2\sin\varphi}.$$

This approximation depends on the shape of the limit domain, as it contains the interior angle. However, we have in (3.8) already a formula stating a connection between the curvature and the interior angle of such a limit domain. As we know the curvature κ, we can isolate the angle and obtain

$$\tilde{\alpha} = 1 + \frac{2}{\pi}\arcsin\left(\kappa\sin\left(\pi/m\right)\right) - \frac{2}{m}.$$

We substitute $\tilde{\alpha}$ into our approximation to obtain

$$\mu_{\text{approx}} = a\cot\varphi - \frac{1 - [1 + (2/\pi)\arcsin\left(\kappa\sin\left(\pi/m\right)\right) - (2/m)]^2}{4\sin\varphi}. \tag{3.9}$$

The result is an approximation for the parameter μ for a specific curvature of the long edge, under the assumption that φ is small. The accuracy of the approximation can be seen in the Figures 21 and 22.

[18]The actual residues have changed signs and are conjugated.

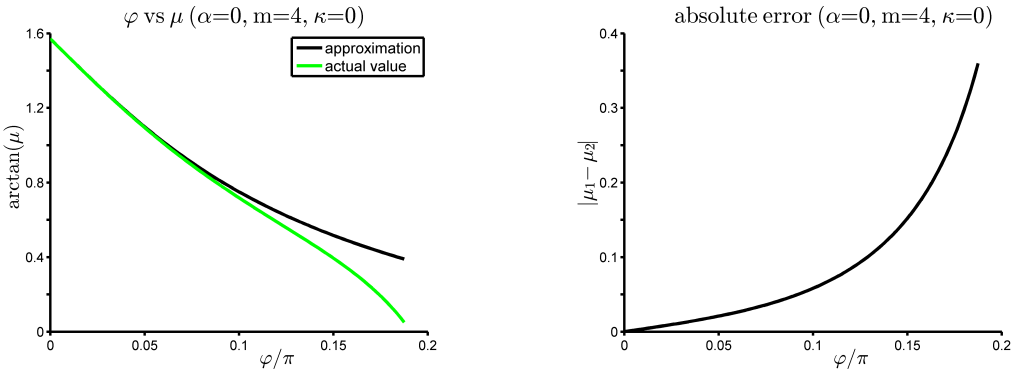

(a) Approximation vs actual values of μ

(b) Absolute error

Figure 21: A comparison of the actual values of μ and the approximation for μ for a changing φ. ($\alpha = 0$, $m = 4$, $\kappa = 0$)

It is important to note that this approximation does not hold for all κ. We assumed a new vertex in the limit case at 1. However, this requires from the geometry that the circle providing the long arc is large enough to at least touch the real axis. Or from an analytic point of view: κ must be in the range of possible values provided by (3.8) i.e. $\kappa \in [-\sin(\pi/m)^{-1}, \sin(\pi/m)^{-1}]$. This can also be seen in the approximation formula itself, as the argument of the arcsin must be between -1 and 1.

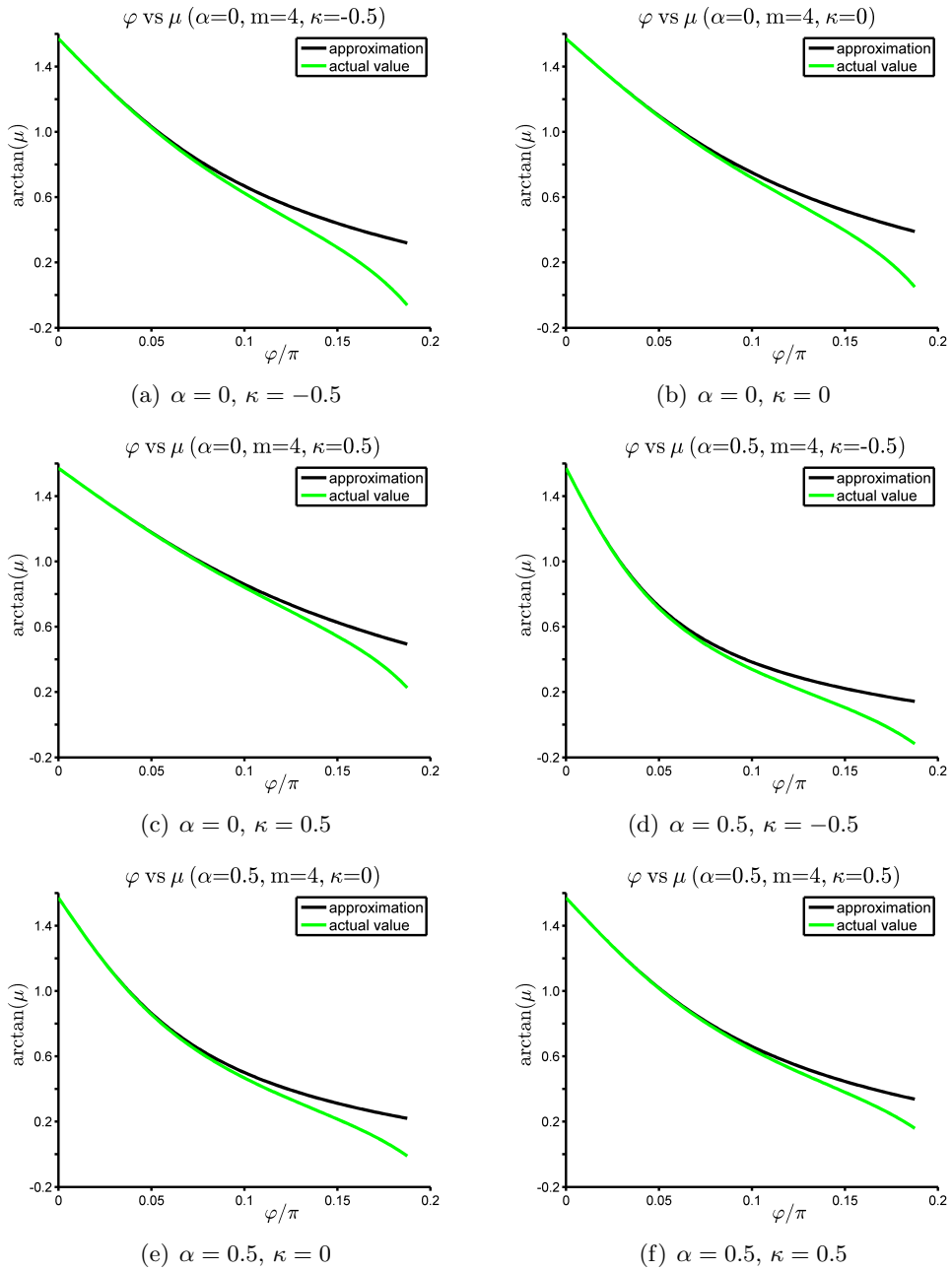

(a) $\alpha = 0$, $\kappa = -0.5$ (b) $\alpha = 0$, $\kappa = 0$

(c) $\alpha = 0$, $\kappa = 0.5$ (d) $\alpha = 0.5$, $\kappa = -0.5$

(e) $\alpha = 0.5$, $\kappa = 0$ (f) $\alpha = 0.5$, $\kappa = 0.5$

Figure 22: The actual values of μ and the approximations for changing φ and different interior angles α and curvatures κ. $(m = 4)$

4 Multiply Connected Circular Arc Polygon Domains

In this chapter, we construct our version of the Schwarzian derivative of the conformal mappings that map from a circular domain D onto a multiply connected circular arc polygon domain (MCCAPD) P (Figure 23). Note that the existence of such mappings is

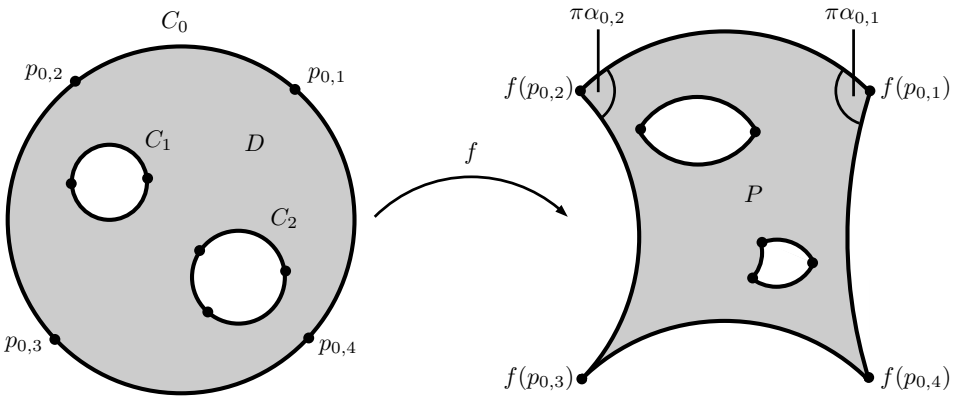

Figure 23: The conformal mapping from a circular domain onto a multiply connected circular arc polygon domain.

ensured by common knowledge about multiply connected conformal mappings [Con95] if D and P are conformally equivalent. Hence, we assume for the following discussion that, for each mapping, D and P are conformally equivalent, because otherwise there would not be any conformal map between them.

Definition 4.1
A circular domain $D \subset \mathbb{C}_\infty$ is a $(m+1)$-connected domain bounded by $m+1$ disjoint non-degenerated circles C_j, where $j = 0, \ldots, m$. The domain is called unbounded if all circles are exterior to each other. It is called bounded if the circles C_j, $j = 1, \ldots, m$, are inside of C_0.
A multiply connected circular arc polygon domain (MCCAPD) $P \subset \mathbb{C}_\infty$ is a $(m+1)$-connected domain bounded by $m+1$ disjoint circular arc polygons P_j, $j = 0, \ldots, m$, where $0 < m \in \mathbb{N}$. (cf. Definition 3.1)

We suppose for each preimage domain D that the circle C_0 is the unit circle $\partial\mathbb{D}$. If not stated otherwise, we further suppose that either zero (bounded case) or infinity (unbounded case) are inside the domain (Figure 24).[19]
We suppose each of the $m+1$ circular arc polygons P_j that bound a MCCAPD to consist of K_j circular arcs. Each of these arcs $\tilde{\zeta}_{j,k}$ is part of some circle $\tilde{C}_{j,k}$. Here the index $j = 0, \ldots, m$ refers to the boundary component, while $k = 1, \ldots, K_j$ refers to the

[19] A common exception is the annulus as canonical domain for doubly connected mappings.

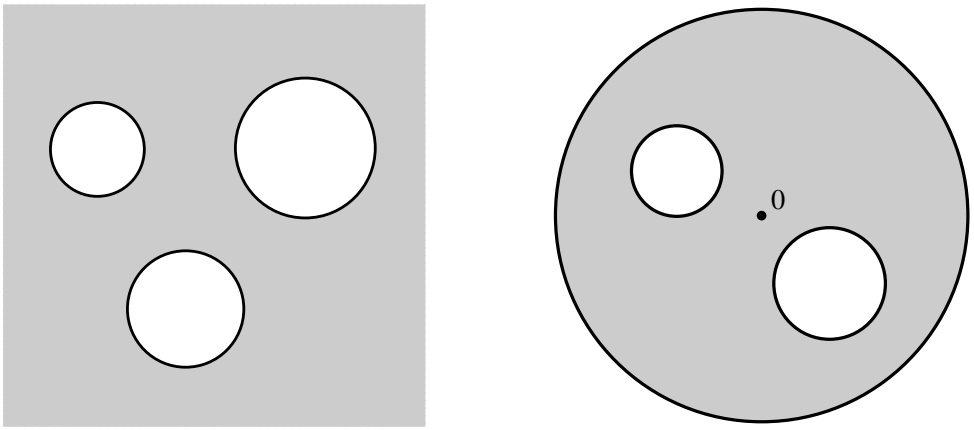

(a) An unbounded circular domain (b) A bounded circular domain

Figure 24: The two different kinds of circular domains.

specific circular arc of the component.
We further suppose the domains to be to the left of the boundary and number the vertices $v_{j,k} = f(p_{j,k})$ of each boundary component P_j accordingly.

4.1 Properties of the Schwarzian Derivative

The first step of our construction is to extend the domain of definition of such a mapping f to its maximum, similarly to the proof of Theorem 3.4 for the simply connected mappings.
We can apply the Schwarz reflection principle to the mapping, since the boundary consists for D, as for P, only of circular arcs. Hence we may extend D over an arc $\zeta_{j,k}$

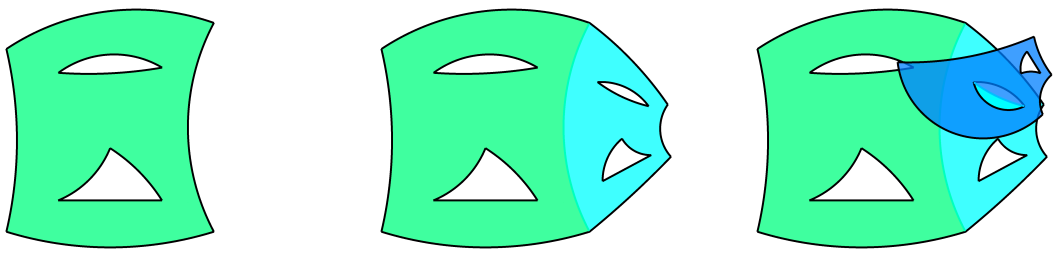

Figure 25: A CAP domain can be extended by reflecting across a boundary arc. The extended domain can then be extended again by reflecting across another arc. We probably lose global univalence in the process.

of the boundary circle C_j and P over $\tilde{\zeta}_{j,k} = f(\zeta_{j,k})$ of the circle $\tilde{C}_{j,k}$. The reflection

in the preimage domain with respect to C_j shall be denoted as s_j while the reflections against $\tilde{C}_{j,k}$ shall be referred to by $\tilde{s}_{j,k}$. We obtain, by this extension of the mapping, the property

$$f(s_j(D)) = \tilde{s}_{j,k}(f(D)) = \tilde{s}_{j,k}(P). \tag{4.1}$$

The index of s and the first index of $\tilde{s}$ have to be equal, while the second index of $\tilde{s}$ can freely be chosen.[20] In this process we may lose global univalence by an overlapping of the extended image domain, but the mapping is still locally injective (Figure 25).
The extended version of D is almost a circular domain. It is bounded by the circles C_n and $s_j(C_n)$, where $n = 0, \ldots, m$ and $n \neq j$, but contains the slit $C_j \setminus \zeta_{j,k}$ (Figure 26). This is because only $\zeta_{j,k}$ is included in the new domain D_1, but not the remaining part of C_j. The extended MCCAPD P_1 is also a MCCAPD, but may be self overlapping with boundary arcs from the circles $\tilde{C}_{n,o}$ and $\tilde{s}_{j,k}(\tilde{C}_{n,o})$, where $(n, o) \neq (j, k)$. If we

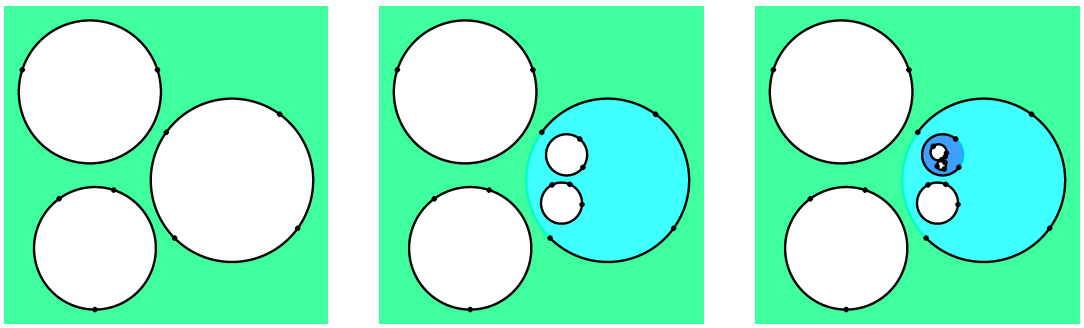

Figure 26: Circular domains can be extended similar to CAP domains. Only the arcs used for the reflection are included into the new (extended) domains. (The here shown extensions match the ones of Figure 25.)

denote the reflections against the new boundary components by σ and $\tilde{\sigma}$, we are able to apply the reflection principle once more to show

$$f(\sigma_i(s_j(D))) = \tilde{\sigma}_{i,l}(\tilde{s}_{j,k}(f(D))).$$

Since two subsequent reflections result in a Möbius transformation, we rewrite this to

$$f(T_{i;j}(D)) = \tilde{T}_{i,l;j,k}(f(D)),$$

where $T_{i;j} = \sigma_i \circ s_j$ and $\tilde{T}_{i,l;j,k} = \tilde{\sigma}_{i,l} \circ \tilde{s}_{j,k}$. To remove the transformation $\tilde{T}_{i,l;j,k}$, which depends on the image domain, we apply the Schwarzian derivative to obtain

$$(T'_{i;j}(z))^2 \{f, T_{i;j}(z)\} = \{f, z\}. \tag{4.2}$$

We also merge the different extensions in this step. Two different extensions, e.g. $\tilde{s}_{j,k}(P)$ and $\tilde{s}_{n,o}(P)$, can be mapped onto each other by a Möbius transformation

$$\tilde{s}_{j,k}(P) = (\tilde{s}_{j,k} \circ \tilde{s}_{n,o})(\tilde{s}_{n,o}(P)) = T_{j,k;n,o}(\tilde{s}_{n,o}(P)).$$

[20] There are several different extensions, depending on the chosen arc $\tilde{\zeta}_{j,k}$ of the image domain.

Hence, both extensions are equal in the context of the Schwarzian derivative. This is also true for all subsequent extensions ensuring that the process of extending the domain does not influence the resulting Schwarzian. Hence we can include all arcs ζ into the domain, as there is for each arc an extension, which includes the arc into the domain

$$D_1 = D \cup \bigcup_{j=0}^{m} s_j(D) \cup \bigcup_{j=0}^{m} \bigcup_{k=1}^{K_j} \zeta_{j,k}.$$

The only points left are the start and end point of each arc, i.e. the preimages of the vertices of the bounding CAPs.[21] To reach the maximum extension of D, we will continue with this procedure of applying the reflection principle.
We want to rewrite equation (4.2) in the context of this maximum extension to a generalised form:

$$(T'(z))^2\{f, T(z)\} = \{f, z\}, \qquad T \in \mathbb{M}(D), \tag{4.3}$$

where $\mathbb{M}(D)$ is the set of all Möbius transformations arising in the extension process. This gives us a functional equation for the Schwarzian derivative of the mapping f, which will be of great use later on.

We further investigate the process of extending D in order to define the set $\mathbb{M}(D)$. The domain D can be extended by a reflection s_j against C_j in the manner described above. The new domain $s_j(D)$ can again be extended by reflecting against a circle $s_j(C_i)$. However, instead of the reflection against $s_j(C_i)$, it is possible to apply the reflection $s_j \circ s_i$ for an equivalent mapping.[22]

Lemma 4.2 ([DEP04])
Let s_j denote the reflection against the circle C_j, $j \in \{0, 1\}$, and $s_{0,1}$ the reflection against the circle $C_{0,1} = s_0(C_1)$.
A reflection through C_1 followed by a reflection through C_0 is the same as the reflection through C_0 followed by a reflection through $C_{0,1}$, i.e. $s_{0,1} \circ s_0 \equiv s_0 \circ s_1$.

We will prefer the version using the reflections against the boundary circles of D, as it results in a simpler notation. Hence, we can express any reflection by $s_{j\ldots i} = s_j \circ \ldots \circ s_i$. Since reflections are self inverse $s_j \circ s_j = \mathrm{id}$, the reflection $s_{j\ldots i}$ can not contain any pair of equal indices not separated by a different index.
We are interested in all the Möbius transformations arising in this context. As noted earlier (Lemma 2.2), two consecutive reflections yield a Möbius transformation. The set of all these Möbius transformations can be described by a group, which is generated by

[21] We will include these points into the domain later on, as they will be poles of the second order of the meromorphic Schwarzian derivative. This can be seen in the following section.

[22] The properties regarding such successive reflections are well covered in the article [DEP04] by DeLillo, Elcrat and Pfaltzgraff, since they used reflections to construct the multiply connected Schwarz-Christoffel mapping.

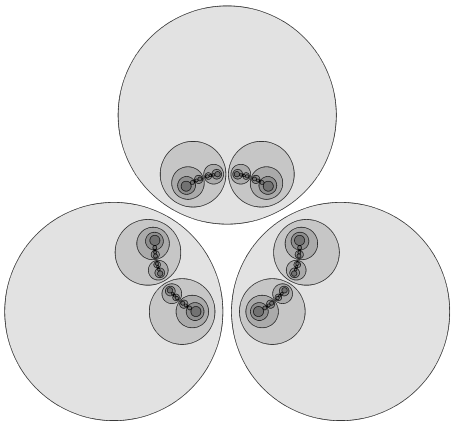

(a) The unbounded domain (white) is extended in the circles by several steps of reflections. The areas get darker with a rising number of reflections necessary to reach them.

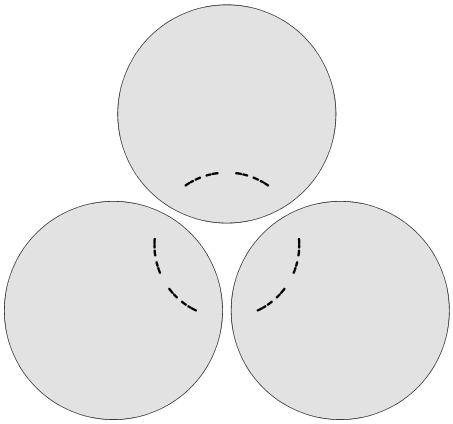

(b) The limit points, i.e. the boundary, for the expansion of the domain which is shown in the left image.

Figure 27: The behavior of the domain if it is extended as described.
The domain is extended 5 times for the left image and 8 times for the limit points on the right side.

the initial transformations $T_{ji} = s_j \circ s_i$, where $j, i = 0, \ldots, m$ and $i \neq j$. However since we have for these transformations

$$T_{ji} \circ T_{il} = (s_j \circ s_i) \circ (s_i \circ s_l) = s_j \circ s_l = T_{jl},$$

the set of generators for the group can be reduced to transformations of the type T_{0j}, where $j = 1, \ldots, m$. This group shall from now on denoted by $\mathbb{M}(D)$, the set of all transformations belonging to the circular domain D. We will furthermore write T_j instead of T_{0j} for ease of notation.
This group can also be seen as a Schottky group (Definition 2.27). Each transformation T_j maps the exterior of C_j onto the interior of $s_0(C_j)$, while C_j is carried into $s_0(C_j)$, as demanded in the definition of the Schottky group. The fundamental region of this group is therefore the exterior of the circle pairs C_j and $C'_j = s_0(C_j)$ for $j = 1, \ldots, m$ or the extension of D over C_0, i.e. $D_R = D \cup C_0 \cup s_0(D)$.
The special construction of the group leads to a somewhat restricted behavior (for example, no additional rotations are permitted) compared to more generic Schottky groups. Hence, this group satisfies, by its construction, the requirements of a symmetric Schottky group (Definition 2.28).
Note that C_0 was arbitrary chosen for the construction of the group. An alternative fundamental region, but with the same group, can be constructed for each boundary circle C_j.

We now return to the extension of the preimage domain D of the mapping, or rather the domain of definition of the Schwarzian derivative of f. If we extend D over C_0, we

obtain the preimage domain $D_R = D \cup C_0 \cup s_0(D)$ for the Schwarzian.[23] Any further extension can then be expressed as either an even number of reflections applied to D ($s_1(s_0(D))$, $s_0(s_1(D))$, ...) or as an odd number of reflections applied to D ($s_0(D)$, $s_1(D)$, ...). Every even number of these reflections is a Möbius transformation of $\mathbb{M}(D)$, while every odd number of reflections can be rewritten, with the use of $s_0 \circ s_0 = \mathrm{id}$, to a transformation of $s_0(D)$

$$s_{i\ldots j}(D) = (s_{i\ldots j} \circ s_0)(s_0(D)) = T_{i\ldots j0}(s_0(D)), \qquad T_{i\ldots j0} \in \mathbb{M}(D).$$

The maximum extension of D is therefore given by $\bigcup_{T\in\mathbb{M}(D)}(T(D_R) \cup \bigcup_{j=0}^{m} T(C_j))$. Since $\mathbb{M}(D)$ is a Kleinian group and $D_R = D \cup C_0 \cup s_0(D)$ its fundamental region, we cover the whole Riemann sphere with the mappings $T(D_R)$ except for the limit set Λ according to Lemma 2.26. Therefore, these limit points represent the boundary of the maximum extension.
Hence, we define the following terms:

Definition 4.3
Let D be a circular domain bounded by $m+1$ disjoint non-degenerated circles C_j, $j = 0, \ldots, m$, which are either all inside or all outside of $C_0 = \partial\mathbb{D}$ and denote by s_j the reflection through the circle C_j.
We define:

- *$D_R := D \cup C_0 \cup s_0(D)$, the extension of D by reflection against the boundary circle C_0.*
- *$\mathbb{S}(D)$, the set of all reflections s_j against the boundary circles C_j, $j = 0, \ldots, m$.*
- *$\mathbb{M}(D)$, the symmetric Schottky group of Möbius transformations matching the fundamental region D_R. It is generated by the transformations $T_j = s_0 \circ s_j$, where $j = 1, \ldots, m$.*
- *Λ, the set of the limit points of $\mathbb{M}(D)$.*
- *$D_E := \mathbb{C}_\infty \setminus \Lambda$, the maximum extension of D by reflections.*

We also introduce a special notation for the Schwarzian derivative of the conformal mappings onto MCCAPDs.

Definition 4.4
The Schwarzian derivative of a conformal mapping f from a circular domain onto a multiply connected circular arc polygon domain is denoted by $\mathcal{S}$.

We also restate the functional equation (4.3) for ease of reference.

[23] We noted above that only the Schwarzian allows us to include the whole circle, as the different extensions over C_0 merge. Here, D_R contains even the preimages of the vertices of the CAP P_0. This inclusion will be justified later on.

Lemma 4.5
The Schwarzian derivative $\mathcal{S}$ of a conformal mapping from the circular domain D onto a multiply connected circular arc polygon domain satisfies the functional equation

$$(T'(z))^2 \mathcal{S}(T(z)) = \mathcal{S}(z), \qquad T \in \mathbb{M}(D).$$

4.1.1 Construction: Transformation

The basic idea for the construction of mappings similar to the Schwarz-Christoffel transformation is that at each vertex in the image domain such a mapping f has to behave like

$$f(z) = (z-p)^\alpha \psi(z). \tag{4.4}$$

In this equation, p refers to the preimage of the vertex (or prevertex), α to the interior angle at the vertex and ψ is an analytic function different from zero at p. ψ represents the remaining part of f. As we apply the Schwarzian derivative, we obtain

$$\{f,z\} = \frac{1-\alpha^2}{2(z-p)^2} + \frac{\psi'(p)}{\psi(p)} \frac{(1-\alpha^2)}{\alpha} \frac{1}{(z-p)} + O((z-p)^0).$$

To shorten the notation, we define

$$\mathcal{S}(z) := \{f,z\}, \qquad a := \frac{1}{2}(1-\alpha^2), \qquad \gamma := \frac{\psi'(p)}{\psi(p)} \frac{(1-\alpha^2)}{\alpha},$$

similarly to the simply connected case.
If we now apply the ideas of the preceding discussion, we can state:

Lemma 4.6
Let P be a multiply connected circular arc polygon domain bounded by the circular arc polygons P_j with the vertices $v_{j,1}, \ldots, v_{j,K_j}$, where $j = 0, \ldots, m$.
The Schwarzian derivative $\mathcal{S}$ of any conformal mapping f from a circular domain D onto P has at each transformed prevertex $T(p)$, where $p \in \{\, p_{j,k} \,|\, p_{j,k} \in C_j;\ f(p_{j,k}) = v_{j,k};\ j = 0, \ldots, m;\ k = 1, \ldots, K_j \,\}$ and $T \in \mathbb{M}(D)$, the expansion

$$\mathcal{S}(z) = \frac{a}{(z-T(p))^2} + \left(\frac{\gamma}{T'(p)} - \frac{aT''(p)}{(T'(p))^2} \right) \frac{1}{z-T(p)} + O(1).$$

Proof. In the preceding section we derived

$$\tilde{T}(f(z)) = f(T(z))$$

for each conformal mapping onto a MCCAPD, where $\tilde{T}$ is a Möbius transformation depending on the shape of the image domain. Combining this with equation (4.4) for

the mappings of the Schwarz-Christoffel type gives

$$\tilde{T}(f(z)) = f(T(z)) = (T(z) - p)^{\alpha}\psi(T(z)), \qquad T \in \mathbb{M}(D).$$

Substituting $p = T(U(p)) = T(q)$, where $U = T^{-1}$, and applying the Schwarzian derivative leads to

$$\begin{aligned}\{f \circ T, z\} &= \frac{a}{(z-q)^2} + \left(T'(q)\frac{\psi'(p)}{\psi(p)}\frac{(1-\alpha^2)}{\alpha} + \frac{(1-\alpha^2)}{2}\frac{T''(q)}{T'(q)}\right)\frac{1}{z-q} + O(1) \\ &= \frac{a}{(z-q)^2} + \left(T'(q)\gamma + a\frac{T''(q)}{T'(q)}\right)\frac{1}{z-q} + O(1).\end{aligned}$$

As we can see, there is also a pole at the transformed prevertex $q = U(p)$ and the residue δ at q can be calculated from the residue γ at p.

$$\delta = T'(q)\gamma + a\frac{T''(q)}{T'(q)}, \qquad T(q) = p.$$

By applying the fact that $T'(q) = (U'(p))^{-1}$ and its derivative, we find

$$\delta = \frac{\gamma}{U'(p)} - \frac{aU''(p)}{(U'(p))^2}, \qquad U \in \mathbb{M}(D). \tag{4.5}$$

If we take all the different prevertices $p_{j,k}$ on the different circles C_j and their transformations into account, the Schwarzian has to contain the sum

$$\sum_{T\in\mathbb{M}(D)}\sum_{j=0}^{m}\sum_{k=1}^{K_j}\left[\frac{a_{j,k}}{(z-T(p_{j,k}))^2} + \left(\frac{\gamma_{j,k}}{T'(p_{j,k})} - \frac{a_{j,k}T''(p_{j,k})}{(T'(p_{j,k}))^2}\right)\frac{1}{z-T(p_{j,k})}\right],$$

and therefore has the stated principle part at each $T(p)$, $T \in \mathbb{M}(D)$. □

Since we will refer to the variables introduced thus far frequently, we restate them in one common definition.

Definition 4.7
Let f be a conformal mapping from a circular domain D bounded by $m+1$ circles C_j, $j = 0, \ldots, m$, onto a MCCAPD P. The number of vertices of each boundary component $P_j = f(C_j)$ shall be denoted by K_j. The interior angle at each vertex $v_{j,k}$ is $\pi\alpha_{j,k}$, $k = 1, \ldots, K_j$, and the preimage of each vertex is $p_{j,k}$, i.e. $f(p_{j,k}) = v_{j,k}$. Therefore we have the following sets:

- $\{p_{j,k} \,|\, p_{j,k} \in C_j; j = 0, \ldots, m; k = 1, \ldots, K_j\}$, *the set of prevertices on the boundary of D.*
- $\{a_{j,k} \,|\, a_{j,k} = \frac{1}{2}(1-\alpha_{j,k}^2); \alpha_{j,k} \in [0,2]; j = 0, \ldots, m; k = 1, \ldots, K_j\}$, *the set referring to the interior angles $\pi\alpha_{j,k}$ at the vertices.*

- $\{\gamma_{j,k} \,|\, j = 0, \dots, m; k = 1, \dots, K_j\}$, *the set of the parameters, which arise in the Schwarzian derivative as residues at the prevertices.*

These sets will be called the "first generation".
With $\mathbb{M}(D)$ according to Definition 4.3, we further have:

- $\{p_{T,j,k} \,|\, p_{T,j,k} = T(p_{j,k}), T \in \mathbb{M}(D)\}$, *the set of transformed prevertices.*
- $\{\gamma_{T,j,k} \,|\, \gamma_{T,j,k} = \frac{\gamma_{j,k}}{T'(p_{j,k})} - \frac{a_{j,k}T''(p_{j,k})}{(T'(p_{j,k}))^2}, T \in \mathbb{M}(D)\}$, *the set of transformed parameters.*

In the context of the mapping, we also define the sum symbols

$$\sum_{j,k} := \sum_{j=0}^{m} \sum_{k=1}^{K_j} \qquad \text{and} \qquad \sum_{T,j,k} := \sum_{T \in \mathbb{M}(D)} \sum_{j=0}^{m} \sum_{k=1}^{K_j}.$$

We denote the set of sets (a, p, γ) generated by transformations of length $n-1$ as the nth generation. Note that each generation after the second has $2m-1$ times as many prevertices/parameters as the preceding one. This leads to an exponential growth in succeeding prevertices/parameters.
The parameters can be grouped to sets $(a, p, \gamma)_{T,j,k}$, representing the location of a pole (prevertex p) and the coefficients for the first (parameter γ) and second power (interior angle as a) at this pole. To shorten the notation, we will skip the indices of these values if the context allows it, or we will denote them by each other, e.g. γ_p is the residue at p, while $\gamma_{T(p)}$ is the residue at $T(p)$.

For easier reference, we introduce a possible candidate $\mathcal{K}$ for the Schwarzian derivative $\mathcal{S}$, which consists of all the principle parts at the prevertices. We also include some additional (yet unknown) terms $\mathcal{A}_C$ to ensure the convergence.

Definition 4.8
The candidate function $\mathcal{K}$ is defined as

$$\mathcal{K}(z) := \sum_{T,j,k} \left(\frac{a_{j,k}}{(z - p_{T,j,k})^2} + \frac{\gamma_{T,j,k}}{z - p_{T,j,k}} + \mathcal{A}_C(z, T, j, k) \right).$$

$\mathcal{K}$ will be redefined as we continue investigating features of the Schwarzian derivative $\mathcal{S}$. For each section, only the last definition of $\mathcal{K}$ is valid.
The candidate function is of particular interest, as it not only includes a subset, but all poles of $\mathcal{S}$ in D_E.

Lemma 4.9
The Schwarzian derivative $\mathcal{S}$ has its only poles in D_E at the prevertices and their transformations.

Proof. The form of the Schwarzian derivative

$$\mathcal{S} = \left(\frac{f''}{f'}\right)' - \frac{1}{2}\left(\frac{f''}{f'}\right)^2$$

implies that every pole has to be either a pole of f'' or a zero of f'. The poles of f'' are also poles of f, but since f is conformal, it has at most one simple pole in D and this only in the case of a mapping onto an unbounded domain. However, according to Lemma 2.14, this pole does not appear in the Schwarzian. This is also true for the boundary excluding the prevertices, as the mapping can be extended. Applying the extension process, the only poles in D_E can be at the prevertices. □

Based on the facts gathered so far, we will regard $\mathcal{S}$ rather as meromorphic function on D_E than as holomorphic function on D_E without the (transformed) prevertices.

Because we already collected all poles of $\mathcal{S}$ in D_E, the functions $\mathcal{A}_C$ have to be analytic in D_E. Hence, the $\mathcal{A}_C$ can only have singularities in Λ. As a consequence, we have found the basic structure of the Schwarzian.

Lemma 4.10
The Schwarzian derivative $\mathcal{S}$ of a MCCAPD mapping is of the form

$$\mathcal{S}(z) = \sum_{T,j,k}\left(\frac{a_{j,k}}{(z-p_{T,j,k})^2} + \frac{\gamma_{T,j,k}}{z-p_{T,j,k}} + \mathcal{A}_C(z,T,j,k)\right) + \mathcal{A}_R(z), \tag{4.6}$$

where the functions $\mathcal{A}_C$ and the function $\mathcal{A}_R$ are analytic in $D_E = \mathbb{C}_\infty \setminus \Lambda$.

Proof. If we combine the Lemmas 4.6 and 4.9, we see that all poles of the Schwarzian in $D_E = \mathbb{C}_\infty \setminus \Lambda$ are given by

$$\sum_{T,j,k}\left(\frac{a_{j,k}}{(z-p_{T,j,k})^2} + \frac{\gamma_{T,j,k}}{z-p_{T,j,k}}\right). \tag{4.7}$$

Any term we may add would then have to be analytic in D_E, i.e. any non-constant term we add has to have a singularity in Λ.
If we denote the terms necessary for the convergence of the sum (4.7) by $\mathcal{A}_C$, we get the candidate function of Definition 4.8

$$\mathcal{K}(z) = \sum_{T,j,k}\left(\frac{a_{j,k}}{(z-p_{T,j,k})^2} + \frac{\gamma_{T,j,k}}{z-p_{T,j,k}} + \mathcal{A}_C(z,T,j,k)\right).$$

Since the Schwarzian and the candidate function have the same poles in D_E, any remaining difference $\mathcal{A}_R = \mathcal{S} - \mathcal{K}$ must be analytic in D_E. We reach the lemma by writing $\mathcal{S} = \mathcal{K} + \mathcal{A}_R$. □

4.1.2 Construction: Reflection

Instead of investigating every second step in the extension process, i.e. the Möbius transformations, we may directly examine the reflections of each step. This allows us to state a functional equation similar to the one of Lemma 4.5.

Lemma 4.11
The Schwarzian derivative $\mathcal{S}$ of a conformal mapping from a circular domain D onto a MCCAPD satisfies for each reflection $s \in \mathbb{S}(D)$ against a boundary circle of D the functional equation

$$\mathcal{S}(z) = \sigma'(z)^2 \overline{\mathcal{S}(\overline{\sigma(z)})}, \qquad \sigma(z) = \overline{s(z)},\ s \in \mathbb{S}(D). \tag{4.8}$$

Proof. The use of reflections led to equation (4.1)

$$f(s(z)) = \tilde{s}(f(z)) \Leftrightarrow f(z) = \tilde{s}(f(s(z))). \tag{4.9}$$

If we introduce the substitutions

$$\tilde{\sigma}(\bar{z}) := \tilde{s}(z), \qquad \overline{\sigma(z)} := s(z), \qquad g(z) := \overline{f(\bar{z})},$$

we obtain

$$(\tilde{s} \circ f \circ s) = (\tilde{\sigma} \circ g \circ \sigma).$$

The advantage of this form is that the new functions are all holomorphic (in comparison to anti-holomorphic reflections) and the functions $\tilde{\sigma}$ and σ are even Möbius transformations. This allows us to apply the Schwarzian derivative to equation (4.9):

$$\{f, z\} = \{\tilde{s} \circ f \circ s, z\} = \{\tilde{\sigma} \circ g \circ \sigma, z\} = \{g \circ \sigma, z\} = \sigma'(z)^2 \{g, \sigma(z)\}.$$

By substituting from g back to f, we find

$$\mathcal{S}(z) = \sigma'(z)^2 \overline{\mathcal{S}(\overline{\sigma(z)})}.$$

Since this is true for each reflection against a boundary circle C_j, the lemma follows. □

If we extend the domain by reflections, the domain is only in the first step reflected against a boundary circle of D. For further extensions, we need to reflect the already extended domain against the new boundary circles $s_i(C_j)$. These new circles are reflections of the initial circles bounding D.
According to Lemma 4.2, we can express any extension by only using reflections against the boundary circles of D, and it is therefore sufficient to investigate the functional equation (4.8) for the initial boundary circles C_j.
We also note the connection to the previous discussion, as we can combine any two

reflections of $\mathbb{S}(D)$ to a Möbius transformation of $\mathbb{M}(D)$

$$s_0 \circ s_j = T_j, \qquad s_j \circ s_0 = T_j^{-1}, \qquad s_i \circ s_j = T_i^{-1} T_j,$$

where $i \neq j$ and $i, j \neq 0$. The functional equation of Lemma 4.5 can therefore be constructed by applying the functional equation of the lemma above twice.

Continuing the investigation, we obtain the following interesting information about the parameters γ:

Lemma 4.12
Let C be a boundary circle C_j of D or a transformation $T(C_j)$, where $T \in \mathbb{M}(D)$, of a boundary circle with center c and radius r and let $s(z) = \frac{r^2}{\bar{z}-\bar{c}} + c$ be the reflection against C.
The parameters γ_p and γ_q corresponding to the prevertices p and $q = s(p)$ (not necessary on C) satisfy the equation

$$\gamma_q = -\frac{(\bar{p} - \bar{c})}{r^2} \left(\overline{\gamma_p}(\bar{p} - \bar{c}) + 2a\right).$$

If p lies on C, this simplifies to

$$\operatorname{Re}\left(\gamma_p(p - c) + a\right) = 0. \tag{4.10}$$

Proof. We already derived the expansion for f in the form

$$\{f, z\} = \frac{a}{(z-p)^2} + \frac{\gamma}{(z-p)} + O((z-p)^0).$$

Therefore g, defined as in the previous proof by $g(z) := \overline{f(\overline{z})}$, has the expansion

$$\{g, z\} = \frac{a}{(z-\bar{p})^2} + \frac{\bar{\gamma}}{(z-\bar{p})} + O((z-\bar{p})^0).$$

We define q by $p = s(q)$, with s being a reflection against one of the boundary circles or against a transformation of a boundary circle. Alternatively, we can write $\overline{p} = \sigma(q)$, where $\sigma(z) = \overline{s(z)}$. We continue to obtain

$$\begin{aligned}\{g \circ \sigma, z\} &= \sigma'(z)^2 \{g, \sigma(z)\} \\ &= \frac{a}{(z-q)^2} + \frac{\sigma''(q)a + \sigma'(q)^2\bar{\gamma}}{\sigma'(q)} \frac{1}{(z-q)} + O((z-q)^0).\end{aligned}$$

This gives us the equation

$$\gamma_q = \sigma'(q)\overline{\gamma_p} + a\frac{\sigma''(q)}{\sigma'(q)}.$$

If we now replace $\sigma'(z) = -r^2(z-c)^{-2}$ in the formula, it alters to

$$\gamma_q = \frac{-r^2}{(q-c)^2}\overline{\gamma_p} + \frac{-2}{(q-c)}a = -\frac{(\bar{p}-\bar{c})}{r^2}\left(\overline{\gamma_p}(\bar{p}-\bar{c}) + 2a\right).$$

We can attain the second statement of the lemma if we reshape the equation to

$$\gamma_q(q-c) + a = -\overline{(\gamma_p(p-c)+a)}.$$

If p lies on the circle C, which is used for the reflection, we have $p = q$ and therefore

$$\gamma_p(p-c) + a = -\overline{(\gamma_p(p-c)+a)}.$$

Hence $\gamma_p(p-c)+a$ must be purely imaginary. □

Equation (4.10) allows us to conclude that each γ can be expressed by one real value similar to the simply connected case in Theorem 3.4. Hence, we want to state our result and introduce a new real parameter.

Lemma 4.13
Each parameter $\gamma_{j,k}$ of Definition 4.7 is completely defined by one real parameter $\mu_{j,k} \in \mathbb{R}$ in the form

$$\gamma_{j,k} = \frac{i\mu_{j,k} - a_{j,k}}{p_{j,k} - c_j},$$

where c_j refers to the center of the boundary circle C_j on which $p_{j,k}$ lies.

Proof. The lemma follows directly from Lemma 4.12 by

$$\mathrm{Re}\left(\gamma(p-c)+a\right) = 0 \quad \Leftrightarrow \quad i\mu = \gamma(p-c)+a,$$

where $\mu \in \mathbb{R}$. Isolating γ yields the result. □

4.1.3 Behavior of the Parameters γ

If we want to investigate the convergence of $\mathcal{K}$, it is reasonable to look into the behavior of the parameters γ.

Lemma 4.14
The parameters $\gamma_{T(p)}$ of $\mathcal{S}$, i.e. the residues at the poles $T(p)$, are unbounded by increasing length of the transformations.

Proof. If we use the common notation for Möbius transformations

$$T(z) = \frac{Az+B}{Cz+D}, \qquad T'(z) = \frac{1}{(Cz+D)^2}, \qquad T''(z) = \frac{-2C}{(Cz+D)^3},$$

where $AD - BC = 1$, we can rewrite $\gamma_{T(p)}$ to

$$\begin{aligned} \gamma_{T(p)} &= (Cp+D)^2\gamma_p + 2aC(Cp+D) \\ &= C^2(p+\tfrac{D}{C})((p+\tfrac{D}{C})\gamma_p + 2a) \end{aligned} \tag{4.11}$$

while "a" refers to the interior angle and is not to be confused with "A" from the transformation.

Since $\mathbb{M}(D)$ is a Schottky group, we can use some of the properties of Kleinian groups. We know from Lemma 2.22 that the radii of the isometric circles $|Cz+D| = 1$ are going to zero for any infinite subset of a group of Möbius transformations, if infinity is not a limit point of the group. (We supposed that infinity is in D_R, and so it can not be a limit point.) The centers on the other hand are clustering around the limit points and have therefore an upper boundary.
In other words, the absolute value of C goes to infinity, while $-\frac{D}{C}$ stays bounded. As γ grows quadratically with C, it will tend to infinity for longer transformations, i.e. $|T| \to \infty \Rightarrow |\gamma_{T(p))}| \to \infty$.

An alternative, more geometric proof is also possible. By extending D, we place infinitely many transformations of D in the complex plain. Since they have to accumulate near the limit points of the group, they have to decrease in size. However, a decrease in size means a derivative smaller then 1, and so as the image shrinks, the derivative also has to get smaller. Therefore the derivative goes to zero, which means that the reciprocal value goes to infinity, but this is the factor applied to γ_p. As above, this is only true if infinity is not a limit point of the group. It would otherwise be possible for the transformed domains to actually increase in size. □

Let us illustrate this behavior with an example. Suppose D is a doubly connected unbounded circular domain. In this case, $\mathbb{M}(D)$ is generated by only one transformation $T = s_0 \circ s_1$. We choose $C_0 = \partial\mathbb{D}$ and therefore have

$$\begin{aligned} s_0(z) = \frac{1}{\overline{z}}, \quad s_1(z) &= \frac{r^2}{\overline{z} - \overline{c_1}} + c_1 \\ \Rightarrow T(z) &= \frac{(r^2 - |c_1|^2)z + c_1}{-\overline{c_1}z + 1}. \end{aligned}$$

If we normalize the Möbius transformation ($AD - BC = 1$) and write it in the form of a matrix, which contains the coefficients, we get

$$T = \frac{1}{r}\begin{pmatrix} |c_1|^2 - r^2 & -c_1 \\ \overline{c_1} & -1 \end{pmatrix}.$$

By choosing some explicit values for the radius and the center of C_1, for example $r = 1$ and $c = 3$, we can calculate the iterations of T

$$T = \begin{pmatrix} 8 & -3 \\ 3 & -1 \end{pmatrix},\ T^2 = \begin{pmatrix} 55 & -21 \\ 21 & -8 \end{pmatrix},\ T^3 = \begin{pmatrix} 377 & -144 \\ 144 & -55 \end{pmatrix},\ \dots$$

We notice that $|C|$ is rising with the length of the transformation (3, 21, 144), while $-\frac{D}{C}$ stays bounded and converges against the limit point inside of $C_0 = \partial\mathbb{D}$ ($\frac{1}{3} \approx 0.33333$, $\frac{8}{21} \approx 0.38095$, $\frac{55}{144} \approx 0.38194$) (Tables 1 and 2).

T^n	$n=1$	2	3	4	5	6	7
C	3	21	144	987	6765	46368	317811
$-\frac{D}{C}$	0.33333	0.38095	0.38194	0.38197	0.38197	0.38197	0.38197

Table 1: The coefficients C tend to infinity, while the quotients $-\frac{D}{C}$ stay bounded, as the length of the transformations increases.

T^n	$n=1$	2	3	4	5	6	7	8	9	10
$\log_{10}(C)$	0.48	1.32	2.16	3.00	3.83	4.65	5.52	6.35	7.17	8.00

Table 2: The coefficients C grow nearly exponential.

If we continue with this example, we may also investigate the behavior of $\sum_{T,j,k} \gamma_{T,j,k}$. Suppose there are two prevertices on each circle C_j

$$\begin{aligned} p_{0,1} &= c_0 + r_0, & p_{0,2} &= c_0 - r_0, \\ p_{1,1} &= c_1 + r_1, & p_{1,2} &= c_1 - r_1, \end{aligned}$$

where $c_j \in \mathbb{R}$ is the center and r_j the radius of C_j, $j = 0, 1$.[24] By the geometry of the image domain, the values $a_{j,1}$, $a_{j,2}$ for each circle C_j must be equal. We even choose all a to be equal:

$$a_{0,1} = a_{0,2} = a_{1,1} = a_{1,2} = a.$$

We will further denote the transformation T, by

$$T = \begin{pmatrix} A & B \\ C & D \end{pmatrix}, \qquad U = T^{-1} = \begin{pmatrix} D & -B \\ -C & A \end{pmatrix}.$$

[24] The circle C_0 was already normalized to $\partial\mathbb{D}$.

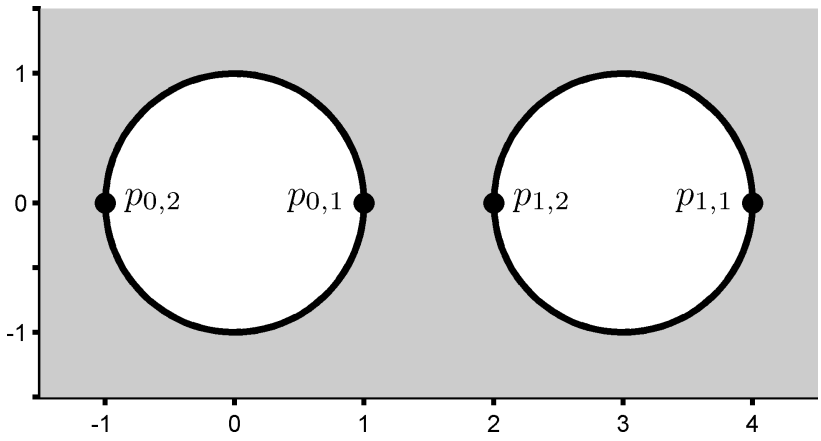

Figure 28: The example domain for $c_1 = 3$ and $r_1 = 1$.

The sum over the γ of the second generation (with applied T and U) is

$$\begin{aligned}\sum_{j,k}\gamma_{T,j,k}+\sum_{j,k}\gamma_{U,j,k} &= \sum_{j,k}((Cp_{j,k}+D)^2\gamma_{j,k}+2C(Cp_{j,k}+D)a)\\ &\quad+\sum_{j,k}((-Cp_{j,k}+A)^2\gamma_{j,k}-2C(-Cp_{j,k}+A)a)\\ &= \sum_{j,k}(C^2(p_{j,k}-u_T)^2\gamma_{j,k}+2C^2(p_{j,k}-u_T)a)\\ &\quad+\sum_{j,k}(C^2(p_{j,k}-u_U)^2\gamma_{j,k}+2C^2(p_{j,k}-u_U)a),\end{aligned}$$

where $u_T = -\frac{D}{C}$ and $u_U = \frac{A}{C}$ are the centers of the isometric circles of the transformations. Since the circles are symmetric to the line with constant real part $\frac{1}{2}(c_0+c_1)$, the centers of the isometric circles are also symmetric. This leads to

$$\begin{aligned}p_{0,2}-u_T &= -(p_{1,1}-u_U), & p_{0,1}-u_T &= -(p_{1,2}-u_U),\\ p_{1,1}-u_T &= -(p_{0,2}-u_U), & p_{1,2}-u_T &= -(p_{0,1}-u_U).\end{aligned}$$

Hence, the factors of a drop out of the sum, which gives us

$$\sum_{j,k}\gamma_{T,j,k}+\sum_{j,k}\gamma_{U,j,k} = \sum_{j,k}C^2(p_{j,k}-u_T)^2\gamma_{j,k}+\sum_{j,k}C^2(p_{j,k}-u_U)^2\gamma_{j,k}.$$

Since $C = c_1$ and $p_{j,k} - u$ are real, the coefficients of the γ are all positive as they are taken to the second power. This is also true for successive applications of T and U. Therefore, the sum over γ for each generation grows, i.e.

$$\sum_{j,k}\gamma_{T,j,k} < \sum_{j,k}\gamma_{V,j,k} \quad \text{for} \quad |T| < |V|,$$

and so the sum $\sum_{T,j,k}\gamma_{T,j,k}$ over all generations tends to infinity, if there are no further requirements for γ.

4.1.4 Idea Regarding the Convergence

Based on the behavior of γ, it is reasonable to assume that $\mathcal{A}_C(z,T,j,k) \neq 0$ to ensure the convergence of $\mathcal{K}$. Referring to Mittag-Leffler's theorem we can expand one of the principal parts of (4.6) around a point l in terms of $(z-l)^{-1}$ to obtain

$$\frac{a}{(z-p)^2}+\frac{\gamma}{(z-p)}=\frac{\gamma}{(z-l)}+\frac{a+\gamma(p-l)}{(z-l)^2}+\frac{2a(p-l)+\gamma(p-l)^2}{(z-l)^3}+O((z-l)^{-4}).$$

Since $\mathcal{A}_C$ can only have poles in Λ, we match each transformation of the circular domain $T(D)$ with a limit point l_T inside the convex hull of $T(D)$. This allows us to state our first approach to the convergence of $\mathcal{K}$.

Lemma 4.15
Let D be a circular domain, infinity an ordinary point of $\mathbb{M}(D)$ lying in D_R and Λ the limit set of $\mathbb{M}(D)$. Further let

$$\varepsilon=\frac{1}{4}\max_{l_1,l_2\in\Lambda}\{|l_1-l_2|\}.$$

The candidate function $\mathcal{K}$ in the form

$$\begin{aligned}\mathcal{K}(z)=&\sum_{j,k}\left(\frac{a_{j,k}}{(z-p_{j,k})^2}+\frac{\gamma_{j,k}}{z-p_{j,k}}\right)\\&+\sum_{T,j,k}{}'\left(\frac{a_{j,k}}{(z-p_{T,j,k})^2}+\frac{\gamma_{T,j,k}}{z-p_{T,j,k}}-\frac{\gamma_{T,j,k}}{(z-l_T)}\right.\\&\left.-\frac{a_{j,k}+\gamma_{T,j,k}(p_{T,j,k}-l_T)}{(z-l_T)^2}-\frac{2a_{j,k}(p_{T,j,k}-l_T)+\gamma_{T,j,k}(p_{T,j,k}-l_T)^2}{(z-l_T)^3}\right),\end{aligned}$$

converges locally uniformly on D, where $l_T\in\Lambda$ and $|T^{-1}(l_T)-T^{-1}(\infty)|>\varepsilon$.
The symbol $\sum'$ indicates the sum without the identity.

We will not rely on this lemma later on, therefore the proof is not stated here, but can be found in the appendix at A.2.
The lemma is none the less quite interesting. The discussion so far allows the convergence only for a similar construction with poles in the limit points. However, the version above is not actually suitable; while it provides the convergence, it is not compatible with the functional equation (Lemma 4.5) of the Schwarzian. If the functional equation is applied to $\mathcal{K}$, the coefficients and the poles do not match any longer. We will therefore search for an invariant expression regarding the functional equation.

4.1.5 Note about the Boundary Values

We are investigating conformal mappings onto MCCAPDs. This means that the boundaries of the image domains consist of circular arcs, while the preimages are bounded by circles.
According to Lemma 2.16, a mapping f from a circular arc $z(t) = re^{it} + c$ onto a circular arc leads to the property

$$(z-c)^2\{f,z\} \in \mathbb{R}$$

for the Schwarzian. Hence in the context of the MCCAPD mapping, we should have

$$(z-c_j)^2\mathcal{S}(z) \in \mathbb{R}, \qquad z \in C_j,\ j = 0,\dots,m, \tag{4.12}$$

where c_j indicates the center of C_j. The only exceptions would be the prevertices, as they are poles of the Schwarzian.

Lemma 4.11 requires the Schwarzian to satisfy the functional equation

$$\mathcal{S}(z) = \sigma'(z)^2\overline{\mathcal{S}(\overline{\sigma(z)})} \tag{4.13}$$

for every reflection $s \in \mathbb{S}(D)$ against one of the boundary circles.
Suppose $z = re^{i\varphi} + c$ to be on a boundary circle C of D, and s to be the reflection against this circle C. We have $s(z) = z$ and σ is defined by $\sigma(z) = \overline{s(z)}$. If a candidate function $\mathcal{K}$ satisfies the functional equation (4.13), we can reshape the equation to

$$\begin{aligned}\mathcal{K}(z) = (\sigma'(z))^2\overline{\mathcal{K}(\overline{\sigma(z)})} = \left(\frac{r}{z-c}\right)^4\overline{\mathcal{K}(z)} = (e^{-i\varphi})^2(\overline{e^{i\varphi}})^2\overline{\mathcal{K}(z)}\\ \Rightarrow\ (e^{i\varphi})^2\mathcal{K}(z) = \overline{(e^{i\varphi})^2\mathcal{K}(z)}.\end{aligned}$$

If we substitute again, but this time with $e^{i\varphi} = \frac{z-c}{r}$, and multiply both sides with r^2, we get

$$(z-c)^2\mathcal{K}(z) = \overline{(z-c)^2\mathcal{K}(z)}, \qquad z \in C_j \setminus \{p_{j,k} | k = 1\dots K_j\},\ j = 0,\dots,m.$$

This means that $(z-c)^2\mathcal{K}(z)$ is real, i.e. the candidate function also satisfies equation (4.12).
Hence, any candidate function that satisfies the functional equation (4.13) also satisfies equation (4.12). It is therefore not necessary to verify if the boundary is actually mapped onto circular arcs.

4.2 Mappings onto Doubly Connected Domains

In most cases the limit set Λ of $\mathbb{M}(D)$ contains an infinite number of points (Lemma 2.25). The only exceptions are the groups generated for doubly connected domains D with only two limit points. Since the analytic parts of $\mathcal{S}$ depend on Λ, we investigate this simplified case first.
While we were supposing for the common case that either zero or infinity should be in D, we switch here to annuli of the form $\mathbb{A} = \{ z \,|\, r < |z| < 1 \}$. Not only are the annuli the most common canonical region for doubly connected mappings, but also the groups $\mathbb{M}(\mathbb{A})$ will be quite simple.
It is sufficient to investigate the mappings from the annuli. If needed, we can change each preimage domain by applying a Möbius transformation. For a given circular domain D, we only have to find the transformation $H \in \mathbb{M}$ which maps D onto a conformally equivalent annulus $\mathbb{A} = H(D)$ (Figure 29). The new Schwarzian $\{f \circ H, z\}$ is then given by $H'(z)^2\{f, H(z)\} = H'(z)^2\mathcal{S}(H(z))$ if f refers to the conformal mapping from this annulus onto the MCCAPD (or *DCCAPD* for *doubly connected circular arc polygon domain*) $f(\mathbb{A}) = f(H(D))$.

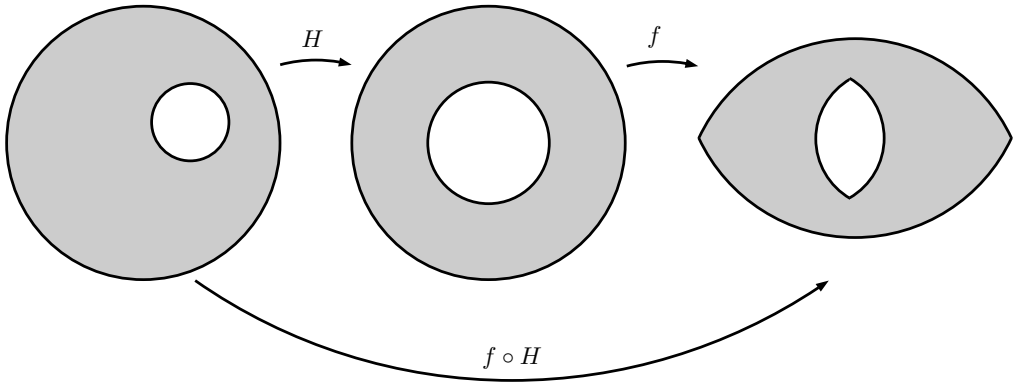

Figure 29: A change of the preimage domain of a mapping f can be established by applying a Möbius transformation H in the form $f \circ H$.

We will restate the results from above, but modify them for annuli. The reflections against the boundaries are $s_0(z) = \frac{1}{\bar{z}}$ and $s_1(z) = \frac{r^2}{\bar{z}}$. The only generating transformation for $\mathbb{M}(\mathbb{A})$ is therefore the scaling $T(z) = r^2 z$, so $\mathbb{M}(\mathbb{A}) = \{ r^{2n} z \,|\, n \in \mathbb{Z} \}$. Hence, the maximum extension of $\mathbb{A}$ is $\mathbb{A}_E := \mathbb{C} \setminus \{0\}$, as the limit points of $\mathbb{M}(\mathbb{A})$ are 0 and ∞. By inserting these values and combining our Lemmas 4.5, 4.10 and 4.11 we get:

Lemma 4.16
The Schwarzian derivative of a conformal mapping from the annulus $\mathbb{A} = \{ z \,|\, r <$

$|z| < 1\}$ *onto a DCCAPD is of the form*

$$\mathcal{S}(z) = \sum_{n=-\infty}^{\infty} \sum_{j,k} \left(\frac{a_{j,k}}{(z - r^{2n} p_{j,k})^2} + \frac{\gamma_{j,k}}{r^{2n}} \frac{1}{z - r^{2n} p_{j,k}} + \mathcal{A}_C(z, n, j, k) \right) + \mathcal{A}_R(z),$$

where the functions $\mathcal{A}_C$ *and* $\mathcal{A}_R$ *are analytic in* $\mathbb{A}_E = \mathbb{C} \setminus \{0\}$*. Further,* $\mathcal{S}$ *satisfies the functional equations*

$$\mathcal{S}(z) = r^4 \mathcal{S}(r^2 z),$$
$$\mathcal{S}(z) = z^{-4} \overline{\mathcal{S}(\overline{z}^{-1})}.$$

We also rewrite $\mathcal{K}$ and Lemma 4.15. The only limit points are 0 and ∞, while the fractions for $l_T = \infty$ vanish. Hence, we have found the following convergence statement:

Lemma 4.17
The candidate function $\mathcal{K}$ *for the annulus* $\mathbb{A} = \{ z \,|\, r < |z| < 1\}$ *of the form*

$$\mathcal{K}(z) = \sum_{n=-\infty}^{\infty} \sum_{j,k} \left(\frac{a_{j,k}}{(z - r^{2n} p_{j,k})^2} + \frac{\gamma_{j,k}}{r^{2n}} \frac{1}{z - r^{2n} p_{j,k}} + \mathcal{A}_C(z, n, j, k) \right)$$

converges uniformly on closed sets $M \subset \mathbb{A}_E$ *not containing prevertices* $r^{2n} p_{j,k}$*, where*

$$\mathcal{A}_C(z, n, j, k) = \begin{cases} -\frac{\gamma_{j,k}}{r^{2n} z} - \frac{a_{j,k} + \gamma_{j,k} p_{j,k}}{z^2} & \text{for } n > 0 \\ 0 & \text{for } n \leq 0 \end{cases}.$$

Proof. Let $M \subset \mathbb{A}_{E,p} := \mathbb{C} \setminus (\{0\} \cup \{r^{2n} p_{j,k}\})$ be a closed subset of $\mathbb{A}_{E,p}$ and $z \in M$. Based on the piecewise definition of $\mathcal{A}_C$, we split up the sum.

If n is negative we have for $r < 1$ and $m = -n$

$$\lim_{m \to \infty} r^{-2m} = \infty \quad \Rightarrow \quad \lim_{m \to \infty} |z - r^{-2m} p_{j,k}| = \infty$$

and so our formula becomes

$$\lim_{m \to \infty} \left(\frac{a_{j,k}}{(z - r^{-2m} p_{j,k})^2} + \frac{\gamma_{j,k}}{r^{-2m}} \frac{1}{(z - r^{-2m} p_{j,k})} \right) = 0,$$

since each of the denominators grow with r^{-4m} while the numerators are fixed.
A more exact formulation gives us

$$\max_{z,m,j,k} \left| \frac{a_{j,k} + (r^{2m} z - p_{j,k}) \gamma_{j,k}}{(r^{2m} z - p_{j,k})^2} \right| = \lambda_1$$

as the terms $|r^{2m} z - p_{j,k}| > \varepsilon > 0$ have a lower boundary for all $z \in M$ and tend to

$|p_{j,k}|$ for rising m. Therefore, we have

$$\left|\frac{a_{j,k}}{(z-r^{-2m}p_{j,k})^2}+\frac{r^{2m}\gamma_{j,k}}{(z-r^{-2m}p_{j,k})}\right| = r^{4m}\left|\frac{a_{j,k}+(r^{2m}z-p_{j,k})\gamma_{j,k}}{(r^{2m}z-p_{j,k})^2}\right| \leq r^{4m}\lambda_1$$

and this concludes for the sum over the negative values of n

$$\begin{aligned}
&\left|\sum_{n=-\infty}^{-1}\sum_{j,k}\left[\frac{a_{j,k}}{(z-r^{2n}p_{j,k})^2}+\frac{\gamma_{j,k}}{r^{2n}}\frac{1}{(z-r^{2n}p_{j,k})}\right]\right| \\
&\leq \sum_{n=-\infty}^{-1}\sum_{j,k}\left|\frac{a_{j,k}}{(z-r^{2n}p_{j,k})^2}+\frac{\gamma_{j,k}}{r^{2n}}\frac{1}{(z-r^{2n}p_{j,k})}\right| \\
&\leq \sum_{m=1}^{\infty} r^{4m}\sum_{j,k}\left|\frac{a_{j,k}+(r^{2m}z-p_{j,k})\gamma_{j,k}}{(r^{2m}z-p_{j,k})^2}\right| \\
&\leq 2\max_j\{K_j\}\lambda_1\sum_{m=1}^{\infty} r^{4m} < \infty.
\end{aligned}$$

The first half is therefore converging locally uniformly on $\mathbb{A}_{E,p}$.

The case of a positive n is less simple. The main problem is that $\frac{\gamma_{j,k}}{r^{2n}}$ goes to infinity for growing n, while the sums

$$\sum_{j=0}^{1}\sum_{k=1}^{K_j}\left(\frac{a_{j,k}}{(z-r^{2n}p_{j,k})^2}+\frac{\gamma_{j,k}}{r^{2n}}\frac{1}{(z-r^{2n}p_{j,k})}-\frac{\gamma_{j,k}}{r^{2n}z}-\frac{a_{j,k}+\gamma_{j,k}p_{j,k}}{z^2}\right)$$

must go to zero. If we investigate one of these summands, we see

$$\begin{aligned}
&\frac{a_{j,k}}{(z-r^{2n}p_{j,k})^2}+\frac{\gamma_{j,k}}{r^{2n}}\frac{1}{(z-r^{2n}p_{j,k})}-\frac{\gamma_{j,k}}{r^{2n}z}-\frac{a_{j,k}+\gamma_{j,k}p_{j,k}}{z^2} \\
&= r^{2n}p_{j,k}\left(a_{j,k}\frac{2z-r^{2n}p_{j,k}}{(z-r^{2n}p_{j,k})^2z^2}+\frac{\gamma_{j,k}p_{j,k}}{(z-r^{2n}p_{j,k})z^2}\right).
\end{aligned}$$

Because r^{2n} goes to zero, the factor $|z-r^{2n}p|$ in the denominator has a lower boundary and tends to $|z|$ for growing n. Since the numerators are also bounded, there must be an upper boundary for the whole expression

$$\max_{z,n,j,k}\left|p_{j,k}\left(a_{j,k}\frac{2z-r^{2n}p_{j,k}}{(z-r^{2n}p_{j,k})^2z^2}+\frac{\gamma_{j,k}p_{j,k}}{(z-r^{2n}p_{j,k})z^2}\right)\right| = \lambda_2.$$

Application of this results in

$$\left|\sum_{n=1}^{\infty}\sum_{j,k}\left[\frac{a_{j,k}}{(z-r^{2n}p_{j,k})^2}+\frac{\gamma_{j,k}}{r^{2n}}\frac{1}{(z-r^{2n}p_{j,k})}+\mathcal{A}_C(z,n,j,k)\right]\right|$$

$$\leq \sum_{n=1}^{\infty} \sum_{j,k} \left| \frac{a_{j,k}}{(z - r^{2n} p_{j,k})^2} + \frac{\gamma_{j,k}}{r^{2n}} \frac{1}{(z - r^{2n} p_{j,k})} + \mathcal{A}_C(z, n, j, k) \right|$$

$$\leq \sum_{n=1}^{\infty} r^{2n} \sum_{j,k} \left| p_{j,k} \left(a_{j,k} \frac{2z - p_{j,k} r^{2n}}{(z - r^{2n} p_{j,k})^2 z^2} + \frac{\gamma_{j,k} p_{j,k}}{(z - r^{2n} p_{j,k}) z^2} \right) \right|$$

$$\leq 2 \max_j \{K_j\} \lambda_2 \sum_{n=1}^{\infty} r^{2n} < \infty.$$

This shows the locally uniformly convergence of $\mathcal{K}$ on $\mathbb{A}_{E,p}$. □

4.2.1 Construction of the Schwarzian Derivative

We have a candidate function in Lemma 4.17, which has the same poles in $\mathbb{A}_E = \mathbb{C} \setminus \{0\}$ as $\mathcal{S}$. The next step would be to ensure the functional equations of Lemma 4.16, but we will need one more result before we continue. We have found the following connection between the parameters of the Schwarzian derivative:

Lemma 4.18
The parameters a, p and γ of the Schwarzian derivative of a conformal mapping from an annulus $\mathbb{A}$ onto a DCCAPD satisfy the equation

$$\sum_{j=0}^{1} \sum_{k=1}^{K_j} (p_{j,k} \gamma_{j,k} + a_{j,k}) = 0, \tag{4.14}$$

where every term $(p_{j,k}\gamma_{j,k} + a_{j,k})$ is purely imaginary.

Proof. If we integrate along the circles $\delta(t) = \rho \exp(it)$, where $1 < \rho < r^{-1}$, and $\zeta(t) = r^2 \delta(t)$, the annulus $\mathbb{A}$ lies between both curves (Figure 30). This is possible, as we extended $\mathcal{S}$ over both boundaries. Based on the residue theorem, the difference of the two integrals can be expressed as the sum over the enclosed residues

$$\int_{\delta} z\mathcal{S}(z)dz - \int_{\zeta} z\mathcal{S}(z)dz = 2\pi i \sum_{j,k} (p_{j,k}\gamma_{j,k} + a_{j,k}), \tag{4.15}$$

since

$$z \left(\frac{a}{(z-p)^2} + \frac{\gamma}{(z-p)} \right) = \frac{ap}{(z-p)^2} + \frac{a + \gamma p}{(z-p)} + \gamma.$$

However, by using the functional equation we obtain

$$\int_\zeta z\mathcal{S}(z)dz = \int_0^{2\pi} r^2\delta(t)\mathcal{S}(r^2\delta(t))r^2\dot{\delta}(t)dt = \int_0^{2\pi} \delta(t)\mathcal{S}(\delta(t))\dot{\delta}(t)dt = \int_\delta z\mathcal{S}(z)dz,$$

and therefore have

$$\int_\delta z\mathcal{S}(z)dz - \int_\zeta z\mathcal{S}(z)dz = \int_\delta z\mathcal{S}(z)dz - \int_\delta z\mathcal{S}(z)dz = 0. \tag{4.16}$$

Combining the equations (4.15) and (4.16) gives us

$$\sum_{j,k}(p_{j,k}\gamma_{j,k} + a_{j,k}) = 0.$$

The statement that each $(p_{j,k}\gamma_{j,k} + a_{j,k})$ is purely imaginary follows from Lemma 4.12. □

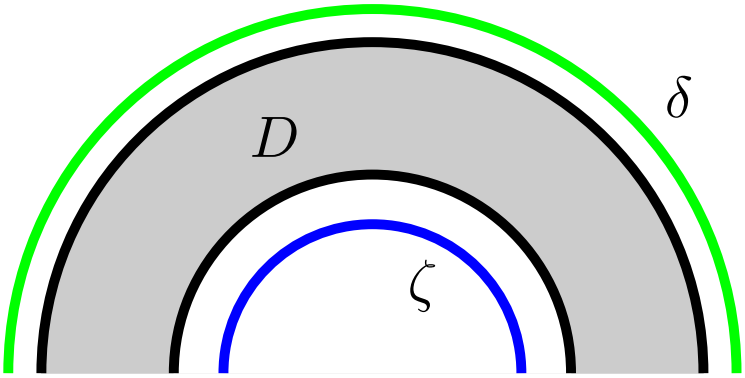

Figure 30: The curves used in the proof of Lemma 4.18 enclose the annulus $r < |z| < 1$. The parametrization δ describes a circle with center zero and a radius greater than 1 and ζ describes a circle whose center is also zero but with a radius smaller than r

To ensure that each term $p_{j,k}\gamma_{j,k} + a_{j,k}$ is purely imaginary, we will use the parameter $\mu_{j,k}$ (Lemma 4.13) with

$$i\mu_{j,k} = p_{j,k}\gamma_{j,k} + a_{j,k}$$

instead of $\gamma_{j,k}$. The restricting equation (4.14) therefore simplifies to

$$\sum_{j=0}^{1}\sum_{k=1}^{K_j}\mu_{j,k} = 0.$$

We will also substitute γ in $\mathcal{K}$ of Lemma 4.17 and apply the restricting equation to further simplify the result.

Lemma 4.19
The candidate function $\mathcal{K}$ for the annulus $\mathbb{A} = \{ z \,|\, r < |z| < 1\}$ of the form

$$\mathcal{K}(z) = \sum_{n=-\infty}^{\infty} \sum_{j,k} \left(\frac{a_{j,k}}{(z - r^{2n} p_{j,k})^2} + \frac{i\mu_{j,k} - a_{j,k}}{r^{2n} p_{j,k} (z - r^{2n} p_{j,k})} - \frac{i\mu_{j,k} - a_{j,k}}{r^{2n} p_{j,k} z} \right),$$

where $\sum_{j,k} \mu_{j,k} = 0$, converges uniformly on closed sets $M \subset \mathbb{A}_E$ not containing prevertices $r^{2n} p_{j,k}$.

Proof. According to Lemma 4.17, we know that

$$\mathcal{K}_1(z) = \sum_{n=-\infty}^{\infty} \sum_{j,k} \left(\frac{a_{j,k}}{(z - r^{2n} p_{j,k})^2} + \frac{i\mu_{j,k} - a_{j,k}}{r^{2n} p_{j,k} (z - r^{2n} p_{j,k})} + \mathcal{A}_1(z, n, j, k) \right),$$

converges locally uniformly on $\mathbb{A}_{E,p} := \mathbb{C} \setminus (\{0\} \cup \{r^{2n} p_{j,k}\})$, where

$$\mathcal{A}_1(z, n, j, k) = \begin{cases} -\frac{i\mu_{j,k} - a_{j,k}}{r^{2n} p_{j,k} z} - \frac{i\mu_{j,k}}{z^2} & \text{for } n > 0 \\ 0 & \text{for } n \leq 0 \end{cases}.$$

The function $\mathcal{K}_1$ will now be modified to match the shape shown in the lemma.
For easier handling, we define

$$\tau_1 := -\sum_{j,k} \frac{i\mu_{j,k} - a_{j,k}}{p_{j,k}}, \qquad \tau_2 := -\sum_{j,k} i\mu_{j,k},$$

and rewrite $\mathcal{K}_1$ by reordering the finite sums to

$$\mathcal{K}_2(z) := \sum_{n=-\infty}^{\infty} \left(\sum_{j,k} \left(\frac{a_{j,k}}{(z - r^{2n} p_{j,k})^2} + \frac{i\mu_{j,k} - a_{j,k}}{r^{2n} p_{j,k} (z - r^{2n} p_{j,k})} \right) + \mathcal{A}_2(z, n, j, k) \right),$$

where

$$\mathcal{A}_2(z, n, j, k) := \begin{cases} \frac{\tau_1}{r^{2n} z} + \frac{\tau_2}{z^2} & \text{for } n > 0 \\ 0 & \text{for } n \leq 0 \end{cases}.$$

$\mathcal{K}_2$ is converging, as its only difference from $\mathcal{K}_1$ is a reordering in the finite part of the sum. We know that τ_2 is zero because of Lemma 4.18, and so we may neglect it in the future.
For negative n, we have

$$\sum_{n=-\infty}^{0} \frac{-\tau_1}{r^{2n} z} = \frac{\tau_1}{(r^2 - 1) z}$$

due to the identity

$$\sum_{n=-\infty}^{0} \frac{1}{r^{2n}} = \sum_{n=0}^{\infty} (r^2)^n = \frac{-1}{r^2-1}.$$

This allows us to define

$$\begin{aligned}\mathcal{K}_3(z) &:= \mathcal{K}_2(z) + \frac{\tau_1}{(r^2-1)z} \\ &= \sum_{n=-\infty}^{\infty} \sum_{j,k} \left(\frac{a_{j,k}}{(z-r^{2n}p_{j,k})^2} + \frac{i\mu_{j,k}-a_{j,k}}{r^{2n}p_{j,k}(z-r^{2n}p_{j,k})} - \frac{i\mu_{j,k}-a_{j,k}}{r^{2n}p_{j,k}z} \right).\end{aligned}$$

$\mathcal{K}_3$ is converging on $\mathbb{A}_{E,p}$ as $\mathcal{K}_2$ is doing so. Reordering the finite part again leads to the form of the lemma. □

With the convergence ensured, we will introduce a form of $\mathcal{K}$, which satisfies the functional equations.

Lemma 4.20
The candidate function $\mathcal{K}$ of the form

$$\mathcal{K}(z) = \sum_{n=-\infty}^{\infty} \sum_{j,k} \left(\frac{a_{j,k}}{(z-r^{2n}p_{j,k})^2} + \frac{i\mu_{j,k}-a_{j,k}}{z(z-r^{2n}p_{j,k})} \right) + \frac{ib_i}{z^2},$$

where $\sum_{j,k} \mu_{j,k} = 0$ and

$$b_i = -\frac{1}{2} \sum_{k=1}^{K_1} \mu_{1,k} \in \mathbb{R},$$

satisfies the equations

$$\begin{aligned}\mathcal{K}(z) &= r^4 \mathcal{K}(r^2 z), \\ \mathcal{K}(z) &= z^{-4} \overline{\mathcal{K}(\overline{z}^{-1})}.\end{aligned}$$

Proof. First we show $\mathcal{K}(z) = z^{-4}\overline{\mathcal{K}(\overline{z}^{-1})}$. For ease of calculation, we define

$$\tau(z,n,j,k) := \frac{a_{j,k}}{(z-p_{n,j,k})^2} + \frac{i\mu_{j,k}-a_{j,k}}{z(z-p_{n,j,k})},$$

where $p_{n,j,k} = r^{2n}p_{j,k}$, to calculate

$$z^{-4}\overline{\tau(\overline{z}^{-1},n,j,k)} = \frac{a_{j,k}}{(z-q)^2} + \frac{i\mu_{j,k}-a_{j,k}}{z(z-q)} - \frac{i\mu_{j,k}}{z^2}$$

where $q = \overline{p_{n,j,k}}^{-1}$. Depending on the circle C_j on which the initial $p_{j,k}$ lies, we have

$$\overline{p_{n,j,k}}^{-1} = \begin{cases} p_{-n,j,k} & \text{for } j = 0 \\ p_{-n-1,j,k} & \text{for } j = 1 \end{cases}.$$

Using this fact, we can reshape the expression above to

$$z^{-4}\overline{\tau(\bar{z}^{-1}, n, j, k)} = \begin{cases} \tau(z, -n, j, k) - \frac{i\mu_{j,k}}{z^2} & \text{for } j = 0 \\ \tau(z, -n-1, j, k) - \frac{i\mu_{j,k}}{z^2} & \text{for } j = 1 \end{cases}. \tag{4.17}$$

The candidate function $\mathcal{K}(z) = \lim_{N\to\infty} \mathcal{K}_N(z)$ is the limit of

$$\begin{aligned} \mathcal{K}_N(z) &= \sum_{n=-N}^{N} \sum_{j,k} \left(\frac{a_{j,k}}{(z - r^{2n} p_{j,k})^2} + \frac{i\mu_{j,k} - a_{j,k}}{z(z - r^{2n} p_{j,k})} \right) + \frac{ib_i}{z^2} \\ &= \sum_{n=-N}^{N} \sum_{j,k} \tau(z, n, j, k) + \frac{ib_i}{z^2}. \end{aligned}$$

For the expression $z^{-4}\overline{\mathcal{K}_N(\overline{z}^{-1})}$ of the functional equation we have, by using equation (4.17),

$$\begin{aligned} z^{-4}\overline{\mathcal{K}_N(\overline{z}^{-1})} &= \sum_{n=-N}^{N} \sum_{j,k} z^{-4}\overline{\tau(\overline{z}^{-1}, n, j, k)} - \frac{ib_i}{z^2} \\ &= \sum_{n=-N}^{N} \left(\sum_{k=1}^{K_0} \tau(z, -n, 0, k) + \sum_{k=1}^{K_1} \tau(z, -n-1, 1, k) \right) - \frac{ib_i}{z^2} \\ &= \sum_{n=-N}^{N} \sum_{k=1}^{K_0} \tau(z, n, 0, k) + \sum_{n=-N-1}^{N-1} \sum_{k=1}^{K_1} \tau(z, n, 1, k) - \frac{ib_i}{z^2}. \end{aligned}$$

The terms $i\mu_{j,k} z^{-2}$ vanish in the sum according to Lemma 4.18, since we have an equal amount of sums $\sum_k i\mu_{j,k} z^{-2}$ for $j = 0$ as for $j = 1$.
If we compare $\mathcal{K}_N(z)$ with $z^{-4}\overline{\mathcal{K}_N(\overline{z}^{-1})}$, we can cancel out the expressions τ with equal parameters. Hence, the difference can be written as

$$\begin{aligned} \mathcal{K}_N(z) - z^{-4}\overline{\mathcal{K}_N(\overline{z}^{-1})} &= \sum_{k=1}^{K_1} \tau(z, N, 1, k) + \frac{ib_i}{z^2} - \left(\sum_{k=1}^{K_1} \tau(z, -N-1, 1, k) - \frac{ib_i}{z^2} \right) \\ &= \sum_{k=1}^{K_1} \left(\frac{a_{1,k}}{(z - r^{2N} p_{1,k})^2} + \frac{i\mu_{1,k} - a_{1,k}}{z(z - r^{2N} p_{1,k})} \right) \\ &\quad - \sum_{k=1}^{K_1} \left(\frac{a_{1,k}}{(z - r^{-2N-2} p_{1,k})^2} + \frac{i\mu_{1,k} - a_{1,k}}{z(z - r^{-2N-2} p_{1,k})} \right) + \frac{2ib_i}{z^2}. \end{aligned}$$

If we now apply the limit for N to infinity, we obtain

$$\lim_{N\to\infty}\left(\mathcal{K}_N(z) - z^{-4}\overline{\mathcal{K}_N(\overline{z}^{-1})}\right) = \sum_{k=1}^{K_1}\left(\frac{a_{1,k}}{z^2} + \frac{i\mu_{1,k} - a_{1,k}}{z^2}\right) + \frac{2ib_i}{z^2}.$$

Hence, the functional equation $\mathcal{K}(z) = z^{-4}\overline{\mathcal{K}(\overline{z}^{-1})}$ holds only if we have

$$b_i = -\frac{1}{2}\sum_{k=1}^{K_1}\mu_{1,k}.$$

Note that b_i is real, as every $\mu_{1,k}$ is real.

For the other functional equation $\mathcal{K}(z) = r^4\mathcal{K}(r^2z)$, we define

$$\tau(z,n) := \sum_{j,k}\left(\frac{a_{j,k}}{(z-p_{n,j,k})^2} + \frac{i\mu_{j,k} - a_{j,k}}{z(z-p_{n,j,k})}\right)$$

and therefore have by calculation

$$r^4\tau(r^2z,n) = \tau(z,n-1).$$

This time the difference of the two sides of the functional equation takes the form

$$\begin{aligned}\mathcal{K}_N(z) - r^4\mathcal{K}_N(r^2z) &= \left(\tau(z,N) + \frac{ib_i}{z^2}\right) - \left(\tau(z,-N-1) + \frac{ib_i}{z^2}\right)\\ &= \tau(z,N) - \tau(z,-N-1)\end{aligned}$$

and in the limit case

$$\lim_{N\to\infty}\left(\mathcal{K}_N(z) - r^4\mathcal{K}_N(r^2z)\right) = \sum_{j,k}\left(\frac{a_{j,k}}{z^2} + \frac{i\mu_{j,k} - a_{j,k}}{z^2}\right) = 0$$

according to Lemma 4.18. This proves the second equation. □

With the functional equations satisfied, we are able to state the remaining difference between $\mathcal{K}$ and $\mathcal{S}$.

Lemma 4.21
The Schwarzian derivative of a conformal mapping of the annulus $\mathbb{A}$ onto a DCCAPD is of the form

$$\mathcal{S}(z) = \mathcal{K}(z) + \frac{b_r}{z^2},$$

where $\mathcal{K}$ as in Lemma 4.20 and $b_r \in \mathbb{R}$.

Proof. The difference $\mathcal{T}(z) := \mathcal{S}(z) - \mathcal{K}(z)$ is holomorphic in $\mathbb{A}_E$, as $\mathcal{S}$ and $\mathcal{K}$ have the same poles in D_E, and further satisfies the equations

$$\mathcal{T}(z) = r^4 \mathcal{T}(r^2 z), \tag{4.18}$$

$$\mathcal{T}(z) = \frac{1}{z^4} \overline{\mathcal{T}\left(\frac{1}{\overline{z}}\right)}, \tag{4.19}$$

as $\mathcal{S}$ and $\mathcal{K}$ satisfy them. Since $\mathcal{T}$ can only have poles at zero and infinity, it must be of the form

$$\mathcal{T}(z) = \sum_{n=-\infty}^{\infty} d_n z^n,$$

but equation (4.18) reduces this to

$$\mathcal{T}(z) = \frac{b_r}{z^2},$$

where $b_r = d_{-2}$, while equation (4.19) provides $b_r \in \mathbb{R}$. □

We restate the last result to explicitly show our version of the Schwarzian derivative for conformal mappings onto doubly connected CAPDs.

Theorem 4.22
Let P be a doubly connected circular arc polygon domain bounded by the circular arc polygons P_j, $j = 0, 1$, with the vertices $v_{j,k}$, $k = 1, \ldots, K_j$, and the interior angles $\alpha_{j,k}\pi$. Further, let $\mathbb{A} = \{ z \,|\, r < |z| < 1 \}$ be the annulus conformally equivalent to P. The Schwarzian derivative $\mathcal{S}$ of any conformal mapping f of $\mathbb{A}$ onto P has the form

$$\mathcal{S}(z) = \sum_{n=-\infty}^{\infty} \sum_{j,k} \left(\frac{a_{j,k}}{(z - r^{2n} p_{j,k})^2} + \frac{i\mu_{j,k} - a_{j,k}}{z(z - r^{2n} p_{j,k})} \right) + \frac{b}{z^2}.$$

The parameters of the formula are the prevertices $p_{j,k} \in \{ p_{j,k} \,|\, p_{j,k} \in C_j,\ f(p_{j,k}) = v_{j,k} \}$, the interior angles $\pi\alpha_{j,k}$ in the form $a_{j,k} = \frac{1}{2}(1 - \alpha_{j,k}^2)$, the additional parameters $\mu_{j,k} \in \mathbb{R}$ and b, where

$$\sum_{k=1}^{K_0} \mu_{0,k} + \sum_{k=1}^{K_1} \mu_{1,k} = 0, \tag{4.20}$$

$$\operatorname{Im}(b) = \frac{1}{2} \sum_{k=1}^{K_0} \mu_{0,k}. \tag{4.21}$$

4.2.2 Mappings from Generic Doubly Connected Circular Domains

Until now, we have only investigated mappings for the case where the preimage domain is an annulus. To get the shape of $\mathcal{S}$ for a more generic doubly connected circular domain D, we apply a Möbius transformation H, where $H(D) = \mathbb{A}$, to the known Schwarzian $\{f, z\}$ for the annulus $\mathbb{A}$ to calculate $\{f \circ H, z\}$, where $f \circ H$ is a conformal mapping from a non-annulus circular domain onto a DCCAPD. The Schottky group

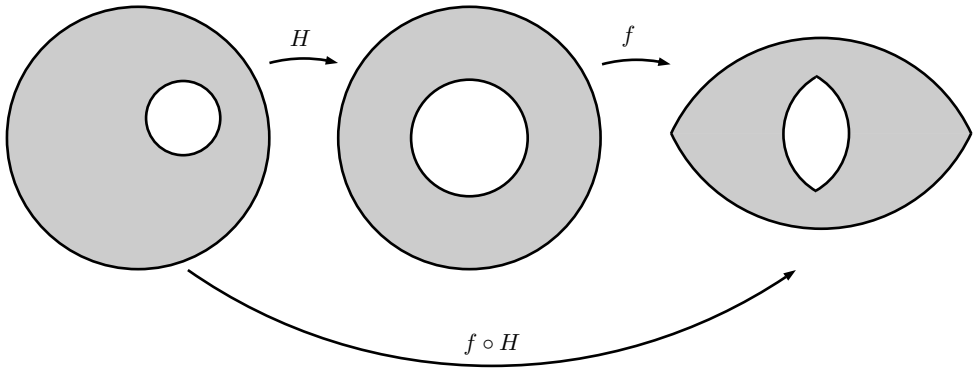

Figure 31: A change of the preimage domain of a mapping f can be established by applying a Möbius transformation H in the form $f \circ H$.

$\mathbb{M}(D)$ still has only two limit points l_1 and l_2, as it is generated by one transformation $T = s_0 \circ s_1$, i.e. $\text{gen}(\mathbb{M}(D)) = \{T, T^{-1}\}$. Hence, the modified version of our version of the Schwarzian is of the form:[25]

Theorem 4.23
Let P be a doubly connected circular arc polygon domain bounded by the circular arc polygons P_j, $j = 0, 1$, with the vertices $v_{j,k}$, $k = 1, \ldots, K_j$, and the interior angles $\alpha_{j,k}\pi$. Further, let D be a doubly connected circular domain conformally equivalent to P and bounded by the circles C_j with the centers c_j. The reflections against the circles C_j are denoted by $s_j \in \mathbb{S}(D)$.
The Schwarzian derivative $\mathcal{S}$ of any conformal mapping f of D onto P has the form

$$\begin{aligned}\mathcal{S}(z) = \sum_{n=-\infty}^{\infty} \sum_{j,k} \Bigg(& \frac{a_{j,k}}{(z - p_{n,j,k})^2} + \frac{\gamma_{n,j,k}}{(z - p_{n,j,k})} \\ & + \frac{(p_{n,j,k} - l_2)\gamma_{n,j,k} + a_{j,k}}{(l_2 - l_1)(z - l_1)} + \frac{(p_{n,j,k} - l_1)\gamma_{n,j,k} + a_{j,k}}{(l_1 - l_2)(z - l_2)} \Bigg) \\ & + \frac{b(l_1 - l_2)^2}{(z - l_1)^2 (z - l_2)^2}.\end{aligned}$$

[25] We use γ instead of μ, to keep the formulas as short as possible.

The parameters of the formula are the prevertices $p_{n,j,k} \in \{T^n(p_{j,k}) \,|\, p_{j,k} \in C_j,\ T = s_0 \circ s_1,\ f(p_{j,k}) = v_{j,k}\}$, *the interior angles* $\pi\alpha_{j,k}$ *in the form* $a_{j,k} = \frac{1}{2}(1-\alpha_{j,k}^2)$ *and the additional parameters* $\gamma_{n,j,k}$ *and* b, *where*

$$\sum_{j,k}\Big((p_{j,k}-l_1)(p_{j,k}-l_2)\gamma_{j,k} + (2p_{j,k}-l_1-l_2)a_{j,k}\Big) = 0, \tag{4.22}$$

$$\mathrm{Im}\,(b) = \frac{1}{2}\sum_{k=1}^{K_0}\frac{(p_{j,k}-l_1)(p_{j,k}-l_2)\gamma_{j,k} + (2p_{j,k}-l_1-l_2)a_{j,k}}{(l_1-l_2)},$$

$$\gamma_{j,k}(p_{j,k}-c_j) + a_{j,k} \in i\mathbb{R}.$$

The limit points of $\mathbb{M}(D)$ *are denoted by* l_1 *and* l_2, *where* l_1 *lies inside* C_1.

Proof. To get the shape of $\mathcal{S}$ for a generic circular domain D, we apply a Möbius transformation to the Schwarzian for the annulus. Since the Schwarzian derivative provides us with

$$\{f \circ H, z\} = H'(z)^2\{f, H(z)\}$$

if H is a Möbius transformation, it is sufficient to calculate the right side of the equation. We define the bounded domain D by $H(D) = \mathbb{A}$, where $H(z) = (Az+B)/(Cz+D)$, $AD-BC = 1$, $H(C_0) = \partial\mathbb{D}$, and $H(C_1) \subset \mathbb{D}$. The new preimage domain has a changed set of parameters. The new prevertices q are given by $q = H^{-1}(p)$. The new parameters δ are given by $\delta = (Cq+D)^{-2}\gamma - 2aC(Cq+D)^{-1}$ if we use equation (4.5). The generating transformation $T = s_0 \circ s_1$ for $\mathbb{M}(D)$ is $H^{-1} \circ G \circ H$, where $G(z) = r^2 z$, while the new limit points are given by the preimages of zero and infinity, i.e.

$$H(l_1) = H\left(-\tfrac{B}{A}\right) = 0, \qquad H(l_2) = H\left(-\tfrac{D}{C}\right) = \infty,$$

where l_1 is inside both circles and we therefore have $l_1 \in \mathrm{ch}(C_1) \subset \mathrm{ch}(C_0)$.
By using these expressions, we obtain the relation

$$\begin{aligned} &H'(z)^2\sum_{j,k}\left(\frac{a}{(H(z)-p)^2} + \frac{\gamma}{(H(z)-p)} - \frac{\gamma}{H(z)}\right) \\ &= \sum_{j,k}\left(\frac{a}{(z-q)^2} + \frac{\delta}{(z-q)} + \frac{\delta(q-l_2)+a}{(l_2-l_1)(z-l_1)} + \frac{\delta(q-l_1)+a}{(l_1-l_2)(z-l_2)}\right). \end{aligned} \tag{4.23}$$

Equation (4.23) contains the sum over j and k because we already used the property

$$\sum_{j,k}(\gamma p + a) = \sum_{j,k}\left((q-l_1)(q-l_2)\delta + (2q-l_1-l_2)a\right) = 0.$$

Actually, the relation for the restricting equation is

$$\gamma p + a = \frac{(q-l_1)(q-l_2)\delta + (2q-l_1-l_2)a}{l_1-l_2},$$

but the difference $(l_1 - l_2)$ is constant and can therefore be removed from the sum. The remaining analytic part $\frac{b}{z^2}$ can be transformed to

$$H'(z)^2 \frac{b}{H(z)^2} = \frac{b(l_1-l_2)^2}{(z-l_1)^2(z-l_2)^2}.$$

Having transformed every part of $\mathcal{S}$ and the restricting equation, the lemma is proven for bounded domains.
An unbounded domain D_U can be reached by using an inversion $U(z) = r_0^2/(z-c_0)+c_0$ with respect to C_0 in the form $(H \circ U)(D_U) = H(D) = \mathbb{A}$. However, the only difference to the result above for bounded domains is the fact that C_1 is outside of C_0 and we therefore have $l_1 \in \mathrm{ch}(C_1)$, $l_2 \in \mathrm{ch}(C_0)$, and $\mathrm{ch}(C_0) \cap \mathrm{ch}(C_1) = \emptyset$. □

An easy way to check the plausibility of the above equation is to let l_2 approach infinity

$$\mathcal{S}(z) = \sum_{n,j,k} \left(\frac{a_{j,k}}{(z-p_{n,j,k})^2} + \frac{\gamma_{n,j,k}}{(z-p_{n,j,k})} + \frac{-\gamma_{n,j,k}}{(z-l_1)} \right) + \frac{b}{(z-l_1)^2}.$$

If additionally l_1 is replaced by zero, the expression simplifies to the form for the annulus, where the limit points are zero and infinity.

Remark

One may wish to prove the restricting equation

$$\sum_{j,k} \frac{(p-l_1)(p-l_2)\gamma + (2p-l_1-l_2)a}{(l_1-l_2)} = 0 \tag{4.24}$$

directly in D. The integration method used for Lemma 4.18 needs to be modified to establish this. The function

$$h(z) := \frac{(z-l_1)(z-l_2)}{(l_1-l_2)}$$

has the interesting properties

$$\begin{aligned} T'(z)^{-1} h(T(z)) &= h(z), \\ \sigma'(z)^{-1} \overline{h(s(z))} &= h(z) \end{aligned} \tag{4.25}$$

regarding transformations of $\mathbb{M}(D)$ and reflections against the boundary components of D. As a consequence, the integral

$$\int_\delta h(z)\mathcal{S}(z)dz$$

is invariant against applications of these transformations/reflections to the integration curve δ,[26] and so it takes the place of the integral

$$\int_\delta z\mathcal{S}(z)dz$$

in the proof of Lemma 4.18. It is interesting to note that the function $g(z) = z$ satisfies the equations (4.25) for the transformations belonging to an annulus.
Applying the proof of Lemma 4.18 yields the wanted result. This can also be seen by the fact that the restricting equation can be written as

$$\sum_{j,k}(h(p)\gamma + h'(p)a) = 0$$

by using h. Furthermore, every term $h(p)\gamma + h'(p)a$ is invariant with respect to the transformations of $\mathbb{M}(D)$.

4.2.3 Validity of the Mappings

We noted in the discussion following Lemma 2.13 that it is in general not possible to say in advance if the solution of a Schwarzian derivative is a valid multiply connected mapping. We further observed that one way to check this would be to verify

$$\int_\delta f^{(k)}(z)dz = 0, \qquad k = 1, 2, 3, \tag{4.26}$$

for curves enclosing exactly one of the boundary components.
For a doubly connected mapping, it is sufficient to integrate around one of the holes in the domain.[27] For the annulus $r < |z| < 1$, we can, for example, set δ to

$$\delta(t) = \frac{r+1}{2}\,\mathrm{e}^{it}$$

and test the three integrals (4.26) along this curve.
The downside is that we first need to solve for f before we can verify the mapping. This leads to the requirement of numerical methods for finding a valid map onto a DCCAPD.

It is reasonable in this context to count the number of free parameters on both sides of such a mapping.
On the image side, a DCCAPD can be defined by its vertices and the curvature[28] of the arcs. Let us denote the number of the vertices by $K := K_0 + K_1$. This gives $3K$ real degrees of freedom from which we must subtract 6 degrees for an applicable Möbius transformation, so we have $3K - 6$ degrees of freedom on the image side.

[26] The integral may still change its sign, if the transformation/reflection applied to the curve changes its direction.

[27] There is only one hole for bounded doubly connected domains, but two holes for unbounded domains.

[28] Here we will need the curvature with a sign to distinguish arcs bounded inwards and arcs bounded outwards.

For the preimage, the Schwarzian contains $3K$ real parameters p, a, μ, while the boundary circles are defined by 6 real values (centers and radii). We further have one real parameter $b_r = \mathrm{Re}\,(b)$ for the analytic remainder. On the other hand, we have to subtract again 6 degrees of freedom for the applicable Möbius transformation. Further we have the restricting equation (-1) and the three integral conditions (-6). Hence we have

$3K$	parameters $p,\ a,\ \mu$
$+\,6$	centers and radii of C_0 and C_1
$+\,1$	$\mathrm{Re}\,(b)$
$-\,6$	Möbius transformation
$-\,1$	restricting equation (4.14)
$-\,6$	integral equations (4.26)
$=3K-6$	

degrees of freedom on the preimage side.
Therefore both sides have the same number of degrees of freedom, but we can choose $3K$ values for the mapping as the integral equations can only be satisfied by changing the remaining values. There are therefore parameter sets (p, a, γ, $\mathrm{Re}\,(b)$, D) which do not lead to a valid doubly connected mapping.

There is also an interesting fact regarding the analytic remainder b_r/z^2. Note that b_r for the analytic remainder is real. The imaginary part b_i is a result of satisfying the functional equations of $\mathcal{S}$. If we calculate the Schwarzian of the function $g(z) = z^\alpha$, we have

$$\{g, z\} = \frac{1-\alpha^2}{2}\frac{1}{z^2}.$$

Therefore the solution of the Schwarzian derivative of b_r/z^2 is $T \circ g$ for a Möbius transformation T and a suitable choice of α. However the function z^α is for $\alpha \neq \pm 1$ not a valid doubly connected mapping of any annulus. It is mapping an annulus onto an annulus with a gap or an overlapping at the negative real axis depending on the choice of α. The remainder can therefore be seen as a way to compensate a gap contained in the solution of the Schwarzian by adjusting the parameter b_r correctly.
In the case of a generic circular domain, the solution for the analytic remainder is of the form

$$\left(\frac{z-l_1}{z-l_2}\right)^\alpha.$$

It has a similar effect as b_r/z^2, but the slit/gap is drawn between the two limit points of $\mathbb{M}(D)$. The slit for the annuli can therefore be seen as a connection between the origin and infinity.

4.2.4 Univalence of the Mappings

If a conformal mapping onto a DCCAPD exists for a given set of parameters, it may still not be univalent. However, there are results for the Schwarzian derivative especially concerning such univalence properties. Best known is the result of Nehari (stated as Lemma 2.17), which demands

$$|\{f, z\}| \leq \frac{6}{(1-|z|^2)^2}, \qquad |z| < 1.$$

as a necessary condition for a mapping from the unit disk. This condition was expanded in several directions since its publishing. A good overview of the development can be found in [Osg98]. For our needs, the most suitable version is one of Gehring [Geh77].

Lemma 4.24 ([Geh77])
If f is analytic and univalent in D, then

$$|\{f, z\}| \leq 6\, dist(z, \partial D)^{-2}$$

in D. The constant 6 is the best possible.

If we define

$$d(z) := \min\{(|z| - r), (1 - |z|)\}$$

for the annulus $\mathbb{A} = \{\, z \,|\, r < |z| < 1\}$, the requirement of the lemma changes to

$$|\mathcal{S}(z)| \leq 6\, d(z)^{-2}, \qquad z \in \mathbb{A}.$$

As this inequality has to be true for all z, it stays true if we integrate inside the annulus along a curve δ.

$$\int_\delta |\mathcal{S}(z)||dz| \leq \int_\delta 6\, d(z)^{-2}|dz|, \qquad \delta \subset \mathbb{A}.$$

While $\int_\delta |\mathcal{S}(z)||dz|$ is hard to calculate, there is a lower boundary

$$\left|\int_\delta \mathcal{S}(z)dz\right| \leq \int_\delta |\mathcal{S}(z)||dz|,$$

which is easier to handle.
If $\delta(t) = \rho e^{it}$ is a circle in $\mathbb{A}$ enclosing C_1, we have

$$\begin{aligned}
\int_\delta \mathcal{S}(z)dz &= 2\pi i \left(\sum_{-\infty}^{0} \sum_k \gamma_{n,0,k} + \sum_{-\infty}^{-1} \sum_k \gamma_{n,1,k} \right) \\
&= 2\pi i \left(\sum_{-\infty}^{0} r^{-2n} \sum_k \gamma_{0,k} + \sum_{-\infty}^{-1} r^{-2n} \sum_k \gamma_{1,k} \right) \\
&= -2\pi i \left(\frac{1}{1-r^2} \sum_k \gamma_{0,k} + \frac{1}{r^{-2}-1} \sum_k \gamma_{1,k} \right)
\end{aligned}$$

and

$$\int_{\delta} 6\, d(z)^{-2}|dz| = 2\pi\rho\; 6\, d(\rho)^{-2}.$$

Setting the radius for δ to $\rho = \frac{r+1}{2}$ to get the largest possible distance to the boundary, we find

$$\left|\frac{\sum_k \gamma_{0,k}}{1-r^2} + \frac{\sum_k \gamma_{1,k}}{r^{-2}-1}\right| \leq 6\left(\frac{1+r}{2}\right)\left(\frac{2}{1-r}\right)^2 = 12\frac{1+r}{(1-r)^2}. \tag{4.27}$$

This gives us a necessary, but not sufficient, condition for univalence, which depends on γ and r. The disadvantage of this inequality is that it is inaccurate. While the initial inequality is accurate in the sense of the best possible constant, the two following estimations are not precise.
If the same inequality is applied to the reflected annulus $1 < |z| < r^{-1}$, we get an altered form

$$\left|\sum_{j,k} \gamma_{j,k}\right| \leq 12\frac{(1+r)(r^{-1}-r)}{(1-r)^2}.$$

4.3 Known Mappings onto Doubly Connected Domains

4.3.1 Mapping Formula of Crowdy and Fokas

There is already a form for the Schwarzian in the doubly connected case, which is provided by Crowdy and Fokas [CF07].

Lemma 4.25 ([CF07])
Let $f(z)$ be the conformal mapping of the annulus $r < |z| < 1$ onto a doubly connected circular polygon domain. Let $\{\pi\alpha_{j,k} \,|\, j = 0, 1;\ k = 1, \ldots, K_j\}$ be the interior angles at the prevertices $\{p_{j,k} \,|\, j = 0, 1;\ k = 1, \ldots, K_j\}$, respectively. Then $\mathcal{T}(z) = z^2\mathcal{S}(z)$ is given by

$$\mathcal{T}(z) = \sum_{j=0}^{1}\sum_{k=1}^{K_j}\left[\left(\frac{\alpha_{j,k}^2 - 1}{2}\right) L\Big(\frac{z}{p_{j,k}}\Big) + i\gamma_{j,k}K\Big(\frac{z}{p_{j,k}}\Big)\right] + c,$$

where $\{\gamma_{j,k} \,|\, j = 0, 1;\ k = 1, \ldots, K_j\}$ are real constants satisfying the conditions

$$\sum_{k=1}^{K_0}\gamma_{0,k} + \sum_{k=1}^{K_1}\gamma_{1,k} = 0, \tag{4.28}$$

while c is a complex constant satisfying

$$c - \overline{c} = -i\sum_{k=1}^{K_1}\gamma_{1,k}. \tag{4.29}$$

The functions L and K in the expression above are constructed by using the Schottky-Klein prime function

$$P(z) := (1 - z)\prod_{n=1}^{\infty}(1 - r^{2k}z)(1 - r^{2k}z^{-1})$$

for the annulus $r < |z| < 1$. They are defined as

$$K(z) := \frac{zP'(z)}{P(z)},$$
$$L(z) := zK'(z).$$

To get a version that is easier to compare to our results, we evaluate them to

$$K(z) = \sum_{n=-\infty}^{0}\left(\frac{r^{2n}}{z - r^{2n}} + 1\right) + \sum_{n=1}^{\infty}\left(\frac{r^{2n}}{z - r^{2n}}\right)$$
$$L(z) = \sum_{n=-\infty}^{\infty}\left(\frac{-(r^{2n})^2}{(z - r^{2n})^2} + \frac{-r^{2n}}{z - r^{2n}}\right).$$

We obtain for each prevertex, by using $\frac{\alpha^2-1}{2} = -a$,

$$-aL\Big(\frac{z}{p}\Big) + i\gamma K\Big(\frac{z}{p}\Big) = \sum_{n=-\infty}^{\infty}\left(\frac{a(r^{2n}p)^2}{(z-r^{2n}p)^2} + \frac{ar^{2n}p}{z-r^{2n}p}\right) + \sum_{n=-\infty}^{0}\left(\frac{i\gamma r^{2n}p}{z-r^{2n}p} + i\gamma\right) + \sum_{n=1}^{\infty}\frac{i\gamma r^{2n}p}{z-r^{2n}p}.$$

Since γ drops out of the sum over the index k according to equation (4.28), we have

$$\mathcal{T}(z) = \sum_{j=0}^{1}\sum_{k=1}^{K_j}\sum_{n=-\infty}^{\infty}\left(\frac{a_{j,k}(r^{2n}p_{j,k})^2}{(z-r^{2n}p_{j,k})^2} + \frac{r^{2n}p_{j,k}(i\gamma_{j,k}+a_{j,k})}{z-r^{2n}p_{j,k}}\right) + c \tag{4.30}$$

In comparison, our form of Theorem 4.22 can be reshaped to

$$\begin{aligned} z^2\mathcal{S}(z) &= z^2\sum_{n=-\infty}^{\infty}\sum_{j,k}\left[\frac{a_{j,k}}{(z-r^{2n}p_{j,k})^2} + \frac{i\mu_{j,k}-a_{j,k}}{z(z-r^{2n}p_{j,k})}\right] + b \\ &= \sum_{n=-\infty}^{\infty}\sum_{j,k}\left[\frac{a_{j,k}(r^{2n}p_{j,k})^2}{(z-r^{2n}p_{j,k})^2} + \frac{r^{2n}p_{j,k}(i\mu_{j,k}+a_{j,k})}{(z-r^{2n}p_{j,k})}\right] + b \end{aligned} \tag{4.31}$$

by using the property $\sum_{j,k} i\mu_{j,k} = 0$ provided by equation (4.20).
The formulas (4.30) and (4.31) are equal, beside some minor differences regarding the notation. Their γ equals our μ and their c equals our b. Also the additional equations (4.28) and (4.20) and the equations (4.29) and (4.21) are equal.

4.3.2 Schwarz-Christoffel Mapping of the Annulus

A polygonal domain is a special case of a circular arc polygon domain. It is therefore reasonable to compare the doubly connected SC mapping with the DCCAPD mapping.[29]
Conformal mappings from annuli onto doubly connected regions bounded by two polygons were already constructed by Komatu in 1945 [Kom45], but we will use the approach of DeLillo, Elcrat and Pfaltzgraff [DEP01]. They stated the pre-Schwarzian of the mappings in the form:[30]

Lemma 4.26 ([DEP01])
Let P be a bounded doubly connected polygonal domain bounded by the polygons P_j, $j = 0, 1$, with the vertices $v_{j,k}$, $k = 1, \ldots, K_j$, and the turning angles $\beta_{j,k}\pi$.
Any conformal mapping f from the annulus $\mathbb{A} = \{z \,|\, r < |z| < 1\}$ onto P has a

[29] This was already done for simply connected domains in Section 3.3.
[30] It is not the final form found in the paper, but the one that is most suitable for our needs.

pre-Schwarzian of the form

$$S(z) = \frac{f''(z)}{f'(z)} = \sum_{n=-\infty}^{\infty} \sum_{j=0}^{1} \sum_{k=1}^{K_j} \frac{\beta_{j,k}}{z - r^{2n} p_{j,k}},$$

where $\{\beta_{j,k} = \alpha_{j,k} - 1 \,|\, \alpha_{j,k} \in [0,2];\ j = 0,1;\ k = 1,\ldots,K_j\}$ *are the turning angles and* $\{p_{j,k} \,|\, j = 0,1;\ k = 1,\ldots,K_j;\ |p_{0,k}| = 1;\ |p_{1,k}| = r;\ f(p_{j,k}) = v_{j,k}\}$ *are the prevertices.*

To derive the Schwarzian derivative from the pre-Schwarzian S, we define

$$S(z) := \lim_{N\to\infty} S_N(z) = \lim_{N\to\infty} \sum_{n=-N}^{N} \sum_{j,k} \frac{\beta_{j,k}}{z - r^{2n} p_{j,k}}$$

and

$$S_N(z, r^{2n} p_{j,k}) := \begin{cases} S_N(z) - \frac{\beta_{j,k}}{z - r^{2n} p_{j,k}} & \text{for } -N \le n \le N \\ S_N(z) & \text{otherwise} \end{cases}.$$

We will denote the derived Schwarzian by $\mathcal{T}$ to distinguish it from our version $\mathcal{S}$ provided by Theorem 4.22. Hence, the solutions of $\mathcal{T}$ will have the property that the image domain can be mapped onto a polygonal domain by a Möbius transformation. To obtain $\mathcal{T}$, we begin with

$$\begin{aligned} \mathcal{T}(z) &= \left(\frac{f''(z)}{f'(z)}\right)' - \frac{1}{2}\left(\frac{f''(z)}{f'(z)}\right)^2 = (S(z))' - \frac{1}{2}(S(z))^2 \\ &= \lim_{N\to\infty} \left((S_N(z))' - \frac{1}{2}(S_N(z))^2 \right). \end{aligned}$$

If we denote the finite version of $\mathcal{T}$ by $\mathcal{T}_N$, we have at each pole

$$\begin{aligned} \mathcal{T}_N(z) &= (S_N(z))' - \frac{1}{2}(S_N(z))^2 = \left(S_N(z,p) + \frac{\beta}{z-p}\right)' - \frac{1}{2}\left(S_N(z,p) + \frac{\beta}{z-p}\right)^2 \\ &= \frac{-\beta}{(z-p)^2} - \frac{1}{2}\frac{\beta^2}{(z-p)^2} - \frac{\beta}{z-p} S_N(z,p) + (S_N(z,p))' - \frac{1}{2}(S_N(z,p))^2 \\ &= \frac{a}{(z-p)^2} - \frac{\beta S_N(p,p)}{(z-p)} + O((z-p)^0), \end{aligned}$$

where $a = \frac{1}{2}(1 - \alpha^2)$ refers to the interior angle as in the preceding discussion. Since S is only composed of poles at the prevertices, the Schwarzian has to have a similar structure, and so we have found

$$\mathcal{T}_N(z) = \sum_{n=-N}^{N} \sum_{j,k} \left(\frac{a_{j,k}}{(z - r^{2n} p_{j,k})^2} + \frac{-\beta_{j,k} S_N(r^{2n} p_{j,k}, r^{2n} p_{j,k})}{(z - r^{2n} p_{j,k})} \right). \tag{4.32}$$

If we compare $\mathcal{T}_N$ with a finite version $\mathcal{S}_N$ of the Schwarzian from Theorem 4.22[31]

$$\mathcal{S}_N(z) = \sum_{n=-N}^{N} \sum_{j,k} \left(\frac{a_{j,k}}{(z - r^{2n} p_{j,k})^2} + \frac{\gamma_{n,j,k}}{(z - r^{2n} p_{j,k})} - \frac{\gamma_{n,j,k}}{z} \right) + \frac{b}{z^2}, \tag{4.33}$$

we notice that they differ in two major aspects. The residues γ at the prevertices are depending in the SC form $\mathcal{T}_N$ on the limit process and the poles at zero ($\frac{\gamma}{z}$ and $\frac{b}{z^2}$) are missing.
We have nonetheless found a formula for the parameters γ if we are mapping onto a DCCAPD that can be mapped onto a polygonal domain.

Lemma 4.27
Let P be a doubly connected circular arc polygon domain that can be mapped onto a bounded polygonal domain by a Möbius transformation.
The parameters γ of the Schwarzian derivative of a conformal mapping of an annulus $\mathbb{A}$ onto P are given by

$$\gamma_{n,j,k} = -\beta_{j,k} S(r^{2n} p_{j,k}, r^{2n} p_{j,k}), \qquad n \in \mathbb{Z},\ j = 0, 1,\ k = 1, \ldots, K_j,$$

where $S(z, p_{n,j,k})$ denotes the pre-Schwarzian S of the SC mapping (Lemma 4.26) of $\mathbb{A}$ onto P without the pole at $p_{n,j,k}$.

Proof. Comparing the residues of the equations (4.32) and (4.33) and letting N go to infinity yields the result

$$\gamma_{n,j,k} = \lim_{N \to \infty} -\beta_{j,k} S_N(r^{2n} p_{j,k}, r^{2n} p_{j,k}).$$

□

The missing parts of equation (4.32) ($\frac{\gamma}{z}$ and $\frac{b}{z^2}$) have to arise from the difference of $\beta S_N(p, p)$ and γ in the limit process. This is because

$$\lim_{N \to \infty} \left(-\beta_{j,k} S_N(r^{2n} p_{j,k}, r^{2n} p_{j,k}) - \gamma_{n,j,k} \right)$$

tends only for a fixed n to zero. However, the residues of the last summands in equation (4.32), i.e. where $n = N$, contain always a significant difference to their corresponding γ, no matter how large N grows. We will compute the parameter b to visualize this behavior.
For the following lemma, we define the notation

$$S_{M,N}(z) := \sum_{n=M}^{N} \sum_{j,k} \frac{\beta_{j,k}}{z - r^{2n} p_{j,k}}.$$

[31] We use γ instead of μ for easier comparison.

Lemma 4.28
Let P be a doubly connected circular arc polygon domain that can be mapped onto a bounded polygonal domain by a Möbius transformation.
The parameter b of the Schwarzian derivative of a conformal mapping of the annulus $\mathbb{A} = \{ z \,|\, r < |z| < 1 \}$ onto P is given by

$$\begin{aligned} b &= \sum_{n=0}^{\infty} \sum_{j,k} p_{j,k} \beta_{j,k} S_{1+n,\infty}(p_{j,k}) \\ &= \sum_{n=0}^{\infty} \sum_{j,k} p_{j,k} \beta_{j,k} \sum_{m=1+n}^{\infty} \sum_{i=0}^{1} \sum_{l=1}^{K_i} \frac{\beta_{i,l}}{p_{j,k} - r^{2m} p_{i,l}}. \end{aligned}$$

Proof. With the definition of $S_{M,N}$, we can split up S into

$$S(z) = S_{-\infty,-N-1}(z) + S_N(z) + S_{N+1,\infty}(z).$$

If we apply this notation also to $S(z,p)$, we have

$$S_N(p,p) = S(p,p) - (S_{-\infty,-N-1}(p) + S_{N+1,\infty}(p))$$

for $r^{2N+1} \le |p| \le r^{-2N}$. The residue in equation (4.32) can therefore be replaced by

$$-\beta S_N(p,p) = \gamma + \beta(S_{-\infty,-N-1}(p) + S_{N+1,\infty}(p)).$$

For further reference, we denote the difference to γ by

$$E_N(p) := \beta \left[S_{-\infty,-N-1}(p) + S_{N+1,\infty}(p) \right].$$

To actually determine b, we note that the difference $\mathcal{T}_N(z) - \mathcal{S}_N(z)$ tends to zero for growing N and all $z \in \mathbb{A}_E = \mathbb{C} \setminus \{0\}$,

$$\lim_{N\to\infty} \mathcal{T}_N(z) - \mathcal{S}_N(z) = 0, \qquad z \in \mathbb{A}_E.$$

Hence, we can state the modified difference

$$\begin{aligned} &\mathcal{T}_N(z) - \left(\mathcal{S}_N(z) - \frac{b}{z^2} \right) \\ &= \sum_{n=-N}^{N} \sum_{j,k} \left(\frac{-\beta_{j,k} S_N(r^{2n} p_{j,k}, r^{2n} p_{j,k})}{(z - r^{2n} p_{j,k})} - \frac{\gamma_{n,j,k}}{(z - r^{2n} p_{j,k})} + \frac{\gamma_{n,j,k}}{z} \right) \\ &= \sum_{n=-N}^{N} \sum_{j,k} \left(\frac{E_N(r^{2n} p_{j,k})}{(z - r^{2n} p_{j,k})} + \frac{\gamma_{n,j,k}}{z} \right) \overset{N\to\infty}{\longrightarrow} \frac{b}{z^2}, \end{aligned} \tag{4.34}$$

which converges[32] to $\frac{b}{z^2}$.

Now, we want to integrate along a circle with center at the origin that is given by the curve $\delta(t) = Re^{2\pi it}$, where $R = 1 + \frac{r}{2}$.[33] We then have

$$\lim_{N\to\infty} \int_\delta z \left(\mathcal{T}_N(z) - \mathcal{S}_N(z) + \frac{b}{z^2} \right) dz = 2\pi i b. \tag{4.35}$$

If we combine the equations (4.34) and (4.35), we obtain

$$\begin{aligned} b &= \lim_{N\to\infty} \frac{1}{2\pi i} \int_\delta z \left(\sum_{n=-N}^{N} \sum_{j,k} \left(\frac{E_N(r^{2n} p_{j,k})}{(z - r^{2n} p_{j,k})} + \frac{\gamma_{n,j,k}}{z} \right) \right) dz \\ &= \lim_{N\to\infty} \sum_{n=0}^{N} \sum_{j,k} r^{2n} p_{j,k} E_N(r^{2n} p_{j,k}). \end{aligned}$$

We know by the convergence of S_N that

$$\lim_{N\to\infty} S_{N+1,\infty}(p) = 0, \quad \lim_{N\to\infty} S_{-\infty,-N-1}(p) = 0,$$

for any fixed p. The pre-Schwarzian S has, like $\mathcal{S}$, a functional equation, namely

$$S(r^2 z) = r^{-2} S(z),$$

which changes for a finite sum to

$$S_{M,N}(r^2 z) = r^{-2} S_{M-1,N-1}(z),$$

where all terms are "shifted to the left". For the last generation $r^{2N} p_{j,k}$ of the prevertices, we therefore have

$$S_{N+1,\infty}(r^{2N} p_{j,k}) = r^{-2N} S_{1,\infty}(p_{j,k}),$$

where $S_{1,\infty}(p_{j,k})$ only depends on $p_{j,k}$ and r^{-2N} goes to infinity for growing N.
By applying this functional equation to the result from above for b we find

$$\begin{aligned} b &= \lim_{N\to\infty} \sum_{n=0}^{N} \sum_{j,k} r^{2n} p_{j,k} \left[\beta_{j,k} \left(S_{-\infty,-N-1}(r^{2n} p_{j,k}) + S_{N+1,\infty}(r^{2n} p_{j,k}) \right) \right] \\ &= \lim_{N\to\infty} \sum_{n=0}^{N} \sum_{j,k} p_{j,k} \beta_{j,k} \left(S_{-\infty,-2N-1+n}(p_{j,k}) + S_{1+n,\infty}(p_{j,k}) \right). \end{aligned}$$

Since the terms $S_{-\infty,-2N-1+n}(p_{j,k})$ vanish for N approaching infinity, we have proven the lemma. □

It is interesting to note that the b provided by the lemma already has the correct real and imaginary part.

While the equation for b holds for all SC mappings, it is not valid for the generic DCCAPD case. The sum of the turning angles $\sum_k \beta_{j,k} = \sum_k (\alpha_{j,k} - 1)$ is for a polygon either 2 or -2 (depending on whether it is an outer or inner boundary component). As this feature is used for demonstrating the convergence of S, the formula for b does not have to yield a value if the interior angles are changed. Therefore, a generalization does not seem possible with this approach.

Example

The simplest double connected polygonal domain has only two vertices on the inner boundary (slit) and three on the outer boundary. To keep the domain as symmetric as possible, we choose four vertices on the outer boundary and have

$$\begin{aligned} p_{0,k} &\in \{1, i, -1, -i\}, & p_{1,k} &\in \{r, -r\}, \\ \beta_{0,k} &= \beta_0 = -\frac{1}{2}, & \beta_{1,k} &= \beta_1 = 1. \end{aligned} \tag{4.36}$$

Some quick calculation yields that for $r = \frac{1}{2}$ we have

$$b = 0.047427\ldots$$

This example shows that $\mathrm{Re}\,(b)$ is actually non-zero. While neither in the simply connected case nor in the pre-Schwarzian of multiply connected SC mappings any additional analytic terms arise, it is inevitable for the Schwarzian derivative of a mapping onto a MCCAPD.
Also for this special example, we can conclude that since b is real, we have

$$\sum_k (\gamma_{0,k} p_{0,k} + a_{0,k}) = \sum_k (\gamma_{1,k} p_{1,k} + a_{1,k}) = 0.$$

As a matter of fact, most of the examples with symmetric domains have provided a real value for b. More values for a variation in r can be seen in Figure 32.

Unbounded SC Mappings

There is also a form of the pre-Schwarzian of conformal mappings that map an annulus onto an unbounded polygonal domain.

[32] The convergence is ensured by the fact that $(S_N(z))' - \frac{1}{2}(S_N(z))^2$ converges by [DEP01] and the remaining sum converges by Lemma 4.19.

[33] The radius is taken large enough to include the annulus $r < |z| < 1$, which is only for easier writing of the sum. Otherwise we would have to distinguish between the prevertices of the initial annulus which lie on the unit circle and those on the inner circle. This is possible as we have already extended the mapping to $\mathbb{C} \setminus \{0\}$.

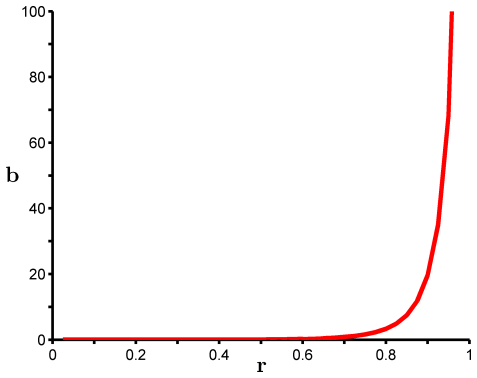

(a) The values of b for $r \in]0,1[$.

(b) The values of $\log_{10}(b)$ for $r \in]0,1[$ to better visualize the growth of b.

Figure 32: The magnitude of b grows very fast for r approaching 1. The values of b are calculated for the prevertices and angles given by (4.36).

Lemma 4.29 ([DEP04])
Let P be an unbounded doubly connected polygonal domain.
Any conformal mapping f of the annulus $\mathbb{A} = \{z \,|\, r < |z| < 1\}$ onto P has a pre-Schwarzian of the form

$$S(z) = \frac{f''(z)}{f'(z)} = \sum_{n=-\infty}^{\infty} \sum_{j=0}^{1} \left(\sum_{k=1}^{K_j} \left(\frac{\beta_{j,k}}{z - r^{2n} p_{j,k}} \right) + \frac{-2}{z - r^{2n} u_j} \right),$$

where $\{\beta_{j,k} = \alpha_{j,k} - 1 | j = 0,1; k = 1,\ldots,K_j\}$ are the turning angles, $\{p_{j,k} | j = 0,1; k = 1,\ldots,K_j; |p_{0,k}| = 1; |p_{1,k}| = r\}$ are the prevertices and $\{u_j | u_0 = \frac{1}{d}; u_1 = d; d \in \mathbb{A}\}$ are the preimages of infinity. The position of d can be chosen arbitrary in $\mathbb{A}$.

Since the image domain is unbounded, the pre-Schwarzian contains some additional terms referring to the preimage of infinity and its reflections/transformations. The choice of these preimages depends on the desired image domains,[34] but can be declared arbitrary (in the form of the parameter d) for the following discussion.
An interesting point is that the terms for infinity are actually required to establish convergence. While in the bounded case the sums of the turning angles are -2 and $+2$ (and therefore cancel each other out), they are $+2$ for both boundary parts in the unbounded case. Hence the terms for infinity with the coefficients -2 are the correct counterpart to ensure convergence.
A similar calculation as in the bounded case yields an adjusted version of our last result regarding b.

[34] In the paper of DeLillo, Elcrat and Pfaltzgraff, the preimage domains are unbounded. They therefore normalize the mappings with $f(\infty) = \infty$, but we use bounded preimage domains and have at the moment no need for a normalization.

Lemma 4.30
Let P be a doubly connected circular arc polygon domain that can be mapped onto an unbounded polygonal domain by a Möbius transformation.
The parameter b of the Schwarzian derivative of a conformal mapping from the annulus $\mathbb{A}$ onto P is given by

$$b = \sum_{n=0}^{\infty} \sum_{j=0}^{1} \left(\sum_{k=1}^{K_j} (p_{j,k}\beta_{j,k} S_{1+n,\infty}(p_{j,k})) - 2u_j S_{1+n,\infty}(u_j) \right).$$

In this case, S refers to the pre-Schwarzian of the unbounded mapping, which includes the terms for infinity.

Validity of the SC Mapping

We observed in Section 4.2.3 that not every set of parameters for the DCCAPD mapping yields a valid doubly connected mapping. We will repeat the parameter count on the preimage and image domains for the SC mapping to get an equivalent statement for this subset of the mappings onto DCCAPDs.

The solving process for the SC mapping is a mere integration in comparison to the differential equation of the CAPD mapping. However, this integration can also be seen as the solving of a differential equation of the first order. We can therefore state an integration condition similar to (2.3) for the Schwarzian derivative, but for a first order equation it is enough to check the first derivative, i.e.

$$\int_{\delta} f'(z)dz = 0, \tag{4.37}$$

where δ is a curve in the preimage annulus enclosing the smaller boundary circle.

If we now count the degrees of freedom of the image and the preimage of such a mapping, we obtain the following:
The image polygons are defined by their vertices. If we denote the sum of all vertices by K, this gives $2K$ real degrees of freedom. Further, we have to subtract 4 degrees, as the domain can be rotated, scaled and translated. Hence there are $2K - 4$ degrees of freedom in the image domain.
On the other hand, we need 6 real values to define the circles of the preimage domain[35] and K for the prevertices. The angles provide only $K - 2$ degrees, as the sums of the turning angles must be ± 2 depending on the boundary component. Subtracting 6 degrees for the application of a Möbius transformation and 2 for the integration

[35] We could also count only one degree of freedom for the inner radius of the annulus instead of the 6 degrees for a generic domain. However, in this case, we only need to subtract one degree for the normalization by a rotation instead of a Möbius transformation. Either way yields the same result, i.e. $6 - 6 = 1 - 1 = 0$.

condition leads to a sum of $2K-4$ real degrees of freedom on the preimage domain.

K	prevertices p
$+\,K-2$	turning angles β
$+\,6$	centers and radii of C_0 and C_1
$-\,6$	Möbius transformation
$-\,2$	integral equation (4.37)
$=2K-4$	

Both sides have $2K-4$ degrees of freedom, but this implies, as for the DCCAPD mapping, that there must be sets of prevertices and angles without a proper image domain. The argument is the same as in Section 4.2.3: We can choose $2K-2$ parameters in comparison to the $2K-4$ degrees of freedom, so there must be sets with image domains breaking the integration condition.
Such an unsatisfied condition appears in the numerical evaluation in the form of images of closed curves without matching start and end points, indicating that the boundary has gaps or overlap and intersect itself.
An example for an alternative approach to the validity of the mappings can be found in Hu's DSCPACK [Hu98], an algorithm for the calculation of doubly connected mappings from annuli onto doubly connected polygonal domains. Each mapping has to satisfy the condition that the two images of the first prevertex on the inner boundary, one gathered directly and one by solving around the hole, have to coincide. This is the same concept as the integration condition, but solved via an alternative method.

We visualize this problem by two different parameter sets for the annulus $0.2 < |z| < 1$. The first set has equal spaced prevertices, where

$$\begin{aligned} \arg(p_0) &= (0.25,\, 0.75,\, 1.25,\, 1.75)\,\pi, & \alpha_0 &= (0.5,\, 0.5,\, 0.5,\, 0.5), \\ \arg(p_1) &= (0,\, 0.5,\, 1,\, 1.5)\,\pi, & \alpha_1 &= (1.5,\, 1.5,\, 1.5,\, 1.5), \end{aligned} \tag{4.38}$$

while the prevertices of the second set are closer together

$$\begin{aligned} \arg(p_0) &= (0.1,\, 0.5,\, 0.8,\, 1.1)\,\pi, & \alpha_0 &= (0.5,\, 0.5,\, 0.5,\, 0.5), \\ \arg(p_1) &= (0.8,\, 1,\, 1.3,\, 1.7)\,\pi, & \alpha_1 &= (1.5,\, 1.5,\, 1.5,\, 1.5). \end{aligned} \tag{4.39}$$

The results can be seen in Figure 33. The images are generated the same way as the examples in Section 5.3.3, while the solving of the Schwarzian is replaced with the integration of the derivative of the Schwarz-Christoffel transformation. A full description of the process can be found in Chapter 5.
The first parameter set (4.38) yields a well shaped polygonal domain, while the second set (4.39) produces a rather distorted imaged domain. The image domain for the second set is self overlapping and therefore the start and end points of each boundary component do not match. Based on the image domain, the set (4.39) does not belong to a valid doubly connected SC transformation.

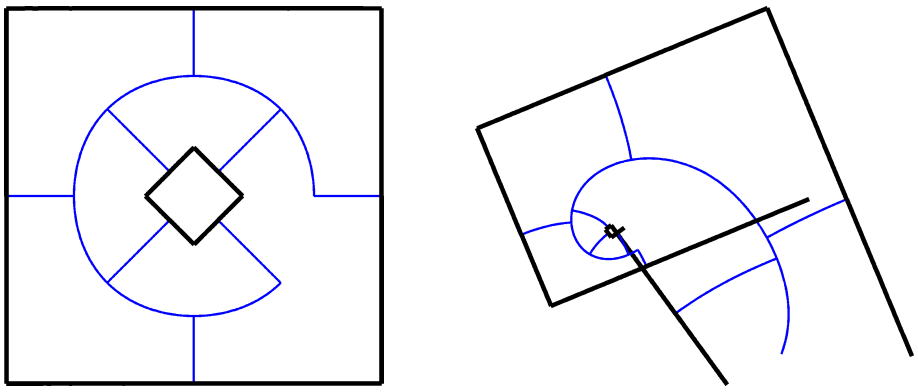

(a) The well shaped result for the parameter set (4.38).

(b) The distorted "boundary" for the parameter set (4.39).

Figure 33: The image domains for the Schwarz-Christoffel transformation of the annulus $0.2 < |z| < 1$ with the parameter sets (4.38) and (4.39) are shown.

4.3.3 Nehari's Mapping onto a Slit Domain

In the monograph [Neh52, p. 293-295] they show a mapping from the annulus $r < |z| < 1$ onto the unit disk minus a symmetric slit on the real axis. The mapping is given by one of Jacobi's elliptic functions

$$f(z) = \sqrt{k}\,\mathrm{sn}\left(\frac{2iK}{\pi}\log\frac{z}{r} + K, r^4\right),$$

where k depends on r and K on the elliptic function.
To compare this to our results, we derive the pre-Schwarzian of $f(z)$ (as shown in Appendix A.3) and find

$$S_N(z) = \sum_{n=-(2N+1)}^{2N+1}\sum_{k=1}^{2}\frac{1}{z - r^{2n}p_k} + \sum_{n=-N}^{N+1}\sum_{k=1}^{2}\frac{-2}{z - r^{4n}u_k}, \tag{4.40}$$

where $p_1 = r$, $p_2 = -r$, $u_1 = ir^{-1}$, $u_2 = -ir^{-1}$, and $S(z) = \lim_{N\to\infty} S_N(z)$.
To understand the pre-Schwarzian, we examine the behavior of the mapping. The inner circle of the annulus is mapped onto a slit in the image domain, so the pre-Schwarzian has to contain two prevertices p_1 and p_2, representing the ends of the slit, as is common for this kind of mapping.
While the prevertices $p_1 = r$ and $p_2 = -r$ are mapped onto real points $v_1 = f(r)$ and $v_2 = f(-r)$, the points ir and $-ir$ are mapped onto zero by the symmetry of the domain. If we extend the preimage and image domain by a reflection against $\partial\mathbb{D}$[36], we cover the whole image plane except the real intervals $]-\infty, v_2^{-1}]$, $[v_2, v_1]$ and $[v_1^{-1}, \infty[$. Zero is reflected onto infinity in this process, so the reflections of ir and $-ir$ through

[36]The unit circle is a boundary component of the image and the preimage domain.

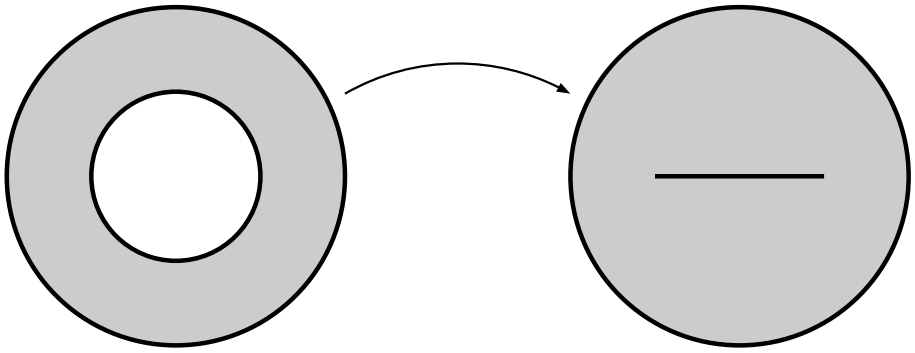

Figure 34: The function given by Nehari conformally maps an annulus onto the unit disk minus a slit on the real axis.

the unit circle are mapped onto infinity and we have $f(ir^{-1}) = f(-ir^{-1}) = \infty$. These poles can therefore be seen at the u_k in the pre-Schwarzian.
An interesting side effect of these poles is that they ensure convergence of the expression above, as can be seen by comparison with the convergence proof of the SC mapping (e.g. [DEP04]). For our investigation, it is enough to know that it was derived from a valid mapping function.

To calculate the Schwarzian derivative from the pre-Schwarzian, we notice that the pre-Schwarzian (4.40) is similar to that of the Schwarz-Christoffel mapping. Hence, it is reasonable to apply similar methods.
We denote the alternative Schwarzian again by $\mathcal{T}$. If we write $S(z) = S(z,p) + \frac{1}{z-p}$, we obtain

$$\begin{aligned}\mathcal{T}(z) = (S(z))' - \frac{1}{2}(S(z))^2 &= \left(S(z,p) + \frac{1}{z-p}\right)' - \frac{1}{2}\left(S(z,p) + \frac{1}{z-p}\right)^2 \\ &= \frac{-1}{(z-p)^2} - \frac{1}{2}\frac{1}{(z-p)^2} - S(z,p)\frac{1}{z-p} + S'(z,p) - \frac{1}{2}(S(z,p))^2 \\ &= \frac{-\frac{3}{2}}{(z-p)^2} - \frac{S(p,p)}{z-p} + \text{analytic},\end{aligned}$$

since $S(z,p)$ is analytic at p. We apply the same method for the poles at u and find a similar result except that the quadratic terms vanish. The resulting Schwarzian is of the form

$$\begin{aligned}\mathcal{T}_N(z) = &\sum_{n=-(2N+1)}^{2N+1}\sum_{k=1}^{2}\left(\frac{-\frac{3}{2}}{(z-r^{2n}p_k)^2} - \frac{S_N(r^{2n}p_k, r^{2n}p_k)}{z-r^{2n}p_k}\right) \\ &+ \sum_{n=-N}^{N+1}\sum_{k=1}^{2}\frac{2\,S_N(r^{4n}u_k, r^{4n}u_k)}{z-r^{4n}u_k},\end{aligned}$$

where $\mathcal{T}(z) = \lim_{N\to\infty}\mathcal{T}_N(z)$. For economy in notation, we introduce $\mathcal{V}_N(p) := S_N(p,p)$,

so we may write

$$\mathcal{T}_N(z) = \sum_{n=-(2N+1)}^{2N+1} \sum_{k=1}^{2} \left(\frac{-\frac{3}{2}}{(z - r^{2n}p_k)^2} - \frac{\mathcal{V}_N(r^{2n}p_k)}{z - r^{2n}p_k} \right) + \sum_{n=-N}^{N+1} \sum_{k=1}^{2} \frac{2\,\mathcal{V}_N(r^{4n}u_k)}{z - r^{4n}u_k}.$$

According to Lemma 2.14, the Schwarzian is not allowed to contain the simple poles of the mapping functions, i.e. the preimages of infinity. Therefore, the poles at $r^{4n}u_k$ have to disappear. This means that the $\mathcal{V}_N(r^{4n}u_k)$ have to go to zero as N approaches infinity. However, as in the case of the SC mapping, this is only true for fixed n. The last summand in $\mathcal{S}_N$, i.e. $\mathcal{V}_N(r^{4(N+1)}u_k)$, has an argument dependent on N and therefore does not shrink. This leads to an error term as in the preceding section for the SC mapping.
There is also an error for $-\mathcal{V}_N(r^{2n}p_k)$ compared to $\gamma_{n,j,k}$. The difference of $-\mathcal{V}_N(r^{2n}p_k)$ and $\gamma_{n,j,k}$ is found following a similar argument to that employed in the case of the SC mapping.

To investigate this behavior, we evaluate $\mathcal{V}_N$ for different arguments and values of N. The behavior of $\mathcal{V}_N(r^{4(N+1)}u_1)$ can be seen in the Tables 3 and 4.

$i\mathcal{V}_N(r^{4n}u_1)$	$N=0$	1	2	3	4
$n=1$	$1.1 \cdot 10^{0}$	$4.6 \cdot 10^{-3}$	$1.8 \cdot 10^{-5}$	$7.1 \cdot 10^{-8}$	$2.8 \cdot 10^{-10}$
$n=2$	–	$1.8 \cdot 10^{1}$	$7.4 \cdot 10^{-2}$	$2.9 \cdot 10^{-4}$	$1.1 \cdot 10^{-6}$
$n=3$	–	–	$2.9 \cdot 10^{2}$	$1.2 \cdot 10^{0}$	$4.7 \cdot 10^{-3}$
$n=4$	–	–	–	$4.6 \cdot 10^{3}$	$1.9 \cdot 10^{1}$
$n=5$	–	–	–	–	$7.4 \cdot 10^{4}$

Table 3: Evaluations of $\mathcal{V}_N(r^{4n}u_1) = \mathcal{V}_N(r^{4n}ir^{-1})$ for $r = 0.5$. The results were multiplied by i to provide positive real values.

$\log_{10}\lvert\mathcal{V}_N(r^{4n}u_1)\rvert$	$N=0$	1	2	3	4	5	6
$n=1$	0	−2	−5	−7	−10	−12	−14
$n=2$	–	1	−1	−4	−6	−8	−11
$n=3$	–	–	2	0	−2	−5	−7
$n=4$	–	–	–	4	1	−1	−4
$n=5$	–	–	–	–	5	2	0
$n=6$	–	–	–	–	–	6	4
$n=7$	–	–	–	–	–	–	7

Table 4: Evaluations of $\mathcal{V}_N(r^{4n}u_1) = \mathcal{V}_N(r^{4n}ir^{-1})$ for $r = 0.5$. The table shows the logarithm to base 10 of the results rounded to integer values.

Furthermore $-\mathcal{V}_N(r^{2n}p_k)$ should tend to $\gamma_{n,k}$. The values for different n and N can be seen in Table 5. The values with the greatest n (for a fixed N) always significantly differ from the actual value of γ, as the relative error remains nearly constant. This fact is shown in Table 6.

$-\mathcal{V}_N(r^{2n}p_1)$	$N=0$	1	2	3	4	∞
$n=0$	3.0000	3.0000	3.0000	3.0000	3.0000	3
$n=1$	13.254	12.005	12.000	12.000	12.000	12
$n=2$	–	48.299	48.001	48.000	48.000	48
$n=3$	–	212.14	192.07	192.00	192.00	192
$n=4$	–	–	772.78	768.02	768.00	768
$n=5$	–	–	3394.2	3073.2	3072.0	3072
$n=6$	–	–	–	12365	12288	12288
$n=7$	–	–	–	54307	49171	49152

Table 5: Evaluations of $-\mathcal{V}_N(r^{2n}p_1) = -\mathcal{V}_N(r^{2n}r)$ for $r = 0.5$. The actual value of $\gamma_{n,1}$ is shown in the last column.

$\log_{10}(E_N(r^{2n}p_1))$	$N=0$	1	2	3	4	5
$n=1$	$-\infty$	$-\infty$	$-\infty$	$-\infty$	$-\infty$	$-\infty$
$n=2$	-1	-4	-6	-9	$-\infty$	$-\infty$
$n=3$	–	-3	-5	-7	-10	$-\infty$
$n=4$	–	-1	-4	-6	-9	$-\infty$
$n=5$	–	–	-3	-5	-7	-10
$n=6$	–	–	-1	-4	-6	-9
$n=7$	–	–	–	-3	-5	-7
$n=8$	–	–	–	-1	-4	-6
$n=9$	–	–	–	–	-3	-5
$n=10$	–	–	–	–	-1	-4

Table 6: The table shows the logarithm of the relative error $E_N(r^{2n}p_1) = |\mathcal{V}_N(r^{2n}p_1)+\gamma_{n,1}|/|\mathcal{V}_N(r^{2n}p_1)-\gamma_{n,1}|$ between $-\mathcal{V}_N(r^{2n}p_1)$ and $\gamma_{n,1}$ for $r = 0.5$. The results were rounded to integer values. The "$-\infty$" represent an error smaller than the numerical precision.

At this point, we halt our investigation. We see that the mapping of Nehari behaves very similar to the Schwarz-Christoffel mapping for the annulus. As previously, some of the terms of the mapping formula onto a DCCAPD only arise in the limit process, and can therefore not directly be seen.

4.4 Mappings onto Domains of Connectivity Three or Greater

We now investigate mappings onto domains with connectivity three or greater. The main change in the geometry is that the limit set Λ is now a perfect set. Hence, there are uncountable many limit points instead of only two. Therefore we can not directly apply the results of Section 4.2, but we may use the basic shape of the Schwarzian.
The Schwarzian for the annulus is according to Theorem 4.22 of the form

$$\mathcal{S}(z) = \sum_{n=-\infty}^{\infty} \sum_{j,k} \left(\frac{a_{j,k}}{(z-p_{n,j,k})^2} + \frac{\gamma_{n,j,k}}{(z-p_{n,j,k})} - \frac{\gamma_{n,j,k}}{z} \right) + \frac{ib_i}{z^2} + \frac{b_r}{z^2}$$

if we use γ instead of μ and $p_{n,j,k} = r^{2n} p_{j,k}$. As the index n represents the transformation applied to p, we may instead use T, i.e. $p_{T,j,k} = T(p_{j,k})$. If we denote the poles referring to the prevertices by

$$\mathcal{R}(z,T) := \sum_{j,k} \left(\frac{a_{j,k}}{(z-p_{T,j,k})^2} + \frac{\gamma_{T,j,k}}{(z-p_{T,j,k})} \right), \tag{4.41}$$

we can divide the Schwarzian into

$$\mathcal{S}(z) = \sum_{T \in \mathbb{M}(D)} \Bigg(\underbrace{\sum_{j,k} \left[\frac{a_{j,k}}{(z-p_{T,j,k})^2} + \frac{\gamma_{T,j,k}}{(z-p_{T,j,k})} \right]}_{\mathcal{R}(z,T)} + \underbrace{\sum_{j,k} \left[-\frac{\gamma_{T,j,k}}{z} \right]}_{\mathcal{A}_C(z,T)} \Bigg) + \underbrace{\frac{ib_i}{z^2}}_{\mathcal{A}_F(z)} + \underbrace{\frac{b_r}{z^2}}_{\mathcal{A}_R(z)}$$

with the principle part and three different analytic components.
The resulting four components can be interpreted as

- $\mathcal{R}(z,T)$: the poles at the prevertices
- $\mathcal{A}_C(z,T)$: the functions necessary to ensure the convergence
- $\mathcal{A}_F(z)$: the function to ensure the functional equation
- $\mathcal{A}_R(z)$: a possible analytic remainder.

Hence, from a more distance point of view, the Schwarzian is of the form

$$\mathcal{S}(z) = \sum_{T \in \mathbb{M}(D)} \left[\mathcal{R}(z,T) + \mathcal{A}_C(z,T) \right] + \mathcal{A}_F(z) + \mathcal{A}_R(z) \tag{4.42}$$

with suitably chosen components, where the functions $\mathcal{A}_C$, $\mathcal{A}_F$ and $\mathcal{A}_R$ can only have poles in Λ.
The target will be to look for suitable functions if the image domain is of a connectivity greater than two. The choices for the doubly connected case are no longer valid if the limit set becomes perfect.

For completeness, we also state the functions for the generic doubly connected case of Theorem 4.23. They are given by

$$\begin{aligned}\mathcal{A}_C(z,T) &= \sum_{j,k}\left(\frac{(p_{T,j,k}-l_2)\gamma_{T,j,k}+a_{j,k}}{(l_2-l_1)(z-l_1)}+\frac{(p_{T,j,k}-l_1)\gamma_{T,j,k}+a_{j,k}}{(l_1-l_2)(z-l_2)}\right),\\ \mathcal{A}_F(z) &= \frac{b_i(l_1-l_2)^2}{(z-l_1)^2(z-l_2)^2},\\ \mathcal{A}_R(z) &= \frac{b_r(l_1-l_2)^2}{(z-l_1)^2(z-l_2)^2}.\end{aligned} \tag{4.43}$$

4.4.1 Construction Revisited: Poincaré Theta Series

There is an alternative approach for constructing the Schwarzian derivative. The functional equation

$$T'(z)^2\mathcal{S}(T(z)) = \mathcal{S}(z)$$

is the same as in the case of the Poincaré theta series (Section 2.5). Utilizing this concept, we can analyze the sum

$$\sum_{T\in\mathbb{M}(D)} T'(z)^2\mathcal{R}(T(z)), \tag{4.44}$$

where $\mathcal{R}$ contains the poles of the first generation, i.e. $\mathcal{R}(z) = \mathcal{R}(z,\mathrm{id})$ for $\mathcal{R}(z,T)$ as defined in equation (4.41).
For the following discussion, we define the abbreviations

$$\begin{aligned}\mathcal{R}_{j,k}(z) &:= \frac{a_{j,k}}{(z-p_{j,k})^2}+\frac{\gamma_{j,k}}{(z-p_{j,k})} =: \mathcal{R}(z,p_{j,k}),\\ \mathcal{R}_j(z) &:= \sum_k \mathcal{R}_{j,k}(z),\\ \mathcal{R}(z) &:= \sum_j \mathcal{R}_j(z),\end{aligned}$$

to further decompose $\mathcal{R}(z)$. We write $\mathcal{R}(z,p)$ instead of $\mathcal{R}(z,p_{j,k})$ if the actual position of the prevertex is not important.

If we transform one of the summands of $\mathcal{R}$ by $T'(z)^2\mathcal{R}(T(z),p)$, we find

$$\begin{aligned}&T'(z)^2\left(\frac{a}{(T(z)-p)^2}+\frac{\gamma}{(T(z)-p)}\right)\\ &= \frac{a}{(z-q)^2}+\frac{\delta}{(z-q)}-\frac{\delta}{(z-u)}-\frac{(q-u)\delta+a}{(z-u)^2}-\frac{(q-u)((q-u)\delta+2a)}{(z-u)^3},\end{aligned} \tag{4.45}$$

where q is the transformed prevertex, δ the transformed parameter γ and u the center of the isometric circle of the transformation, $T(u)=\infty$. Hence the sum (4.44) contains

poles at the centers of the isometric circles, which are not allowed by the basic idea of the mappings (Lemma 4.9).
By comparing the form of equation (4.45) with Lemma 4.15, we note that both formulas are very similar. This is reasonable, as the Poincarè series automatically provides the convergence. The only difference is in the choice of the poles.

To compensate for the poles in D_E, we introduce an additional term $\mathcal{A}_C$

$$\sum_{T\in\mathbb{M}(D)} T'(z)^2 \left[\mathcal{R}(T(z)) + \mathcal{A}_C(T(z))\right].$$

The sum (or theta series) already satisfies the functional equation with respect to the transformations (Lemma 4.5), but might not satisfy the one with respect to the reflections (Lemma 4.11). We add a correction term $\mathcal{A}_F$ to rectify this problem

$$\mathcal{K}(z) = \sum_{T\in\mathbb{M}(D)} T'(z)^2 \left[\mathcal{R}(T(z)) + \mathcal{A}_C(T(z))\right] + \mathcal{A}_F(z).$$

The remaining difference $\mathcal{A}_R = \mathcal{S} - \mathcal{K}$ between $\mathcal{K}$ and $\mathcal{S}$ can only be a function analytic in D_E and has to itself satisfy the functional equations. The Schwarzian $\mathcal{S}$ is therefore of the form

$$\mathcal{S}(z) = \sum_{T\in\mathbb{M}(D)} T'(z)^2 \left[\mathcal{R}(T(z)) + \mathcal{A}_C(T(z))\right] + \mathcal{A}_F(z) + \mathcal{A}_R(z). \tag{4.46}$$

This notation differs little from equation (4.42), where the differences are the form of the sum and the interpretation of $\mathcal{A}_C$.
In the first case (4.42), we sum the poles at the prevertices and add $\mathcal{A}_C$ to ensure the convergence. In the second case (4.46), the convergence is already guaranteed and we only need $\mathcal{A}_C$ to eliminate the additional poles arising in the construction process.

If we compare this to the doubly connected case of Theorem 4.23, we may set

$$\begin{aligned}\mathcal{A}_C(z) := \sum_{j,k} \Bigg(&\frac{(p_{j,k}-l_2)\gamma_{j,k}+a_{j,k}}{(l_2-l_1)(z-l_1)} + \frac{(p_{j,k}-l_1)\gamma_{j,k}+a_{j,k}}{(l_1-l_2)(z-l_2)} \\ &+ \frac{(p_{j,k}-l_1)(p_{j,k}-l_2)\gamma_{j,k}+(2p_{j,k}-l_1-l_2)a_{j,k}}{2(l_2-l_1)(z-l_1)^2} \\ &+ \frac{(p_{j,k}-l_1)(p_{j,k}-l_2)\gamma_{j,k}+(2p_{j,k}-l_1-l_2)a_{j,k}}{2(l_1-l_2)(z-l_2)^2}\Bigg)\end{aligned} \tag{4.47}$$

which is equivalent to $\mathcal{A}_C(z,\mathrm{id})$, as it is shown in equation (4.43). To actually see that (4.47) is equal to

$$\mathcal{A}_C(z,\mathrm{id}) := \sum_{j,k} \left(\frac{(p_{j,k}-l_2)\gamma_{j,k}+a_{j,k}}{(l_2-l_1)(z-l_1)} + \frac{(p_{j,k}-l_1)\gamma_{j,k}+a_{j,k}}{(l_1-l_2)(z-l_2)} \right), \tag{4.48}$$

we need the restricting equation (4.22). If we apply (4.22) to (4.47), the poles of the second order vanish.

The advantage of notation (4.47) in comparison to (4.48) is that it allows the direct calculation of

$$T'(z)^2\mathcal{A}_C(T(z)) = \mathcal{A}_C(z,T) + \sum_{j,k}\left(\frac{\delta_{j,k}}{(z-u)} + \frac{(q_{j,k}-u)\delta_{j,k}+a_{j,k}}{(z-u)^2} + \frac{(q_{j,k}-u)((q_{j,k}-u)\delta_{j,k}+2a_{j,k})}{(z-u)^3}\right)$$

which gives us with (4.45)

$$T'(z)^2\left[\mathcal{R}(T(z)) + \mathcal{A}_C(T(z))\right] = \mathcal{R}(z,T) + \mathcal{A}_C(z,T).$$

Hence the forms (4.42) and (4.46) are equivalent for the doubly connected case.

In the following discussion, we will prefer the formulation that employs the Poincaré theta series as it allows us to neglect the consideration of convergence. The goal of the following sections will therefore be to construct the common Schwarzian derivative of the mappings as a Poincaré series by finding suitable components $\mathcal{A}_C$, $\mathcal{A}_F$ and $\mathcal{A}_R$.

4.4.2 Correction Terms for the Poincaré Theta Series

We stated that $\mathcal{S}$ is of the form

$$\mathcal{S}(z) = \sum_{T\in\mathbb{M}(D)} T'(z)^2\left[\mathcal{R}(T(z)) + \mathcal{A}_C(T(z))\right] + \mathcal{A}_F(z) + \mathcal{A}_R(z),$$

where $\mathcal{R}$ is already known. We wish to find a function $\mathcal{A}_C$ that eliminates the poles resulting due to the construction in the form of a Poincaré series. Further, we need to find $\mathcal{A}_F$ to ensure the functional equations.

Compensating for the Poles in D_E: $\mathcal{A}_C$

We require from $\mathcal{A}_C$ that

$$T'(z)\left[\mathcal{R}(T(z)) + \mathcal{A}_C(T(z))\right]$$

does not have a pole at u, where $T(u) = \infty$, or any other point in D_E. Since the functions $\mathcal{A}$ are not allowed to have poles in D_E, $\mathcal{A}_C$ consists of terms with poles in Λ. However, poles in Λ influence the convergence of the Poincaré series as seen in Lemma 2.43. It is therefore reasonable to choose only first order poles and demand the property $\sum |C|^{-2} < \infty$ of the Schottky group $\mathbb{M}(D)$.

The poles we wish to eliminate are the ones of $T'(z)^2\mathcal{R}(T(z),p)$ in u

$$T'(z)^2\mathcal{R}(T(z),p) = -\frac{(q-u)((q-u)\delta+2a)}{(z-u)^3} - \frac{(q-u)\delta+a}{(z-u)^2} - \frac{\delta}{(z-u)} + O(1).$$

In comparison, we have for a pole of order one with weight w in a limit point l

$$T'(z)^2 \frac{w}{T(z)-l} = \frac{C^{-2}w}{(l'-u)^2(z-l')} - \frac{C^{-2}w}{(z-u)^3} - \frac{C^{-2}w}{(l'-u)(z-u)^2} - \frac{C^{-2}w}{(l'-u)^2(z-u)},$$

where $l = T(l')$ and $T(z) = (Az+B)/(Cz+D)$. The point l' is also a limit point, because any transformation of the group maps the limit set onto itself.
We will set up a system of equations to solve for the weights w, where to compensate for the third order pole, we will need at least three different weights. We will use four terms, to also establish the functional equation regarding the reflections.
The analytic function $\mathcal{A}_C$ will be constructed using the following steps:

1. Search for a function $\mathcal{A}_{C,j,k}$ that is analytic in D_E in order to compensate the pole arising in $\mathcal{R}_{j,k}$ by the application of any transformation T.
2. Construct a function $\mathcal{A}_{C,j}$ of the $\mathcal{A}_{C,j,k}$ for all prevertices on one circle C_j represented by $\mathcal{R}_j$.
3. Combine the preceding results to produce one $\mathcal{A}_C$ that matches $\mathcal{R}$.

Lemma 4.31
Let $L = \{l_1, l_2, l_3, l_4\} \subset \Lambda$, the parameters p, a, γ as in $\mathcal{R}(z,p)$, $p \neq c \in D_E$, and define

$$\lambda_1(i) := (l_i - c), \quad \lambda_2(i) := (l_i - c)\sum_{\substack{n=1\\n\neq i}}^{4}(l_n - c), \quad \lambda_3(i) := \prod_{\substack{n=1\\n\neq i}}^{4}(l_n - c),$$

$$\lambda_4(i) := \prod_{\substack{n=1\\n\neq i}}^{4}(l_n - l_i), \quad \lambda_2 := \sum_{n=1}^{3}\sum_{i=n+1}^{4}(l_i - c)(l_n - c),$$

$$\tau_1 := \gamma, \quad \tau_2 := (p-c)\gamma + a, \quad \tau_3 := (p-c)((p-c)\gamma + 2a).$$

The function

$$\mathcal{A}_C(z,p,c,L) := \sum_{i=1}^{4} \frac{\lambda_1(i)\tau_3 + (\frac{\lambda_2}{2} - \lambda_2(i))\tau_2 - \lambda_3(i)\tau_1}{\lambda_4(i)(z-l_i)}$$

has the property that for each $T \in \mathbb{M}(D)$, where $T(u) = \infty$,

$$T'(z)^2(\mathcal{R}(T(z),p) + \mathcal{A}_C(T(z),p,c,L)) = O((z-u)^0),$$

i.e. the expression does not have a pole at u.

We use $\lambda(i)$ instead of the more accurate $\lambda(i,c,L)$ for economy of notation.

Proof. The application of T changes the residue of $\mathcal{R}(z,p)$, as the location of the pole changes to $q = T^{-1}(p)$. Ensuring a calculation dependent only on the the pre-transformation values, we introduce v that $T(\infty) = v$, and write

$$\begin{aligned}
&T'(z)^2\mathcal{R}(T(z),p)\\
&= -\frac{C^{-2}\gamma}{(z-u)^3} + \frac{(p-v)\gamma+a}{(z-u)^2} - \frac{C^2(p-v)((p-v)\gamma+2a)}{(z-u)} + O((z-u)^0),\\
&T'(z)^2\frac{w}{T(z)-l} = \frac{-C^{-2}w}{(z-u)^3} + \frac{(l-v)w}{(z-u)^2} + \frac{-C^2(l-v)^2w}{(z-u)} + O((z-u)^0),
\end{aligned}$$

where $T(z) = (Az+B)/(Cz+D)$. Our object will be to find four suitable weights w for four different limit points $l_1, l_2, l_3, l_4 \in \Lambda$ to compensate the poles at u of $T'(z)^2\mathcal{R}(T(z),p)$.
If we set up the four equations, we get the system

$$\begin{pmatrix} -C^2(l_1-v)^2 & -C^2(l_2-v)^2 & -C^2(l_3-v)^2 & -C^2(l_4-v)^2 \\ l_1-v & l_2-v & l_3-v & l_4-v \\ -C^{-2} & -C^{-2} & -C^{-2} & -C^{-2} \end{pmatrix} \begin{pmatrix} w_1 \\ w_2 \\ w_3 \\ w_4 \end{pmatrix} = \begin{pmatrix} C^2(p-v)((p-v)\gamma+2a) \\ -((p-v)\gamma+a) \\ C^{-2}\gamma \end{pmatrix}$$

with the solution

$$\begin{pmatrix} w_1 \\ w_2 \\ w_3 \\ w_4 \end{pmatrix} = \begin{pmatrix} \frac{-(l_2-l_4)(l_3-l_4)t}{(l_3-l_1)(l_2-l_1)} - \frac{(p-l_2)(p-l_3)\gamma+(2p-l_2-l_3)}{(l_3-l_1)(l_2-l_1)} \\ \frac{-(l_1-l_4)(l_3-l_4)t}{(l_1-l_2)(l_3-l_2)} - \frac{(p-l_1)(p-l_3)\gamma+(2p-l_1-l_3)}{(l_1-l_2)(l_3-l_2)} \\ \frac{-(l_1-l_4)(l_2-l_4)t}{(l_1-l_3)(l_2-l_3)} - \frac{(p-l_1)(p-l_2)\gamma+(2p-l_1-l_2)}{(l_1-l_3)(l_2-l_3)} \\ t \end{pmatrix}$$

where t denotes the remaining complex degree of freedom introduced by the under-determined system.
As the choice for t is rather complicated, we choose the abbreviations

$$\lambda_1(i) := (l_i - c), \quad \lambda_2(i) := (l_i - c)\sum_{\substack{n=1\\n\neq i}}^{4}(l_n - c), \quad \lambda_3(i) := \prod_{\substack{n=1\\n\neq i}}^{4}(l_n - c),$$

$$\lambda_4(i) := \prod_{\substack{n=1\\n\neq i}}^{4}(l_n - l_i), \quad \lambda_2 := \sum_{n=1}^{3}\sum_{i=n+1}^{4}(l_i - c)(l_n - c),$$

$$\tau_1 := \gamma, \quad \tau_2 := (p-c)\gamma + a, \quad \tau_3 := (p-c)((p-c)\gamma + 2a),$$

and set t to

$$t = \frac{\lambda_1(4)\tau_3 + (\frac{\lambda_2}{2} - \lambda_2(4))\tau_2 - \lambda_3(4)\tau_1}{\lambda_4(4)}.$$

As a result, we have

$$\begin{pmatrix} w_1 \\ w_2 \\ w_3 \\ w_4 \end{pmatrix} = \begin{pmatrix} [\lambda_1(1)\tau_3 + (\frac{\lambda_2}{2} - \lambda_2(1))\tau_2 - \lambda_3(1)\tau_1]\lambda_4(1)^{-1} \\ [\lambda_1(2)\tau_3 + (\frac{\lambda_2}{2} - \lambda_2(2))\tau_2 - \lambda_3(2)\tau_1]\lambda_4(2)^{-1} \\ [\lambda_1(3)\tau_3 + (\frac{\lambda_2}{2} - \lambda_2(3))\tau_2 - \lambda_3(3)\tau_1]\lambda_4(3)^{-1} \\ [\lambda_1(4)\tau_3 + (\frac{\lambda_2}{2} - \lambda_2(4))\tau_2 - \lambda_3(4)\tau_1]\lambda_4(4)^{-1} \end{pmatrix}.$$

If we form the fractions of the weights and poles, we obtain

$$\mathcal{A}_C(z, p, c, L) = \sum_{i=1}^{4} \frac{\lambda_1(i)\tau_3 + (\frac{\lambda_2}{2} - \lambda_2(i))\tau_2 - \lambda_3(i)\tau_1}{\lambda_4(i)(z - l_i)}.$$

□

The advantage of this choice for $\mathcal{A}_C(z, p, c, L)$ is that it also satisfies the functional equation regarding the reflection against a boundary circle, if the parameters are set accordingly.

Lemma 4.32
Let $s_j \in \mathbb{S}(D)$ be the reflection against the circle C_j, with center c_j and radius r_j. Suppose

$$\begin{aligned} &p \in C_j, && \gamma(p - c_j) + a \in i\mathbb{R}, \\ &L_j = \{l_1, l_2, l_3, l_4\} \subset \Lambda, && l_1 = s_j(l_2), l_3 = s_j(l_4), \\ &s_j(z) = \frac{r_j^2}{\bar{z} - \bar{c_j}} + c_j = \overline{\sigma_j(z)}, && \sigma_j'(z) = \frac{-r_j^2}{(z - c_j)^2}. \end{aligned}$$

The function

$$\mathcal{T}(z) = \mathcal{R}(z, p) + \mathcal{A}_C(z, p, c_j, L_j),$$

where $\mathcal{A}_C$ as in Lemma 4.31, has the property

$$\sigma_j'(z)^2 \overline{\mathcal{T}(s_j(z))} = \mathcal{T}(z).$$

Proof. It can be shown by a direct (and very lengthy) calculation that

$$\sigma_j'(z)^2 \overline{\mathcal{T}(s_j(z))} - \mathcal{T}(z) = 0.$$

It is essential adjust $\overline{\mathcal{T}(s_j(z))}$ to match $\mathcal{T}(z)$ by using the substitutions

$$\begin{aligned} &p = s_j(p), \quad \gamma = -r^{-2}\overline{(p - c_j)((p - c_j)\gamma + 2a)}, \\ &l_1 = s_j(l_2), \quad l_2 = s_j(l_1), \quad l_3 = s_j(l_4), \quad l_4 = s_j(l_3). \end{aligned}$$

□

To handle this rather complicated correction term, we collect the above in a definition.

Definition 4.33
The values $p_{j,k}$, $a_{j,k}$ and $\gamma_{j,k}$ are defined according to Definition 4.7.
Let $s_j \in \mathbb{S}(D)$ be the reflection against the circle C_j with center c_j and radius r_j. Further, let $L_j = \{l_{j,i} \,|\, l_{j,1} = s_j(l_{j,2}),\, l_{j,3} = s_j(l_{j,4}),\, i = 1,2,3,4\} \subset \Lambda$ be a set of limit points pairwise symmetric to C_j.
The rational functions $\mathcal{R}$ are defined by

$$\mathcal{R}_{j,k}(z) := \frac{a_{j,k}}{(z-p_{j,k})^2} + \frac{\gamma_{j,k}}{(z-p_{j,k})}, \quad \mathcal{R}_j(z) := \sum_k \mathcal{R}_{j,k}(z), \quad \mathcal{R}(z) := \sum_j \mathcal{R}_j(z).$$

The function $\mathcal{A}_{C;j,k}$ is defined by

$$\mathcal{A}_{C;j,k}(z) := \sum_{i=1}^{4} \frac{\lambda_1(j,i)\tau_3(j,k) + (\frac{\lambda_2(j)}{2} - \lambda_2(j,i))\tau_2(j,k) - \lambda_3(j,i)\tau_1(j,k)}{\lambda_4(j,i)(z-l_{j,i})},$$

where

$$\lambda_1(j,i) := (l_{j,i} - c_j), \qquad \lambda_2(j,i) := (l_{j,i} - c_j) \sum_{\substack{n=1 \\ n\neq i}}^{4} (l_{j,n} - c_j),$$

$$\lambda_3(j,i) := \prod_{\substack{n=1 \\ n\neq i}}^{4} (l_{j,n} - c_j), \qquad \lambda_4(j,i) := \prod_{\substack{n=1 \\ n\neq i}}^{4} (l_{j,n} - l_{j,i}),$$

$$\lambda_2(j) := \sum_{n=1}^{3} \sum_{i=n+1}^{4} (l_{j,i} - c_j)(l_{j,n} - c_j),$$

and

$$\tau_1(j,k) := \gamma_{j,k}, \quad \tau_2(j,k) := (p_{j,k} - c_j)\gamma_{j,k} + a_{j,k},$$
$$\tau_3(j,k) := (p_{j,k} - c_j)((p_{j,k} - c_j)\gamma_{j,k} + 2a_{j,k}).$$

Further versions of $\mathcal{A}_C$ are defined by

$$\mathcal{A}_{C;j}(z) := \sum_k \mathcal{A}_{C;j,k}(z) \qquad \text{and} \qquad \mathcal{A}_C(z) := \sum_{j,k} \mathcal{A}_{C;j,k}(z).$$

We will need to refer very often to the property $\sum_{T\in G} |C_T|^{-2} < \infty$ of the sum of the coefficients C_T of the Möbius transformations $T(z) = (A_T z + B_T)/(C_T z + D_T)$ of a group G. To shorten the notation, we will skip the index of the sum and write "G satisfies $\sum |C|^{-2} < \infty$".

We have by now an analytic function for one prevertex, which will be modified to cover all the prevertices of one boundary circle.

Lemma 4.34
Suppose the Schottky group $\mathbb{M}(D)$ satisfies $\sum |C|^{-2} < \infty$. Let further $\mathcal{R}_j$ and $\mathcal{A}_{C;j}$ be as in Definition 4.33, then

$$\mathcal{K}(z) = \sum_{T \in \mathbb{M}(D)} T'(z)^2 \left(\mathcal{R}_j(T(z)) + \mathcal{A}_{C;j}(T(z))\right)$$

satisfies the functional equations

$$\begin{aligned} T'(z)^2 \mathcal{K}(T(z)) &= \mathcal{K}(z), \qquad && T \in \mathbb{M}(D), \\ \sigma'(z)^2 \overline{\mathcal{K}(s(z))} &= \mathcal{K}(z), \qquad && s \in \mathbb{S}(D),\ \overline{\sigma(z)} = s(z). \end{aligned}$$

Proof. The terms $\mathcal{A}_{C;j}(z)$ contain a finite number of first order poles at some limit points. The convergence of $\mathcal{K}$ is ensured by the fact that we demanded $\sum |C|^{-2} < \infty$ and Lemma 2.43, i.e. $\mathcal{K}$ is a (modified) Poincaré theta series. As a Poincaré series, $\mathcal{K}$ satisfies the functional equation

$$T'(z)^2 \mathcal{K}(T(z)) = \mathcal{K}(z), \qquad T \in \mathbb{M}(D).$$

We state some auxiliary calculations before we continue the proof with respect to the second functional equation. Every succession of an even number of reflections is a Möbius transformation. Hence

$$V = s_1 \circ T \circ s_2$$

is a Möbius transformation, as T also consists of an even number of reflections. To derive V, we may rewrite it in the form

$$V = s_1 \circ T \circ s_2 = \rho_1 \circ U \circ \sigma_2,$$

where $\rho_1(\overline{z}) = s_1(z)$, $\overline{U(\overline{z})} = T(z)$, $\overline{\sigma_2(z)} = s_2(z)$, to obtain a sequence of holomorphic functions. Differentiation yields

$$\begin{aligned} V'(z) &= \rho_1'(U(\sigma_2(z)))U'(\sigma_2(z))\sigma_2'(z) \\ &= \overline{\sigma_1'(T(s_2(z)))T'(s_2(z))}\sigma_2'(z) \end{aligned} \tag{4.49}$$

by using $\overline{\rho_1(\overline{z})} = \sigma_1(z) = \overline{s_1(z)}$.
Returning to the initial problem, we know from Lemma 4.32 that

$$\sigma_j'(z)^2 \overline{\mathcal{T}(s_j(z))} = \mathcal{T}(z), \tag{4.50}$$

where

$$\mathcal{T}(z) = \mathcal{R}_j(z) + \mathcal{A}_{C;j}(z) = \sum_k (\mathcal{R}_{j,k}(z) + \mathcal{A}_{C;j,k}(z))$$

for the reflection against the circle C_j. We can therefore calculate for every term $T'(z)^2\mathcal{T}(T(z))$ in $\mathcal{K}$,

$$\begin{aligned}\sigma_k'(z)^2\overline{T'(s_k(z))^2\mathcal{T}(T(s_k(z)))} &\overset{(4.50)}{=} \sigma_k'(z)^2\overline{T'(s_k(z))^2\sigma_j'[T(s_k(z))]^2}\mathcal{T}[s_j(T(s_k(z)))]\\ &= \left(\overline{\sigma_j'[T(s_k(z))]T'(s_k(z))}\sigma_k'(z)\right)^2\mathcal{T}[(\underbrace{s_j\circ T\circ s_k}_{V})(z)]\\ &\overset{(4.49)}{=} V'(z)^2\mathcal{T}(V(z))\end{aligned}$$

by using (4.49) and (4.50) as indicated. This gives for $\mathcal{K}$

$$\begin{aligned}\sigma_k'(z)^2\overline{\mathcal{K}(s_k(z))} &= \sum_T \sigma_k'(z)^2\overline{T'(s_k(z))^2\mathcal{T}(T(s_k(z)))}\\ &= \sum_V V'(z)^2\mathcal{T}(V(z)) = \mathcal{K}(z).\end{aligned}$$

It is important to note that every V is not only a Möbius transformation, but based on its construction also in $\mathbb{M}(D)$. Hence, the sums over V and T are equal except for some shifting. As the Poincaré series converges absolutely, a shifting of the terms does not change the result. □

The last step of our construction is to further extend the correction term to cover all prevertices.

Lemma 4.35
Suppose the Schottky group $\mathbb{M}(D)$ satisfies $\sum|C|^{-2}<\infty$. Let $\mathcal{R}$ and $\mathcal{A}_C$ be defined according to Definition 4.33. The function

$$\mathcal{K}(z)=\sum_{T\in\mathbb{M}(D)} T'(z)^2\left(\mathcal{R}(T(z))+\mathcal{A}_C(T(z))\right)$$

satisfies the functional equations

$$\begin{aligned}T'(z)^2\mathcal{K}(T(z)) &= \mathcal{K}(z), \qquad && T\in\mathbb{M}(D),\\ \sigma'(z)^2\overline{\mathcal{K}(s(z))} &= \mathcal{K}(z), && s\in\mathbb{S}(D),\ \overline{\sigma(z)}=s(z).\end{aligned}$$

Proof. If we split $\mathcal{K}$ into $m+1$ functions

$$\mathcal{K}_j(z)=\sum_{T\in\mathbb{M}(D)} T'(z)^2\left(\mathcal{R}_j(T(z))+\mathcal{A}_{C;j}(T(z))\right),$$

we can apply Lemma 4.34 to each $\mathcal{K}_j$. Combining them again into $\mathcal{K}$ proves the lemma. □

The function $\mathcal{K}$ is already very close to the Schwarzian derivative $\mathcal{S}$, since it has the same poles in D_E as $\mathcal{S}$ and is analytic otherwise. Additionally, it already satisfies the functional equations for the transformations of the group $\mathbb{M}(D)$ and the reflections of $\mathbb{S}(D)$.

Establishing the Functional Equations: $\mathcal{A}_F$

We have noted for the doubly connected case that there is a component $\mathcal{A}_F$ necessary to establish the functional equations. However, according to Lemma 4.35, the case of a greater connectivity does not need such a correction term. This discrepancy can be understood by considering the size of the limit sets.
We need at least four different first order poles at limit points for the construction of $\mathcal{A}_C$ as shown above, but $\mathbb{M}(D)$ provides only two limit points if D is a doubly connected domain. We therefore need to also use second order poles in the construction of a function $\mathcal{A}_C$ to get four different weights. This can be seen in equation (4.47), as it contains the mentioned first and second order poles.
According to the convergence discussion so far, this would require $\sum |C|^0 < \infty$ for $\mathbb{M}(D)$, which is only possible for finite groups. Hence, not even the doubly connected domains can satisfy this requirement.
The Schwarzian is nonetheless converging as the second order poles cancel out in the sum over j and k by the restricting equation (4.14). This means that we no longer can assume absolute convergence as the order of the summands becomes crucial. Without the absolute convergence, the reordering of the poles as it was used in the proof of Lemma 4.35 is not applicable. As a consequence, we need a function $\mathcal{A}_F$ to ensure that the functional equations are satisfied.

Summary

Lemma 4.35 provides us with a function, which has the same poles in D_E as $\mathcal{S}$ and is analytic otherwise. Hence, we can state our version of the Schwarzian derivative for a CAPD mapping of connectivity three or greater.

Theorem 4.36
Let P be a multiply connected circular arc polygon domain of connectivity three or greater, bounded by the circular arc polygons P_j, where $j = 0, \dots, m$ and $m \geq 2$, with the vertices $v_{j,k}$, $k = 1, \dots, K_j$, and the interior angles $\alpha_{j,k}\pi$. Further, let D be a $(m+1)$-connected circular domain conformally equivalent to P, where $\mathbb{M}(D)$ satisfies $\sum |C|^{-2} < \infty$.
The Schwarzian derivative $\mathcal{S}$ of any conformal mapping f of D onto P has the form

$$\mathcal{S}(z) = \sum_{T \in \mathbb{M}(D)} T'(z)^2 \left[\mathcal{R}(T(z)) + \mathcal{A}_C(T(z))\right] + \mathcal{A}_R(z),$$

where $\mathcal{R}$ and $\mathcal{A}_C$ are as in Definition 4.33 and $\mathcal{A}_R$ is a function that is analytic in D_E

and satisfies the equations

$$T'(z)^2 \mathcal{A}_R(T(z)) = \mathcal{A}_R(z),$$
$$\sigma'(z)^2 \overline{\mathcal{A}_R(s(z))} = \mathcal{A}_R(z),$$

for all transformations $T \in \mathbb{M}(D)$ *and all reflections* $s \in \mathbb{S}(D)$, *where* $\overline{\sigma(z)} = s(z)$.

Proof. The function $\mathcal{K}$ from Lemma 4.35 has the same poles as $\mathcal{S}$ in D_E and also satisfies the same functional equations. The difference

$$\mathcal{A}_R(z) = \mathcal{S}(z) - \mathcal{K}(z)$$

must therefore be analytic in D_E and also has to satisfy the functional equations. Hence $\mathcal{S}$ is of the form

$$\mathcal{S}(z) = \sum_{T \in \mathbb{M}(D)} T'(z)^2 \left[\mathcal{R}(T(z)) + \mathcal{A}_C(T(z))\right] + \mathcal{A}_R(z).$$

□

Note that $\mathcal{A}_C$ is not unique; for example, we did not even specify the limit points used for the construction. However, based on common knowledge about multiply connected conformal mappings, the combination of $\mathcal{A}_C$ and $\mathcal{A}_R$ has to be unique.

As the construction of $\mathcal{S}$ is rather complicated, we outline the steps needed:

1. Define a circular domain D by defining the boundary circles.
2. Define values for p, a and γ to form $\mathcal{R}$ as in Definition 4.33.
3. Find for each boundary circle C_j two pairs of limit points symmetric to it.
4. Construct for each prevertex a function $\mathcal{A}_{C;j,k}$ as in Definition 4.33, using the limit points of the last step and sum the $\mathcal{A}_{C;j,k}$ to get $\mathcal{A}_C$.
5. Generate the transformations of $\mathbb{M}(D)$ and calculate the Poincaré theta series.
6. Add a suitable analytic function $\mathcal{A}_R$.

The only information missing is a way to construct the function $\mathcal{A}_R$ of the last step. This issue will be discussed in the following sections.

Each $\mathcal{A}_{C;j,k}$ can be written as a Laurent series converging outside every circle with center $p_{j,k}$, that enclose all prevertices $p_{T,j,k}$ and all limit points:

$$\mathcal{A}_{C;j,k}(z) = -\frac{a_{j,k}}{(z-p_{j,k})^2} - \frac{\gamma_{j,k}}{(z-p_{j,k})} + O((z-p)^{-3}).$$

Comparing this with Lemma 4.15 shows that $\mathcal{A}_C$ can also be seen as a term to ensure the convergence of the series.

4.4.3 Analytic Remainder

We need a function $\mathcal{A}_R$ that completes the Schwarzian derivative, and we require this function $\mathcal{A}_R$ to be analytic in D_E and to satisfy the functional equation

$$\sigma_j'(z)^2\overline{\mathcal{A}_R(s_j(z))} = \left(\frac{r_j}{z-c_j}\right)^4 \overline{\mathcal{A}_R(s_j(z))} = \mathcal{A}_R(z) \tag{4.51}$$

for each boundary circle C_j of D. Here, r_j and c_j denote again the radius and the center of the circle C_j, while s_j is the reflection against it.[37]
The functional equation can be transformed to

$$(z-c_j)^2\,\mathcal{A}_R(z) \in \mathbb{R}, \qquad z \in C_j,$$

or equivalently

$$\mathrm{Im}[(z-c_j)^2\mathcal{A}_R(z)] = 0, \qquad z \in C_j, \tag{4.52}$$

as already discussed in Section 4.1.5. An alternative approach would therefore be to find a function analytic in D and continuous on the boundary ∂D with the boundary conditions (4.52). This resembles the Riemann-Hilbert boundary value problem.

Definition 4.37
Let D be a (multiply) connected domain $D \subset \mathbb{C}_\infty$ and the functions λ and d Hölder continuous on the boundary ∂D of D.
The search for a function ϕ, analytic in D and continuous in $\overline{D} = D \cup \partial D$, which satisfies the boundary conditions

$$\mathrm{Re}[\overline{\lambda(z)}\phi(z)] = d(z), \quad z \in \partial D,$$

is called the Riemann-Hilbert problem.
When $d \equiv 0$, the problem

$$\mathrm{Re}[\overline{\lambda(z)}\phi(z)] = 0, \quad z \in \partial D,$$

is called the homogeneous Riemann-Hilbert problem.

If we define the functions

$$\phi(z) := i\mathcal{A}_R(z), \qquad z \in D \cup \partial D,$$
$$\lambda(z) := \begin{cases} (z-c_0)^{-2} & \text{for } z \in C_0 \\ (z-c_1)^{-2} & \text{for } z \in C_1 \\ \dots & \dots \\ (z-c_m)^{-2} & \text{for } z \in C_m \end{cases},$$

[37] The functional equation regarding the transformations follows by applying the equation for the reflections twice.

the search for $\mathcal{A}_R$ is equivalent to the search for solutions of the homogeneous Riemann-Hilbert problem

$$\mathrm{Re}[\overline{\lambda(z)}\phi(z)] = 0, \qquad z \in \partial D.$$

While this approach allows us to solve for $\mathcal{A}_R$ by the methods of boundary value problems, we are more interested in the basic structure of the solutions.
Any real linear combination of two solutions ϕ_1 and ϕ_2 is also itself a solution of the problem

$$\begin{aligned} &\mathrm{Re}[\overline{\lambda(z)}\phi_1(z)] = \mathrm{Re}[\overline{\lambda(z)}\phi_2(z)] = 0 \\ &\Rightarrow \mathrm{Re}[\overline{\lambda(z)}(b_1\phi_1(z) + b_2\phi_2(z))] = 0, \qquad b_1, b_2 \in \mathbb{R}. \end{aligned}$$

The number L of linearly independent solutions of the Riemann-Hilbert problem is investigated in several publications (e.g. [Gak66], [Vek62], [Nas09]) and can be calculated via the following lemma.

Definition 4.38
The index χ of the Riemann-Hilbert problem

$$\mathrm{Re}[\overline{\lambda(z)}\phi(z)] = d(z), \qquad z \in \partial D,$$

is defined by

$$\chi := \mathrm{wind}_{\partial D}\, \lambda(z) = \frac{1}{2\pi} \int_{\partial D} d \arg \lambda(z).$$

Lemma 4.39 ([Gak66, p. 347],[Vek62])
Let D be a $(m+1)$-connected domain.
If the index of the homogeneous Riemann-Hilbert problem $\chi > m-1$, then the number L of linearly independent solutions of the problem is given by

$$L = 2\chi - (m-1).$$

This allows us to state for our case:

Lemma 4.40
Let D be a $(m+1)$-connected bounded circular domain, where $m > 1$, bounded by the $m+1$ circles C_j with centers c_j.
The homogeneous Riemann-Hilbert problem

$$\mathrm{Re}[\overline{\lambda(z)}\phi(z)] = 0, \qquad z \in \partial D,$$

where

$$\lambda(z) = \begin{cases} (z-c_0)^{-2} & \text{for } z \in C_0 \\ (z-c_1)^{-2} & \text{for } z \in C_1 \\ \dots & \dots \\ (z-c_m)^{-2} & \text{for } z \in C_m \end{cases},$$

has $L = 3m - 3$ linearly independent solutions.

Proof. To apply Lemma 4.39, we must first calculate the index of the problem. Since we wish the domain to be to the left of the boundary, the circles C_j, where $j = 1, \dots, m$, have to be orientated clockwise and C_0 has to be orientated counterclockwise. We have for each boundary component

$$\chi_j = \begin{cases} -2 & \text{for } j = 0 \\ +2 & \text{for } j = 1, \dots, m \end{cases}$$

and therefore for the index

$$\chi = \sum_{j=0}^{m} \chi_j = 2m - 2.$$

Since we have $\chi = 2m - 2 > m - 1$ for $m > 1$, we can use Lemma 4.39 and obtain

$$L = 2\chi - (m-1) = 3m - 3.$$

□

Note that the statement above is not valid for doubly connected domains ($m = 1$). If the domain is an annulus, the index is $\chi = 0$ for the problem, and the condition of Lemma 4.39 $\chi > m - 1$ is violated. However, we have already found the only linearly independent solution z^{-2} for the annulus in Lemma 4.21.

The solutions for an unbounded domain can be reached by extending the solutions for a suitable bounded domain across the outer boundary component C_0.
Alternatively the same number of linearly independent solutions for unbounded domains can be gathered by calculating the index $\chi_u = 2m + 2$ and applying Lemma 4.39. However, the result of the lemma has to be reduced in this case. The functional equation evaluated at c_j implies a fourth order zero at infinity. This reduces the number of linearly independent solutions by eight, corresponding to the eight real restrictions implied by the zero. Hence, we find

$$L_u = 2\chi_u - (m-1) - 8 = 3m - 3.$$

Lemma 4.41
Let the functions $\mathcal{B}_i$, where $i = 1, \dots, 3m-3$, be linearly independent and analytic in D_E. Let each of them also satisfy the functional equation (4.51).
The analytic function $\mathcal{A}_R$ of Theorem 4.36 is completely defined by the analytic functions $\mathcal{B}_i$ and the real values $b_i \in \mathbb{R}$, $i = 1, \dots, 3m-3$, in the form

$$\mathcal{A}_R(z) = \sum_{i=1}^{3m-3} b_i \mathcal{B}_i(z).$$

Proof. According to Lemma 4.40, the $3m-3$ functions $\mathcal{B}_i$ form a basis for all analytic functions in D that satisfy the boundary condition

$$\mathrm{Re}[\overline{\lambda(z)}\phi(z)] = 0, \qquad z \in \partial D.$$

Hence, any function satisfying this boundary condition can be constructed by a linear combination of the functions $\mathcal{B}_i$ with $3m-3$ real weights b_i. Extending the functions across the boundary of D gives the functions analytic in D_E. □

We may interpret the whole search for the Schwarzian $\mathcal{S}$ as a Riemann-Hilbert problem. This was for example done in [Mit12b] for the SC mapping.
In this way, we can see the Poincarè series $\sum T'(z)^2(\mathcal{R}(T(z))+\mathcal{A}_C(T(z)))$ containing the poles as the solution of the inhomogeneous problem, while we may add a homogeneous solution, i.e. $\mathcal{A}_R$, to the result as it is possible for any boundary value problem.

We retain b_i as notation for further work, as these values completely define $\mathcal{A}_R$ for a given basis. The functions $\mathcal{B}_i$ only depend on the domain D.

Definition 4.42
The function

$$\mathcal{A}_R(z) = \mathcal{A}_R(z, b) = \mathcal{A}_R(z, b, \mathcal{B}) = \sum_{i=1}^{3m-3} b_i \mathcal{B}_i(z)$$

is defined by the two vectors

$$\mathcal{B} = \mathcal{B}(D) = (\mathcal{B}_1, \mathcal{B}_2, \dots, \mathcal{B}_{3m-3}),$$
$$b = (b_1, b_2, \dots, b_{3m-3}) \in \mathbb{R}^{3m-3},$$

where $\mathcal{B}$ describes a basis for the analytic functions on D_E satisfying the functional equation (4.51).

With this description of $\mathcal{A}_R$, we are able to refine our result of Theorem 4.36, and state one of our main results:

Theorem 4.43
Let P be a multiply connected circular arc polygon domain of connectivity three or greater, bounded by the circular arc polygons P_j, where $j = 0, \ldots, m$ and $m \geq 2$, with the vertices $v_{j,k}$, $k = 1, \ldots, K_j$, and the interior angles $\alpha_{j,k}\pi$. Further, let D be a $(m+1)$-connected circular domain conformally equivalent to P, where $\mathbb{M}(D)$ satisfies $\sum |C|^{-2} < \infty$.
The Schwarzian derivative $\mathcal{S}$ of any conformal mapping f of D onto P has the form

$$\mathcal{S}(z) = \sum_{T \in \mathbb{M}(D)} T'(z)^2 \left[\mathcal{R}(T(z)) + \mathcal{A}_C(T(z))\right] + \mathcal{A}_R(z, b),$$

where $\mathcal{R}$ and $\mathcal{A}_C$ are as in Definition 4.33 and $\mathcal{A}_R$ is as in Definition 4.42.

Degrees of Freedom of the Schwarzian Derivative

We counted in Section 4.2.3 the degrees of freedom of doubly connected mappings onto CAPDs. The theorem above allows us to also count the degrees for a mapping onto a MCCAPD of a connectivity greater than two.
Let $K := \sum_j K_j$ again indicate the total number of vertices on the boundary of the MCCAPD.

We first describe a MCCAPD for the image domain. Each circular arc polygon bounding the domain can be characterized by its vertices together with the curvature of its edges. We therefore get $3K$ real parameters for the whole domain. Since we can normalize the domain by the application of a Möbius transformation, we subtract 6 real parameters, resulting in $3K - 6$ parameters for the image domain.

On the preimage side, we have K real parameters for the prevertices, as they can be identified by their arguments in relation to the center of their circles. For these circles we need additional $3(m+1) = 3m+3$ real parameters for the centers and radii. There are also K interior angles and K parameters γ. The parameters γ can be described by real values according to Lemma 4.12. Further, we have $3m-3$ real parameters b to set for the analytic remainder.
We have to subtract six real degrees of freedom for the normalization we apply via a Möbius transformation. We must also ensure a valid mapping, by demanding the integrals

$$\int_\delta f^{(k)}(z)dz, \qquad k = 1, 2, 3,$$

to be zero for curves δ enclosing only one of the circles C_j, where $j = 1, \ldots, m$. This gives an additional $6m$ degrees to subtract.

Summing these values results in

$3K$	the parameters p, a, γ
$+ 3m + 3$	the centers and radii
$+ 3m - 3$	the parameters b of the analytic remainder
$- 6$	normalization by a Möbius transformation
$- 6m$	integral equations for validity
$= 3K - 6.$	

Hence both sides have the same number of degrees of freedom.

This allows the same conclusion as in Section 4.2.3 for the doubly connected mappings: Not every set of parameters has to yield a valid mapping onto a MCCAPD.

4.4.4 Analytic Remainder Construction I: Laurent Series

While we know that there are $3m-3$ basis functions for $\mathcal{A}_R$, we need to construct them. We will use the notation $\mathcal{A}$ instead of $\mathcal{B}_i$ or $\mathcal{A}_R$, as they have the same properties. We will further suppose that D is an unbounded circular domain.

We know from the functional equation

$$T'(z)^2 \mathcal{A}(T(z)) = \mathcal{A}(z)$$

that $\mathcal{A}$ has a zero of the fourth order at infinity. This follows by evaluating the functional equation for u, where $T(u) = \infty$, and the fact that by definition $\mathcal{A}(u)$ must be finite, as u is not a limit point. As a result, the integrals

$$\int_\Gamma z^k \mathcal{A}(z) dz = 0, \qquad k = 0, 1, 2, \tag{4.53}$$

must be zero, if Γ is a curve close enough to infinity. In other words: Γ has to enclose all of the boundary circles C_j of D.
To utilize this result, we write $\mathcal{A}$ as a sum of Laurent series[38] expanded around the centers c_j of the circles C_j bounding D

$$\mathcal{A}(z) = \sum_{j=0}^{m} \sum_{n=1}^{\infty} \frac{d(n,j)}{(z - c_j)^n}. \tag{4.54}$$

This notation is defined outside of every circle C_j, and is therefore valid everywhere in D. An alternate version would be an expansion around just one of the centers c_j

$$\mathcal{A}(z) = \sum_{n=-\infty}^{\infty} \frac{d(n,j)}{(z - c_j)^n}, \tag{4.55}$$

[38] The sum of the series has no constant coefficient, as $\mathcal{A}$ has a zero at infinity.

defining $\mathcal{A}$ in an annulus surrounding C_j. In this form, we can apply the functional equation

$$\mathcal{A}(z) = \sigma_j'(z)^2 \overline{\mathcal{A}(s_j(z))}$$

to obtain

$$\sum_{n=-\infty}^{\infty} \frac{d(n,j)}{(z-c_j)^n} = \sum_{n=-\infty}^{\infty} \frac{r_j^{-2n+4}\overline{d(n,j)}}{(z-c_j)^{-n+4}} = \sum_{n=-\infty}^{\infty} \frac{r_j^{2n-4}\overline{d(-n+4,j)}}{(z-c_j)^n}.$$

We now have

$$d(n,j) = r_j^{2n-4}\overline{d(-n+4,j)}, \tag{4.56}$$

which gives for the first three coefficients

$$d(1,j) = r_j^{-2}\,\overline{d(3,j)}, \qquad d(2,j) = \overline{d(2,j)}, \qquad d(3,j) = r_j^2\,\overline{d(1,j)}.$$

Since $d(2,j)$ is real and $d(3,j)$ can be calculated from $d(1,j)$, we can represent these three coefficients by only three real values.
We also have, by calculating the integrals (4.53) for equation (4.54),

$$\begin{aligned} &\sum_{j=0}^{m} d(1,j) = 0, \\ &\sum_{j=0}^{m} [c_j d(1,j) + d(2,j)] = 0, \\ &\sum_{j=0}^{m} \left[c_j^2 d(1,j) + 2c_j d(2,j) + d(3,j)\right] = 0. \end{aligned} \tag{4.57}$$

With 3 real parameters per circle and 6 restricting real equations, all of the first three coefficients of all expansions in (4.54) are defined by $3(m+1) - 6 = 3m - 3$ real values. This matches exactly the number of linearly independent functions according to Lemma 4.40. The solutions of the system (4.57) therefore correspond to the basis functions $\mathcal{B}_i$, since linear combinations of the $\mathcal{B}_i$ result in linear combinations of the coefficients $d(n,j)$.
This yields a way to verify the linear independence of the functions. If the vectors

$$(\operatorname{Re} d(1,0), \operatorname{Im} d(1,0), d(2,0), \operatorname{Re} d(1,1), \operatorname{Im} d(1,1), \ldots, \operatorname{Im} d(1,m), d(2,m))$$

are linearly independent, so are the functions.

We may now calculate the remaining coefficients from those already known, allowing us to directly generate a basis.
Suppose we know the expansions for every circle but one, say C_k, in (4.54). We would be able to calculate the regular part with the coefficients $d(-l,k)$, where $l \geq 0$, in (4.55) by using

$$\sum_{l=0}^{\infty} d(-l,k)(z-c_k)^l = \sum_{j\neq k} \sum_{n=1}^{\infty} \frac{d(n,j)}{(z-c_j)^n}.$$

Differentiation and evaluation at c_k yields the formula

$$d(-l,k) = \sum_{j\neq k}\sum_{n=1}^{\infty}(-1)^l\binom{l+n-1}{l}c(k,j)^{-(l+n)}d(n,j),$$

for all $l \in \mathbb{N}\cup\{0\}$. Here $c(k,j) := c_k - c_j$ denotes the difference between two of the centers. We further shorten the notation by writing

$$w(l,n) := (-1)^l\binom{l+n-1}{l}$$

for the weight of $d(n,j)$.
Using (4.56) we can replace $d(-l,k)$ and find

$$r_k^{-2l-4}\overline{d(l+4,k)} = \sum_{j\neq k}\sum_{n=1}^{\infty}\frac{w(l,n)}{c(k,j)^{(l+n)}}d(n,j). \tag{4.58}$$

Returning to the task of determining the unknown coefficients, we define

$$\lambda(l,k) := \sum_{j\neq k}\sum_{n=1}^{3}\frac{w(l,n)}{c(k,j)^{(l+n)}}d(n,j),$$

which allows us to reshape equation (4.58) to

$$\sum_{j\neq k}\sum_{n=4}^{\infty}\frac{w(l,n)}{c(k,j)^{(l+n)}}d(n,j) - r_k^{-2l-4}\overline{d(l+4,k)} = -\lambda(l,k), \tag{4.59}$$

where $l = 0,\dots,\infty$ and $k = 0,\dots,m$.
The remaining coefficients may be calculated from this system of equations. The downside of this approach is the fact that the system has an infinite dimension, demanding methods such as the Banach fixed-point theorem, which itself demands some convergence conditions.[39] Some alternative constructions are therefore presented in the following.
This system can nonetheless be of great use from the numerical point of view. In the numerics, it is enough to calculate a finite number of coefficients for an approximation, which can be achieved by reducing the system to a suitable amount of variables and solving it by common numerical methods.

Bounded Domains

The concept above holds only for unbounded domains. For bounded domains equation (4.54) changes to

$$\mathcal{A}(z) = \sum_{n=0}^{\infty}d(-n,0)(z-c_j)^n + \sum_{j=1}^{m}\sum_{n=1}^{\infty}\frac{d(n,j)}{(z-c_j)^n},$$

[39] Results from the Riemann-Hilbert problems allow statements regarding the convergence of successive approximations, but we will not further follow this approach.

as we need a Taylor series without negative powers for the bounding circle C_0.
A possible approach is to calculate a function $\mathcal{A}$ for the unbounded domain $s_0(D)$ and then calculate the version for the bounded domain D by using the functional equation $\sigma_0'(z)^2\overline{\mathcal{A}(s_0(z))} = \mathcal{A}(z)$.

Let us denote the boundary circles $s_0(C_j)$ of $s_0(D)$ by C_j' with center c_j' and the coefficients for the corresponding expansion by $d'(n,j)$.
Suppose the expansion for the circles C_j' to be known. We want to apply the functional equation to it. The centers c_j' are mapped onto the points $s_0(c_j') = \tilde{c}_j$ in this process. These points lie inside the circles C_j. The expansion around the $\tilde{c}_j$ with the coefficients $\tilde{d}(n,j)$ can be calculated from the expansion around the c_j' by

$$\begin{aligned}
\tilde{d}(1,j) &= -\overline{d'(1,j)}\frac{r_0^2}{(c_0-\tilde{c}_j)^2} + \overline{d'(2,j)}\frac{2}{(c_0-\tilde{c}_j)} - \overline{d'(3,j)}\frac{1}{r_0^2}\\
\tilde{d}(2,j) &= \overline{d'(2,j)} - \overline{d'(3,j)}\frac{(c_0-\tilde{c}_j)}{r_0^2}\\
\tilde{d}(3,j) &= -\overline{d'(3,j)}\frac{(c_0-\tilde{c}_j)^2}{r_0^2}\\
\tilde{d}(l,j) &= \sum_{n=0}^{\infty}(-1)^l\,\overline{d'(l+n,j)}\binom{l-4+n}{l-4}\frac{(c_0-\tilde{c}_j)^{2l-4+n}}{r_0^{2l-4+2n}} \qquad \text{for } l\geq 4,
\end{aligned}$$

where $j = 1,\dots,m$. Since $\tilde{c}_j = s_0(c_j') \neq c_j$, we shift the expansion point to c_j. We calculate the correct coefficients d by

$$d(l,j) = \sum_{n=1}^{l}\binom{l-1}{n-1}\tilde{d}(n,j)(\tilde{c}_j - c_j)^{l-n}$$

where $l = 1,\dots,\infty$ and $j = 1,\dots,m$. This gives us the desired values for the circles C_j, where $j = 1,\dots,m$.
The expansion for C_0 can be calculated by using the expansions around the c_j' in the form

$$\sum_{l=0}^{\infty} d(-l,0)(z-c_0)^l = \sum_{j=1}^{m}\sum_{n=1}^{\infty}\frac{d'(n,j)}{(z-c_j')^n}.$$

The individual coefficients can again be computed by differentiation and evaluation at $z = c_0$.

Doubly Connected Domains

A problem with the system of equations (4.57) and the doubly connected case is that $3m-3$ is zero for $m = 1$. However, as shown earlier, there exists one linearly independent analytic function.
This behavior can be justified by the fact that the 6 real equations are not linearly independent for $m = 1$. There are actually only 5 real equations for doubly connected domains. This leaves one degree of freedom for the one known basis function.

4.4.5 Analytic Remainder Construction II: First Order Poles

One way to construct the functions $\mathcal{B}_i$ would be to use the same method as we have used previously by constructing $\mathcal{A}_C$.
The first step would be to construct a function $\mathcal{T}$, where $\mathcal{T}$ and $\sigma'(z)^2\overline{\mathcal{T}(s(z))}$ are without any poles in D_E. This can be established by using a linear system of equations as in the proof of Lemma 4.31. It should further be invariant against at least one reflection s_j in the form of the functional equation.

Lemma 4.44
Let $\{l_1, l_2, l_3, l_4\} \subset \Lambda$, $l_1 = s(l_2)$, $l_3 = s(l_4)$, $s \in \mathbb{S}(D)$, and $\overline{\sigma(z)} = s(z)$.
The function

$$\mathcal{T}(z) = \frac{-(l_1 - l_2)(l_3 - l_4)}{(z - l_1)(z - l_2)(z - l_3)(z - l_4)}$$

satisfies the functional equation

$$\sigma'(z)^2\overline{\mathcal{T}(s(z))} = \mathcal{T}(z).$$

Proof. The statement of the lemma can be gathered directly by calculation.
Each of the terms $(l_i - l_j)$ can be replaced by the expression

$$(l_i - l_j) = \overline{\left(\frac{-r^2(s(l_i) - s(l_j))}{(s(l_i) - c)(s(l_j) - c)}\right)},$$

where $s(z) = r^2/(\overline{z} - \overline{c}) + c$. We then have

$$\begin{aligned}\sigma'(z)^2\overline{\mathcal{T}(s(z))} &= \frac{r^4}{(z-c)^4}\overline{\left(\frac{-(l_1 - l_2)(l_3 - l_4)}{(s(z) - l_1)(s(z) - l_2)(s(z) - l_3)(s(z) - l_4)}\right)} \\ &= \frac{-(s(l_1) - s(l_2))(s(l_3) - s(l_4))}{(z - s(l_1))(z - s(l_2))(z - s(l_3))(z - s(l_4))} = \mathcal{T}(z)\end{aligned}$$

□

We now construct a Poincaré theta series with the function $\mathcal{T}$, which satisfies all our requirements for an analytic remainder of the Schwarzian derivative $\mathcal{S}$. Hence, we state an explicit formula to describe the basis functions $\mathcal{B}_i$.

Lemma 4.45
Let $\{l_1, l_2, l_3, l_4\} \subset \Lambda$, $l_1 = s_j(l_2)$, $l_3 = s_j(l_4)$, and $s_j \in \mathbb{S}(D)$ the reflection against the boundary circle C_j. Let further $\mathbb{M}(D)$ satisfy the property $\sum |C|^{-2} < \infty$.

The function

$$\mathcal{A}(z) = \sum_{T \in \mathbb{M}(D)} T'(z)^2 \mathcal{T}(T(z)),$$

where

$$\mathcal{T}(z) = \frac{-(l_1 - l_2)(l_3 - l_4)}{(z - l_1)(z - l_2)(z - l_3)(z - l_4)},$$

satisfies the functional equations

$$\begin{aligned} T'(z)^2 \mathcal{A}(T(z)) &= \mathcal{A}(z), \qquad T \in \mathbb{M}(D), \\ \sigma'(z)^2 \overline{\mathcal{A}(s(z))} &= \mathcal{A}(z), \qquad s \in \mathbb{S}(D),\ \overline{\sigma(z)} = s(z), \end{aligned}$$

and is analytic in D_E.

Proof. We have according to Lemma 4.44

$$\sigma_j'(z)^2 \overline{\mathcal{T}(s_j(z))} = \mathcal{T}(z). \tag{4.60}$$

Since $\mathcal{T}$ contains simple poles at several limit points, we require according to Lemma 2.43 the convergence condition $\sum |C|^{-2} < \infty$ to construct the Poincaré series

$$\mathcal{A}(z) = \sum_{T \in \mathbb{M}(D)} T'(z)^2 \mathcal{T}(T(z))$$

that satisfies the functional equation

$$T'(z)^2 \mathcal{A}(T(z)) = \mathcal{A}(z), \qquad T \in \mathbb{M}(D).$$

The equation

$$\sigma'(z)^2 \overline{\mathcal{A}(s(z))} = \mathcal{A}(z), \qquad s \in \mathbb{S}(D),\ \overline{\sigma(z)} = s(z),$$

can be shown by applying the proof of Lemma 4.34 by using (4.60). □

4.4.6 Analytic Remainder Construction III: Second Order Poles

Based on Lemma 4.23, we have in the doubly connected case the analytic remainder

$$\mathcal{A}(z) = \frac{b(l_1 - l_2)^2}{(z - l_1)^2 (z - l_2)^2}, \qquad b \in \mathbb{R},$$

where l_1 and l_2 are the fixed points of the generator T of $\mathbb{M}(D)$. Since all functions in $\mathbb{M}(D)$ are of the form T^n, $n \in \mathbb{Z}$, these two fixed points are actually all the fixed points of all transformations.

To apply this concept to domains of a connectivity greater then two, we have to modify it. Let D in the following be a $(m+1)$-connected circular domain ($m > 1$) and $\mathbb{M}(D)$ the corresponding Schottky group. The set $\mathbb{M}(D)$ is generated by more than one transformation. Hence, we need to further specify the fixed points and write

$$\mathcal{A}(z,T) := \frac{(l_{T,1} - l_{T,2})^2}{(z - l_{T,1})^2 (z - l_{T,2})^2},$$

where $l_{T,1}$ and $l_{T,2}$ are the fixed points of T.[40]

Lemma 4.46
Let $T \in \mathbb{M}(D) \setminus \{id\}$ and $l_{T,1}$ and $l_{T,2}$ be the fixed points of T. The function

$$\mathcal{A}(z,T) = \frac{(l_{T,1} - l_{T,2})^2}{(z - l_{T,1})^2 (z - l_{T,2})^2}$$

has the properties

$$\begin{aligned} \mathcal{A}(z,T^n) &= \mathcal{A}(z,T), && n \in \mathbb{Z} \setminus \{0\}, \\ \sigma'(z)^2 \overline{\mathcal{A}(s(z),T)} &= \mathcal{A}(z, s \circ T \circ s), && s \in \mathbb{S}(D),\ \sigma(z) = \overline{s(z)}, \\ U'(z)^2 \mathcal{A}(U(z),T) &= \mathcal{A}(z, U^{-1}TU), && U \in \mathbb{M}(D). \end{aligned} \tag{4.61}$$

Proof. The first equation $\mathcal{A}(z,T^n) = \mathcal{A}(z,T)$, where $n \in \mathbb{Z} \setminus \{0\}$, follows directly from the definition of $\mathcal{A}(z,T)$, as each T^n has the same fixed points as T.
The second equation can be gathered by calculating

$$\sigma'(z)^2 \overline{\mathcal{A}(s(z),T)} = \frac{(s(l_{T,1}) - s(l_{T,2}))^2}{(z - s(l_{T,1}))^2 (z - s(l_{T,2}))^2}.$$

Each point $s(l_T)$ has the property

$$(s \circ T \circ s)(s(l_T)) = (s \circ T)(l_T) = s(l_T)$$

and is therefore a fixed point of the Möbius transformation $s \circ T \circ s$.
A similar calculation for $U'(z)^2 \mathcal{A}(U(z),T)$ yields the third equation. □

To reduce the number of different notations $\mathcal{A}(z,T^n)$ for the same function $\mathcal{A}(z,T)$, we demand that the denoting transformation T can not be written as the nth power of another transformation U, where $n > 1$, i.e. $T \neq U^n$ for all $U \in \mathbb{M}(D)$ and $n > 1$. We still have $\mathcal{A}(z,T) = \mathcal{A}(z,T^{-1})$.

The lemma above contains the Möbius transformation $s \circ T \circ s$, which needs some interpretation. We begin with a definition and introduce a new operator.

[40] Note that we have $\mathcal{A}(z,T) = \mathcal{T}(z)$ for $l_{T,1} = l_1$, $l_{T,2} = l_2$, $l_1 = l_4$, where $\mathcal{T}$ is from Lemma 4.45.

Definition 4.47
For a Schottky group $\mathbb{M}(D)$, the operator $*$ for a Möbius transformation $U = U_1 \dots U_n$ of the group, where $U_j \in \text{gen}(\mathbb{M}(D))$, $j = 1, \dots, n$, inverses each (extended) generator U_j used to compose U, i.e.

$$U^* = (U_1 \dots U_n)^* = U_1^{-1} \dots U_n^{-1}.$$

It has the properties

$$(U^*)^* = U \quad \text{and} \quad (UV)^* = U^* V^*.$$

The definition above is only reasonable for a Schottky group and a specific set of generators, since the factorization would not otherwise be unique. As these requirements are satisfied by our construction of $\mathbb{M}(D)$, we suppose them to be satisfied for the following statements.

Lemma 4.48
For any transformation $U \in \mathbb{M}(D)$ and reflection $s_j \in \mathbb{S}(D)$ against a boundary circle C_j of D, the following is true

$$s_0 U s_0 = U^*$$

and for $j \neq 0$

$$s_j U s_j = T_j^{-1} U^* T_j,$$

where $T_j = s_0 \circ s_j \in \text{gen}(\mathbb{M}(D))$.

Proof. We denote the members of $\text{gen}(\mathbb{M}(D))$ by $T_j^{\pm 1}$. According to the definition of $\mathbb{M}(D)$, the (extended) generators are of the form

$$T_j = s_0 \circ s_j, \qquad T_j^{-1} = s_j \circ s_0.$$

We simplify the notation by using only the indices of the reflections

$$T_j = (0j), \qquad T_j^{-1} = (j0).$$

Suppose we have a transformation $U = U_1 U_2 \dots U_n$, where each U_k is a generator. We can replace U_1 by $T_i^{\pm 1}$, U_2 by $T_j^{\pm 1}$ and so on. The application of s_0 yields

$$s_0 U s_0 = \begin{cases} s_0 T_i T_j \dots & = 0(0i)(0j)\dots = (i0)(j0)\dots = T_i^{-1} T_j^{-1} \dots \\ s_0 T_i T_j^{-1} \dots & = 0(0i)(j0)\dots = (i0)(0j)\dots = T_i^{-1} T_j \dots \\ s_0 T_i^{-1} T_j \dots & = 0(i0)(0j)\dots = (0i)(j0)\dots = T_i T_j^{-1} \dots \\ s_0 T_i^{-1} T_j^{-1} \dots & = 0(i0)(j0)\dots = (0i)(0j)\dots = T_i T_j \dots \end{cases}$$

The s_0 to the left of U changes the grouping of the reflections. It either cancels out the reflection s_0 of T_i, changing it to T_i^{-1}, or adds the reflection to change T_i^{-1} to T_i. This modification of the first transformations leads to a "spare reflection" s_0 grouped to the next transformation or borrows a reflection from the following transformation. In either case, the process continues in the same way with all following transformations. Since we also append s_0 to U, the total number of reflections is still even and they can all be grouped to Möbius transformations.
It may be necessary to insert the identity $\mathrm{id} = s_0 \circ s_0$ in the form of two successive reflections against C_0 to get pairs $(0j)$ and $(j0)$ as seen for $s_0 T_i T_j^{-1} \ldots$ above.
The same identity is used if we apply s_j, where $j \neq 0$. We insert a pair $s_0 \circ s_0$ between s_j and U at both ends and proceed as above.

$$s_j U s_j = s_j s_0 s_0 U s_0 s_0 s_j = (j0)0U0(0j) = T_j^{-1} U^* T_j.$$

□

It is important to note that the "piecewise" inversion of a transformation in the form of the $*$ operator is not equal to the inversion of the transformation itself (save for some special symmetries, e.g. $(TUT)^{-1} = T^{-1}U^{-1}T^{-1}$).

We can now rewrite the functional equation (4.61) for $\mathcal{A}(z,T)$ as

$$\sigma_j'(z)^2 \overline{\mathcal{A}(s_j(z),T)} = \mathcal{A}(z, T_j^{-1} T^* T_j).$$

The next step in the construction of an analytic function $\mathcal{A}$ would be to build a Poincaré series with $\mathcal{A}(z,T)$, but this is not possible as $\mathcal{A}(z,T)$ contains second order poles at limit points. Second order poles would demand the unsatisfiable property $\sum |C|^0 < \infty$ of the group $\mathbb{M}(D)$.
This "not-convergence" property can easily be seen by summing over the subset $\{T^n \,|\, n \in \mathbb{Z}\} \subset \mathbb{M}(D)$

$$\sum_{n=-\infty}^{\infty} [(T^n)'(z)]^2 \mathcal{A}(T^n(z),T) = \sum_{n=-\infty}^{\infty} \mathcal{A}(z,T) = \mathcal{A}(z,T) \sum_{n=-\infty}^{\infty} 1 = \infty$$

by using the properties from Lemma 4.46. The sum tends to infinity, as we count the same term infinite times. To avoid this problem, we must ensure for the sum over the transformations V that $V'(z)^2 \mathcal{A}(V(z),T) \neq \mathcal{A}(z,T)$.

Definition 4.49
Two transformations $U, V \in \mathbb{M}(D)$ are equivalent with respect to $T, W \in \mathbb{M}(D)$

$$U \; {}_T\!\sim_W V$$

if

$$U'(z)^2 \mathcal{A}(U(z),T) = V'(z)^2 \mathcal{A}(V(z),W), \qquad z \in D.$$

Two sets of transformations $M_1, M_2 \subset \mathbb{M}(D)$ are called equivalent, if for each $V \in M_1$ there is exactly one equivalent $U \in M_2$ and for each $U \in M_2$ there is exactly one equivalent $V \in M_1$.

We write $\sim_T$ instead of ${}_T\sim_T$ and we write $\sim$ instead of $\sim_T$ if the transformation is known by the context.

We need a suitable subset $\mathbb{M}(D,T) \subset \mathbb{M}(D)$ to avoid the problem of counting the same term multiple times, as occurred for T^n above. $\mathbb{M}(D,T)$ should have the property that each pair of transformations $U, V \in \mathbb{M}(D,T)$, where $U \neq V$, is not equivalent $U \not\sim V$ with respect to $\mathcal{A}(z,T)$. Hence, we have to exclude powers of T and transformations $U = T^{\pm 1}V$ starting with $T^{\pm 1}$.
We also do not want transformations T that can be written as either $T = V^{-1}WV$ or $T = W^n$, $n > 1$, to denote a set $\mathbb{M}(D,T)$. In such a case, we will use $\mathbb{M}(D,W)$ instead. Refining this idea leads to the following definition.

Definition 4.50
The subset $\mathbb{M}(D)^\circ \subset \mathbb{M}(D)$ contains all transformations $T \in \mathbb{M}(D)$ that, for all $U \in \mathbb{M}(D)$ and all $n > 1$, satisfy the properties $T \neq U^n$ and $|U^{-1}TU| \geq |T|$.
The subset $\mathbb{M}(D,T) \subset \mathbb{M}(D)$, where $T = T_1 \dots T_m \in \mathbb{M}(D)^\circ$, $T_k \in \operatorname{gen}(\mathbb{M}(D))$ for $k = 1, \dots, m$, is defined by

$$\mathbb{M}(D,T) := \{V \,|\, V = V_1 \dots V_n,\, V_j \in \operatorname{gen}(\mathbb{M}(D)),\, V_1 \neq T_m^{-1},\, V_1 \dots V_m \neq T\} \cup \{id\}.$$

For a transformation $T \in \operatorname{gen}(\mathbb{M}(D))$, this simplifies to

$$\mathbb{M}(D,T) := \{V \,|\, V = V_1 \dots V_n,\, V_j \in \operatorname{gen}(\mathbb{M}(D)),\, V_1 \notin \{T, T^{-1}\}\} \cup \{id\}.$$

The definition for $\mathbb{M}(D,T)$ is more complicated if T is not a generator. The reason can be shown by an example.
Suppose $\mathbb{M}(D)$ is generated by T and U, then $\mathbb{M}(D)$ contains for example $W = TUT$. If we apply a transformation V in the manner as above, we have $V^{-1}WV = V^{-1}TUTV$. If we choose $V = W$ and apply the transformations of $W = TUT$ one after another, we obtain

$$(TUT)^{-1}TUT(TUT) = (UT)^{-1}UTT(UT) = (T)^{-1}TTU(T) = TUT$$

or in a simplified notation

$$TUT \xrightarrow{T} UTT \xrightarrow{U} TTU \xrightarrow{T} TUT.$$

If we apply the transformations of W^{-1} instead, we have

$$TUT \xrightarrow{T^{-1}} TTU \xrightarrow{U^{-1}} UTT \xrightarrow{T^{-1}} TUT.$$

By applying successively the transformation W or the transformation W^{-1}, the results are rotating through a subset of the transformations with the same length as W.[41]

[41] The rotations of W could also be denoted as circular shifts of the generators used to compose W.

The order differs, but the resulting transformations are the same for W and W^{-1}. We therefore have to successively apply either $W_1 \dots W_{m-1}$ or $(W_2 \dots W_m)^{-1}$, but not both, otherwise we would include some transformations multiple times. It is further not valid to apply W or its inverse completely, since the result would again be W, as $W \sim_W \mathrm{id}$. The restriction to one of the two paths can be accomplished by $V_1 \neq W_m^{-1}$ (or $V_1 \neq W_1$). To prohibit the application of W itself (or W^{-1}), we may demand $V_1 \dots V_m \neq W$ (or $V_1 \dots V_m \neq W^{-1}$). This leads to

$$\mathbb{M}(D,W) = \{V \mid V = V_1 \dots V_n,\, V_j \in \mathrm{gen}(\mathbb{M}(D)),\, V_1 \neq W_m^{-1},\, V_1 \dots V_m \neq W\} \cup \{\mathrm{id}\}$$

or equivalently

$$\mathbb{M}(D,W) = \{V \mid V = V_1 \dots V_n,\, V_j \in \mathrm{gen}(\mathbb{M}(D)),\, V_1 \neq W_1,\, V_1 \dots V_m \neq W^{-1}\} \cup \{\mathrm{id}\}.$$

Lemma 4.51
No two transformations $U, V \in \mathbb{M}(D,T)$, where $U \neq V$ and $T \in \mathbb{M}(D)^\circ$, are equivalent $U \not\sim_T V$.

Proof. For two equivalent transformations $U \sim V$, we would have $(VU^{-1})T(UV^{-1}) = T$, where $VU^{-1} \neq \mathrm{id}$. Since T can not be written as $T = W^n$, there is no rotation of T that equals T itself. This can be seen by investigating the proof of Lemma 2.37. Hence, we must have $(VU^{-1}) = T^m$, where $m \in \mathbb{Z}$, which is not possible by the restrictions for the elements of $\mathbb{M}(D,T)$. □

To easier denote the behavior of rotating the transformations, we introduce some new notations.

Definition 4.52
Let $T = T_1 \dots T_n \in \mathbb{M}(D)$ and $T_j \in \mathrm{gen}(\mathbb{M}(D))$, where $j = 1, \dots, n$. The set of rotations is defined by

$$\mathrm{rot}^+(T) := \{(T_1 \dots T_n),\, (T_2 \dots T_n T_1),\, \dots,\, (T_n T_1 \dots T_{n-1})\},$$
$$\mathrm{rot}^-(T) := \{U^{-1} \mid U \in \mathrm{rot}^+(T)\},$$
$$\mathrm{rot}(T) := \mathrm{rot}^+(T) \cup \mathrm{rot}^-(T).$$

We want to combine the results so far and state the following properties of the set $\mathbb{M}(D,T)$.

Lemma 4.53
For a set $\mathbb{M}(D,T)$, $T \in \mathbb{M}(D)^\circ$ the following is true

- $\mathbb{M}(D,T) \;{}_T\!\sim_{T^{-1}} \mathbb{M}(D,T^{-1})$
- $V \in \mathbb{M}(D,T) \Rightarrow V^* \in \mathbb{M}(D,T^*)$

- $\mathbb{M}(D,T)\ {}_T\!\sim_{T^*}\mathbb{M}(D,T^*)$ *if* $T^* \in \mathrm{rot}(T)$
- $\mathbb{M}(D,T)\ {}_T\!\not\sim_{T^*}\mathbb{M}(D,T^*)$ *if* $T^* \notin \mathrm{rot}(T)$

Proof. The first property follows directly from $\mathcal{A}(z,T) = \mathcal{A}(z,T^{-1})$, as shown in Lemma 4.46.
The second property can be gathered by the definitions of $*$ and $\mathbb{M}(D,T)$.
The third and fourth property follow from the fact that $\mathbb{M}(D,T)$ (by its construction) covers all rotations of T. If T^* is a rotation of T, i.e. $T^* = U^{-1}TU$, where $U \in \mathbb{M}(D,T)$, the sets must be equivalent. This also holds if T^* is the inverse of a rotation according to the first property.
If T^* is not a rotation, we have $T^* \neq U^{-1}TU$ for every $U \in \mathbb{M}(D,T)$. Hence the identity in $\mathbb{M}(D,T^*)$ has no equivalent element in $\mathbb{M}(D,T)$, so the sets can not be equivalent. □

With this preparation, we can now prove the convergence of the following sum:

Lemma 4.54
Let D be a circular domain, $\infty \in D_R$, and $T \in \mathbb{M}(D)^\circ$. The sum

$$\sum_{V\in\mathbb{M}(D,T)} V'(z)^2\mathcal{A}(V(z),T) \tag{4.62}$$

converges locally uniformly on D_E and is analytic in D_E.

Proof. We know from Lemmas 2.25 and 2.31 that every fixed point is a limit point. We further know from Lemma 4.46 that

$$V'(z)^2\mathcal{A}(V(z),T) = \mathcal{A}(z,V^{-1}TV) = \frac{(l_1-l_2)^2}{(z-l_1)^2(z-l_2)^2},$$

where $l_j = V^{-1}(l_{T,j})$, $j = 1,2$, are the fixed points of $V^{-1}TV$ and $l_{T,j}$, $j = 1,2$, are the fixed points of T. Hence, the sum (4.62) has no poles in D_E, because every transformation $V(l)$, $V \in \mathbb{M}(D)$, of a limit point is again a limit point. This also means that for a closed subset $M \subset D_E$ and $z \in M$, the denominators of all $\mathcal{A}(z,V^{-1}TV)$ have a common lower boundary $\lambda > 0$. On the other hand, the numerator can be written as

$$(l_1-l_2)^2 = \left(V^{-1}(l_{T,1}) - V^{-1}(l_{T,2})\right)^2 = \left(\frac{l_{T,1}-l_{T,2}}{C^2(l_{T,1}-u)(l_{T,2}-u)}\right)^2$$

where $V^{-1}(z) = (Az+B)/(Cz+D)$ and $u = -\frac{D}{C} = V(\infty)$, except for $V = \mathrm{id}$. The differences $|l_{T,j} - V(\infty)|$ have a lower boundary $\mu > 0$ according to Lemma 2.36 and

the definition of $\mathbb{M}(D,T)$. If we combine these results, we can state for every term

$$|\mathcal{A}(z, V^{-1}TV)| \leq \left| \frac{(l_{T,1} - l_{T,2})^2}{C^4 \mu^2 \lambda} \right| = |C|^{-4} \nu$$

and for the sum, excluding the term for $V = id$,

$$\left| \sum_{V \in \mathbb{M}(D,T)} V'(z)^2 \mathcal{A}(V(z), T) \right| \leq \sum_{V \in \mathbb{M}(D,T)} |\mathcal{A}(z, V^{-1}TV)| \leq \nu \sum_{V \in \mathbb{M}(D,T)} |C|^{-4} < \infty.$$

□

With convergence ensured, we now prepare for showing the functional equations.

Lemma 4.55
For transformations $T \in \mathbb{M}(D)^\circ$ and $V \in \text{gen}(\mathbb{M}(D))$, we have

$$\{\, UV \mid U \in \mathbb{M}(D,T) \,\} \sim \mathbb{M}(D,T),$$

i.e. appending a transformation V to the transformations of $\mathbb{M}(D,T)$ yields a set equivalent to $\mathbb{M}(D,T)$.

Proof. The transformations $U \in \mathbb{M}(D,T)$ are, in comparison with the ones in $\mathbb{M}(D)$, restricted by choices of the transformations in $\text{gen}(\mathbb{M}(D))$ used in their construction, where we must have

$$U_1 \neq T_m^{-1} \quad \text{and} \quad U_1 \dots U_m \neq T.$$

There are two ways that the combination UV can break these conditions. The appending of T_m^{-1} to the identity yields $UV = T_m^{-1}$, while the appending of T_m to $T_1 \dots T_{m-1}$ yields T. If we append neither of these two transformation but $V \in \text{gen}(\mathbb{M}(D)) \setminus \{T_m^{-1}, T_m\}$, we get an equivalent set, as the transformations ending with V^{-1} and the ones not ending with V^{-1} merely exchange places.
We take a closer look at the critical transformations, i.e. the ones that can break the conditions of $\mathbb{M}(D,T)$. Listing the transformations of the group $\mathbb{M}(D,T)$ for the appending of T_m^{-1} or T_m gives

U	$W \sim UT_m^{-1}$	$W \sim UT_m$
id	$T_1 \dots T_{m-1}$	T_m
T_m	id	T_m^2
$T_1 \dots T_{m-1}$	$T_1 \dots T_{m-1} T_m^{-1}$	id
$U_1 \dots U_n$	$U_1 \dots U_n T_m^{-1}$ or $U_1 \dots U_{n-1}$	$U_1 \dots U_n T_m$ or $U_1 \dots U_{n-1}$

In the context of equivalent functions, we only have a rotation in the set if we apply either T_m^{-1} or T_m. The sets $\mathbb{M}(D,T)$ and $\{\, UV \mid U \in \mathbb{M}(D,T) \,\}$ are therefore equivalent for all $V \in \mathrm{gen}(\mathbb{M}(D))$. □

One problem remains: The application of a reflection leads to the $*$ operator, but according to Lemma 4.53, we may leave the set $\mathbb{M}(D,T)$ in the process. To deal with this issue, we define the analytic functions $\mathcal{A}_T$ in the following way, and hence determine another way to describe the analytic functions that can be used to construct the basis functions $\mathcal{B}_i$.

Definition 4.56
Let $T \in \mathbb{M}(D)^\circ$. The function $\mathcal{A}_T$ is defined by

$$\mathcal{A}_T(z) := \sum_{V \in \mathbb{M}(D,T)} V'(z)^2 \mathcal{A}(V(z),T) + \sum_{V \in \mathbb{M}(D,T^*)} V'(z)^2 \mathcal{A}(V(z),T^*)$$

if $T^* \notin \mathrm{rot}(T)$, or

$$\mathcal{A}_T(z) := \sum_{V \in \mathbb{M}(D,T)} V'(z)^2 \mathcal{A}(V(z),T)$$

if $T^* \in \mathrm{rot}(T)$.

With all preparation complete, we may now show that the functions of the definition above satisfy our requirements for the analytic remainder functions.
Note that the following lemma does not require the Schottky group $\mathbb{M}(D)$ to satisfy the property $\sum |C|^{-2} < \infty$.

Lemma 4.57
The function $\mathcal{A}_T$ of Definition 4.56, where $T \in \mathbb{M}(D)^\circ$, is analytic everywhere in $D_E = \mathbb{C}_\infty \setminus \Lambda$ and satisfies the equations

$$\sigma'(z)^2 \overline{\mathcal{A}_T(s(z))} = \mathcal{A}_T(z), \qquad \sigma(z) = \overline{s(z)},\ s \in \mathbb{S}(D),$$
$$U'(z)^2 \mathcal{A}_T(U(z)) = \mathcal{A}_T(z), \qquad U \in \mathbb{M}(D).$$

Proof. The function $\mathcal{A}_T$ is analytic in D_E, as only poles in Λ were used in its construction. We therefore have three properties to prove: the convergence, the functional equation related to transformations and the functional equation related to reflections.

convergence
The convergence is already covered in Lemma 4.54. It may have to be applied twice: once for the sum over $\mathbb{M}(D,T)$ and once for the sum over $\mathbb{M}(D,T^*)$.

transformation
If we apply a transformation U to $\mathcal{A}_T$, we have for every term $V'(z)^2\mathcal{A}(V(z),T)$ in the sum over $\mathbb{M}(D,T)$

$$U'(z)^2V'(U(z))^2\mathcal{A}(V(U(z)),T) = W'(z)^2\mathcal{A}(W(z),T),$$

where $W = VU$. However, according to Lemma 4.55, the set containing all transformations W is equivalent to $\mathbb{M}(D,T)$, so the sum is unchanged as the reordering is permitted by the absolute convergence of the sum.
The same can be repeated for the sum over $\mathbb{M}(D,T^*)$.

reflection
In the case of reflections, we have for each term in the sum over $\mathbb{M}(D,T)$

$$\sigma_j'(z)^2\overline{\mathcal{A}(s_j(z),V^{-1}TV)} = \mathcal{A}(z,s_jV^{-1}TVs_j) = \mathcal{A}(z,W^{-1}T^*W),$$

where $W = V^*U_j$ and $U_j = s_0 \circ s_j \in \mathrm{gen}(\mathbb{M}(D))$. This time, W is in the set $\mathbb{M}(D,T^*)$.
If $T^* \in \mathrm{rot}(T)$, we have $\mathbb{M}(D,T^*) \sim \mathbb{M}(D,T)$, so the sum does not change.
If $T^* \notin \mathrm{rot}(T)$, we have two sums (the one over $\mathbb{M}(D,T)$ and the one over $\mathbb{M}(D,T^*)$) by the definition of $\mathcal{A}_T$. These two sums interchange as $(T^*)^* = T$, so the sum of the sums does not change.

□

4.5 Known Mappings onto Domains of Connectivity Three or Greater

There are not many known non-trivial conformal mappings for multiply connected domains, especially for connectivity three or greater.
The Schwarz-Christoffel transformation for multiply connected domains is probably the most well known class of mappings. Two major forms of these mappings exist. The first was stated by DeLillo, Elcrat and Pfaltzgraff [DEP04] and was constructed similar to our mappings onto MCCAPDs. The second was established by Crowdy [Cro05] and uses the so called Schottky-Klein prime function, which was later on also utilized to construct further mappings [CM06].
The problem with these two forms is that they are not easy to use for a comparison. We have already seen in Section 4.3.2 that the terms not directly associated with the prevertices arise in the limit process. With the increased size of the limit set Λ, extracting useful information becomes extremely difficult.
We can still compare the conditions necessary for the convergence in both cases. Since we can derive a suitable Schwarzian from a SC mapping, the Schwarzian, at least for some mappings, must converge under the same conditions as the pre-Schwarzian in the SC scenario.
Beforehand, we must introduce the mappings itself.

Before we continue with the SC mapping, we note that there is also a form for the MCCAPD mapping from Crowdy, Fokas and Green [CFG11], but the article contains no comparable form of the mappings.

4.5.1 Schwarz-Christoffel Mapping of Multiply Connected Domains

Definition 4.58 ([DEP04])
For a circular domain bounded by the $m+1$ circles C_j with centers c_j and radii r_j, the separation modulus Δ is defined by

$$\Delta := \max_{i,j,i\neq j} \mu_{ij}^{sep},$$

where

$$\mu_{ij}^{sep} := \frac{r_i + r_j}{|c_i - c_j|}, \qquad i,j = 0,\dots,m;\ i \neq j.$$

Lemma 4.59 ([DEP04])
Let P be an unbounded $(m+1)$-connected polygonal region, $\infty \in P$ and D a conformally equivalent circular domain. Further, suppose D satisfies the separation property $\Delta < m^{-1/4}$ for $m > 1$. Then D is mapped conformally onto P by a function of the

form $Af(z) + B$ *where*

$$f(z) = \int^z \prod_{j=0}^{m} \prod_{k=1}^{K_j} \left[\prod_{i=0,\nu\in\sigma_i(j)}^{\infty} \left(\frac{\zeta - p_{j,k,\nu}}{\zeta - u_{j,\nu}} \right) \right]^{\beta_{j,k}} d\zeta. \tag{4.63}$$

The separation parameter Δ *is given explicitly in terms of the radii and centers of the circular boundary components of* D.

The mapping formula is gained in the article by showing that the function S of the following definition is the pre-Schwarzian $S = \frac{f''}{f'}$ of the mappings.

Definition 4.60 ([DEP04])
The function $S(z)$ *is defined by the following limit*

$$S(z) = \lim_{N\to\infty} S_N(z),$$

where

$$S_N(z) = \sum_{i=0}^{N} \sum_{j=0}^{m} \sum_{\nu\in\sigma_i(j)} \sum_{k=1}^{K_j} \frac{\beta_{j,k}(p_{j,k,\nu} - u_{j,\nu})}{(z - p_{j,k,\nu})(z - u_{j,\nu})}$$

The index ν in the sum and the product above refers to a sequence of reflections against the boundary circles of D.
We have already noted that the basic structure regarding the poles in the plain can be gathered either by reflections or by transformations. In the article [DEP04] reflections were used for the construction, so the prevertices above would be read as

$$p_{j,k,\nu} = s_\nu(p_{j,k}) = (s_{\nu_1} \circ s_{\nu_2} \circ \ldots \circ s_{\nu_i})(p_{j,k}),$$

where s_ν refers to a reflection generated by successive application of reflections in $\mathbb{S}(D)$ against the boundary circles of D. The sequence of these reflections is defined by ν. The set $\sigma_i(j)$ is defined as all valid[42] reflection sequences of length i not ending with the index j, i.e. the first applied reflection is not s_j. This condition is necessary to avoid the sum containing one prevertex several times, as we have $s_j(p_{j,k}) = p_{j,k}$. The notation can therefore be compared to the $p_{T,j,k} = T(p_{j,k})$ used in our construction. Essentially we have

$$\lim_{N\to\infty} \sum_{j=0}^{N} \sum_{\nu\in\sigma_j(i)} \approx \sum_{T\in\mathbb{M}(D)}$$

The main reason that we can not directly rewrite the pre-Schwarzian of the SC mapping in a form that uses transformations is the appearance of poles at the reflections of infinity

[42] Valid means that no successive indices are equal, as $s_j \circ s_j = \mathrm{id}$, which would reduce the length of the sequence.

$u_{j,\nu} = s_\nu(u_j) = s_\nu(s_j(\infty))$. They do not show up in the Schwarzian derivative, but in the pre-Schwarzian with residue -2. This behavior can be seen in the proof of Lemma 2.14.
In the form of DeLillo, Elcrat and Pfaltzgraff the poles at the prevertices on each (reflected) circle and the reflections of infinity are grouped together. This is not easy to denote with transformations. We have, beside the sheer ordering of the poles, the problem that each pole at u is either given by $T(\infty)$ or by $T(s_0(\infty))$, where s_0 is the reflection against the circle C_0. We will investigate the sum to illustrate this problem.
In the first step the prevertices on the circle C_j are grouped with the reflection of infinity against C_j, i.e. $c_j = u_j = s_j(\infty)$. Let us, for example, observe the prevertices $p_{0,k}$ on C_0 and c_0. In the next step they are reflected by, for example, s_1 to $s_1(p_{0,k})$ and $s_1(c_0)$. Bringing them to our notation gives

$$\begin{aligned} s_1(p_{0,k}) &= s_1(s_0(p_{0,k})) = T_1^{-1}(p_{0,k}), \\ s_1(c_0) &= s_1(s_0(\infty)) = T_1^{-1}(\infty), \end{aligned}$$

by using the identity $p_{0,k} = s_0(p_{0,k})$. If we further apply s_2, we get in the same manner

$$\begin{aligned} s_2(s_1(p_{0,k})) &= (s_2 \circ s_0 \circ s_0 \circ s_1)(p_{0,k}) = (T_2^{-1} \circ T_1)(p_{0,k}), \\ s_2(s_1(c_0)) &= (s_2 \circ s_0 \circ s_0 \circ s_1)(c_0) = (T_2^{-1} \circ T_1)(c_0), \end{aligned}$$

by using $s_0 \circ s_0 = \mathrm{id}$.
Proceeding with this construction shows that we have to group any $T(p_{j,k})$ either with $T(\infty)$ or with $T(c_j)$, depending on whether the first applied reflection in T is s_j or not. We still might try to write the pre-Schwarzian, including some reordering, in the form

$$\begin{aligned} S(z) = &\sum_{j,k} \left(\frac{\beta_{j,k}}{z - p_{j,k}} \right) + \frac{-2}{z - s_0(\infty)} \\ &+ \sum_{T \in \mathbb{M}(D) \setminus \{\mathrm{id}\}} \left[\sum_{j,k} \left(\frac{\beta_{j,k}}{z - p_{T,j,k}} \right) + \frac{-2}{z - T(s_0(\infty))} + \frac{-2}{z - T(\infty)} \right]. \end{aligned}$$

The downside of this formulation is the possible loss of convergence of the sum by the reordering of the terms.

4.5.2 Convergence of the Schwarz-Christoffel Transformation

The importance of the ordering of the poles becomes obvious, when we consider if

$$S(z) = \sum_{i=0}^{\infty} \sum_{j=0}^{m} \sum_{\nu \in \sigma_i(j)} \sum_{k=1}^{K_j} \frac{\beta_{j,k}(p_{j,k,\nu} - u_{j,\nu})}{(z - p_{j,k,\nu})(z - u_{j,\nu})}$$

is converging for $z \in D$. Within this special ordering, the sum contains the expression $p_{j,k,\nu} - u_{j,\nu}$. We know already that by either reflection or transformation, the images

of the boundary circles are shrinking with the number of reflections/transformations applied, but each $u_{j,\nu}$ is inside a circle $C_{j,\nu}$ on which the reflected prevertices $p_{j,k,\nu}$ lie. Hence $|p_{j,k,\nu} - u_{j,\nu}|$ is smaller than twice the radius $r_{j,\nu}$ of the reflected circle $C_{j,\nu} = s_\nu(C_j)$ and therefore goes to zero.
The remaining open issues are whether the difference is going quickly enough to zero and how this depends on the geometry of D.
To provide the necessary context for the following discussion, we sketch the convergence proof of [DEP04].

Lemma 4.61 ([DEP04])
For a $(m+1)$-connected circular domain D, where $m \geq 1$, satisfying the separation condition

$$\Delta < m^{-1/4},$$

the function S converges uniformly on closed sets $G \subset D$.

Proof. First we note that there is an upper boundary for

$$\max \left| \frac{\beta_{j,k}}{(z - p_{j,k,\nu})(z - u_{j,\nu})} \right| \leq \delta,$$

as both factors in the denominator are bounded: The prevertices $p_{j,k,\nu}$ and the $u_{j,\nu}$ are all inside or on the boundary circles C_j. There is therefore a positive distance between each of them and any $z \in G \subset D$.
We will further need the property

$$\sum_{j=0}^{m} \sum_{\nu \in \sigma_n(j)} r_{j,\nu}^2 \leq \Delta^{4n} \sum_{j=0}^{m} r_j^2$$

taken from [DEP04], where [Hen86] is referred. $r_{j,\nu}$ indicates the radius of the circle $s_\nu(C_j)$, r_j the radius of the circle C_j and $\sigma_n(j)$ all sequences of reflections of length n with the first reflection not being s_j.
If we now define $A_i(z)$ as the summands of S_N by

$$|S_N(z)| = \left| \sum_{i=0}^{N} A_i(z) \right| \leq \sum_{i=0}^{N} |A_i(z)|,$$

we can write with $K_{\max} := \max_j\{K_j\}$, $|p_{j,k,\nu} - u_{j,\nu}| \leq 2r_{j,\nu}$ and the Cauchy-Schwarz

inequality

$$\begin{aligned}
|A_i(z)| &= \left| \sum_{j=0}^{m} \sum_{\nu \in \sigma_i(j)} \sum_{k=1}^{K_j} \frac{\beta_{j,k}(p_{j,k,\nu} - u_{j,\nu})}{(z - p_{j,k,\nu})(z - u_{j,\nu})} \right| \\
&\leq \sum_{j=0}^{m} \sum_{\nu \in \sigma_i(j)} \sum_{k=1}^{K_j} \frac{|\beta_{j,k}||p_{j,k,\nu} - u_{j,\nu}|}{|(z - p_{j,k,\nu})(z - u_{j,\nu})|} \\
&\leq \sum_{j=0}^{m} \sum_{\nu \in \sigma_i(j)} \sum_{k=1}^{K_j} 2\,\delta\, r_{j,\nu} \leq 2\delta K_{\max} \sum_{j=0}^{m} \sum_{\nu \in \sigma_i(j)} r_{j,\nu} \\
&\leq 2\delta K_{\max} \left(\sum_{j=0}^{m} \sum_{\nu \in \sigma_i(j)} r_{j,\nu}^2 \right)^{1/2} \left(\sum_{j=0}^{m} \sum_{\nu \in \sigma_i(j)} 1 \right)^{1/2} \\
&\leq 2\delta K_{\max} \left(\sum_{j=0}^{m} \sum_{\nu \in \sigma_i(j)} r_{j,\nu}^2 \right)^{1/2} \sqrt{m+1}\, m^{i/2} \\
&\leq 2\delta K_{\max} \Delta^{2i} \left(\sum_{j=0}^{m} r_j^2 \right)^{1/2} \sqrt{m+1}\, m^{i/2} \\
&\leq \tilde{\delta} \Delta^{2i} m^{i/2} = \tilde{\delta} \left(\Delta^2 \sqrt{m} \right)^i,
\end{aligned}$$

where $\tilde{\delta}$ contains the constant terms, i.e. $\tilde{\delta} = 2\delta K_{\max} \left(\sum_{j=0}^{m} r_j^2 \right)^{1/2} \sqrt{m+1}$. Therefore we have for S_N

$$|S_N(z)| \leq \sum_{i=0}^{N} |A_i(z)| \leq \sum_{i=0}^{N} \tilde{\delta} \left(\Delta^2 \sqrt{m} \right)^i.$$

Hence, S_N converges if $\Delta^2 \sqrt{m} < 1$. □

The critical point in the proof is whether the sum

$$\sum_{i=0}^{\infty} \sum_{j=0}^{m} \sum_{\nu \in \sigma_i(j)} r_{j,\nu}$$

over the radii of all the (reflected) circles converges. To ensure the convergence, the separation condition and the Cauchy-Schwarz inequality are needed.
By replacing the reflections with transformations, we can rewrite the sum as

$$\sum_{T \in \mathbb{M}(D)}^{\infty} \sum_{j=0}^{m} r_{j,T}$$

covering the same radii as in the version above. A similar sum already appeared in Lemma 2.46. This allows us to state our own convergence criteria.

Lemma 4.62
Let D be a $(m+1)$-connected circular domain, where $m \geq 1$ and $\mathbb{M}(D)$ satisfies the condition $\sum |C|^{-2} < \infty$.
The pre-Schwarzian S converges uniformly on closed sets $G \subset D$.

Proof. The difference between

$$\sum_{i=0}^{\infty} \sum_{j=0}^{m} \sum_{\nu \in \sigma_i(j)} r_{j,\nu} = \sum_{T \in \mathbb{M}(D)}^{\infty} \sum_{j=0}^{m} r_{j,T}$$

and the sum from Lemma 2.46

$$\sum_{T \in \mathbb{M}(D)} \sum_{j=1}^{m} r_{j,T}$$

is that the sum in the lemma covers only the transformations of the circles with index $j = 1, \ldots, m$ as the circle C_0 does not appear as a boundary circle of the fundamental region, since C_0 was used in the construction of $\mathbb{M}(D)$.
However each of the circles $T(C_0)$ ($T \neq \mathrm{id}$) is inside of at least one other circle $U(C_j)$, where $j = 1, \ldots, m$, and $T, U \in \mathbb{M}(D)$. We choose the $U(C_j)$ with the smallest radius still enclosing $T(C_0)$ and have

$$r_{0,T} < r_{j,U}.$$

To also include the $r_{0,T}$ in the sum, we count the corresponding $r_{j,U}$ twice. Or we may count every radius twice, which yields

$$\sum_{T \in \mathbb{M}(D)}^{\infty} \sum_{j=0}^{m} r_{j,T} < 2 \sum_{T \in \mathbb{M}(D)} \sum_{j=1}^{m} r_{j,T} + r_0.$$

The right side of the inequality converges for $\sum |C|^{-2} < \infty$ according to Lemma 2.46. The statement of the lemma follows if this result is used in the proof of Lemma 4.61. □

The condition $\sum |C|^{-2} < \infty$ matches our requirement for the MCCAPD mapping, so both mapping formulas essentially have the same requirement regarding the convergence.
This allows us to use all the results regarding $\sum |C|^{-2} < \infty$ for establishing the convergence of the pre-Schwarzian of the SC mapping.

Lemma 4.63
For a triply connected circular domain D the pre-Schwarzian S converges uniformly on close sets $G \subset D$.

Proof. Construct $\mathbb{M}(D)$. The circle C_0 separates the fundamental region D_R into triply connected regions as demanded in Lemma 2.45. Therefore we have $\sum |C|^{-2} < \infty$. □

This means on the other hand that the separation condition stated above would also allow us to assume the convergence for the MCCAPD mapping.

Note

An alternative approach would be to note that the distance $p_{j,k,\nu} - u_{j,\nu}$ shrinks with $|C|^{-2}$. The sum over A_i therefore converges if $\sum |C|^{-2}$ converges. The result itself can easily be shown by a simple calculation, but a clear notation would not be easy, as $u_{j,\nu}$ can be $T(\infty)$ or $T(c_j)$, leading us to investigate separate cases.

4.5.3 Recent Results Regarding the Convergence of the SC Mapping

Until now, we have used the convergence condition $\sum |C|^{-2} < \infty$, while for the SC mapping the condition $\Delta < m^{-1/4}$ was used. We already noticed that both conditions are equivalent for the SC mapping, but the question remains whether these conditions are necessary at all.

The requirement $\sum |C|^{-2} < \infty$ originates from the convergence of the Poincaré theta series, which is shown by demonstrating its absolute convergence. Mityushev stated in his article [Mit98] that by replacing the absolute locally uniform convergence by locally uniform convergence, we can alter the condition $\nu \geq 2$ in Lemma 2.40 to $\nu \geq 1$ for symmetric Schottky groups. However, the convergence for $\nu \geq 1$ is equivalent to the condition $\sum |C|^{-2} < \infty$.[43] An application of this result to our discussion may allow to discard the convergence conditions stated so far.

Meanwhile Mityushev also directly applied the methods of boundary value problems to the topic of (multiply connected) conformal mappings [Mit12a], [Mit12b]. The article [Mit12b] is especially of interest, as it shows the convergence of the Schwarz-Christoffel transformation for multiply connected domains without any convergence restrictions. He constructed a version of the SC mapping by solving a Riemann-Hilbert problem (Definition 4.37), where in his construction no restrictions regarding the convergence arise.

[43] See also the discussion at the end of Section 2.5.

5 Numerical Approaches to the CAPD Mapping

There are several points worth noticing in the numerical evaluation of conformal mappings onto CAPDs. Since we only know the Schwarzian derivative of the mappings, any evaluation includes the solving of a third order differential equation.
An important aspect of the numerical solving process is a suitable choice of the curves for the calculation. To investigate the mapping behavior, a full grid may be useful. If we are only interested in the shape of the boundary, we only need to "touch" each boundary arc once, which requires significantly less calculation effort. We show our approach for handling this problem in Section 5.2.

Before we can solve the Schwarzian, we first have to calculate it. The term "calculate" refers to the fact that if we start with a preimage domain D and a complete set of prevertices, interior angles and parameters, we still need the extension of the domain. Hence, we have to calculate the transformations of $\mathbb{M}(D)$ to set up the Poincaré series. We present our algorithms for this issue in Section 5.4.

The last step in the solving process would be the determination of the analytic remainder for a given mapping. As we are missing an explicit calculation routine, this will lead to some iterative solving methods to find the most suitable parameters to ensure a valid mapping, where possible.

We will focus on multiply connected mappings, but most of the results can also be used for the simply connected case. Since the structure for doubly connected domains and the ones with connectivity three or greater differ significantly, we will cover the two cases separately.

5.1 Solving the Schwarzian Derivative

The solving process for the Schwarzian derivative does not differ for simply and multiply connected domains. The result may not be valid for multiply connected domains as discussed in the note which follows Lemma 2.13, but this does not influence the computation.

Since the Schwarzian derivative is a differential operator, we have to solve a differential equation of the third order, however we know already by Lemma 2.13 that we can alternatively solve two differential equations of the second order instead.
The details of setting up the system of differential equations can be found in the Appendix B.1.

5.2 Choosing Suitable Paths for an Evaluation

The common way to evaluate a mapping that is given in the form of a differential equation at a specific point z_1 is to start at a point z_0 with initial values for $f(z_0)$ and

its derivatives and solve along some curve ζ, where $\zeta(0) = z_0$ and $\zeta(1) = z_1$.
The curve should satisfy the property that it lies completely in the preimage domain D. This is complicated by the fact that in our case D contains several holes that should be avoided. While the Schwarzian is defined in $C_\infty \setminus \Lambda$, we are moving from the image domain $f(D)$ to a reflection of it by crossing its boundary. If we return into D across a

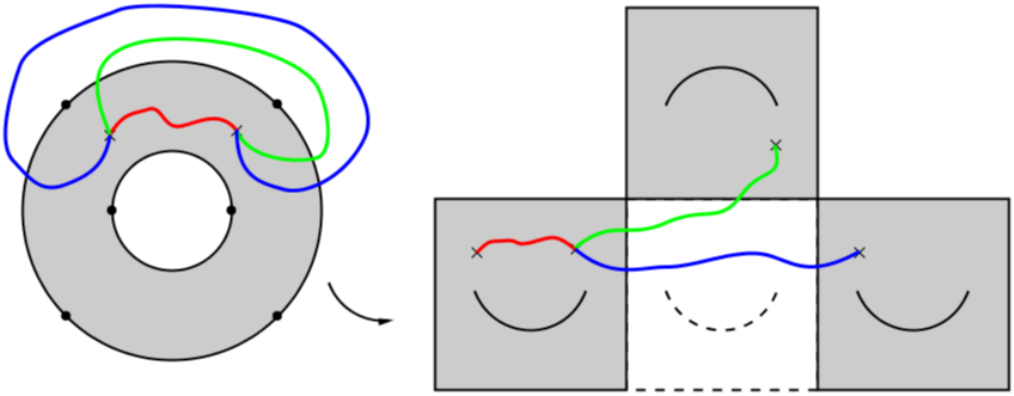

Figure 35: If the solving process leaves D, it may end in a transformed version of the image domain.

pre-arc different to the one we crossed in leaving, we are actually moving into a Möbius transformed version of $f(D)$ (Figure 35). The safest way is to remain solely in D.
It is also reasonable to stay away from the prevertices for computational reasons. As each prevertex is a pole of the second order, it is sensible to assume some numerical difficulties, if the curve approaches them too close.

We will now present our algorithm for choosing suitable paths.[44] It was used to generate the images of the numerical evaluations of the mappings shown in the Sections 5.3.3 and 5.4.4.

5.2.1 Reaching the Boundary Components

We are not only interested in some specific points, but in the shape of the image domain. We will therefore start with a concept to evaluate the boundary.
We know that the boundary consists of circular arcs. Each of these arcs is part of a circle $\tilde{C}_{j,k}$. If we know all these circles, we can calculate the boundary of the domain.[45] To find the circle corresponding to an arc, we need a path from z_0 to a boundary point z_1, which is mapped onto this arc. If we reach the boundary, we get $f(z_1)$, $f'(z_1)$ and

[44] We use the term "path" in addition to "curve" to indicate that we are actually interested in orientated curves, because we have to start each curve in z_0.

[45] For the actual calculation, we may need some additional information, like the interior angles and the orientation of the curves. However, all these values are either known beforehand or gathered in the process of the calculation.

$f''(z_1)$ as a result of solving the differential equation. $f(z_1)$ gives a point that is part of the circle in question; $f'(z_1)$ gives the orientation of the curve and the direction in which the center of the circle can be found; finally $f''(z_1)$ provides us with the curvature/the radius of the circle. Hence the boundary is known if we have the solution of the differential equation at one point of each boundary arc. The actual computation of the boundary using these points on the boundary can be found in the Appendix B.2.

In the following, we will present one possible way to select the paths. This method was used to generate the images of the mapping behavior, which are shown in the following sections.
We will for now suppose that each line segment from z_0 to the center of a boundary circle C_j is not intersected by another boundary circle than C_j itself.
The idea is to get close to each of the boundary circles and then solve (with some distance) around them. Whenever we need a point from the boundary, we solve from the "orbit" to this specific point.

We have to specify the points we want to reach. Since we need to keep some distance from the prevertices, a suitable choice would be the midpoints of the pre-arcs:

$$\begin{aligned}\varphi_{2,j,k} &:= \frac{1}{2}\left(\arg(p_{j,k} - c_j) + \arg(p_{j,k+1} - c_j)\right),\\ z_{2,j,k} &:= r_j \exp(i\varphi_{2,j,k}) + c_j.\end{aligned}$$

We also need to know how far we can stay away from the circles, so we compute the minimum distance between the circles and divide it by three[46][47]

$$d := \frac{1}{3} \min_{j,i,j\neq i} \left\{|c_j - c_i| - r_j - r_i\right\}.$$

Now we solve from the starting point z_0 in the direction of c_j to a point $z_{1,j,0}$ that has the distance d from C_j:

$$\begin{aligned}\varphi_{1,j,0} &:= \arg(z_0 - c_j),\\ z_{1,j,0} &:= (r_j + d)\exp(i\varphi_{1,j,0}) + c_j.\end{aligned}$$

Beginning in $z_{1,j,0}$, we solve along the circle $(r_j + d)\exp(it) + c_j$ and stop at the points

$$z_{1,j,k} := (r_j + d)\exp(i\varphi_{2,j,k}) + c_j$$

with the same arguments $\varphi_{2,j,k}$ with respect to the center c_j as the points $z_{2,j,k}$. From each of these points $z_{1,j,k}$, we solve along a line segment to the corresponding point $z_{2,j,k}$.
Combining this leads to the first version of our algorithm:

[46] The factor $\frac{1}{3}$ was chosen arbitrary. Any factor smaller than one half is reasonable.
[47] The formula for d has to be modified for the circle C_0 of bounded domains.

Algorithm 1:

1: **for all** circles C_j **do**
2: solve from z_0 to $z_{1,j,0}$
3: **for all** prevertices $p_{j,k}$ on C_j **do**
4: solve from $z_{1,j,k-1}$ to $z_{1,j,k}$ along the circle $(r_j + d)\exp(it) + c_j$
5: solve from $z_{1,j,k}$ to $z_{2,j,k}$
6: calculate the circle for the image of the arc between $p_{j,k}$ and $p_{j,k+1}$
7: **end for**
8: **end for**

There are some facts to note regarding the algorithm:

- Depending on the location of z_0, it may be necessary to solve away from C_j to reach $z_{1,j,0}$
- If D is a bounded domain, there is one outer circle C_0. We have to replace the radius $(r_0 + d)$ by $(r_0 - d)$ for $z_{1,0,0} = (r_0 - d)\exp(i\varphi_{1,0,0}) + c_0$. The argument $\varphi_{1,0,0}$ can be set to any value as long as we ensure that the line segment between z_0 and $z_{1,0,0}$ is not intersected by any boundary circle.
- It is probably not the best option to solve directly from $z_{1,j,0}$ to $z_{1,j,1}$. In most cases, there will be a $z_{1,j,k}$, which lies (argument-wise) closer to $z_{1,j,0}$ than $z_{1,j,1}$. Changing the order may reduce the calculation time.

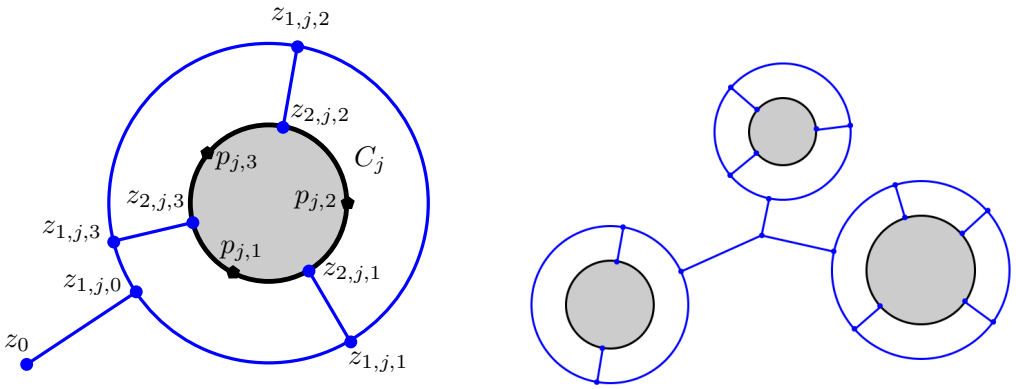

(a) Starting in z_0, the algorithm solves around C_j and touches each pre-arc once.

(b) All boundary circles are covered in the solving process.

Figure 36: A close up figure showing the behavior of the algorithm and a figure of the whole domain. The domain is colored white, while the areas outside of the domain are colored gray.

We supposed above that the line segment between z_0 and C_j lies completely in D or, in other words, is not intersected by another boundary circle. If this condition is not satisfied, the algorithm has to be altered.

If the connection between z_0 and C_1 is, for example, intersected by C_2, we will say that C_1 is in the shadow of C_2. (Imagine z_0 as a light source.)

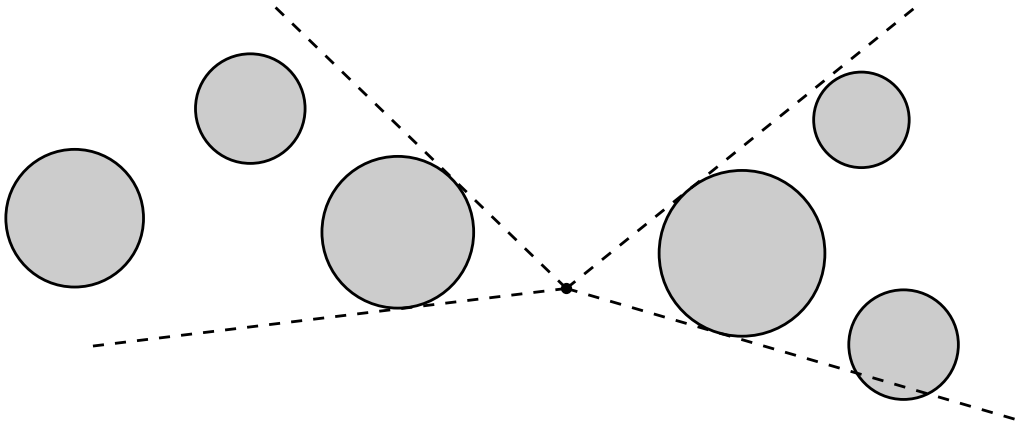

Figure 37: Some circles may be in the "shadow" of other circles and are therefore not reachable by a line segment starting in z_0.

First we reorder the circles with respect to their distance to z_0, i.e.

$$|c_j - z_0| - r_j \leq |c_{j+1} - z_0| - r_{j+1}.$$

We then assess whether each circle C_j is in the shadow of one of the other circles C_k, for $k < j$. If it is not in the shadow of another circle, we can proceed as above (i.e. line segment from z_0, etc.). Otherwise, the circle will be connected to the closest circle C_l, where $l < j$. If a circle C_j is connected to a circle C_l, we will not solve from z_0 to C_j, but from C_l to C_j. Therefore, we need a point $z_{0,l,j}$ on the orbit of C_l that will be connected to an alternative $z_{1,j,0}$ in the orbit of C_j:

$$\begin{aligned} \varphi_{1,j,0} &:= \arg(c_l - c_j), \\ z_{0,l,j} &:= (r_l + d)\exp(i\varphi_{1,j,0} + i\pi) + c_l, \\ z_{1,j,0} &:= (r_j + d)\exp(i\varphi_{1,j,0}) + c_j. \end{aligned}$$

Expanding our algorithm according to this concept gives:

Algorithm 2:

order the circles C_j according to their distance to z_0
for all circles C_j **do**
    if C_j is in the shadow of another circle **then**
        search the closest circle C_l, where $l < j$
        solve from $z_{1,l,0}$ to $z_{0,l,j}$ (circular arc)
        solve from $z_{0,l,j}$ to $z_{1,j,0}$ (line segment)
    else
        solve from z_0 to $z_{1,j,0}$ (line segment)

```
    end if
    for all prevertices p_{j,k} on C_j do
        solve from z_{1,j,k-1} to z_{1,j,k} along the circle (r_j + d) exp(it) + c_j
        solve from z_{1,j,k} to z_{2,j,k}
        calculate the circle for the image of the arc between p_{j,k} and p_{j,k+1}
    end for
end for
```

The notes of the preceding algorithm also hold here. This includes the remark about bounded domains, while this time C_0 can also be covered by shadows of other circles. Note that it may be useful to calculate the connections of the circles before calculating the arcs. The calculation of the $z_{0,l,j}$ can then be included in the calculation of the $z_{1,l,k}$. This will save some calculation time.

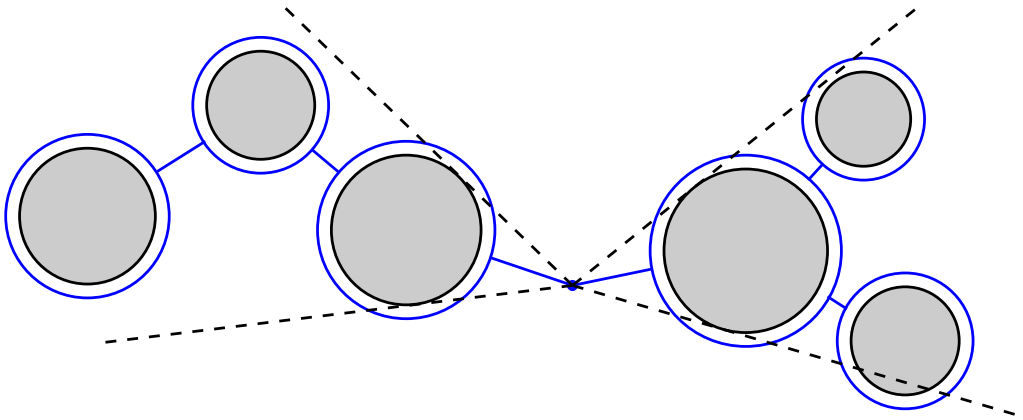

Figure 38: The shadow circles are connected according to the suggested algorithm.

While the algorithm holds for all circular domains, it can be simplified for special preimage domains.
If the circular domain is an annulus, we can place the points $z_{1,0,k}$ and $z_{1,1,k}$ on the same circle. A reasonable choice for this circle would be $\frac{1+r}{2}\exp(it)$ (Figure 39(a)).
It further simplifies for simply connected domains. Since the unit disk is a convex domain, we can reach all $z_{2,0,k}$ directly by line segments starting in z_0 (Figure 39(b)).

5.2.2 Reaching a Single Point

If we intend to reach only a single point, we can simplify the algorithm constructed for the boundary. If we want to solve from z_0 to a point z_2, the line segment connecting the points is probably intersected by some boundary circles C_j. To avoid these circles, we use a similar concept to the one above.

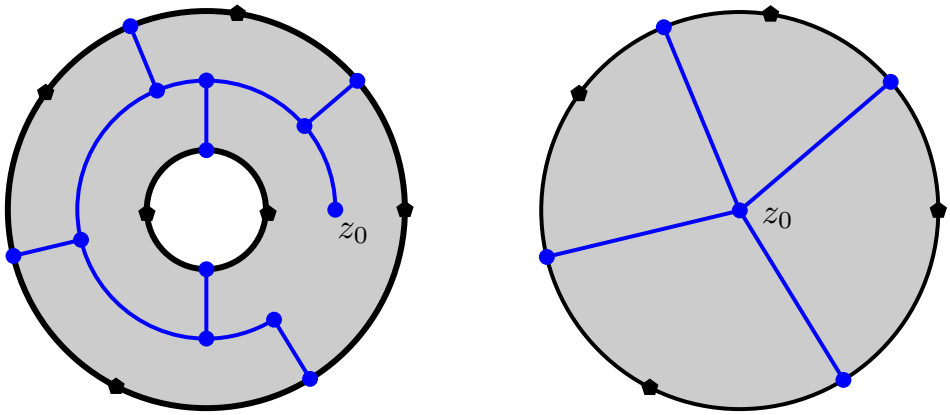

(a) If a circular domain is an annulus, one common orbit is enough to reach all boundary arcs.

(b) Every boundary point of the unit disk can be reached by a line segment starting in the origin.

Figure 39: The algorithm can be simplified for special circular domains.

We again use the orbit of each circle by extending its radius by a suitable constant d, so the path has to avoid the circles

$$C_j^o : \ |z - c_j| = r_j + d.$$

Hence, we calculate the intersection points of the line segment between z_0 and z_2 and the circles C_j^o. We get two points $z_{1,j,1}$ and $z_{1,j,2}$ for each intersected circle. If the line segment only touches the circle, the resulting touching point can be discarded. We therefore get $2n$ intersection points if n circles are intersected. We further sort the points by the distance to z_0

$$|z_{1,\nu} - z_0| < |z_{1,\nu+1} - z_0|, \qquad \nu = 1, \ldots, 2n\,,$$

where each pair $z_{1,\nu}$, $z_{1,\nu+1}$, for an odd-numbered ν, belongs to the same circle.
All that remains is to connect the points to reach z_2. We have line segments between the pairs $(z_0, z_{1,1})$, $(z_{1,2n}, z_2)$ and every combination $(z_{1,\nu}, z_{1,\nu+1})$ with an even-numbered ν. The pairs of points on the same orbit C_j^o can be connected by a circular arc that is part of the corresponding orbit. It is reasonable to choose the shorter one of the two possible arcs.

Algorithm 3:

```
1: calculate the line segment L between z_0 and z_2
2: for all orbit C_j^o do
3:     if C_j^o and L intersect then
4:         calculate the intersection points
5:         save them together with the corresponding orbits
```

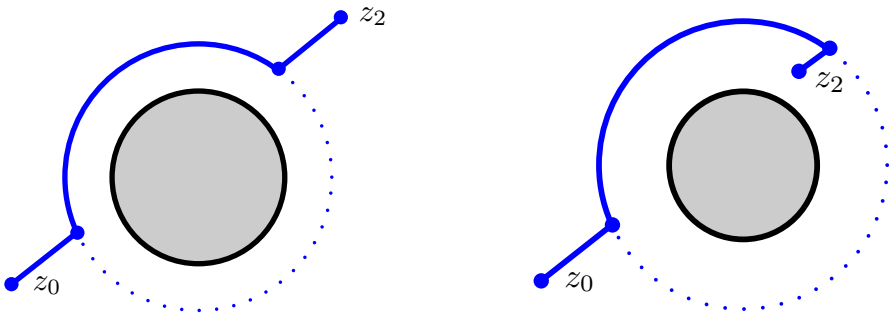

(a) Replacing parts of the line segment connecting z_0 and z_2 with arcs of the intersected orbits yields a suitable path.

(b) If a point lies inside an orbit, we may approach that point by solving into the orbit instead of reducing the size of the orbit.

Figure 40: To solve from z_0 to a point z_2, we may need to avoid the boundary circles by surrounding them.

```
    end if
end for
sort the intersection points and orbits according to their distance to z_0
solve from z_0 to z_{1,1} along a line segment
for all z_{1,ν} do
    if ν is odd then
        solve from z_{1,ν} to z_{1,ν+1} along the shorter arc of C^o_{j(ν)} connecting them
    else
        solve from z_{1,ν} to z_{1,ν+1} along the line segment connecting them
    end if
end for
solve from z_{1,2n} to z_2 along a line segment
```

This solving method is only reasonable for single points. If more points are needed, one may want to further analyze the situation. If, for example, all points of the set M are on a line segment, it is more efficient to start the solving process only for one point $z_2 \in M$ in z_0. All the remaining points can then easily be reached from z_2 instead of starting again in z_0.
Hence, there is in most cases a more efficient way to evaluate special structures, where the calculation of the boundary may be seen as an example.

5.3 Mappings onto Doubly Connected Domains

We now discuss the case of doubly connected domains before we continue with mappings of domains of a greater connectivity. The calculation of the Schwarzian derivative is

easier to handle in the case of connectivity two, based on the linear structure of the underlying Schottky group.
The goal of this section is the "forward mapping" of a doubly connected domain: By choosing D, p, a and μ, we calculate the image domain $f(D)$.
The formula for the mapping of an annulus is much easier then the one for generic doubly connected domains. Nonetheless, one might want to use an unbounded preimage domain to map onto an unbounded image domain for computational reasons. An annulus would contain in this case the preimage of infinity, which can lead to numerical issues. We will therefore try to cover both cases in our discussion.

We will suppose the preimage domains to be normalized, and so assume C_0 to be the unit circle for bounded and unbounded domains. Hence, three degrees of freedom remain for further normalization. We want the bounded domains to be annuli and normalize the second circle accordingly. Each annulus is then defined by $r < |z| < 1$.
For unbounded domains, we can normalize the center of the circle C_1 to be on the positive real axis $c_1 \in \mathbb{R}^+$ and set the radius to one. The conformal module of the domain is therefore only depending on the real value of the center c_1.
The remaining degree of freedom for both domain types can be used to set the argument of one of the prevertices.

To calculate an image domain, we have to perform several steps:

1. **Choose a preimage domain D**
   Since we have chosen a specific normalization, this means we have to select an inner radius r for an annulus or a center $c_1 \in \mathbb{R}^+$ for the unbounded case.

2. **Choose the prevertices p, interior angles $\pi\alpha$ and parameters μ**
   The values a can be calculated based on the angles $\pi\alpha$, and the γ for the unbounded case can be calculated from the μ. The best way to define the prevertices is by their arguments with respect to the center of their circles.

3. **Test for the restricting equation**
   If the equation is not satisfied, we have to modify one of the sets. If we want to keep p and a, we have to modify μ. We either change one value of μ or project the μ into a subspace of $\mathbb{R}^n$ (with n according to the number of parameters) such that the restricting equation is satisfied.
   We also calculate b_i for the analytic remainder at this point.

4. **Calculate the Schwarzian**
   To evaluate the Schwarzian, we need to extend the domain as discussed or, for a numerical point of view, we must calculate the terms of the sum. This calculation is necessary for the unbounded case, but might be skipped for an annulus, as the formula in that case only depends on the factor r^{2n}.

5. **Search for the best parameter b_r**
   The analytic remainder of the Schwarzian is defined by the geometry of D and the parameter b_r. For the final mapping, we need to find the best possible value.

6. **Evaluate the mapping**
   After all values have been found, we can evaluate the mapping and, for example, calculate a specific point, the boundary, or a grid. A method for reaching the specific components were already presented in Section 5.2.

We now consider steps 4 and 5 in more detail.

5.3.1 Calculating the Schwarzian Derivative

The Schwarzian derivative for the bounded and for the unbounded case is given in the form of an infinite sum. For the numerical evaluation, we truncate it to a finite version. Suppose for the following that the preimage domain is known and the parameters p, a and μ are given and satisfy the restricting equation.

Annulus

The Schwarzian derivative for the mapping onto an annulus in given in Theorem 4.22, but we have to use the finite form

$$\mathcal{S}_N(z) = \sum_{n=-N}^{N} \sum_{j,k} \left(\frac{a_{j,k}}{(z - r^{2n} p_{j,k})^2} + \frac{i\mu_{j,k} - a_{j,k}}{z(z - r^{2n} p_{j,k})} \right) + \frac{b_r + ib_i}{z^2}.$$

Unbounded Domain

The form for an unbounded preimage domain is more complicated, and takes the form

$$\begin{aligned} \mathcal{S}_N(z) = \sum_{n=-N}^{N} \sum_{j,k} \Bigg(& \frac{a_{j,k}}{(z - p_{n,j,k})^2} + \frac{\gamma_{n,j,k}}{(z - p_{n,j,k})} \\ & + \frac{(p_{n,j,k} - l_2)\gamma_{n,j,k} + a_{j,k}}{(l_2 - l_1)(z - l_1)} + \frac{(p_{n,j,k} - l_1)\gamma_{n,j,k} + a_{j,k}}{(l_1 - l_2)(z - l_2)} \Bigg) \\ & + \frac{(b_r + ib_i)(l_1 - l_2)^2}{(z - l_1)^2 (z - l_2)^2}. \end{aligned}$$

First we complete our set of parameters. We calculate the γ according to Lemma 4.13 by using

$$\gamma_{j,k} = \frac{i\mu_{j,k} - a_{j,k}}{p_{j,k} - c_j}.$$

We then calculate[48] the generating transformation $T = s_0 \circ s_1$. Any other transformation of $\mathbb{M}(D) = \{T^n \mid n \in \mathbb{Z}\}$ can directly be calculated with T. The transformation T is also needed to calculate the limit points l_1, l_2 as they are the fixed points of T, and so we look for the solutions of the equation $z = T(z)$.

[48] A formula is given in Lemma 2.29, but it lacks the normalization $AD - BC = 1$.

We must now decide if we want to calculate the values beyond the first generation by using reflections or transformations. We can calculate the prevertices $p_{n,j,k}$ by reflecting them successively against the boundary circles. The corresponding values for γ follow from Lemma 4.12 by

$$\gamma_{s(p)} = -\frac{(\bar{p}-\bar{c})}{r^2}\left(\overline{\gamma_p}(\bar{p}-\bar{c})+2a\right),$$

where c and r are the center and radius of the circle used for the reflection $s(z) = \frac{r^2}{\bar{z}-\bar{c}}+c$. Alternatively, we can transform the prevertices by applying $U = T^n$ and calculate γ, according to Lemma 4.6, by

$$\gamma_{U(p)} = \frac{\gamma_p}{U'(p)} - \frac{aU''(p)}{(U'(p))^2}.$$

We prefer transformations for the computation, as they are easier to perform. Therefore, our suggestion for an algorithm handling the task of calculating the values is of the form:

Algorithm 4:

```
 1: set the maximum depth N
 2: load the domain D and the sets p, a, μ
 3: modify μ to satisfy the restricting equation
 4: compute T and the set γ
 5: save the values p, a, γ in values[0][0]
 6: for d ∈ {−1, 1} do
 7:     define U := T^d and V := U
 8:     for n from 1 to N do
 9:         for all tuples (p, a, γ) in values[0][0] do
10:             calculate q = U(p) and δ = γ_{U(p)}
11:             store the combination (q, δ, a) in values[d][n]
12:         end for
13:         set U := U ∘ V
14:     end for
15: end for
```

Here "*values*" is a suitable structure to store all the information.

5.3.2 Analytic Remainder

Recall the interpretation of the analytic remainder. The main geometry of the domain is already determined by the Schwarzian derivative before the analytic remainder is added. We have set the correct interior angles by our choice of a and the functional equations guarantee that the boundary consists of circular arcs. We have yet to ensure that the Schwarzian leads to a valid mapping.

We cannot guarantee that every closed curve is mapped onto a closed curve. Consider as an example the mapping of the annulus $r < |z| < 1$ by the function $g(z) = z^x$, where $x \in \mathbb{R}$. The closed curve $\delta(t) = \rho \exp(2\pi i t)$, where $r < \rho < 1$ and $t \in [0, 1]$, is only mapped onto a closed simple curve for $x \in \{1, -1\}$. Otherwise, we have $g(\delta(0)) \neq g(\delta(1))$, or the curve revolve about the origin (e.g. $x = 2$). Hence g describes only for $x \in \{1, -1\}$ a valid doubly connected mapping.
In Section 2.2, after Lemma 2.13, we concluded that we can verify a mapping by using the integrals (2.3), i.e.

$$\int_\delta f^{(k)}(z)dz = 0, \qquad k = 1, 2, 3.$$

The integrals ensure that $f^{(k)}(a^+) = f^{(k)}(a^-)$ for each $k \in \mathbb{N}_0$ if we solve along a closed curve surrounding a hole of D, where a is the coinciding start (a^+) and end point (a^-) of such a curve. The same property can be tested by solving the Schwarzian along closed curves and directly comparing the results to the initial values.

For an annulus, we can solve either clockwise or counterclockwise around C_1 starting at some point $a \in \mathbb{R}^+ \cup \mathbb{A}$. Afterwards, we test if $f^{(k)}(a^+) = f^{(k)}(a^-)$.
For any non-annulus domain, we can choose any closed curve δ surrounding C_1 and test if $f^{(k)}(\delta(0)) = f^{(k)}(\delta(1))$.
We define by $\mathcal{S}(z, b_r)$ the Schwarzian not only depending on z but also on b_r. We therefore denote the solution of this Schwarzian derivative by $f(z, b_r)$. Hence, we look for the zeros of the functions

$$\begin{aligned} g_0(b_r) = g_0(b_r, \delta) &:= |f(\delta(0), b_r) - f(\delta(1), b_r)|, \\ g_1(b_r) = g_1(b_r, \delta) &:= |f'(\delta(0), b_r) - f'(\delta(1), b_r)|, \\ g_2(b_r) = g_2(b_r, \delta) &:= |f''(\delta(0), b_r) - f''(\delta(1), b_r)|, \end{aligned}$$

where $b_r \in \mathbb{R}$ and $\delta \subset D$ is a suitable curve. The interior of δ should contain one boundary component, i.e. it should surround C_1.
If the mapping $f(z, b_{r,0})$ is valid, $g_k(b_{r,0}, \delta)$ must be zero for all $\delta \subset D$ and $k = 0, 1, 2$. This is only a necessary and not a sufficient condition for any specific δ. It is possible for $f(\delta, b_{r,0})$ to revolve about C_1 twice and still have $g_k(b_{r,0}) = 0$.
We can nonetheless use this idea for a way to search for a suitable b_r. We can find a candidate by

Algorithm 5:

1: calculate $\mathcal{S}(z, b)$
2: set $\rho := \frac{1}{2}(1 + r_1)$ (annulus) or $\rho := \frac{1}{2}c_1$ (unbounded domain)
3: define $\delta(t) := \rho \exp(2\pi i t) + c_1$
4: define $g_k(b)$
5: search a common zero of all $g_k(b)$ and save it as $b_{r,0}$

As stated, Algorithm 5 does not have to yield a correct result, but works quite well in many cases. The algorithm does not even have to yield a result at all in the form of a

zero since, according to Section 4.2.3, there might be no suitable b_r for a specific set of D, p, a and μ.

While not further investigated, the information on differential equations outlined in the Appendix A.4 could lead to some useful results that could be used to restrict the choices for the parameters in the context of valid mappings.

5.3.3 Examples

We created two different algorithms for the visualization of the mappings, so we must discuss their behavior to allow a proper interpretation.
The first algorithm solves the Schwarzian along the paths described in Section 5.2 and plots the results. The Schwarzian is also solved along the boundary of the domain, as soon as a boundary arc is reached. To avoid numerical issues, the solving process maintains a distance from the prevertices, resulting in visible gaps in the image domains. An example is shown in Figure 41.

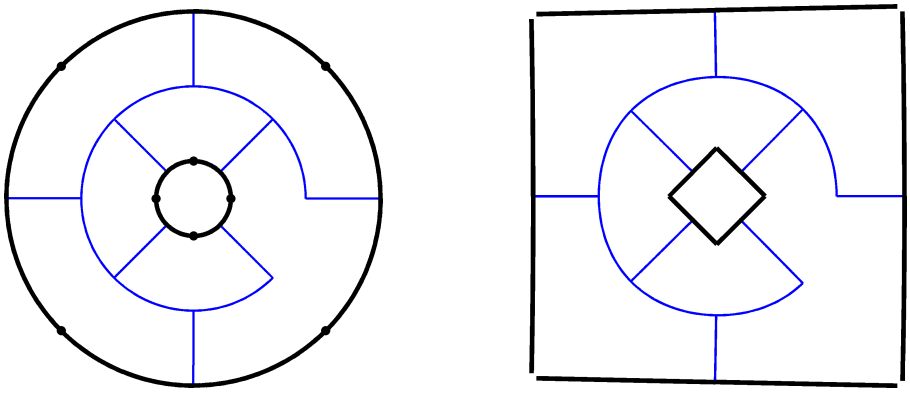

(a) Preimage: The path surrounds the inner circle and touches each prearc of the boundary.

(b) Image: The images of the path and of the boundary.

Figure 41: The first algorithm shows the path used for reaching the boundary (blue) and the actual behavior at the boundary (black). The boundary has gaps at the vertices, as the algorithm avoids to touch the prevertices.

We solve along the boundary to visualize the exact behavior of such a mapping. This allows us to determine the existence of any gaps or overlaps in the image domain. It also allows to verify if the boundary consists of circular arcs.
The second algorithm also uses the paths of Section 5.2, but only to solve for a point on each boundary component. Then, the boundary circles for the image domain are calculated with these points. These circles allow the algorithm to calculate the boundary and the vertices. Also a grid is added to further visualize the behavior of the investigated mapping. An example of the result of the second algorithm is shown in Figure 42.

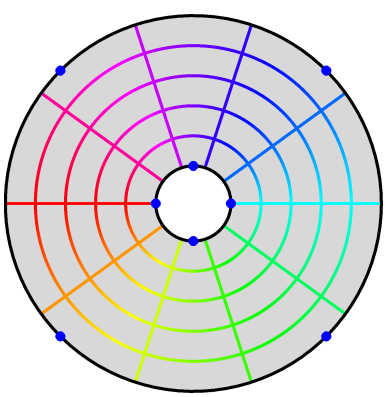

(a) Preimage: The concentric mesh is colored according to the argument of the grid points.

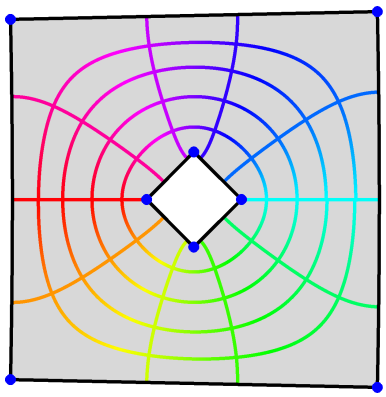

(b) Image: The boundary is closed and shows the vertices, as they are calculated by the algorithm. The color of the grid corresponds to the argument of its preimage points.

Figure 42: The second algorithm calculates the boundary and the vertices with information of the circles $\tilde{C}_{j,k}$ that provide the boundary arcs. The interior of the domain is filled with a mesh.

The grid also contains a safety gap towards the boundary to avoid touching the prevertices. The gaps only become visible if an image domain is elongated as shown in Figure 43.

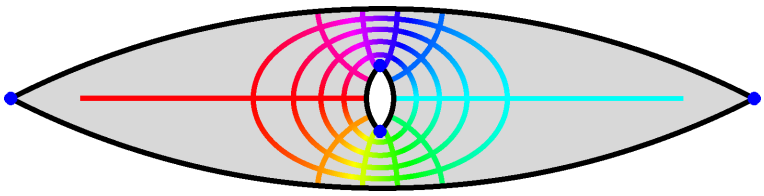

Figure 43: The great distortion of elongated regions shows that the grid calculation does not touch the prevertices or the boundary.

We visualize the influence of the different parameters by an example mapping. We set $r = 0.3$ and

$$\begin{array}{lll} p_{0,1} = 1, & p_{0,2} = -1, & \alpha_{0,1} = \alpha_{0,2} = 0.5, \\ p_{1,1} = 0.3\exp\left(i\pi/4\right), & p_{1,2} = -0.3\exp\left(i\pi/4\right), & \alpha_{1,1} = \alpha_{1,2} = 1.6\,. \end{array} \tag{5.1}$$

A suitable set for μ is given by[49]

$$\begin{aligned} \mu_{0,1} &= 0.1404\ldots, & \mu_{0,2} &= 0.1401\ldots, \\ \mu_{1,1} &= -0.1407\ldots, & \mu_{1,2} &= -0.1397\ldots, \\ b_i &= -0.1402\ldots, & b_r &= 0.0372\ldots. \end{aligned} \tag{5.2}$$

The resulting image domain can be seen in Figure 44 for the initial values $f(0.65) = 0$,

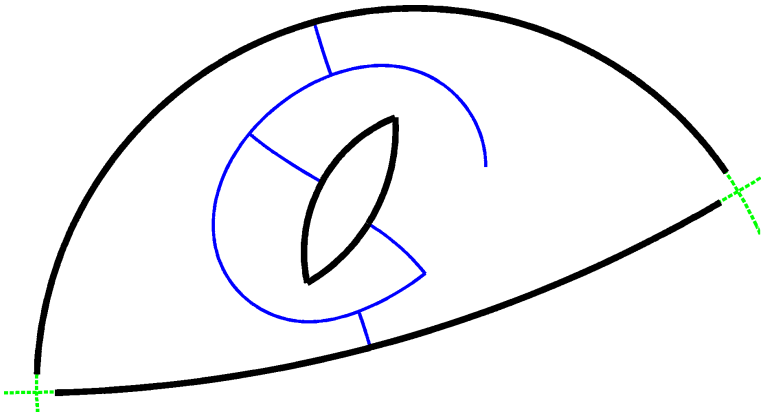

Figure 44: The image domain for the prevertices (5.1) and the parameters (5.2). The dashed green circles $\tilde{C}_{j,k}$ indicate the theoretical boundary, while the black line shows the actual result.

$f'(0.65) = 1$ and $f''(0.65) = 1.5$.
We modified the plotting algorithm in this case by adding the calculated circles $\tilde{C}_{j,k}$ of the image domain. As in the second algorithm, we compute these circles at the points where the (blue) path touches the boundary. We see in Figure 44 that the solution gathered for the boundary (black line) overlaps with the result for the (green dashed) circles. Hence, the circles only become visible if we approach the vertices.
We have done this to show the distortion that appears for insufficient parameters. If we, for example, choose parameters not satisfying the restricting equation (4.20), the solution at the boundary and the calculated circles do not have to match. The result for the values

$$\begin{aligned} \mu_{0,1} &= 0.02, & \mu_{0,2} &= 0.02, \\ \mu_{1,1} &= -0.1, & \mu_{1,2} &= 0.1, \end{aligned} \tag{5.3}$$

which do not satisfy the equation, can be seen in Figure 45.
If we break this condition, the functional equations of the Schwarzian are no longer satisfied. As we discussed in Section 4.1.5, the functional equation is connected to the fact that the boundary consists of circular arcs. While the domain shown in Figure 45 is self overlapping, the fact that the boundary curves are not circular arcs is crucial. This can be seen by comparing the black boundary with the green dashed circles.

[49] The values were optimized by numerical routines.

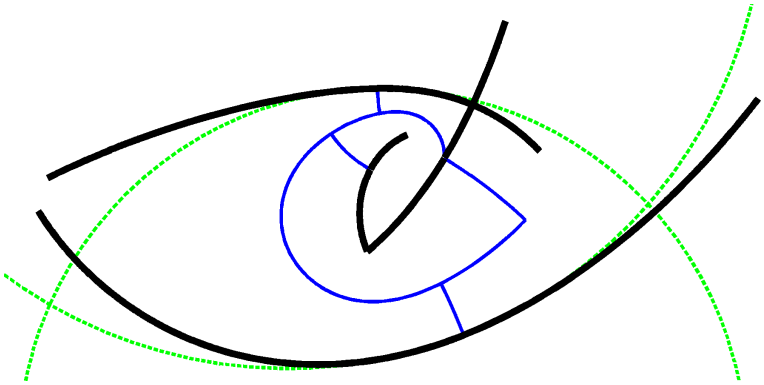

Figure 45: The parameters μ of equation (5.3) do not satisfy the restricting equation. As a result, the green dashed and the black solid lines do not match. The curvature of the actual boundary (black) even changes for each arc.

A similar effect occurs if we set the imaginary part b_i of b to a value not satisfying equation (4.21). For Figure 46 we used again the μ given by (5.2), but changed b_i to zero.
The curvature of the boundary arcs changes in this case, as the mapping does not satisfy the functional equations. In this example, the lower of the two outer boundary arcs

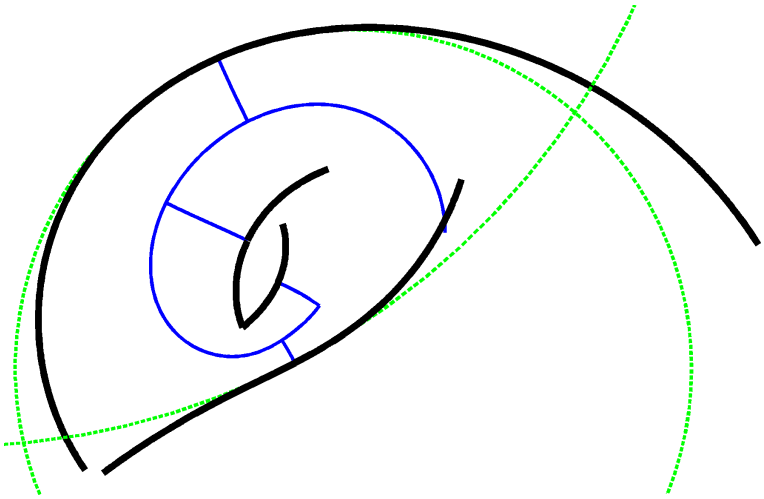

Figure 46: The boundary curvature changes for the image domain for the parameters (5.2) and $b_i = 0$. The curvature of the lower outer boundary arc changes in sign.

even changes the sign of the curvature and therefore gives us a good visualization of the "not a circular arc" property.
The Schwarzian still satisfies the functional equations, if the real part b_r of b is incorrect.

We define the values shown in (5.2), but set b_r to zero. The result is displayed in Figure 47.
The results for the boundary and the calculated circles match this time. With the func-

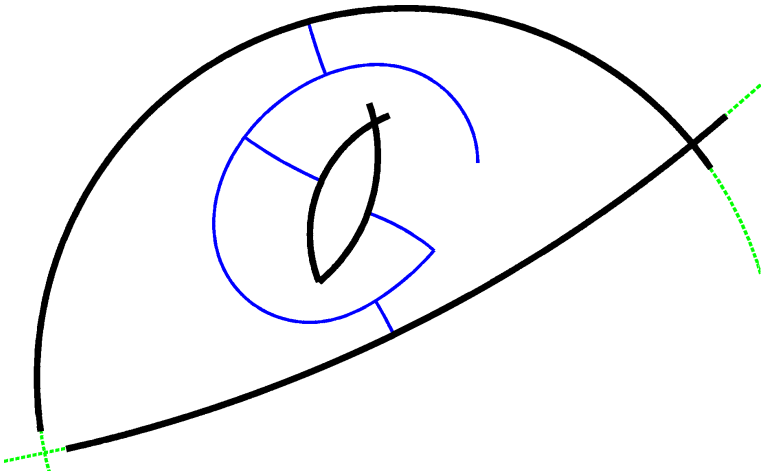

Figure 47: The image domain is self overlapping for the parameters (5.2) and $b_r = 0$. This can be seen at the right vertex where the two boundary arcs cross.

tional equations satisfied, the boundary consists only of circular arcs. As we discussed in Section 4.2.3, a invalid choice for b_r lead to an invalid mapping. The image therefore shows an overlapping domain, as the boundary arcs intersect. This is best seen at the right vertex of the outer boundary component.

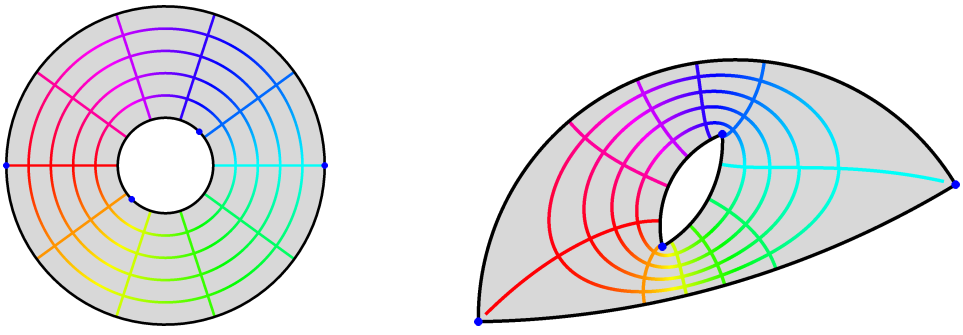

(a) Preimage (b) Image

Figure 48: A full grid plot of the domain shown in Figure 44

The next example will illustrate the influence of the parameters μ on the boundary of the domain. We set $r = 0.2$ and choose in the form of vectors

$$\begin{aligned} p_0 &= (\exp(0.25\,i\,\pi), \exp(0.75\,i\,\pi), \exp(1.25\,i\,\pi), \exp(1.75\,i\,\pi)), \\ \alpha_0 &= (0.5, 0.5, 0.5, 0.5), \qquad \mu_0 = \lambda(1, -1, 1, -1), \\ p_1 &= (0.2, -0.2), \quad \alpha_1 = (1.5, 1.5), \quad \mu_1 = (0, 0). \end{aligned} \tag{5.4}$$

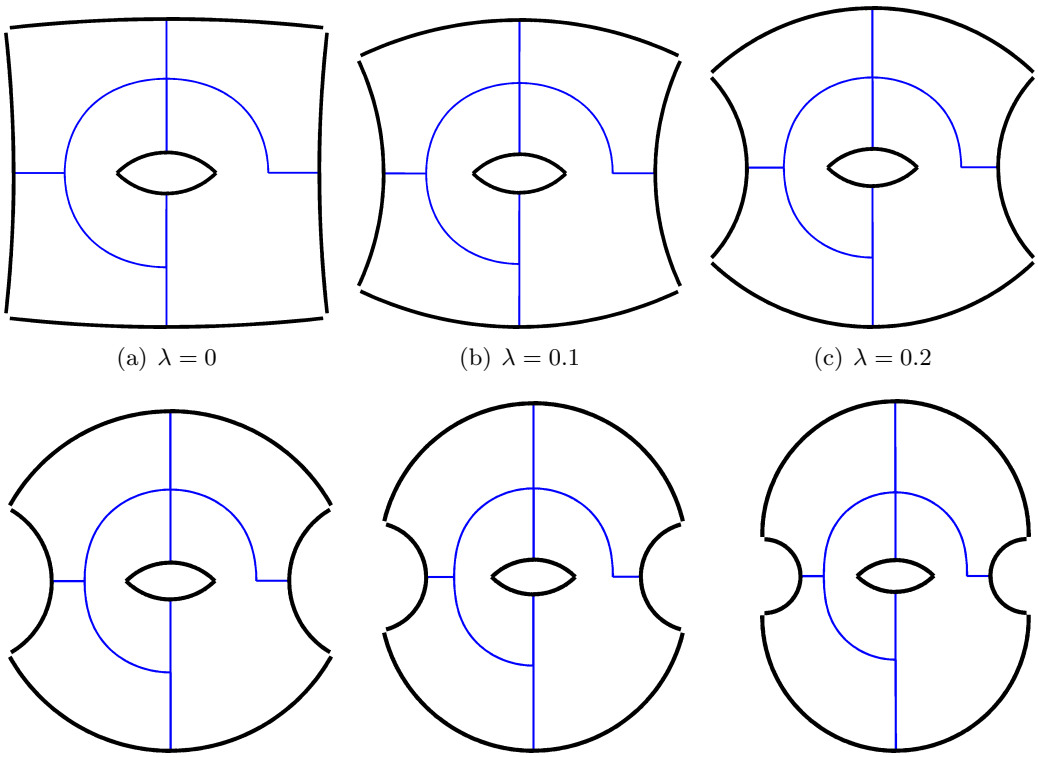

(a) $\lambda = 0$ (b) $\lambda = 0.1$ (c) $\lambda = 0.2$

(d) $\lambda = 0.3$ (e) $\lambda = 0.4$ (f) $\lambda = 0.5$

Figure 49: The image domain for the parameters (5.4) changes with the choice for λ. The ratio of the curvatures of the outer boundary arcs changes with an increasing value for λ.

If we modify the weight $\lambda \in \mathbb{R}$ of the parameters $\mu_{0,k}$ of the outer boundary component, the image domain changes. This is shown in Figure 49, where λ is altered from 0 to 0.5 by steps of 0.1.
The image domain is symmetric, as the prevertices and the values for the μ also contain a symmetry. Hence, we have two different curvatures for the outer boundary arcs.[50] If we now change λ, we notice that the ratio between the two curvatures changes if λ grows. This behavior is similar to the simply connected case. As a matter of fact, the inner boundary component is nearly unchanged as we alter the outer boundary. A reason for this might be that we keep the values for $\mu_{1,1}$ and $\mu_{1,2}$ unchanged. Note that we are only able to keep these values unchanged as the choice of λ does not influence the restricting equation.

We have not shown any pictures of unbounded doubly connected domains, as the algorithmic behavior is similar to that seen in unbounded domains of connectivity three

[50] The symmetry of the domain requires a suitable normalization.

or greater and the influence of the parameters is similar to that seen for the annuli. Corresponding images for unbounded domains can be found in the following section.

5.4 Mappings onto Domains of Connectivity Three or Greater

The forward map for a MCCAPD mapping of connectivity three or greater is constructed using a similar procedure to that used in the case of an doubly connected CAPD mapping. The major difference is that we have to calculate a basis for the analytic remainder before we can find a suitable set of parameters b. Moreover, the calculation of the Schwarzian derivative becomes significantly more difficult. On the other hand, we will not have to verify any restricting equations.
As for the doubly connected mappings, we suppose the domain D and the parameters p, a and μ to be given and calculate the image domain $f(D)$.
We do not specify a special normalization for the circular domains, as it would have less impact here as in the doubly connected case. We still suppose that $0 \in D$ for bounded domains or $\infty \in D$ for unbounded domains. In this way, we avoid limit points in the neighborhood of infinity. It may still be advantageous to set C_0 to be the unit circle.

The process of constructing a evaluable mapping consists of the following steps:

1. **Choose a preimage domain D**
   Select the centers and radii of the boundary circles C_j of D.

2. **Choose the prevertices p, interior angles $\pi\alpha$ and parameters μ**
   The values a can be calculated based on the α and the prevertices p are defined by their argument with respect to the center of the corresponding boundary circle. The γ are calculated from the μ to ensure $(p-c)\gamma + a \in i\mathbb{R}$.

3. **Calculate the Schwarzian**
   To (pre)calculate the Schwarzian we either calculate all the transformations of $\mathbb{M}(D)$ or the poles and weights of the poles of the Schwarzian. This calculation also includes $\mathcal{A}_C$.

4. **Calculate a basis for the analytic remainder**
   We compute $3m-3$ analytic basis functions for the domain D.

5. **Search for the best parameter set b**
   We look for a set of parameters b, such that the analytic remainder leads to a valid multiply connected mapping.

6. **Evaluate the mapping**
   After all values are set, we evaluate the mapping and, for example, calculate a specific point, the boundary, or a grid. The calculation of the boundary may be accomplished by the algorithm provided in Section 5.2.

5.4.1 Calculating the Schwarzian Derivative

According to Theorem 4.36, the Schwarzian derivative of a conformal mapping onto a domain of connectivity three or greater is of the form

$$\mathcal{S}(z) = \sum_{T \in \mathbb{M}(D)} T'(z)^2 \left[\mathcal{R}(T(z)) + \mathcal{A}_C(T(z))\right] + \mathcal{A}_R(z).$$

We omit $\mathcal{A}_R(z)$ for now and focus on the Poincarè series contained in the Schwarzian derivative. To evaluate it, we need the initial rational function

$$\mathcal{F}(z) := \mathcal{R}(z) + \mathcal{A}_C(z)$$

and the transformations T of the group $\mathbb{M}(D)$.

We begin with the calculation of $\mathcal{F}$. It contains the poles of the first generation and their corresponding terms, and is therefore of the form

$$\mathcal{F}(z) = \sum_{j,k} \left(\frac{a_{j,k}}{(z - p_{j,k})^2} + \frac{\gamma_{j,k}}{(z - p_{j,k})} \right) + \sum_{j,k} \sum_{i=1}^{4} \frac{w_{j,k,i}}{(z - l_{j,i})}. \tag{5.5}$$

The $w_{j,k,i}$ represent the weights at the limit points used for $\mathcal{A}_C$. The actual values of these weights can be found in Definition 4.33, but they do not matter for the following discussion. It is enough to know that each set $\{ w_{j,k,i} \,|\, i = 1, \ldots, 4 \}$ corresponding to a prevertex $p_{j,k}$ can be calculated with the limit points $L_j = \{ l_{j,i} \,|\, l_{j,1} = s_j(l_{j,2}),\, l_{j,3} = s_j(l_{j,4}),\, i = 1, \ldots, 4 \}$, the center c_j of the corresponding circle C_j and the values belonging to the prevertex ($p_{j,k}$, $a_{j,k}$, $\gamma_{j,k}$). We can sum the weights over the index k to $w_{j,i} = \sum_k w_{j,k,i}$ as the poles $l_{j,i}$ do not depend on k.

As we supposed D and all $p_{j,k}$, $\alpha_{j,k}$ and $\mu_{j,k}$ to be known, we can calculate $a_{j,k}$ by $a_{j,k} = \frac{1}{2}(1 - \alpha_{j,k}^2)$ and $\gamma_{j,k}$ by $\gamma_{j,k} = \frac{i\mu_{j,k} - a_{j,k}}{p_{j,k} - c_j}$. We still need to calculate the limit points $l_{j,i}$ and weights $w_{j,i}$. Each set

$$L_j = \{ l_{j,i} \,|\, l_{j,1} = s_j(l_{j,2}),\, l_{j,3} = s_j(l_{j,4}),\, i = 1, \ldots, 4 \}$$

contains limit points symmetric to C_j, as s_j indicates the reflection against C_j. One method of calculating suitable limit points $l_{j,i}$ is to compute the fixed points of $s_j \circ s_\nu$ and $s_j \circ s_\eta$, where $\nu, \eta = 0, \ldots, m$, $\nu \neq j$, $\eta \neq j$, and $\nu \neq \eta$.
Let l_1 be a fixed point of $s_j \circ s_\nu$. We therefore have

$$(s_j \circ s_\nu)(l_1) = l_1 \Leftrightarrow s_j(l_1) = s_\nu(l_1)$$

and define $l_2 = s_j(l_1) = s_\nu(l_1)$. The point l_2 is also a fixed point as we have

$$(s_j \circ s_\nu)(l_2) = (s_j \circ s_\nu)(s_\nu(l_1)) = s_j(l_1) = l_2$$

and l_1 and l_2 are symmetric with respect to C_j. According to Lemma 2.25, both fixed points are also limit points.
With the $l_{j,i}$ known, we may also calculate the weights $w_{j,i}$. Hence we state the following algorithm to calculate the poles and coefficients of $\mathcal{F}$.

Algorithm 6:

set the values D, $p_{j,k}$, $\alpha_{j,k}$ and $\mu_{j,k}$
calculate the $a_{j,k}$ and $\gamma_{j,k}$
set the reflections s_j
compute L_0 as fixed points of $s_0 \circ s_1$ and $s_0 \circ s_2$
compute L_1 as fixed points of $s_1 \circ s_0$ and $s_1 \circ s_2$
calculate the $w_{0,i}$ and $w_{1,i}$ for $i = 1, \ldots, 4$
for j from 2 to m **do**
    compute L_j as fixed points of $s_j \circ s_0$ and $s_j \circ s_1$
    calculate the $w_{j,i}$ for $i = 1, \ldots, 4$
end for

Calculating the Poincaré series

With $\mathcal{F}$ set, we calculate the Poincaré series

$$\sum_{T \in \mathbb{M}(D)} T'(z)^2 \mathcal{F}(T(z)).$$

First, we truncate the Poincaré series to make it calculable. A natural way to do this is to restrict the length of the transformations. We will therefore use

$$\mathbb{M}(D, N) := \{\, T \mid T \in \mathbb{M}(D),\ |T| \leq N \} \tag{5.6}$$

instead of $\mathbb{M}(D)$ for the numerics.
There are two principal ways to compute the series. While both versions are mathematically equal, they have different computational errors.

The first method is to sum over the terms $T'(z)^2 \mathcal{F}(T(z))$ as it is suggested by the definition of the series. To set up the sum, we have to calculate all T in $\mathbb{M}(D, N)$:

Algorithm 7:

set the maximum transformation depth N
calculate the generating transformations of $\mathbb{M}(D)$ and their inverses
save them in $T[1]$
for n from 2 to N **do**
    for all transformations U in $T[n-1]$ **do**
        for all transformations V in $T[1]$ **do**
            if V is not inverse to the last applied transformation of U **then**
                calculate $U \circ V$
                save the result in $T[n]$[new number]
            end if
        end for
    end for
end for

The results are stored in a structure T in the form T[length][number]. The value "length" refers to the length $|T|$ of the transformation T. The formulation "V is not inverse to the last transformation of U" is necessary because the length of a transformation is reduced if we apply the inverse of the last applied generating transformation. With the set $\mathbb{M}(D, N)$, we are able to calculate the Poincarè series using the terms $T'(z)^2\mathcal{F}(T(z))$. Note that we need to include the term $\mathcal{F}(z)$ in the sum, as the set $\mathbb{M}(D, N)$ constructed above does not contain the identity.

The second method is to pre-calculate the $\mathcal{F}_T = T'(z)^2\mathcal{F}(T(z))$ in the form

$$\mathcal{F}_T(z) = \sum_{j,k}\left(\frac{a_{j,k}}{(z-q_{j,k})^2} + \frac{\delta_{j,k}}{(z-q_{j,k})}\right) + \sum_j \sum_{i=1}^{4} \frac{\tilde{w}_{j,i}}{(z-\tilde{l}_{j,i})}$$

by transforming $\mathcal{F}$ (given by equation (5.5)), where

$$p_{j,k} = T(q_{j,k}), \qquad \delta_{j,k} = T'(q_{j,k})\gamma_{j,k} + \frac{a_{j,k}T''(q_{j,k})}{T'(q_{j,k})},$$

$$l_{j,i} = T(\tilde{l}_{j,i}), \qquad \tilde{w}_{j,i} = T'(\tilde{l}_{j,i})w_{j,i}.$$

Since this calculation can not only be applied to the first generation, we may want to calculate $\mathcal{F}_{T\circ U} = U'(z)^2\mathcal{F}_T(U(z))$ in the same way, but starting with $\mathcal{F}_T$ instead of $\mathcal{F}$. This allows us to calculate each $\mathcal{F}_T$ directly by successive applications of the generators of $\mathbb{M}(D)$ without calculating $\mathbb{M}(D, N)$ in advance. Hence, we can alter our current approach to:

Algorithm 8:

```
1: set the maximum transformation depth N
2: calculate the generating transformations of M(D) and their inverses
3: save them in T
4: store the parameters of F (i.e. p_{j,k}, a_{j,k}, γ_{j,k}, l_{j,i}, w_{j,i}) in values[0][1]
5: for n from 1 to N do
6:     for all rational functions F_T in values[n − 1] do
7:         for all transformations U in T do
8:             if U is not inverse to the last applied transformation of F_T then
9:                 transform the poles p and l with U
10:                calculate the corresponding weights γ and w
11:                save the results in values[n][new number]
12:            end if
13:        end for
14:    end for
15: end for
```

Numerical Stability

Both versions of the Poincarè series, either the one using $T'(z)^2\mathcal{F}(T(z))$ or the one with $\mathcal{F}_T(z)$, contain some numerical problems.

To set up the correct context for the following discussion, we have to remember that the coefficients of the Möbius transformations $T(z) = (Az + B)/(Cz + D)$ grow very fast with an increasing length, while the quotients $-\frac{D}{C}$ stay bounded. This becomes crucial as the coefficients appear in several positions of our formula. The derivatives $T'(z)^2$ shrink with $|C|^{-4}$, while the parameters γ grow with $|C|^2$.
For visualization, we show the magnitude of the weight C^2 of γ in the form of iterations T^n of a transformation T in Table 7. Here T is the successive reflection against the unit circle $\partial\mathbb{D}$ and a circle C_1 with center c and radius r. We can see that the coefficients of

$\log_{10}(\lvert C\rvert^2)$	$n=1$	2	3	4	5	6	7	8	9	10
$c=3,\ r=1$	0.96	2.64	4.32	6.00	7.66	9.30	11.0	12.7	14.3	16.0
$c=5,\ r=1$	1.40	4.12	6.86	9.56	12.3	15.0	17.7	20.4	23.2	26.0
$c=5,\ r=2$	0.80	2.80	4.78	6.78	8.78	10.8	12.8	14.8	16.7	18.8
$c=7,\ r=1$	1.70	5.04	8.40	11.7	15.0	18.4	21.8	25.2	28.4	31.8

Table 7: The table shows the growth of the factor C^2, where C is the corresponding coefficient of a transformation T^n. The transformation T maps $\partial\mathbb{D}$ onto the circle C_1 with center c and radius r.

T^n grow like $O(\exp(n))$, which leads to problems in the numerics.
The common data type for numerics is the double precision floating point number. This type has about 16 significant decimal digits. We must assume that the last digit contains some form of rounding error. As a consequence, if we multiply any value x by a number in the size of 10^{16}, the result contains a rounding error equal in size to the original x. In our case, we would see this in calculating γ. Depending on the geometry of D, even a small number of transformations lead to a formula, which contains parameters with rounding errors greater than the absolute value of the parameters of the first generation.

The idea behind the convergence of the Poincaré series $\sum T'(z)^\nu \mathcal{R}(T(z))$ is that the derivatives T' in the form $T'(z)^\nu$ are tending to zero for $z \in D$ and $|T| \to \infty$, while the rational functions $\mathcal{R}(T(z))$ stay bounded. In our case, the rational functions $\mathcal{F}(T(z))$ are not bounded, but the $T'(z)^2$ are shrinking quickly enough to ensure the convergence. From a numerical point of view, this means that we are multiplying numbers of very different magnitudes.
There is another difficulty in the denominator $T(z) - l$ in $\mathcal{A}_C(T(z))$. The subtraction of equal sized numbers lead to the numerical problem of a loss of significance [DR08, Chapter 2.2]. Hence the result becomes very inaccurate if $T(z)$ tends to l.

On the other hand, the denominators of $\mathcal{F}_T(z)$ have a lower boundary for all $z \in D$. This is a consequence of the combination of the shrinking $T'(z)^2$ and growing $\mathcal{F}(T(z))$. The result is an overall shrinking expression $\mathcal{F}_T(z)$. The shrinking relies on the fact that the different parts of $\mathcal{F}_T(z)$ cancel each other out. The usage of $\mathcal{F}_T(z)$ is therefore also vulnerable to a loss of significance. This becomes especially critical, as the weights of the different terms (e.g. $\gamma_{T,j,k}$) grow with the length of the transformations. The numerical errors for longer transformations can therefore be greater than the correct values for shorter transformations, leaving only corrupt results.

Both versions incur numerical problems if we include lengthy transformations, i.e. the N in $\mathbb{M}(D, N)$ of equation (5.6) gets too large. However, we need a large N to obtain accurate results by the convergence of the sum. One of the main targets for the numerical evaluation is therefore to find an equilibrium between the accuracy provided by the limit process and the errors that grow with the length of the transformations.

Calculation Speed

We state some notes regarding the calculation speed of the evaluation. Many numerical software packages use multi-dimensional arrays as standard data type (e.g. MatLab, Octave, ...). They handle them very quickly in comparison with more complicated data types like structures. This fact can especially be used at two different points in the calculation process.

If we prepare or set up the sum for the Schwarzian as in the Algorithms 7 and 8, we obtain some rather expensive[51] structures. Since the Schwarzian has to be evaluated very often, it is reasonable to restructure the data to a form which can be evaluated more quickly. Since the order of the terms is not important for a finite sum, we may create a single vector or matrix for each parameter type. Using vectors and matrices instead of loops results in a significant quicker calculation.
This vectorization can for example be done by the following algorithm if we want to convert the results of Algorithm 8.

Algorithm 9:

```
for n from 0 to N do
    for all sets S in values[n] do
        for all combinations belonging to one prevertex of S do
            save the current prevertex as new element of the vector p
            save also a and γ as new elements of corresponding vectors
            save the limit points (for A_C) as a new row in the matrix l
            save the weights for the limit points as a new row in the matrix w
        end for
    end for
end for
```

If we use the concept of transformations (based on Algorithm 7), we can use a matrix containing the coefficients of each transformation in a row, thus evaluating the Schwarzian without loops.

The use of matrices is also useful in the calculation of the Möbius transformations. If we write the coefficients of the Möbius transformations in the form of a matrix, i.e.

$$T = \begin{pmatrix} A & B \\ C & D \end{pmatrix},$$

[51] Expensive in the context of calculation time.

we can calculate the composition of two transformations $U \circ T$ by a simple matrix multiplication.[52]

5.4.2 Basis Functions for the Analytic Remainder

The analytic remainder $\mathcal{A}_R$ of the Schwarzian derivative can be expressed as a real linear combination of $3m-3$ basis functions according to Lemma 4.41. We therefore need $3m-3$ linearly independent functions $\mathcal{B}_i$ with the correct properties and suitable weights b_i.

First we calculate $3m-3$ basis functions. We already presented three different ways to construct suitable functions in the Sections 4.4.4, 4.4.5 and 4.4.6, but we must ensure that we are only constructing linearly independent functions or we have to reduce the resulting set of functions to only contain linearly independent elements.

The versions of Lemma 4.45 (Section 4.4.5) and of Definition 4.56 (Section 4.4.6) for such functions $\mathcal{B}_i$ are very similar from a numerical point of view. Both versions resemble a Poincaré theta series, but the second covers only a subset of the transformations of the group.
Hence, both of them can be pre-calculated in the manner described in the previous section. The only difference is that we only need the mentioned subset $\mathbb{M}(D,T,N)$ of the transformations $\mathbb{M}(D)$ for the second option. We alter our algorithm for $\mathbb{M}(D,N)$ to compute only the required subset.

Algorithm 10:

```
 1: set T and the maximum transformation depth N
 2: calculate the generating transformations of M(D) and their inverses
 3: save them in G
 4: copy G to V[0] except for the one transformation equal to T_m^{-1}
 5: for n from 1 to N do
 6:     for all transformations U in V[n-1] do
 7:         for all transformations W in G do
 8:             if W is not inverse to the last transformation of U then
 9:                 if U ∘ W is not T then
10:                     calculate U ∘ W
11:                     save the result in V[n][new number]
12:                 end if
13:             end if
14:         end for
15:     end for
16: end for
```

[52] This fact can be proven by calculation.

We are also able to calculate the basis functions by using only the poles and weights as discussed in the previous section for $\mathcal{F}_T$. This may be done by a modification of Algorithm 8.
After calculating several functions $\mathcal{B}_i$ by different initial limit points or transformations, we need to verify if they are linearly independent. This can be done by using the information of Section 4.4.4 that the first three coefficients of all Laurent series of equation (4.54) together completely define the function. Hence, calculating these coefficients represented by three real values and testing the vectors of the $\mathbb{R}^{3m+3}$ for linear dependence is sufficient.[53]

Alternatively, we can directly construct the functions in the form

$$\mathcal{B}_i(z) = \sum_{j=0}^{m} \sum_{n=1}^{N} \frac{d_i(n,j)}{(z-c_j)^n}$$

of equation (4.54), but with a finite number of coefficients $d_i(n,j)$. We already stated in Section 4.4.4 that the coefficients can be computed by constructing a system of equations based on a finite version of formula (4.59)

$$\sum_{j\neq k} \sum_{n=4}^{N} \omega(l,n) c(k,j)^{-(l+n)} d_i(n,j) - r_k^{-2l-4} \overline{d_i(l+4,k)} = -\lambda_i(l,k), \tag{5.7}$$

where

$$\omega(l,n) = (-1)^l \binom{l+n-1}{l}, \qquad c(k,j) = c_k - c_j,$$

$$\lambda_i(l,k) = \sum_{j\neq k} \sum_{n=1}^{3} \omega(l,n) c(k,j)^{-(l+n)} d_i(n,j).$$

Hence, we set up the system

$$Wd = \lambda, \tag{5.8}$$

where W is a matrix containing the weights for the $d_i(n,j)$, d is a vector constructed of the $d_i(n,j)$ and λ is a vector consisting of the $\lambda_i(l,k)$. The matrix and the vectors cover all combinations of $l = 0,\dots,N-4$ and $k = 0,\dots,m$. Solving this system for d yields the coefficients to calculate an approximation of $\mathcal{B}_i$.
The first three coefficients $d_i(n,j)$ for each circle, which are needed to calculate the $\lambda_i(l,k)$, can be acquired by solving the system of linear equations (4.57). Actually, a basis for the kernel of the linear system gives us a set of initial values to calculate $3m-3$ linearly independent functions $\mathcal{B}_i$. Hence, we have found the following algorithm:

[53] This method is only valid for unbounded domains. The initial domain may need to be transformed accordingly.

Algorithm 11:
1: set the number of coefficients N
2: set up the system of equations (4.57)
3: calculate a basis B for the null space of the system
4: generate the matrix W based on (5.7)
5: **for all** elements in B **do**
6: calculate the $\lambda(l,k)$ and generate the vector λ
7: solve the system $Wd = \lambda$ for d
8: save the solution
9: **end for**

This method also leads to some numerical issues.[54] Since the absolute value of the $\omega(l,n)$ rise very fast for large l, the system (5.8) loses stability for large N, or equivalently the condition number of W rises with N. Again, the best N is not necessary a large one.

While the construction above is designed for unbounded circular domains, basis functions for bounded domains can be calculated by the procedure stated at the end of Section 4.4.4.

1. Extend the circular domain D over the outer boundary circle C_0.
2. Calculate the basis functions for the unbounded extension $s_0(D)$.
3. Transform the solutions to be defined on D.

5.4.3 Validity of the Mappings

We discussed at the end of Section 4.4.3 that not all combinations of parameters of the Schwarzian yield a valid mapping. To verify if the result of a mapping is valid, we may apply the same method as for the doubly connected domains. The main difference is that we have to investigate m curves instead of only one.
Let $\delta_j(t)$, where $t \in [0,1]$, be the parametrization of a circle in D enclosing only the boundary circle C_j. To verify the conditions (2.3), we solve from $\delta_j(0)$ to $\delta_j(1)$ and compare the results to the initial values. For a valid mapping, the values for $\delta_j(0)$ and $\delta_j(1)$ must be equal. Hence, we investigate the values

$$g_{j,l} := f^{(l)}(\delta_j(0)) - f^{(l)}(\delta_j(1)), \qquad j = 1,\dots,m,\ l = 0,1,2.$$

If all of them are zero, we have a necessary (but not sufficient) condition for validity.

As for the doubly connected case, we can use this idea to find an analytic remainder, which matches the mapping function as much as possible with respect to a valid

[54] The problems of the Poincaré series, which apply to the first two methods, where already covered in the previous section.

mapping. Since the analytic remainder is defined by

$$\mathcal{A}_R(z) = \sum_{i=1}^{3m-3} b_i \mathcal{B}_i(z),$$

we have to find suitable weights $b_i \in \mathbb{R}$ for the linear combination, if the $\mathcal{B}_i$ are given. As the $g_{j,l}$ depend on $b = (b_1, \ldots, b_{3m-3})$, we can establish an error function

$$E(b) := \sum_{j=1}^{m} \sum_{l=1}^{3} |g_{j,l}(b)|.$$

Now we must find a zero of E by numerical methods to obtain a suitable choice for b.

5.4.4 Examples

The algorithms for the plotting of a CAPD mapping of connectivity three or greater are similar to the ones of the doubly connected case. The greatest difference is the usage

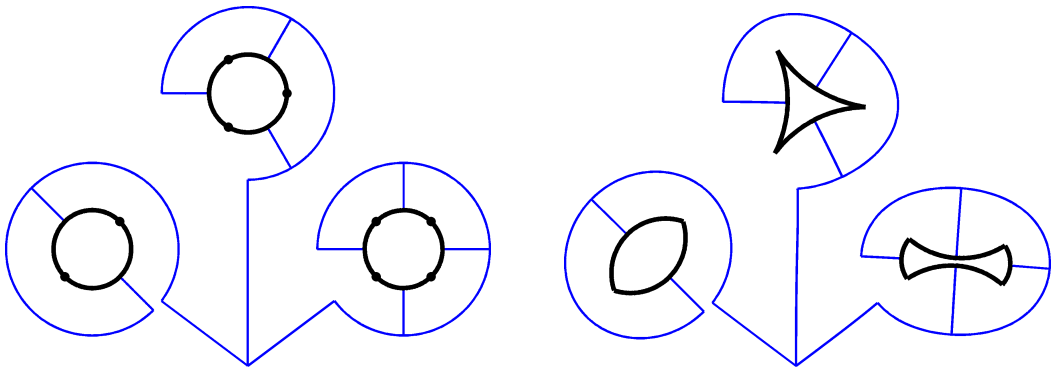

(a) Preimage: The blue paths to reach the boundary are chosen according to Section 5.2. The black boundary is then calculated.

(b) Image: The blue image of the paths and the black image of the boundary are shown.

Figure 50: The first algorithm reaches out from a starting point to touch each boundary arc. At each of these arcs, the behavior at the boundary is calculated. Here a triple connected unbounded domain is shown.

of the Schwarzian for MCCAPD mappings instead of the one for the mappings onto DCCAPDs.
The algorithm generating the grid is further modified. Since there is no obvious choice for a grid, we place a small grid around each boundary circle to visualize the mapping behavior, and also change the coloring. Each boundary component is now painted in a different color to distinguish them, and each grid uses the color of its corresponding boundary component (Figure 51).

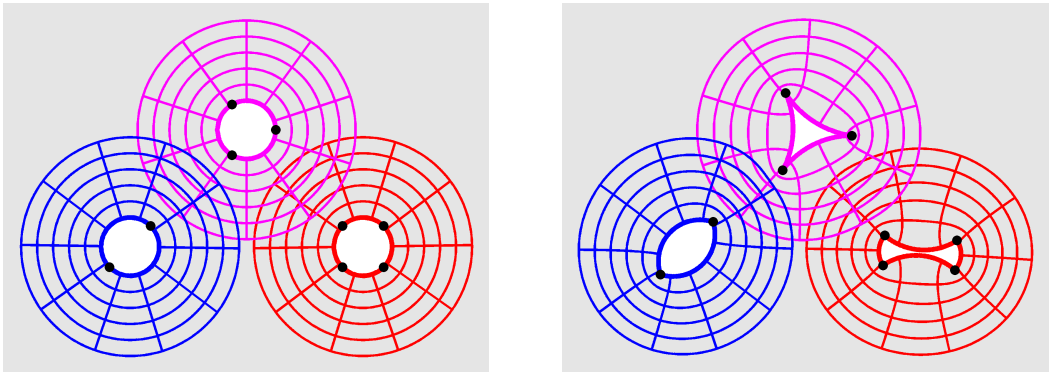

Figure 51: The second algorithm plots the boundary, the vertices and a grid around each boundary component. Each boundary component is painted in a different color for ease of matching with its preimage. The corresponding grid has the same color as the boundary. Here the triply connected domain of Figure 50 is shown once again.

While there is no restricting equation for the MCCAPD mappings, we still have the problem of overlapping image domains. The results are similar to the doubly connected mappings, so we refer to the images presented in Section 5.3.3 for visualization.
However, this problem becomes of greater interest, as the search for valid parameter sets is more difficult than in the case of doubly connected domains, and any search algorithm will take longer as the number of parameters increases. This is the main reason why most of the images show boundary components containing some kind of symmetry. These domains are easier to handle with respect to their parameters (Figures 53 to 56).

We noted in the doubly connected case that the behavior of the image domains with respect to the prevertices p and the parameters μ is similar to the simply connected case. This holds also for an even greater connectivity.
Hence, we want to set up an example similar to (5.4) of the doubly connected case. We define the parameters for the outer boundary C_0 by

$$\begin{aligned} c_0 = 0, \quad r_0 = 1, \qquad & \arg(p_0 - c_0) = (\,0.25, 0.75, 1.25, 1.75\,)\,\pi, \\ \alpha_0 = (\,0.5, 0.5, 0.5, 0.5\,), \qquad & \mu_0 = \lambda(\,1, -1, 1, -1\,). \end{aligned} \tag{5.9}$$

Again, the values of μ depend on an additional parameter $\lambda \in \mathbb{R}$. The parameters for the inner two boundary components are defined by

$$\begin{aligned} c_1 = 0.5, \quad r_1 = 0.1, \qquad & c_2 = -0.5, \quad r_2 = 0.1, \\ \arg(p_1 - c_1) = (\,0, 1\,)\,\pi, \qquad & \arg(p_2 - c_2) = (\,0, 1\,)\,\pi, \\ \alpha_1 = (\,1.5, 1.5\,), \qquad & \alpha_2 = (\,1.5, 1.5\,), \\ \mu_1 = (\,0, 0\,), \qquad & \mu_2 = (\,0, 0\,). \end{aligned} \tag{5.10}$$

By changing λ, we obtain image domains very similar to the ones for the doubly connected mappings. The results can be seen in Figure 52.

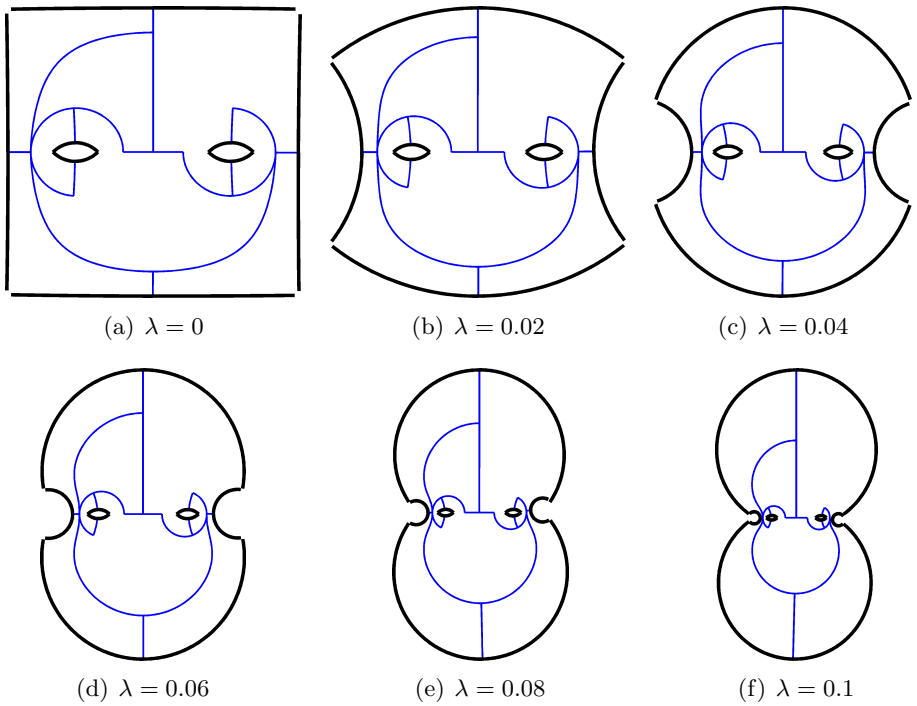

(a) $\lambda = 0$ (b) $\lambda = 0.02$ (c) $\lambda = 0.04$

(d) $\lambda = 0.06$ (e) $\lambda = 0.08$ (f) $\lambda = 0.1$

Figure 52: The image domain for the parameters given by (5.9) and (5.10) changes with the choice for λ. The difference in curvature of two successive outer boundary arcs increases with an increasing value for λ.

If we compare Figure 52 with Figure 49 of the doubly connected mappings, we notice one more fact: The ratio of the curvature is changing faster in the images of the triply connected domains, while the values for λ increase slower. The λ for double connectivity ranges from 0 to 0.5, while the λ for the triply connected case ranges from 0 to 0.1. While the basic behavior in both cases is equal, the actual results still depend on the shape of D.

One point to remember while investigating the image domain of any kind of CAPD mapping is this: The visual impression of a result depends significantly on the initial values. We adjusted these values for the produced images to keep the basic properties of the results constant. For example, we kept the curvature of the arcs of the outer boundary pairwise equal for the images regarding the changing parameters in Figure 52.
The fact that a CAP looks very different for different initial values/Möbius transformations was already shown in Figure 14.

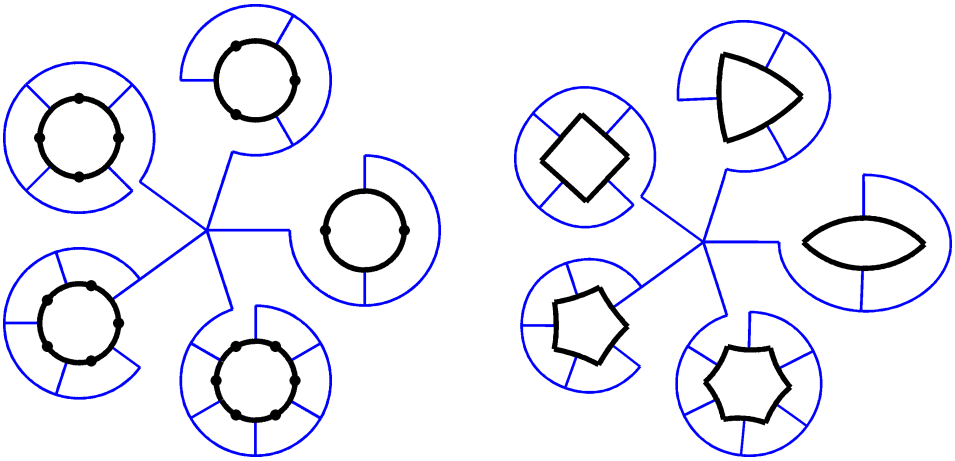

Figure 53: The image of the boundary for a domain of connectivity five.

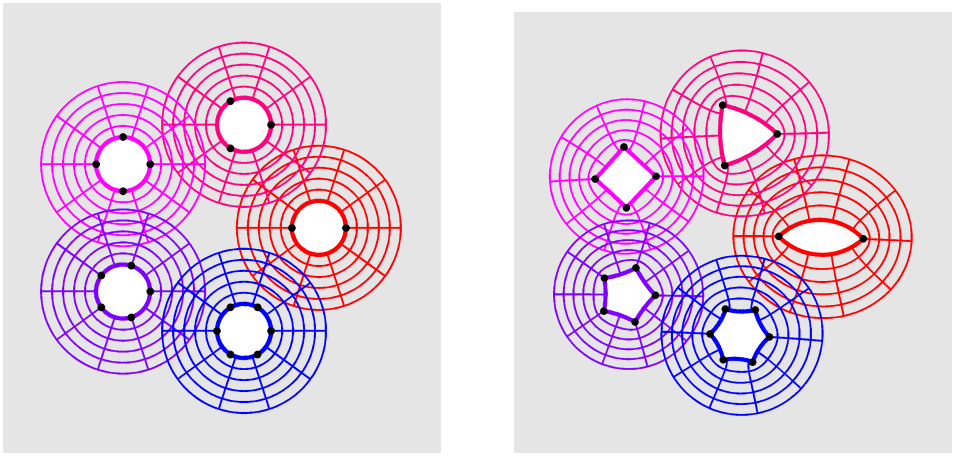

(a) Preimage (b) Image

Figure 54: The domain of connectivity five (Figure 53), where the vertices and surrounding grids are shown.

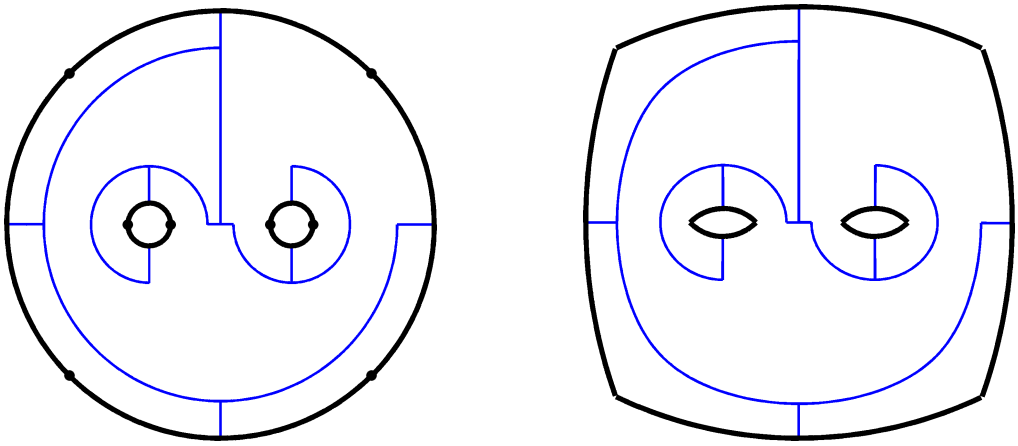

(a) Preimage (b) Image

Figure 55: The first algorithm for a bounded triply connected domain.

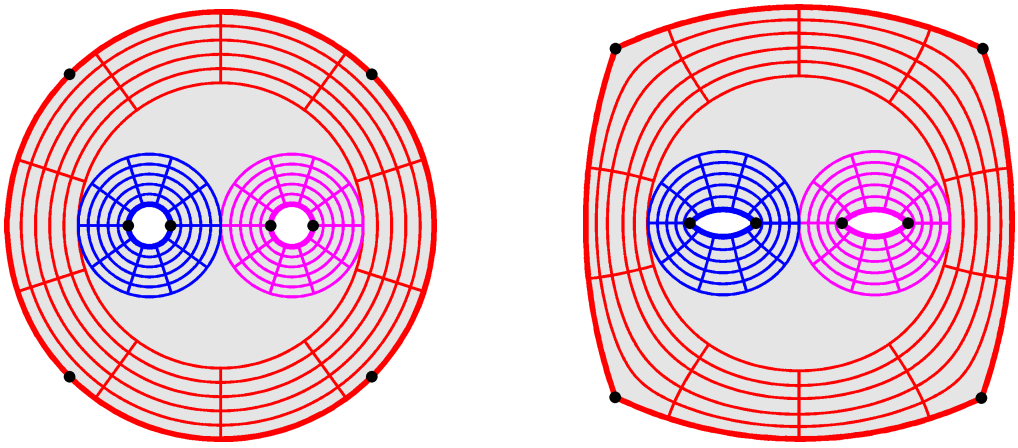

(a) Preimage (b) Image

Figure 56: The second algorithm for the bounded triply connected domain of Figure 55.

5.5 Approach to the Parameter Problem

To map onto a specific image domain, we must find the correct parameters for the Schwarzian derivative. This is known as the "parameter problem" in the context of the Schwarz-Christoffel transformation.
The best known approaches to this topic for simply connected circular arc polygon domains are from Bjørstad and Grosse ([BG87]) and from Howell ([How90], [How93]). We now extend their concepts to handle conformal mappings onto multiply connected domains.

5.5.1 Numerical Solving the Parameter Problem

The Schwarzian derivative for MCCAPD mappings contains four groups of parameters: the prevertices p, the interior angles $\alpha\pi$ in the form of a, the parameters μ and the linear combination for $\mathcal{A}_R$ given by b. We also need a conformally equivalent preimage domain, and so we need the boundary circles of a suitable circular domain D in form of their centers c and radii r.
If we denote the number of all prevertices of all circles by $K := \sum_j K_j$, we need $3K$ real values to describe the parameters p, a and μ. For a $(m+1)$-connected domain D, it takes $3(m+1)$ real values to determine the boundary circles and there are $3(m-1)$ linearly independent analytic functions $\mathcal{B}_i$ to construct $\mathcal{A}_R$. Since the target MCCAPD P is known, we already know the interior angles and therefore the values a. We also have to take a normalizing Möbius transformation for the preimage domain D into account. We therefore have to find real values in the quantities

$3K$	parameters p, a, μ
$-K$	known interior angles
$+2(m+1)$	centers c
$+(m+1)$	radii r
$+3(m-1)$	parameter b
-6	normalization by Möbius transformation
$=2K+6m-6.$	

We combine these values to one parameter vector $\overrightarrow{x}$. Note that not all $\overrightarrow{x}$ are valid, as for example not every combination of centers and radii yields a circular domain.

We now need a way to describe the image domain of a MCCAPD mapping to be able to compare it with other MCCAPDs. Any CAP domain can be characterized by its vertices and the curvature of its arcs. If we denote the number of all vertices as above by K, the domain is given by $3K$ real values. By supposing the interior angles to be fixed, this reduces to $2K$ real values.[55] Since we can apply a Möbius transformation to the mapping, we can normalize each CAPD by six degrees of freedom. This leaves us

[55] See the next section for further discussion about the geometry of CAPDs.

with $2K-6$ real values to identify a CAPD. As we are dealing with a MCCAPD that is generated by a mapping, we need to verify the validity of the image domain by the three integral equations (2.3) for m of the $m+1$ boundary components. This gives a further $6m$ real values to take into account.

$2K$	vertices
$+K$	curvatures
$-K$	known interior angles
-6	normalization by Möbius transformation
$+6m$	integral equations
$=2K+6m-6$	

Overall, this results in $2K+6m-6$ values to describe a CAPD, so we can compare two CAPDs P_1 and P_2 by $2K+6m-6$ values, i.e. define an operator d measuring the distance $d(P_1,P_2)\in\mathbb{R}^{2K+6m-6}$.

Since both sides have the same numbers of degrees of freedom we can apply methods similar to those of the parameter problem for the SC mapping. Hence, if we are looking for a domain P_0, we will need a function $E:\mathbb{R}^{2K+6m-6}\to\mathbb{R}^{2K+6m-6}$ taking $\overrightarrow{x}$ as an input and returning the distance between the CAP domains $P(\overrightarrow{x})$ and P_0, where $P(\overrightarrow{x})$ denotes the image domain for the parameter vector $\overrightarrow{x}$. With this function, we only need to find a zero of $E(\overrightarrow{x}):=d(P(\overrightarrow{x}),P_0)$ by numerical optimization routines like quasi-Newton methods to get the correct parameters.
The function E should contain the following steps

Algorithm 12:

1: pre-calculate the Schwarzian for the parameter vector $\overrightarrow{x}$
2: calculate a basis for the analytic remainder and set $\mathcal{A}_R$
3: compute the boundary of the image domain
4: normalize the domain
5: compare the current image domain with the target domain P_0
6: return the difference as a vector of $\mathbb{R}^{2K+6m-6}$

Any search algorithm will vary the values in $\overrightarrow{x}$ to find the zero of E, but this method presents two problems. The first is that the order of the prevertices on each circle is not allowed to change. As this problem also occurs for the Schwarz-Christoffel transformation, there is already a solution to this problem, as given by a clever substitution for the arguments of the prevertices found in [DT02].
More critical is the second issue that the basis for the analytic remainder changes if we change the preimage domain, so the coefficients b_i can not be applied to the same functions $\mathcal{B}_i$ as in the previous step.
A possible solution to this problem would be to remove the search for b from E and do it in a subroutine in each step of E, where the conditions for a good b can for example be the validity of the mapping as we discussed above.

Algorithm 13:
1: pre-calculate the Schwarzian for the parameter vector $\overrightarrow{x}$
2: calculate a basis for the analytic remainder
3: search for the best choice of b
4: use the calculated value of b for the following steps
5: compute the boundary of the image domain
6: normalize the domain
7: compare the current image domain with the target domain P_0
8: return the difference as a vector

The downside of Algorithm 13 is that the problem is no longer quadratic, forcing us to use other numerical solvers.

5.5.2 Geometry of Circular Arc Polygon Domains

Degrees of Freedom of a CAP

To compare the image CAPD of a mapping and the wanted CAPD P_0, we need a way to describe the bounding circular arc polygons.

A CAP is completely defined if we know all the vertices and the curvatures of all the edges. This gives $3K$ degrees of freedom for a CAP with K vertices/edges. For the parameter problem, the interior angles of the CAP are set, as we are looking for a specific CAPD. Subtracting these K degrees of freedom means we have to identify the CAP by the $2K$ remaining degrees.
The vertices alone are not suitable to identify the CAP. This can be seen by an example from [BG87] shown in Figure 57. Suppose the vertices of a rectangle to be given. If one

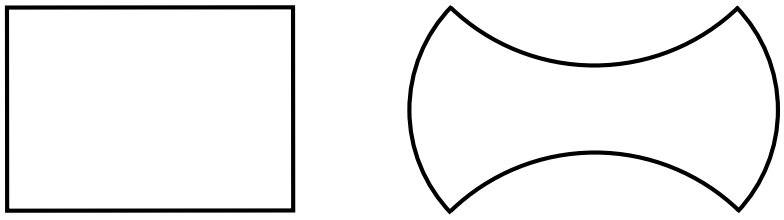

Figure 57: Both domains have the same position of the vertices and the same interior angles but differ in their shape. [BG87]

side is bend inwards, we can keep the interior angles by alternately bending the other sides either outwards or inwards. Therefore, the same vertices and interior angles allow us to construct several different CAPs. We could for example handle this problem by replacing the 2 real degrees of freedom of one vertex by the values of two curvatures.

Hence, one way to construct a CAP by $2K$ real values would be the following:
Each circular arc represents five degrees of freedom: three for the circle and two for the starting and end point. We can therefore fix the first edge by setting the vertices v_1, v_2 and the curvature κ_1 of the edge. For the second edge, we already have three information: the vertex v_2 and the interior angle between the first and the second edge. The remaining two points of information can be established by the vertex v_3. We can continue in this manner through the vertices until v_{K-1}. Up to this point we used $5 + 2(K-3) = 2K-1$ real information for the construction, leaving one degree of freedom open for the last two edges. We can use this remaining degree to set the curvature κ_{K-1} of the second to last edge. In this way, we obtain the circle $\tilde{C}_{K-1}$ for this edge, where the starting point is already given by v_{K-1}. Since the CAP is a closed curve, we can also use the first circle $\tilde{C}_1$ and v_1 for the calculation of the last edge. With $\tilde{C}_1$, $\tilde{C}_{K-1}$, v_1 and the angles between the circles, we are able to calculate $\tilde{C}_K$.[56] The last vertex v_K can afterwards be computed as the intersection point of the circles $\tilde{C}_{K-1}$ and $\tilde{C}_K$.[57]

A problem with this and many other approaches is that it is only valid for CAPs that are simple curves. If at least one arc is larger than 2π in argument, the construction is no longer valid. While such arcs are not used for our construction of circular arc polygons, they might still appear in the numerics. This topic is further discussed in [How90].

Normalization of MCCAPD Mappings

As the preimage and the image domain of a MCCAPD mapping can be transformed by Möbius transformations, we need some normalization for these domains.
For the preimage domain, a circular domain, we can use three of the six real degrees of freedom provided by a Möbius transformation to set C_0 to the unit circle $\partial\mathbb{D}$. The remaining three can be used to set further circle properties, prevertices or a combination of both. A suggestion would be to set the first prevertex on C_0 to 1 and the center of C_1 to a specific value like 10 or $1/2$ depending whether D is unbounded or bounded. These normalized values have then to be excluded from the parameter vector $\overrightarrow{x}$.
The image domain can be normalized by setting either the vertices or the curvatures to the values we wish. One easy method is to set three vertices to the required values. This allows to directly calculate the Möbius transformation for the normalization by the cross-ratio of the points. Afterwards we apply the transformation to the image domain to move all other vertices accordingly.

[56] By interpreting the interior angles as inversive distances between the circles, one can easily set up a system of equations.

[57] The calculation of the last vertex may becomes difficult for specific configurations of curvatures and angles [How90], but this problem can be handled by changing the curvatures by using other prevertices for the normalization.

Measuring the Difference between Circular Arc Polygon Domains

With the discussion so far, we have supposed two MCCAPDs P and $\tilde{P}$ to be equal if they satisfy for all boundary CAPs the equations

$$\begin{aligned} v_{j,k} - \tilde{v}_{j,k} &= 0, \qquad j = 0, \ldots, m,\ k = 1, \ldots, K_j - 1, \\ \kappa_{j,k} - \tilde{\kappa}_{j,k} &= 0, \qquad j = 0, \ldots, m,\ k = 1, K_j - 1, \end{aligned}$$

where we exclude three vertices for the normalization. If $P(\overrightarrow{x})$ is generated by a MCCAPD mapping $f(z, \overrightarrow{x})$ with the parameter vector $\overrightarrow{x}$, we also have to verify the validity of the mapping with regard to

$$\int_{\delta_j} f^{(l)}(z, \overrightarrow{x}) dz = 0, \qquad j = 1, \ldots, m,\ l = 1, 2, 3.$$

We already suggested in Section 5.4.3 that we may verify

$$g_{j,l}(\overrightarrow{x}) = f^{(l)}(\delta_j(0), \overrightarrow{x}) - f^{(l)}(\delta_j(1), \overrightarrow{x}) = 0, \qquad j = 1, \ldots, m,\ l = 0, 1, 2,$$

instead as this version demands less calculation time. Hence, we have found the formulas

$$\begin{aligned} v_{j,k}(\overrightarrow{x}) - \tilde{v}_{j,k} &= 0, && 2K - 2(m+1) - 6 \text{ real equations}, \\ \kappa_{j,k}(\overrightarrow{x}) - \tilde{\kappa}_{j,k} &= 0, && 2(m+1) \text{ real equations}, \\ \mathrm{Re}\,(g_{j,l}(\overrightarrow{x})) &= 0, && 3m \text{ real equations}, \\ \mathrm{Im}\,(g_{j,l}(\overrightarrow{x})) &= 0, && 3m \text{ real equations}, \end{aligned}$$

where $K = \sum_j K_j$, resulting in $2K + 6m - 6$ real equations.
This gives a system of equations as needed for Algorithm 12.

With this system of equations, we have found a way to measure the difference between two CAPDs P and $\tilde{P}$, i.e. we have a function $d(P, \tilde{P})$. We are also able to compute the boundary of a MCCAPD $P(\overrightarrow{x})$ defined by the parameters $\overrightarrow{x}$. Hence, for a given target MCCAPD P_0, the function $E(\overrightarrow{x}) = d(P(\overrightarrow{x}), P_0) : \mathbb{R}^{2K+6m-6} \to \mathbb{R}^{2K+6m-6}$ is given. This allows us to perform the solving of the parameter problem as the search for the zero $\overrightarrow{x_0}$ of the function E.

At this point, we may apply a lot of the knowledge already gathered for the Schwarz-Christoffel parameter problem [DT02]. This includes transformations of the parameters to forms which are more suitable for numerical solvers and variations in the equation system such as replacing the vertices by lengths and curvatures.

5.6 Current State of the Schwarz-Christoffel Transformation

The most influential articles about the numerical computation of multiply connected Schwarz-Christoffel maps are written by DeLillo, Elcrat, Kropf and Pfaltzgraff. After stating the initial formula for the mappings in [DEP04], they evolve the numeric for the computation by improving the evaluation of the mappings and introducing approaches

to the parameter problem ([DDEP06], [DK10]). The results were published later in [DK11].

The even more recent article [DEKP13] introduces an interesting approach to the evaluation of the mapping function. The mapping formula (4.63)

$$f(z) = \int^z \prod_{j=0}^{m} \prod_{k=1}^{K_j} \left[\prod_{i=0,\nu\in\sigma_i(j)}^{\infty} \left(\frac{\zeta - p_{j,k,\nu}}{\zeta - u_{j,\nu}} \right) \right]^{\beta_{j,k}} d\zeta$$

is rewritten to

$$f(z) = \int^z \prod_{j=0}^{m} \prod_{k=1}^{K_j} [f_{j,k}(\zeta)]^{\beta_{j,k}} \, d\zeta,$$

where

$$f_{j,k}(z) = \prod_{i=0,\nu\in\sigma_i(j)}^{\infty} \left(\frac{z - p_{j,k,\nu}}{z - u_{j,\nu}} \right).$$

Since $f_{j,k}$ is defined by an infinite product, it yields most of the numerical problems. Therefore it is approximated by a method using Laurent series to avoid the reflections necessary for the original $f_{j,k}$. This approach may also be useful for the MCCAPD mapping.

6 Conclusion

Considering all our results, there are three different but to some degree similar versions for the Schwarzian derivative of conformal mappings onto CAPDs, depending on the connectivity of the domains. All three versions depend on the parameters p, a and μ and the geometry of the preimage domain. In addition, there are restricting equations for the parameters p, a and μ and the mapping formula contains an analytic remainder that has to be correctly chosen. Note that the number of restricting equations is reduced and the number of parameters for the analytic remainder grows if the connectivity becomes greater.

simply connected Theorem 3.4 (page 36)
3 restricting equations, 0 parameters for the analytic remainder

doubly connected Theorem 4.22 (page 76) and Theorem 4.23 (page 77)
1 restricting equation, 1 parameter for the analytic remainder

multiply connected Theorem 4.36 (page 108)
0 restricting equations, $3m - 3$ parameters for the analytic remainder

With these results, we are able to find for each simply or multiply connected CAPD P a conformal mapping from a circular domain[58] onto P,[59] but the search for the mapping becomes more difficult if the connectivity of P grows. The common problem for all of these versions is the choice and interpretation of the parameters. This becomes even more crucial as not every parameter set yields a valid mapping in the case of multiply connected domains.

For the individual parts of this thesis, we have the following results and open topics:

6.1 Simply Connected CAP Domains

We discussed the properties of conformal mappings onto simply connected CAP domains and investigated the behavior of the parameters μ for some special CAP domains. We noticed that $|\mu|$ rises as the prevertices cluster together (Section 3.2) and that there is a connection between the curvatures of the arcs and the values of the μ (Section 3.4). We even provide an explicit formula for the μ if the image domain can be mapped onto a polygonal domain by a Möbius transformation. This result is gathered by comparison with the classical Schwarz-Christoffel transformation (Section 3.3).

If we combine our three results, we see that the μ depend on the distances between the prevertices, the interior angles $\pi\alpha$ and the curvatures of the boundary arcs. The best way to see this connection to the prevertices and angles is Lemma 3.6, where the curvature is zero for all boundary arcs if a suitable normalization is applied. The formula

[58] The unit disk is a special case of a circular domain.
[59] There is still a restriction regarding the convergence for domains of connectivity four or greater.

presented in the lemma allows us to directly investigate this connection. Otherwise, equation (3.9) also contains the curvature, but the equation is only an approximation for the μ. Hence, it allows us only to make some estimations.

While we showed a connection of the parameters μ with the prevertices, the interior angles and the curvature of the boundary arcs of the image domain, the main problem of an accurate description of the μ remains. The usage of curvatures for the description of the μ always depends on the normalization of the actual image domain, so it would be useful to replace the curvatures by a value that does not depend on the normalization. It would even be better to replace the μ by parameters that are independent of the other parameters of the mapping.
Even with an interpretation of the μ, the classical Schwarz-Christoffel parameter problem would remain, and so any improvements in this direction would also be appreciated.

6.2 Multiply Connected CAP Domains

We collected properties of the Schwarzian derivative of conformal mappings onto multiply connected CAP domains by extending the domain of definition of such mappings to its maximum (Section 4.1) and used these properties afterwards for the construction of the Schwarzian. We established a Schwarzian derivative for conformal mappings onto doubly connected CAP domains (Section 4.2) and one for mappings onto CAP domains with connectivity three or greater (Section 4.4).
While the form for connectivity two is fixed, the form for connectivity three or greater can be modified by the choice of $\mathcal{A}_C$ and the basis for $\mathcal{A}_R$. We found a choice for $\mathcal{A}_C$ that satisfies the requirements of the mappings, and we also presented three versions for the basis functions $\mathcal{B}_i$ of $\mathcal{A}_R$.
These results were then compared to existing mappings onto CAPDs and to mappings onto domains that can be interpreted as special cases of CAPDs, for example the Schwarz-Christoffel transformation (Section 4.3 and Section 4.5).

In summary, we found formulas to conformally map onto multiply connected circular arc polygon domains and verified them by comparison to existing formulas that cover similar mappings. We are therefore able to conformally map onto every CAPD (of finite connectivity) as long as we find the correct parameters.
A comparison of our proofs of the multiply connected mappings and our proof of Theorem 3.4 for simply connected mappings allows us to see that all cases of mappings onto CAPDs are constructed in a similar way by extending the domain of definition. However, the different preimage domains lead to different results including the analytic remainder and different numbers of restricting equations.

We note for further work that the conformal mappings onto MCCAPDs can be improved by simplifying $\mathcal{A}_C$ and $\mathcal{A}_R$. Our choice for $\mathcal{A}_C$ is rather complicated, and there might be a better choice or at least a simplification. We presented several version to find a basis for $\mathcal{A}_R$, but there is still room for improvement. It would be useful to find a set of basis functions of greater computational simplicity. This includes the problem of

ensuring the linear independence of the constructed functions.
As the (normalized) conformal mappings onto CAPDs are unique, there must also be a connection between the choice of $\mathcal{A}_C$ and the parameters b of $\mathcal{A}_R$. A combination of both terms would perhaps lead to a simpler form of the Schwarzian.
It would also be advantageous to remove the convergence requirement for the mapping by using current results regarding Poincaré theta series.

The mappings onto multiply connected CAP domains pose the problem of choosing suitable parameters to obtain a valid mapping. We are at the moment restricted to testing this property by evaluating each mapping and checking the image domain for overlapping parts and gaps. Hence, some conditions for the parameters to ensure a valid mapping without testing the result would be beneficial. The main goal should nonetheless be a full description of the subspace of valid parameters. Based on the Carathéodory convergence theorem, this subspace is at least connected and open.

Even for a valid set of parameters, we have a lack of information regarding the parameters μ for multiply connected image domains. Some of the numerical generated images lead us to expect a similar behavior as for simply connected domains, but this conjecture needs verification.

6.3 Numeric for CAPD Mappings

We presented the necessary background and methods for the numerical evaluation of conformal mappings onto multiply connected CAP domains and an approach for numerically solving the parameter problem:

- Calculation of the Schwarzian derivative
- Paths in order to solve the Schwarzian along them
- Calculation of the boundary and the vertices
- A system of equations to approach the parameter problem

We are therefore able to handle the common numerical tasks regarding conformal mappings: We can find the correct parameters for a specific circular arc polygon domain and we are able to evaluate the resulting mapping everywhere in its domain of definition and determine its boundary.

However, many of the individual procedures still need testing and improvements to obtain a robust algorithm for the calculation of the mapping.
This especially includes the parameter problem. As for similar problems, the robustness of the algorithm depends heavily on the quality of the used system of equations. Hence, one may try to use as many techniques as possible from the better investigated Schwarz-Christoffel transformation and modify them for the needs of CAP boundaries.
There are also ideas like approximating parts of the formula by Laurent series expansions [DEKP13] (Section 5.6) that may be applied to improve the mappings.

A Additional Notes

A.1 Restricting Equations for the CAPD Mapping onto Polygonal Domains

The parameters μ of the conformal mappings of the unit disk onto CAPDs have to satisfy the equations (3.1)

$$\sum_{k=1}^{n} \mu_k = \sum_{k=1}^{n} p_k(a_k + i\mu_k) = 0$$

of Theorem 3.4. We wish to verify these equations for the parameters

$$\mu_k = -\frac{(\alpha_k - 1)}{2} \sum_{j \neq k} (\alpha_j - 1) \cot \frac{\varphi_j - \varphi_k}{2}, \qquad k = 1, \ldots, n,$$

of Lemma 3.6 that were calculated for CAPD mappings onto polygonal domains. To shorten the notation, we introduce

$$\lambda(j,k) := (\alpha_j - 1)(\alpha_k - 1).$$

For the first equation

$$\sum_{k=1}^{n} \mu_k = 0$$

we have

$$\begin{aligned}
\sum_{k=1}^{n} \mu_k &= -\frac{1}{2} \sum_{k=1}^{n} \sum_{j \neq k} \lambda(j,k) \cot \frac{\varphi_j - \varphi_k}{2} \\
&= -\frac{1}{2} \sum_{k=1}^{n-1} \sum_{j=k+1}^{n} \left(\lambda(j,k) \cot \frac{\varphi_j - \varphi_k}{2} + \lambda(k,j) \cot \frac{\varphi_k - \varphi_j}{2} \right) = 0
\end{aligned}$$

by reordering the sum, the fact that λ is symmetric ($\lambda(j,k) = \lambda(k,j)$), and that cotangent is an odd function ($\cot(-x) = -\cot(x)$).

The second equation can be split up into two, considering the real and the imaginary part.

$$\begin{aligned}
\sum_{k=1}^{n} p_k(a_k + i\mu_k) &= \sum_{k=1}^{n} (\cos(\varphi_k) + i \sin(\varphi_k))(a_k + i\mu_k) \\
&= \sum_{k=1}^{n} \left[(a_k \cos(\varphi_k) - \mu_k \sin(\varphi_k)) + i\,(a_k \sin(\varphi_k) + \mu_k \cos(\varphi_k)) \right] \\
&= \tau_r + i\tau_i
\end{aligned}$$

If we continue with the real part τ_r of the equation, we find

$$\begin{aligned}\tau_r &= \sum_{k=1}^{n}\left[a_k\cos(\varphi_k) - \sin(\varphi_k)\left(-\frac{1}{2}\sum_{j\neq k}\left(\lambda(k,j)\cot\frac{\varphi_j-\varphi_k}{2}\right)\right)\right]\\ &= \sum_{k=1}^{n} a_k\cos(\varphi_k) + \frac{1}{2}\sum_{k=1}^{n}\sum_{j\neq k}\lambda(k,j)\sin(\varphi_k)\cot\frac{\varphi_j-\varphi_k}{2}\\ &= \sum_{k=1}^{n} a_k\cos(\varphi_k) + \frac{1}{2}\sum_{k=1}^{n-1}\sum_{j=k+1}^{n}\lambda(k,j)\cot\frac{\varphi_j-\varphi_k}{2}\left(\sin(\varphi_k)-\sin(\varphi_j)\right).\end{aligned}$$

By using the identity

$$\cot\frac{\varphi_1-\varphi_2}{2}\left(\sin(\varphi_2)-\sin(\varphi_1)\right) = -\cos(\varphi_1)-\cos(\varphi_2)$$

and reestablishing the original order, we have

$$\begin{aligned}\tau_r &= \sum_{k=1}^{n} a_k\cos(\varphi_k) - \frac{1}{2}\sum_{k=1}^{n-1}\sum_{j=k+1}^{n}\lambda(k,j)\left(\cos(\varphi_j)+\cos(\varphi_k)\right)\\ &= \sum_{k=1}^{n} a_k\cos(\varphi_k) - \frac{1}{2}\sum_{k=1}^{n}(\alpha_k-1)\cos(\varphi_k)\sum_{j\neq k}(\alpha_j-1).\end{aligned}$$

Since polygons satisfy the geometric property $\sum_{k=1}^{n}(\alpha_k-1) = -2$, we have the equation $\sum_{j\neq k}(\alpha_j-1) = -2-(\alpha_k-1)$ at our disposal. Hence, we can further transform the real part τ_r to

$$\begin{aligned}\tau_r &= \sum_{k=1}^{n} a_k\cos(\varphi_k) - \frac{1}{2}\sum_{k=1}^{n}(\alpha_k-1)\cos(\varphi_k)(-2-(\alpha_k-1))\\ &= \sum_{k=1}^{n} a_k\cos(\varphi_k) - \frac{1}{2}\sum_{k=1}^{n}(1-\alpha_k^2)\cos(\varphi_k)\\ &= \sum_{k=1}^{n} a_k\cos(\varphi_k) - \sum_{k=1}^{n} a_k\cos(\varphi_k) = 0,\end{aligned}$$

since a_k is defined by $a_k = \frac{1}{2}(1-\alpha_k^2)$.
The same techniques can be used to simplify the imaginary part τ_i to zero, which demonstrates the second restricting equation.

A.2 Proof of the Convergence Lemma 4.15

We will state the proof of Lemma 4.15 that was omitted in Section 4.1.4.

Lemma A.1
Let D be a circular domain, infinity an ordinary point of $\mathbb{M}(D)$ lying in D_R and Λ the limit set of $\mathbb{M}(D)$. Further let

$$\varepsilon = \frac{1}{4} \max_{l_1, l_2 \in \Lambda} \{|l_1 - l_2|\}.$$

The candidate function $\mathcal{K}$ in the form

$$\begin{aligned}\mathcal{K}(z) = &\sum_{j,k} \left(\frac{a_{j,k}}{(z - p_{j,k})^2} + \frac{\gamma_{j,k}}{z - p_{j,k}} \right) \\ &+ \sum_{T,j,k}{}' \left(\frac{a_{j,k}}{(z - p_{T,j,k})^2} + \frac{\gamma_{T,j,k}}{z - p_{T,j,k}} - \frac{\gamma_{T,j,k}}{(z - l_T)} \right. \\ &\left. - \frac{a_{j,k} + \gamma_{T,j,k}(p_{T,j,k} - l_T)}{(z - l_T)^2} - \frac{2a_{j,k}(p_{T,j,k} - l_T) + \gamma_{T,j,k}(p_{T,j,k} - l_T)^2}{(z - l_T)^3} \right),\end{aligned}$$

converges locally uniformly on D, where $l_T \in \Lambda$ and $|T^{-1}(l_T) - T^{-1}(\infty)| > \varepsilon$. The symbol $\sum'$ indicates the sum without the identity.

Proof. We will start with a discussion of the behavior of the group $\mathbb{M}(D)$. Since infinity is an ordinary point, the limit set is bounded and all the images of the circles C_j are of finite length, i.e. the set of transformed prevertices is also bounded. All images of infinity lie either in a circle C_j or $T(C_j)$, where $j = 1, \ldots, m$, and so the points $T(\infty)$ are also bounded.
To show the convergence, we need to investigate the sum

$$\begin{aligned}\sum_{T,j,k}{}' \left(\frac{a_{j,k}}{(z - p_{T,j,k})^2} + \frac{\gamma_{T,j,k}}{z - p_{T,j,k}} - \frac{\gamma_{T,j,k}}{(z - l_T)} \right. \\ \left. - \frac{a_{j,k} + \gamma_{T,j,k}(p_{T,j,k} - l_T)}{(z - l_T)^2} - \frac{2a_{j,k}(p_{T,j,k} - l_T) + \gamma_{T,j,k}(p_{T,j,k} - l_T)^2}{(z - l_T)^3} \right).\end{aligned}$$

If we split up the terms and sort them with respect to a and γ, we see that

$$\frac{a}{(z-p)^2} - \frac{a}{(z-l)^2} - \frac{2a(p-l)}{(z-l)^3} = \frac{a(p-l)^2(2(z-p)+(z-l))}{(z-p)^2(z-l)^3} \tag{A.1}$$

$$\frac{\gamma}{(z-p)} - \frac{\gamma}{(z-l)} - \frac{\gamma(p-l)}{(z-l)^2} - \frac{\gamma(p-l)^2}{(z-l)^3} = \frac{\gamma(p-l)^3}{(z-p)(z-l)^3}. \tag{A.2}$$

(The indices were skipped to shorten the notation.) To investigate the behavior of these two fractions, we start with their numerators. We are able to rewrite the difference

$p_{T,j,k} - l_T$ to

$$p_{T,j,k} - l_T = T(p_{j,k}) - T(\tau_T) = \frac{1}{C^2} \frac{p_{j,k} - \tau_T}{(p_{j,k} + \frac{D}{C})(\tau_T + \frac{D}{C})} \tag{A.3}$$

if we use $p_{T,j,k} = T(p_{j,k})$, $\tau_T := T^{-1}(l_T)$ and $T(z) = \frac{Az+B}{Cz+D}$. We further shorten our notation by $u_T = -\frac{D}{C} = T^{-1}(\infty)$.
The $p_{j,k}$, τ_T and u_T are bounded due to the behavior of $\mathbb{M}(D)$. The differences $p_{j,k} - \tau_T$ and $p_{j,k} - u_T$ have a lower and an upper boundary, since the $p_{j,k}$ lie on the circles C_j, while each τ_T and u_T lie inside of a circle C_j or $T(C_j)$ with a positive distance to the corresponding circle C_j or $T(C_j)$. The difference $\tau_T - u_T$ has also a lower boundary, as demanded by $|\tau_T - u_T| = |T^{-1}(l_T) - T^{-1}(\infty)| > \varepsilon$. Hence, there is an upper boundary

$$\delta = \max_{T,j,k} \left\{ \left| \frac{p_{j,k} - \tau_T}{(p_{j,k} - u_T)(\tau_T - u_T)} \right| \right\}$$

for the quotient of equation (A.3). We therefore have for the absolute value of the difference $p_{T,j,k} - l_T$

$$|p_{T,j,k} - l_T| \leq |C|^{-2}\delta.$$

For z from a closed subset $M \subset D$, we can repeat the argument to find a boundary for the remaining components of equation (A.1)

$$\left| \frac{2(z - p_{T,j,k}) + (z - l_T)}{(z - p_{T,j,k})^2 (z - l_T)^3} \right| \leq \mu_1$$

for all indices T, j, k and $z \in M$.
Applying this together with $K := \sum_{j=0}^{m} K_j$ and $\max_{j,k} \{|a_{j,k}|\} \leq \frac{3}{2}$ to the sum over the expression (A.1) shows

$$\begin{aligned}
&\left| \sum_{T,j,k}{}' \frac{a_{j,k}(p_{T,j,k} - l_T)^2 (2(z - p_{T,j,k}) + (z - l_T))}{(z - p_{T,j,k})^2 (z - l_T)^3} \right| \\
&\leq \sum_{T,j,k}{}' |a_{j,k}| |p_{T,j,k} - l_T|^2 \left| \frac{2(z - p_{T,j,k}) + (z - l_T)}{(z - p_{T,j,k})^2 (z - l_T)^3} \right| \\
&\leq \frac{3}{2} \mu_1 \sum_{T,j,k}{}' |p_{T,j,k} - l_T|^2 \\
&\leq \frac{3}{2} \mu_1 \sum_{T}{}' \left(|C|^{-4} \delta^2 \sum_{j} K_j \right) \\
&\leq \frac{3}{2} \mu_1 \delta^2 K \sum_{T}{}' |C|^{-4} = \lambda_1 \sum_{T}{}' |C|^{-4}.
\end{aligned}$$

We have to be more careful for the second part, since the $\gamma_{T,j,k}$ increase with the length of T in their absolute value. The correlation between $\gamma_{T,j,k}$ and $\gamma_{j,k}$ (first generation γ) is, according to (4.11),

$$\begin{aligned}\gamma_{T,j,k} &= (Cp_{j,k}+D)^2\gamma_{j,k} + 2a_{j,k}C(Cp_{j,k}+D)\\ &= C^2(p_{j,k}-u_T)\left[(p_{j,k}-u_T)\gamma_{j,k}+2a_{j,k}\right].\end{aligned}$$

Since all factors excluding the C^2 are bounded, we can introduce a new positive constant μ_2, where

$$\left|\frac{\gamma_{T,j,k}}{(z-p_{T,j,k})(z-l_T)^3}\right| \le |C|^2\mu_2.$$

Therefore we can write

$$\begin{aligned}&\left|\sum_{T,j,k}{}' \frac{\gamma_{T,j,k}(p_{T,j,k}-l_T)^3}{(z-p_{T,j,k})(z-l_T)^3}\right| \le \sum_{T,j,k}{}' |p_{T,j,k}-l_T|^3 \left|\frac{\gamma_{T,j,k}}{(z-p_{T,j,k})(z-l_T)^3}\right|\\ &\le \sum_{T,j,k}{}' \left(|C|^{-6}\delta^3|C|^2\mu_2\right) \le \delta^3\mu_2 K\sum_{T}{}' |C|^{-4} = \lambda_2\sum_{T}{}' |C|^{-4}.\end{aligned}$$

If we combine the results, we see

$$\begin{aligned}&\sum_{T,j,k}{}'\left|\frac{a_{j,k}}{(z-p_{T,j,k})^2}+\frac{\gamma_{T,j,k}}{z-p_{T,j,k}}-\frac{\gamma_{T,j,k}}{(z-l_T)}\right.\\ &\qquad\left.-\frac{a_{j,k}+\gamma_{T,j,k}(p_{T,j,k}-l_T)}{(z-l_T)^2}-\frac{2a_{j,k}(p_{T,j,k}-l_T)+\gamma_{T,j,k}(p_{T,j,k}-l_T)^2}{(z-l_T)^3}\right|\\ &\le(\lambda_1+\lambda_2)\sum_{T}{}' |C|^{-4},\end{aligned}$$

where the sum $\sum_{T}{}' |C|^{-4}$ converges according to Lemma 2.41.
If we also introduce an upper bound λ_3 for the absolute value of the first generation, we have

$$|\mathcal{K}(z)| \le \lambda_3 + (\lambda_1+\lambda_2)\sum_{T}{}' |C|^{-4} < \infty.$$

Thus we have proven the locally uniformly convergence of $\mathcal{K}$ in D. □

The geometric interpretation of the condition $|T^{-1}(l_T) - T^{-1}(\infty)| > \varepsilon$ is that we have to ensure that each l_T lies in the convex hull of the domain $T(D_R)$. This property is necessary, as we require the distance $|p_{T,j,k} - l_T|$ to shrink with the same speed as the diameter of the domains $T(D_R)$.
Note that the proof would actually allow the statement "$\mathcal{K}$ converges uniformly on closed subsets of $\mathbb{C}_\infty$ neither containing limit points nor prevertices".

A.3 Calculation of the Pre-Schwarzian of Nehari's Slit Mapping

We wish to calculate the pre-Schwarzian of the function

$$f(z) = \sqrt{k}\,\mathrm{sn}\left(\frac{2iK}{\pi}\log\frac{z}{r} + K, r^4\right)$$

that conformally maps the annulus $r < |z| < 1$ onto the unit disk minus a symmetric slit on the real axis. Since the following discussion is based on [Neh52, p. 293-295], we need to state some basic properties of the functions sn, cn and dn. The functions cn and dn have the product expansions

$$\mathrm{cn}(z,q) = \frac{\sqrt[4]{q(1-k^2)}}{\sqrt{k}}\,\zeta\,\frac{\prod_{n=0}^{\infty}(1+q^{2n}\zeta^{-2})\prod_{n=1}^{\infty}(1+q^{2n}\zeta^{2})}{\prod_{n=0}^{\infty}(1-q^{2n+1}\zeta^{-2})\prod_{n=0}^{\infty}(1-q^{2n+1}\zeta^{2})},$$

$$\mathrm{dn}(z,q) = \sqrt[4]{1-k^2}\,\frac{\prod_{n=0}^{\infty}(1+q^{2n+1}\zeta^{-2})\prod_{n=0}^{\infty}(1+q^{2n+1}\zeta^{2})}{\prod_{n=0}^{\infty}(1-q^{2n+1}\zeta^{-2})\prod_{n=0}^{\infty}(1-q^{2n+1}\zeta^{2})},$$

where $\zeta = e^{\frac{\pi i z}{2K}}$. We do not need an expansion for sn as it has the property

$$\frac{d}{dz}\mathrm{sn}(z) = \mathrm{cn}(z)\,\mathrm{dn}(z). \tag{A.4}$$

Hence, the derivative of f is of the form

$$f'(z) = \frac{2irK\sqrt{k}}{\pi z}\,\mathrm{cn}\left(\frac{2iK}{\pi}\log\frac{z}{r} + K, r^4\right)\,\mathrm{dn}\left(\frac{2iK}{\pi}\log\frac{z}{r} + K, r^4\right)$$

if we use equation (A.4). For $\zeta = i\frac{r}{z}$ and $q = r^4$, we can use the product forms

$$\mathrm{cn}\left(\frac{2iK}{\pi}\log\frac{z}{r} + K, r^4\right) = \frac{ir\sqrt[4]{r^4(1-k^2)}}{\sqrt{k}\,z}\,\frac{\prod_{n=0}^{\infty}(1-(r^4)^{2n}(\frac{z}{r})^2)\prod_{n=1}^{\infty}(1-(r^4)^{2n}(\frac{r}{z})^2)}{\prod_{n=0}^{\infty}(1+(r^4)^{2n+1}(\frac{z}{r})^2)\prod_{n=0}^{\infty}(1+(r^4)^{2n+1}(\frac{r}{z})^2)},$$

$$\mathrm{dn}\left(\frac{2iK}{\pi}\log\frac{z}{r} + K, r^4\right) = \sqrt[4]{1-k^2}\,\frac{\prod_{n=0}^{\infty}(1-(r^4)^{2n+1}(\frac{z}{r})^2)\prod_{n=0}^{\infty}(1-(r^4)^{2n+1}(\frac{r}{z})^2)}{\prod_{n=0}^{\infty}(1+(r^4)^{2n+1}(\frac{z}{r})^2)\prod_{n=0}^{\infty}(1+(r^4)^{2n+1}(\frac{r}{z})^2)}.$$

For further investigations, we will use a finite form, and so define

$$f' = \lim_{N\to\infty} f'_N,$$

where f'_N contains only finite products up to N. If we take logarithm of f'_N, we obtain

$$\begin{aligned}\log f'_N(z) =& \log\left(\frac{-2r^3K\sqrt{1-k^2}}{\pi}\right) - 2\log(z)\\ &+ \sum_{n=0}^{N}\log\left(1-(r^4)^{2n}(\tfrac{z}{r})^2\right) + \sum_{n=1}^{N}\log\left(1-(r^4)^{2n}(\tfrac{r}{z})^2\right)\\ &+ \sum_{n=0}^{N}\log\left(1-(r^4)^{2n+1}(\tfrac{z}{r})^2\right) + \sum_{n=0}^{N}\log\left(1-(r^4)^{2n+1}(\tfrac{r}{z})^2\right)\\ &- 2\sum_{n=0}^{N}\log\left(1+(r^4)^{2n+1}(\tfrac{z}{r})^2\right) - 2\sum_{n=0}^{N}\log\left(1+(r^4)^{2n+1}(\tfrac{r}{z})^2\right).\end{aligned}$$

We can rewrite the terms $1-(r^4)^{2n}(\frac{z}{r})^2 = (1-(r^2)^{2n}\frac{z}{r})(1+(r^2)^{2n}\frac{z}{r})$ and differentiate $\log f'_N(z)$ to find

$$\begin{aligned}\frac{d}{dz}\log f'_N(z) =& \frac{-2}{z} + \sum_{n=0}^{2N+1}\left(\frac{1}{z-(r^2)^{-n}r} + \frac{1}{z+(r^2)^{-n}r}\right)\\ &+ \sum_{n=1}^{2N+1}\left(\frac{1}{z-(r^2)^{n}r} + \frac{1}{z+(r^2)^{n}r} + \frac{-2}{z}\right)\\ &+ \sum_{n=0}^{N}\left(\frac{-2}{z-(r^2)^{-2n}ir^{-1}} + \frac{-2}{z+(r^2)^{-2n}ir^{-1}}\right)\\ &+ \sum_{n=0}^{N}\left(\frac{-2}{z-(r^2)^{2(n+1)}ir^{-1}} + \frac{-2}{z+(r^2)^{2(n+1)}ir^{-1}} + \frac{4}{z}\right).\end{aligned}$$

We have $2(N+1)$ terms $\frac{-2}{z}$ (one in the beginning and $2N+1$ in the sum) and $N+1$ terms $\frac{4}{z}$, which thus cancel out. Therefore we can write

$$\begin{aligned}\frac{d}{dz}\log f'_N(z) =& \sum_{n=-(2N+1)}^{2N+1}\left(\frac{1}{z-(r^2)^{n}r} + \frac{1}{z+(r^2)^{n}r}\right)\\ &+ \sum_{n=-N}^{N+1}\left(\frac{-2}{z-(r^2)^{2n}ir^{-1}} + \frac{-2}{z+(r^2)^{2n}ir^{-1}}\right).\end{aligned}$$

If we introduce the poles p_k and u_k, we can write the pre-Schwarzian as

$$S_N(z) = \sum_{n=-(2N+1)}^{2N+1}\sum_{k=1}^{2}\frac{1}{z-r^{2n}p_k} + \sum_{n=-N}^{N+1}\sum_{k=1}^{2}\frac{-2}{z-r^{4n}u_k},$$

where $p_1 = r$, $p_2 = -r$, $u_1 = ir^{-1}$, $u_2 = -ir^{-1}$, and $S(z) = \lim_{N\to\infty} S_N(z)$.

A.4 Validity of the Mappings by Methods of Differential Equations

If the Schwarzian Derivative is known, one may calculate a corresponding mapping function by solving the differential equation

$$y'' + \frac{1}{2}\mathcal{S}y = 0 \tag{A.5}$$

for two linearly independent solutions. Therefore, it is reasonable to investigate the solutions of the equation to get information about the behavior of the mapping itself. One feature of interest for multiply connected domains is whether the function describes a valid multiply connected mapping.
An example of a statement gathered from differential equations is the univalence criteria of Nehari [Neh48]

$$|\{f, z\}| \leq \frac{6}{(1-|z|^2)^2}, \qquad |z| < 1,$$

which was proven by using the Sturm comparison theorem.

Suppose we wish to solve the Schwarzian along a closed curve $\delta \subset D$. As the curve is closed, it can be seen as a periodic function $\delta(t) = \delta(t + 2\pi)$.
Since a closed curve is mapped onto a closed curve, we require $f(\delta(0)) = f(\delta(2\pi))$ for the mapping to be valid. Since the solution of the Schwarzian is given in the form of a ratio, we have

$$f(z) = \frac{y_1(z)}{y_2(z)}$$

for two independent solutions y_j of (A.5). If we now define

$$v_j(t) := y_j(\delta(t)), \qquad j = 1, 2\,,$$

we can rewrite the problem to

$$f(\delta(0)) = f(\delta(2\pi)) \quad \Leftrightarrow \quad v_j(0) = \sigma(2\pi) v_j(2\pi),$$

where we have added a possible factor σ that vanishes in forming the quotient.
The transformed equation (A.5) for v is[60]

$$v'' - \frac{\ddot{\delta}}{\dot{\delta}} v' + (\dot{\delta})^2 \frac{1}{2}\mathcal{S}v = 0. \tag{A.6}$$

Since the coefficients are 2π periodic, we can apply several techniques for solving ordinary differential equations. Based on the Floquet theory (e.g. [Tes12]), we notice that σ must be constant. Since every solution of (A.6) must have the same σ, both Floquet multipliers must be equal. Based on the structure of the equation, they must equal 1.

We can further transform ([MW66, p. 51]) this equation with

$$w(t) := \exp\left(-\frac{1}{2}\ln\left(\dot{\delta}(t)\right) + \frac{1}{2}\ln\left(\dot{\delta}(0)\right)\right) v(t)$$

[60] See the next section for a derivation of the formula.

into the form of Hill's equation

$$w'' + \mathcal{T} w = 0,$$

where

$$\mathcal{T} = \frac{1}{2}\frac{d}{dt}\left(\frac{\ddot{\delta}}{\dot{\delta}}\right) - \frac{1}{4}\left(\frac{\ddot{\delta}}{\dot{\delta}}\right)^2 + \frac{\dot{\delta}^2}{2}\mathcal{S}(\delta).$$

In this form, the problem of two independent (anti-)periodic solutions is known as the coexistence problem [MW66, ch. 7].
The disadvantage is that there is a lack of statements on equations with generic coefficient functions, while there are some well analyzed special cases. Additionally, most of the statements demand real coefficient functions.

Even if every solution for every curve is periodic, this does not exclude the cases, where some points are surrounded multiple times by the image curve of δ or where the image curve is not simple.
If we choose the initial value of v_1 to be zero, f has zeros at $\delta(0)$ and $\delta(2\pi)$. To cover at least some of the cases stated above, there should not be any more additional zeros on δ. Equivalently v_1 can not have any zeros for $t \in (0, 2\pi)$. This leads to the concept of Sturm-Liouville equations [Zet05], where the boundary values are fixed and, as one aspect, the number of the zeros of the solutions is investigated.

B Basic Calculations for the Evaluation of the Schwarzian Derivative

B.1 System of Differential Equations

We stated already in Lemma 2.13 that the Schwarzian Derivative $\{f, z\} = \mathcal{S}(z)$ can be solved by solving the differential equation

$$y'' + \frac{1}{2}\mathcal{S}y = 0$$

for two independent solutions y_1, y_2. The actual mapping function is then given by the quotient $f = y_1/y_2$. Note that the initial values of the differential equations correspond to the degrees of freedom provided by the Möbius transformations.

In most cases, it is sufficient to calculate the solution only along a curve γ, for example, if we are only interested in some special points. If we use numerics, we are in any case restricted to solving along a curve.
We now state the transformation of the differential equation for the sake of completeness. With $y(\gamma(t)) = v(t)$ we have:

$$y = v, \qquad y' = (\dot{\gamma})^{-1}v', \qquad y'' = (\dot{\gamma})^{-2}\left(v'' - \frac{\ddot{\gamma}}{\dot{\gamma}}v'\right).$$

This gives

$$v'' - \frac{\ddot{\gamma}}{\dot{\gamma}}v' + (\dot{\gamma})^2\frac{1}{2}\mathcal{S}v = 0.$$

We have for the two common curves, a concentric circle and a straight line:

$$\begin{aligned} \text{circle } \gamma(t) = re^{it}: &\qquad v'' - iv' - r^2e^{2it}\frac{1}{2}\mathcal{S}v = 0 \\ \text{line } \gamma(t) = te^{i\varphi}: &\qquad v'' + e^{2i\varphi}\frac{1}{2}\mathcal{S}v = 0 \end{aligned}$$

A note regarding the numerics: It reasonable to solve for both solutions v_1 and v_2 in one system of differential equations instead of two. Combining them reduces the number of evaluations of the Schwarzian resulting in a significantly reduced calculation time.

B.1.1 Initial Values

The initial values of f, y_1, and y_2 are connected by

$$\begin{aligned} f(z_0) = \frac{y_1(z_0)}{y_2(z_0)}, \quad f'(z_0) = \frac{y_1'(z_0)y_2(z_0) - y_1(z_0)y_2'(z_0)}{y_2(z_0)^2}, \\ f''(z_0) = 2y_2'(z_0)\frac{y_1(z_0)y_2'(z_0) - y_1'(z_0)y_2(z_0)}{y_2(z_0)^3}. \end{aligned} \tag{B.1}$$

Normalizing this by setting $y_2(z_0) = 1$, we reach

$$f(z_0) = y_1(z_0), \quad f'(z_0) = y_1'(z_0) - y_1(z_0)y_2'(z_0),$$
$$f''(z_0) = 2y_2'(z_0)\left(y_1(z_0)y_2'(z_0) - y_1'(z_0)\right).$$

Solving the equations for y gives

$$y_1(z_0) = f(z_0), \qquad y_2(z_0) = 1,$$
$$y_1'(z_0) = \frac{2f'(z_0)^2 - f(z_0)f''(z_0)}{2f'(z_0)}, \qquad y_2'(z_0) = -\frac{f''(z_0)}{2f'(z_0)}.$$

Hence, if we have initial values for f, we can calculate the initial values for y_1 and y_2 by the equations above. To switch to the differential equation for the curve γ, we have to compute the initial values for $v_j(t) = y_j(\gamma(t))$, where $\gamma(0) = z_0$, by

$$v_j(0) = y_j(z_0), \qquad v_j'(0) = \dot{\gamma}(0)y_j'(z_0).$$

After solving the differential equation for $v_1(1)$ and $v_2(1)$, we can use the equations (B.1) to calculate the values $f(z_1)$, $f'(z_1)$ and $f''(z_1)$, where $z_1 = \gamma(1)$.

We may wish to change the image domain by applying a Möbius transformation. This can be done after the solving process or beforehand by modifying the initial values. As we will change the initial values in any case, we begin with the simple set

$$f(z_0) = 0, \qquad f'(z_0) = 1, \qquad f''(z_0) = 0,$$

and obtain for y

$$y_1(z_0) = 0, \qquad y_1'(z_0) = 1, \qquad y_2(z_0) = 1, \qquad y_2'(z_0) = 0.$$

If we apply the transformation $T(z) = (az + b)/(cz + d)$ to find $g = T \circ f$ we have

$$g(z_0) = \frac{b}{d}, \qquad g'(z_0) = \frac{1}{d^2}, \qquad g''(z_0) = \frac{-2c}{d^3}$$

and so we set for the transformed function $g = u_1/u_2$ the initial values to

$$u_1(z_0) = b, \qquad u_1'(z_0) = a, \qquad u_2(z_0) = d, \qquad u_2'(z_0) = c.$$

Hence, if we want to change the mapping by a Möbius transformation, we can apply the coefficients directly to the initial values of the differential equation.

B.2 Boundary Calculation

B.2.1 Calculate the Circles Providing the Boundary

To calculate the boundary of an CAP domain, we must calculate the circles providing the boundary arcs. Each pre-arc $\zeta_{j,k} \subset C_j$ is mapped onto a circular arc $f(\zeta_{j,k}) = \delta_{j,k} \subset \tilde{C}_{j,k}$. If we solve from some point z_0 to a boundary point z_1, we get $f(z_1)$, $f'(z_1)$ and $f''(z_1)$ as a result of the differential equation. The goal is to calculate $\tilde{C}_{j,k}$ from these

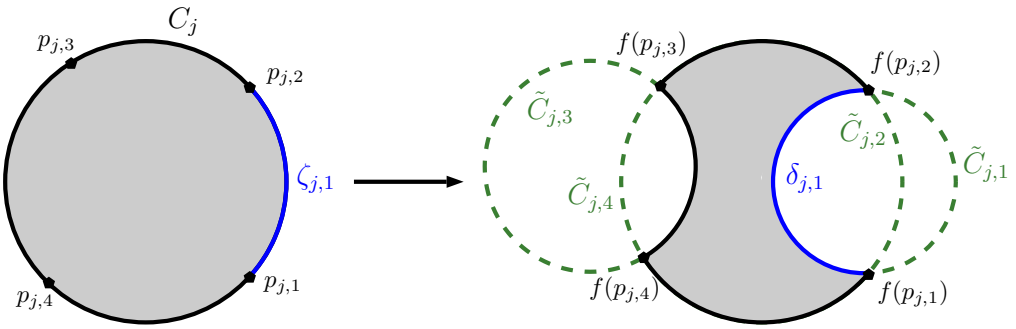

Figure 58: Each boundary circle C_j is mapped onto a circular arc polygon domain. The pre-arcs $\zeta_{j,k}$ are mapped onto the circular arcs $\delta_{j,k}$. Each $\delta_{j,k}$ is part of a circle $\tilde{C}_{j,k}$. In the special case shown above, the circles $\tilde{C}_{j,2}$ and $\tilde{C}_{j,4}$ are equal.

three values.
For the preimage arc, we have

$$\zeta(t) = re^{it/r} + c, \qquad \dot{\zeta}(t) = ie^{it/r}, \qquad \ddot{\zeta}(t) = -\frac{1}{r}e^{it/r}$$

and for the image arc

$$\delta(t) = f(\zeta(t)), \qquad \dot{\delta}(t) = f'(\zeta(t))\dot{\zeta}(t), \qquad \ddot{\delta}(t) = f''(\zeta(t))\dot{\zeta}(t)^2 + f'(\zeta(t))\ddot{\zeta}(t).$$

For a specific point z_1, we set $t = \arg(z_1 - c)$ to calculate the above quantities.[61] We can then calculate the curvature κ and the normal vector $\vec{n}$ of the image curve by

$$\kappa = |f'|^{-1}\,\mathrm{Im}(\ddot{\delta}/\dot{\delta}), \qquad \vec{n} = i\,\mathrm{sign}(\kappa)\,(\dot{\delta}/|\dot{\delta}|),$$

which allows us to calculate

$$\tilde{r} = |\kappa|^{-1}, \qquad \tilde{c} = f + \vec{n}\tilde{r},$$

the radius and center of the circle $\tilde{C}$.

B.2.2 Calculation of the Vertices

We wish to calculate the vertices of the image domain by using the circles $\tilde{C}_{j,k}$. With these vertices, we then also know the arcs of the circles $\tilde{C}_{j,k}$ that form the boundary of the domain.
The previous step of the calculation does not only provide us with the circles $\tilde{C}_{j,k}$ but also with the direction that the boundary takes on them, i.e. clockwise or counterclockwise. Combining these information together with the interior angles of the domain allows us to calculate the vertices.

[61] We can skip the parameter, since t is fixed in the following notation.

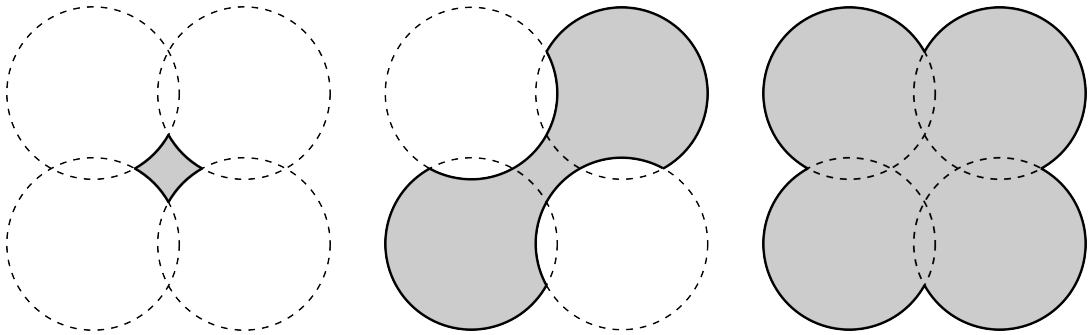

Figure 59: The same set of circles can be used to construct different boundaries for circular arc polygon domains.

Let us look at two of the circles $\tilde{C}_{j,k}$ e.g. $\tilde{C}_{0,1}$ and $\tilde{C}_{0,2}$. The two circles will intersect at two points and we must choose the correct one as the vertex. This problem becomes trivial if the circles only touch each other at one point.

Let us denote the curvature of $\tilde{C}_{0,1}$ and $\tilde{C}_{0,2}$ by κ_1 and κ_2 and the interior angle by $\alpha\pi$. Suppose the center of $\tilde{C}_{0,1}$ is at 1 and the center of $\tilde{C}_{0,2}$ is at -1. We have one vertex v_1 with a positive imaginary part and one vertex v_2 with a negative imaginary part. There are eight different scenarios, as we have two directions for each circle and two vertices to choose from. Listing these cases shows that for each pair of directions we can

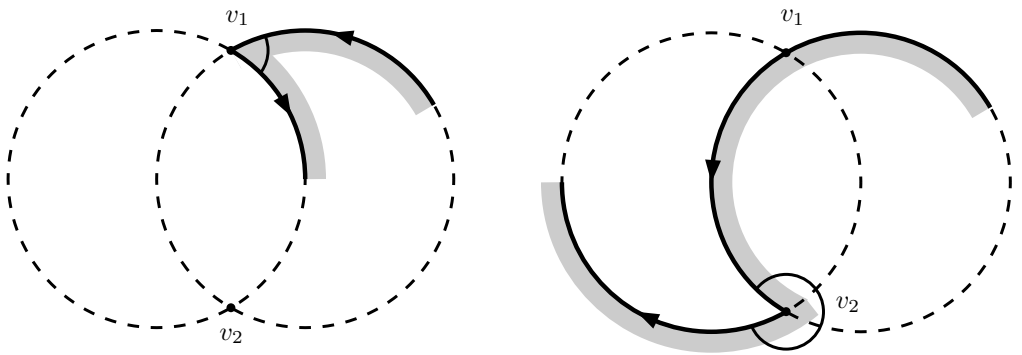

(a) For the vertex v_1, the interior angle is smaller than π.

(b) For the vertex v_2, the interior angle is greater than π.

Figure 60: The curvature for $\tilde{C}_{0,1}$ (right circle) is positive (counterclockwise) and the curvature for $\tilde{C}_{0,2}$ (left circle) is negative (clockwise). For an interior angle smaller than π, we have to choose the upper vertex v_1. For an interior angle greater than π, we have to choose the lower vertex v_2.

distinguish the intersection points by the interior angle. One point produces an interior angle smaller than π ($\alpha < 1$), while the other produces an angle larger than π ($\alpha > 1$).

The results can be found in Table 8(a), and a simplified version is shown in Table 8(b). With the circles $\tilde{C}_{j,k}$, the curvature of the boundary arcs and the vertices we have completely defined the boundary.

$\text{sign}(\kappa_1)$	$\text{sign}(\kappa_2)$	α	vertex
$+1$	$+1$	> 1	v_1
$+1$	$+1$	< 1	v_2
$+1$	-1	> 1	v_2
$+1$	-1	< 1	v_1
-1	$+1$	> 1	v_2
-1	$+1$	< 1	v_1
-1	-1	> 1	v_1
-1	-1	< 1	v_2

(a) The vertex can be chosen by the signs of the curvatures and the interior angle

$\text{sign}(\kappa_1\kappa_2)$	α	vertex
$+1$	> 1	v_1
$+1$	< 1	v_2
-1	> 1	v_2
-1	< 1	v_1

(b) The table to the left can be simplified by investigating only the product of the signs.

Table 8: We may choose the correct vertex by the signs of the curvatures of the arcs and the interior angle.

Note that this approach does not cover the case where two consecutive circular arcs are provided by the same circle. This occurs at the end point of a slit ($\alpha = 2$) or if we artificially split up a boundary arc in several parts ($\alpha = 1$). If this happens, we must approximate the vertices by numerical means.

References

[Ahl73] Lars V. Ahlfors. *Conformal Invariants*. AMS Chelsea Publishing, Providence, Rhode Island, 1973.

[Aka64] Tohru Akaza. Poincaré theta series and singular sets of Schottky groups. *Nagoya Mathematical Journal*, 24:43–65, 1964.

[BG87] Petter Bjørstad and Eric Grosse. Conformal mapping of circular arc polygons. *SIAM Journal on Scientific and Statistical Computing*, 8(1):19–32, 1987.

[Bur91] William Burnside. On a class of automorphic functions. *Proceedings of the London Mathematical Society*, 23:49–88, 1891.

[Cas08] James Case. Breakthrough in conformal mapping. *SIAM News*, 41(1):1–3, 2008.

[CF07] Darren G. Crowdy and Athanassios S. Fokas. Conformal mappings to a doubly connected polycircular arc domain. *Proceedings of the Royal Society A*, 463:1885–1907, 2007.

[CFG11] Darren G. Crowdy, Athanassios S. Fokas, and Christopher C. Green. Conformal mappings to multiply connected polycircular arc domains. *Computational Methods and Function Theory*, 11(2):685–706, 2011.

[CM06] Darren G. Crowdy and Jonathan S. Marshall. Conformal mappings between canonical multiply connected domains. *Computational Methods and Function Theory*, 6(1):59–76, 2006.

[Con95] John B. Conway. *Functions of One Complex Variable II*, volume 159 of *Gradute Texts in Mathematics*. Springer, New York, 1995.

[CP01] Martin Chuaqui and Christian Pommerenke. An integral representation formula of the Schwarzian derivative. *Computational Methods and Function Theory*, 1:155–163, 2001.

[Cro05] Darren G. Crowdy. The Schwarz–Christoffel mapping to bounded multiply connected polygonal domains. *Proceedings of the Royal Society*, 461:2653–2678, 2005.

[DDEP06] Thomas K. DeLillo, Tobin A. Driscoll, Alan R. Elcrat, and John A. Pfaltzgraff. Computation of multiply connected Schwarz-Christoffel maps for exterior domains. *Computational Methods and Function Theory*, 6(2):301–315, 2006.

[DEKP13] Thomas K. DeLillo, Alan R. Elcrat, Everett H. Kropf, and John A. Pfaltzgraff. Efficient calculation of Schwarz-Christoffel transformations for mul-

tiply connected domains using Laurent series. *Computational Methods and Function Theory*, 13(2):307–336, 08 2013.

[DEP01] Thomas K. DeLillo, Alan R. Elcrat, and John A. Pfaltzgraff. Schwarz-Christoffel mapping of the annulus. *Society for Industrial and Applied Mathematics*, 43(3):469–477, 2001.

[DEP04] Thomas K. DeLillo, Alan R. Elcrat, and John A. Pfaltzgraff. Schwarz-Christoffel mapping of multiply connected domains. *Journal d'Analyse Mathematique*, 94(1):14–47, 2004.

[DK10] Thomas K. DeLillo and Everett H. Kropf. Slit maps and Schwarz-Christoffel maps for multiply connected domains. *Electronic Transactions on Numerical Analysis*, 36:195–223, 2010.

[DK11] Thomas K. DeLillo and Everett H. Kropf. Numerical computation of the Schwarz-Christoffel transformation for multiply connected domains. *SIAM Journal on Scientific Computing*, 33(3):1369–1394, 2011.

[DR08] Wolfgang Dahmen and Arnold Reusken. *Numerik für Ingenieure und Naturwissenschaftler*. Springer, Berlin, zweite auflage edition, 2008.

[DT02] Tobin A. Driscoll and Lloyd N. Trefethen. *Schwarz-Christoffel Mapping*. Cambridge University Press, Cambridge, 2002.

[For51] Lester R. Ford. *Automorphic Functions*. Chelsea Publishing Company, New York, 2nd edition edition, 1951.

[Gak66] Fedor D. Gakhov. *Boundary Value Problems*. Pergamon Press, Oxford, 1966.

[Geh77] Frederick W. Gehring. Univalent functions and the Schwarzian derivative. *Comment. Math. Helvetici*, 52:561–572, 1977.

[Hen74] Peter Henrici. *Applied and Computational Complex Analysis*, volume 1. Wiley Classics Library, New York, 1974.

[Hen86] Peter Henrici. *Applied and Computational Complex Analysis*, volume 3. Wiley Classics Library, New York, 1986.

[Hil62] Einar Hille. *Analytic Function Theory*, volume 2. Ginn and Co., Boston, 1962.

[Hil76] Einar Hille. *Ordinary Differential Equations in the Complex Domain*. John Wiley & Sons, New York, 1976.

[How90] Louis H. Howell. *Computation of Conformal Maps by Modified Schwarz-Christoffel Transformations*. PhD thesis, Massachusetts Institute of Technology, 1990.

[How93] Louis H. Howell. Numerical conformal mapping of circular arc polygons. *Journal of Computational and Applied Mathematics*, 46:7–28, 1993.

[Hu98] Chenglie Hu. Algorithm 785: A software package for computing Schwarz-Christoffel confromal transformation for doubly connected polygonal regions. *ACM Transactions on Mathematical Software*, 24(3):317–333, 1998.

[Kom45] Yusaku Komatu. Darstellungen der in einem Kreisringe analytischen Funktionen nebst den Anwendungen auf konforme Abbildung über Polygonalringgebiete. *Jap. J. Math.*, 19:203–215, 1945.

[Mas88] Bernard Maskit. *Kleinian Groups*. Springer-Verlag, Berlin, 1988.

[Mit98] Vladimir Mityushev. Convergence of the Poincaré series for some classical Schottky groups. *Proceedings of the American Mathematical Society*, 126(8):2399–2406, 1998.

[Mit12a] Vladimir Mityushev. Riemann-Hilbert problems for multiply connected domains and circular slit maps. *Computational Methods and Function Theory*, 11(2):575–590, 2012.

[Mit12b] Vladimir Mityushev. Schwarz-Christoffel formula for multiply connected domains. *Computational Methods and Function Theory*, 12(2):449–463, 2012.

[MW66] Wilhelm Magnus and Stanley Winkler. *Hill's Equation*. John Wiley & Sons, New York, 1966.

[Nas09] Mohamed M. S. Nasser. The Riemann-Hilbert problem and the generalized Neumann kernel on unbounded multiply connected regions. *The University Research Journal (IBB University)*, 20:47–60, 2009.

[Neh48] Zeev Nehari. The Schwarzian derivative and schlicht functions. *Bulletin of the American Mathematical Society*, 55:545–551, 1948.

[Neh52] Zeev Nehari. *Conformal Mapping*. McGraw-Hill Book Co., New York, 1952.

[Osg98] Brad Osgood. Old and new on the Schwarzian derivative. *Quasiconformal Mappings and Analysis*, 1:275–308, 1998.

[PK09] Michael R. Porter and Vladislav V. Kravchenko. Conformal mapping of right circular quadrilaterals. *arXiv*, 2009.

[Por05] Michael R. Porter. Numerical calculation of conformal mapping to a disk minus finitely many horocycles. *Computational Methods and Function Theory*, 5(2):471–488, 2005.

[Sch69] Hermann A. Schwarz. Ueber einige Abbildungsaufgaben. *Journal für die reine und angewandte Mathematik*, 70:105–120, 1869.

[Sch87] Friedrich H. Schottky. Ueber eine specielle Function, welche bei einer bestimmten linearen Transformation ihres Arguments unverändert bleibt. *Journal fuer die reine und angewandte Mathematik*, 101:227–272, 1887.

[Tes12] Gerald Teschl. *Ordinary Differential Equations and Dynamical Systems*, volume 140 of *Graduate Studies in Mathematics*. American Mathematical Society, Providence, Rhode Island, 2012.

[Vek62] Il'ja N. Vekua. *Generalized Analytic Functions*. Pergamon Press, Oxford, 1962.

[Zet05] Anton Zettl. *Sturm-Liouville Theory*, volume 121 of *Mathematical Surveys and Monographs*. American Mathematical Society, Providence, Rhode Island, 2005.

Index